

**The battle of human restriction factor APOBEC3
with SIV and HIV Vifs**

Zhang Zeli



The battle of human restriction factor APOBEC3 with SIV and HIV Vifs

Inaugural dissertation

for the attainment of the title of doctor
in the Faculty of Mathematics and Natural Sciences
at the Heinrich Heine University Düsseldorf

presented by

Zeli Zhang
from Wuhan, China

Düsseldorf, 02/2018

From the institute for **Clinic for Gastroenterology, Hepatology, and Infectiology, Medical faculty**, at the Heinrich Heine University Düsseldorf

Published by permission of the
Faculty of Mathematics and Natural Sciences at
Heinrich Heine University Düsseldorf

Supervisor: Prof. Dr. Carsten Münk
Co-supervisor: Prof. Dr. Holger Gohlke

Date of the oral examination:

Contents

Contents	1
Summary	2
Publications	4
Introduction	5
References	24
Chapter I	28
Chapter II	46
Chapter III	83
Acknowledgements	113
Declaration	114

Summary

Apolipoprotein B mRNA-editing enzyme, catalytic polypeptide-like 3s (APOBEC3s, A3s) are potent restriction factors of human immunodeficiency virus type 1/simian immunodeficiency viruses (HIV-1/SIV). The family of human (h) APOBEC3 restriction factors is formed by seven different proteins, hA3A–D and hA3F–H. To overcome the restriction of A3s, lentiviruses encode Vif proteins that directly bind A3s and induce them for proteasomal degradation. However, the molecular interaction of diverse lentiviral Vif proteins with A3 proteins of distinct species is poorly understood. The Vif interaction with A3s is likely of unique importance for the capacity of lentiviruses to infect new host species.

In current study, HIV-1 Vif was identified to be resistant to simian A3C, such as rhesus monkey (rh) A3C and sooty-mangabey monkey (smm) A3C. The simian A3Cs prevented the functional interaction with HIV-1 Vif due to presence of specific residues (N/H130 and Q133). In addition, a natural HIV-1 Vif (F-1 Vif) was characterized that failed to induce the degradation of hA3C and hA3F. The results were instrumental to describe in F-1 Vif an internal salt bridge of E171-K167-D101 that influences the Vif-mediated degradation of hA3C and hA3F. This finding indicates a novel mechanism, demonstrating that internal interactions outside the A3 binding region in HIV-1 Vif are able to influence the capacity to induce degradation of A3s. Additionally, in current study, I also identified that HIV-2, SIVmac and SIVagm Vif could target the so-called linker domain of feline A3Z2Z3 for degradation, which provides a fundamental basis for developing HIV or SIV animal model in felines.

To understand a role of human A3s during the zoonotic transmission of SIV of chimpanzee (SIVcpz) to humans, I investigated the impact of human A3s on the replication of SIVcpz. The hA3B and hA3H haplotype II strongly reduced the

infectivity of SIVcpz, because both of them are resistant to SIVcpz Vifs. Human A3H haplotype II inhibited SIVcpz by deaminase dependent as well independent mechanisms. Moreover, most SIV and HIV lineage Vif proteins could degrade chimpanzee A3H, but no Vifs from SIVcpz and SIV of gorilla (SIVgor) lineages antagonized hA3H haplotype II. Expression of hA3H hapII in human T cells efficiently blocked the spreading replication of SIVcpz. The spreading replication of SIVcpz was also restricted by high levels of A3H protein in human PBMCs. Thus, the data suggest that stably expressed hA3H protects humans against the cross-species transmission of SIVcpz and that SIVcpz spillover to humans may have started in individuals that harbor haplotypes of unstable A3H proteins.

Taken together, these findings indicate that A3s are able to form a barrier to prevent the spread of lentiviruses between different species. Further studies are required to develop strategies to overcome the species-specific antagonism of Vifs to develop new animal model for HIV-1.

Publications

This thesis is based on the following publications:

1. **Zhang Z**, Gu Q, de Manuel Montero M, Bravo IG, Marques-Bonet T, Häussinger D, Münk C. 2017. Stably expressed APOBEC3H forms a barrier for cross-species transmission of simian immunodeficiency virus of chimpanzee to humans. **PLoS Pathogens** 13(12): e1006746. (selected as highlighted study with press release)
2. **Zhang Z***, **Gu Q***, Jaguva Vasudevan AA, Jeyaraj M, Schmidt S, Zielonka J, Perkovic M, Heckel JO, Cichutek K, Häussinger D, Smits SH, Münk C. 2016. Vif Proteins from Diverse Human Immunodeficiency Virus/Simian Immunodeficiency Virus Lineages Have Distinct Binding Sites in A3C. **Journal of virology** 90:10193-10208. * equal first author
3. **Zhang Z**, Gu Q, Jaguva Vasudevan AA, Hain A, Kloke BP, Hasheminasab S, Mulnaes D, Sato K, Cichutek K, Häussinger D, Bravo IG, Smits SH, Gohlke H, Münk C. 2016. Determinants of FIV and HIV Vif sensitivity of feline APOBEC3 restriction factors. **Retrovirology** 13:46.

Additional publications:

1. **Gu Q***, **Zhang Z***, Gertzen CGW, Häussinger D, Gohlke H, Münk C. 2017. Identification of a conserved interface of HIV-1 and FIV Vifs with Cullin 5. **Journal of virology**. * equal first author
2. **Gu Q***, **Zhang Z***, Cano Ortiz L, Franco AC, Häussinger D, Münk C. 2016. Feline Immunodeficiency Virus Vif N-Terminal Residues Selectively Counteract Feline APOBEC3s. **Journal of virology** 90:10545-10557.* equal first author

Introduction

Retroviruses

Retroviruses are a group of single-stranded positive RNA viruses that have a DNA intermediate. Once a retrovirus enters the host cell, the virus utilizes its reverse transcriptase (RT) to generate DNA (complementary DNA or cDNA) by using its RNA genome as the template. Then, using this cDNA as a template, the second plus-strand DNA is synthesized. The RT was discovered by Howard Temin and David Baltimore in 1970 and was described as an RNA-directed DNA polymerase. This discovery led to the award of the Nobel Prize in Physiology or Medicine in 1975. By the reverse transcription process, the viral RNA genome is converted into double-stranded DNA. Then, this double-stranded DNA is integrated into the host chromosome and, at this point, is called a provirus. The integrated viral DNA will replicate together with the host genome and be passed on to the progeny cells. Due to the ability of retroviruses to integrate, they are currently used for gene delivery systems and gene therapy.

Classification

Retroviruses are found as exogenous retroviruses and endogenous retroviruses. Exogenous retroviruses are infectious RNA-containing viruses that are able to transmit among their host. Retroviruses are classified into six genera, including *Alpharetroviruses*, *Betaretroviruses*, *Gammaretroviruses*, *Deltaretroviruses*, *Epsilonretroviruses*, *Lentiviruses* and *Spumaviruses*. Retroviruses infect only one specific species or are limited to closely related species, e.g. human immunodeficiency virus (HIV) infects only human and chimpanzee. The classification of retroviruses is shown in table 1 (Weiss, 1996).

Genus	Type species
<i>Alpharetrovirus</i>	ALV, RSV
<i>Betaretrovirus</i>	MMTV
<i>Gammaretrovirus</i>	MLV, FLV
<i>Deltaretrovirus</i>	BLV, HTLV
<i>Epsilonretrovirus</i>	WDSV
<i>Lentivirus</i>	EIAV, FIV, SIV, HIV
<i>Spumavirus</i>	SFV, FFV,

Table1. The genera of retrovirus. ALV: Avian leucosis virus, RSV: Rous sarcoma virus, MMTV: Mouse mammary tumor virus, MLV: Murine leukemia virus, FLV: Feline leukemia virus, BLV: Bovine leukemia virus, HTLV: Human T-lymphotropic virus, WDSV: Walleye dermal sarcoma virus, EIAV: Equine infectious anemia virus, FIV: Feline immunodeficiency virus, SIV: Simian immunodeficiency virus, HIV: Human immunodeficiency virus, SFV: Simian foamy virus, FFV: Feline foamy virus.

Endogenous retroviruses (ERVs) are endogenous viral elements in vertebrate genomes. They are part of vertebrate genome, for example, human ERV (HERV) that comprises up to 5% - 8% of the human genome (Belshaw et al., 2004) or porcine endogenous retroviruses that are a potential zoonotic risk when using porcine tissues and organs in xenotransplantation (Denner, 2016).

Structure

All retroviruses have the basic proviral genome structure 5'-LTR-*gag-pol-env*-LTR-3' (Fig. 1A). The 5'-LTR (long terminal repeat) acts as a promoter that initiates the transcription of the retrovirus, and the transcription is terminated by a polyadenylation signal located in the 3'-LTR. The structural and accessory proteins are expressed by full-length and spliced RNAs. The *gag* of retroviruses encodes the viral matrix (MA), capsid (CA), and nucleocapsid (NC) proteins, and *pol* encodes the viral enzymes (protease, reverse transcriptase, integrase and some viruses encode dUTPase) that are essential for viral replication (Fig. 1B). The *env* portion expresses the viral glycoprotein (Fig. 1B). Retroviruses form particles of around 100–150 nm. The outer viral membrane is derived from the

cell membrane and contains the viral glycoproteins, which are important for viral attachment and entry into the target cells. Two identical copies of the viral single-stranded RNA genome are packaged into particles by interaction with the Gag precursor protein during viral release from the cell. The closed capsid together with the packaged viral proteins and the genome constitute the viral core (Fig. 1B).

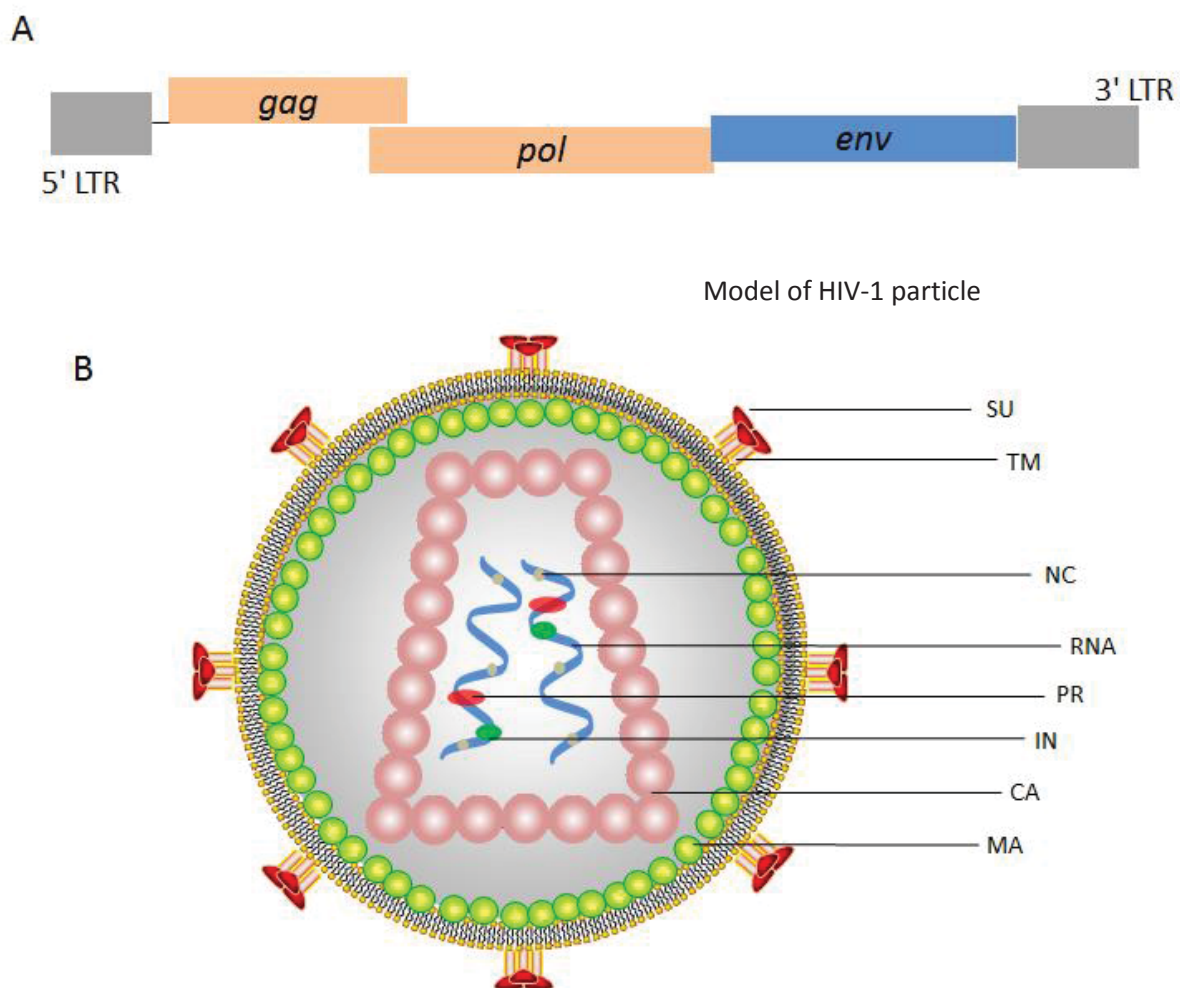


Figure 1: (A) Overview of the genome structure of a simple retrovirus. The 5' and 3' long terminal repeats (LTRs) were shown. The main structural genes: *gag*, *pol* and *env* were represented. **(B) Components of HIV-1 particle.** The *env* of HIV-1 expresses viral surface protein (SU) and transmembrane protein (TM), the *gag* encodes viral matrix (MA), capsid (CA), nucleocapsid (NC) proteins. The *pol* expresses protease (PR), reverse transcriptase (RT) and integrase (IN).

Replication cycle of retroviruses

The replication cycle of retroviruses includes four main steps as follows: viral entry and uncoating; reverse transcription and integration; transcription and splicing; assembly and release.

Viral entry and uncoating

The entry of retroviruses is mediated by the interaction of viral Env with the receptor on the surface of target cells (Fig. 2). Different retroviruses or strains may use distinct cellular receptors (Clapham and McKnight, 2002). For example, HIV-1 utilizes CD4 as its main receptor and CCR5 or CXCR4 as a co-receptor (Clapham and McKnight, 2002), although replication of several HIV-1 strains has been shown to be independent of CD4 (Zerhouni et al., 2004). SIVs have similar receptor utilization. FIV exploits CD134 as its main receptor for viral entry (de Parseval et al., 2004; Shimojima et al., 2004), while the glucose transporter (GLUT1) was recently identified as the receptor for HTLV (Manel et al., 2003). Whether HTLV uses other cell surface molecules as a receptor remains unknown.

The interaction of Env with its receptor/co-receptor, and in some viruses an additional exposure to low pH, induces Env conformational changes, which lead to virus–cell membrane fusion (Blumenthal et al., 2012). The interaction of the viral Env with its receptors is one of the targets for screening inhibitors to block viral replication.

After viral entry, uncoating of the core happens likely in the cytoplasm or near the nuclear membrane (Fig. 2). Currently, little is known about the retroviral uncoating step, but it is predicted to depend on specific cellular factors and ATP (adenosine triphosphate) (Arhel, 2010). It is still controversial where and when

HIV capsids uncoat and the role of reverse transcription in the uncoating remains elusive.

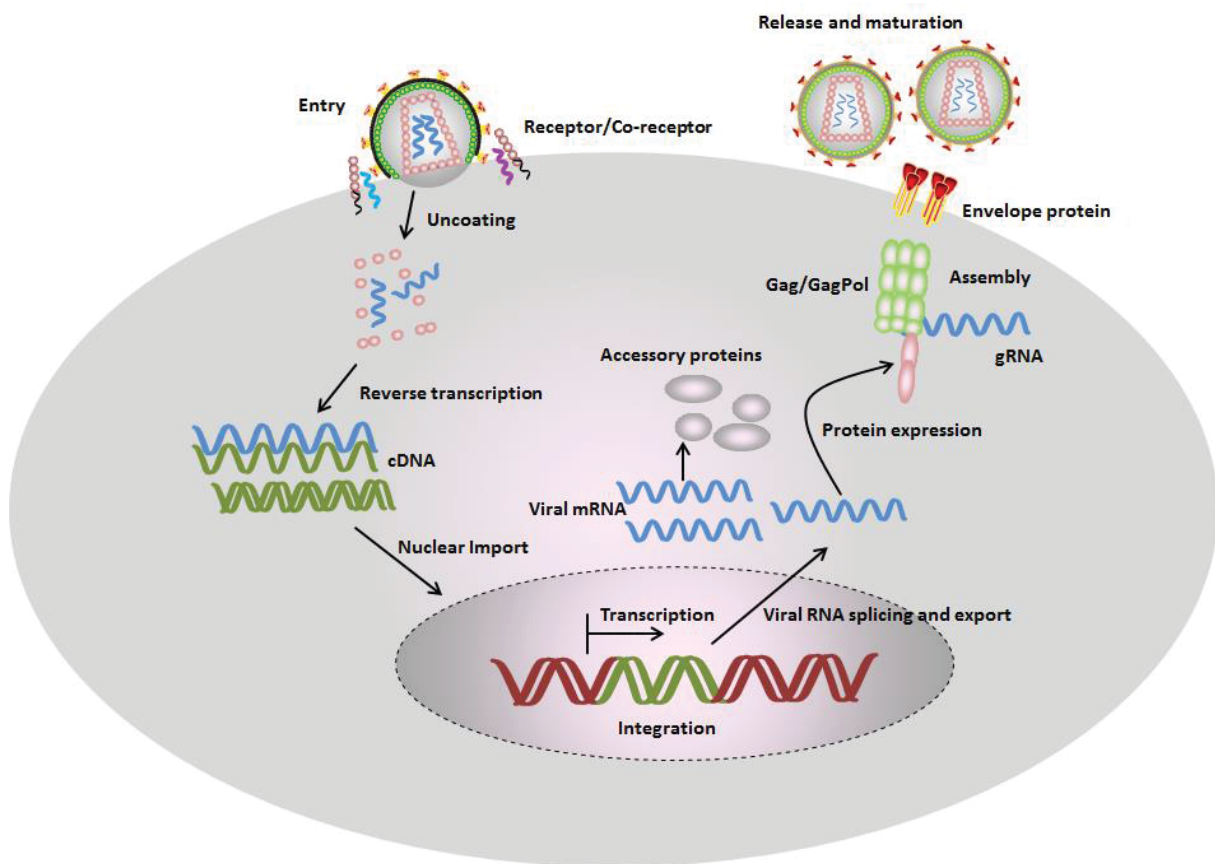


Figure 2: The replication cycle of retroviruses. The main steps are included: viral entry and uncoating; reverse transcription and integration; transcription and splicing; assembly and release.

Reverse transcription and integration

Reverse transcription is the process of generating cDNA from the viral RNA template by the viral reverse transcriptase enzyme. This step is mainly associated with the retroviruses (Fig. 2), but hepatitis B virus (HBV), which is a dsDNA virus, also has the ability to perform reverse transcription (Beck and Nassal, 2007). The retroviral reverse transcriptase has three enzyme activities: (a) RNA-dependent DNA polymerase, which synthesizes the retroviral minus-strand cDNA from the viral plus-strand RNA; (b) RNase H, which catalyzes the

cleavage of RNA in RNA/DNA duplexes; and (c) DNA-dependent DNA polymerase, which synthesizes the plus-strand DNA by using the minus-strand cDNA as the template (Whitcomb and Hughes, 1992). Reverse transcription initiates by annealing a cellular tRNA to the viral primer binding site (PBS) which is used as primer, leading to the synthesis of a short minus-strand DNA containing viral R and U5 sequences. Then, this minus-strand DNA anneals to the 3' end of the viral genome (3' R element) by strand transfer, resulting in the extension of viral minus-strand DNA. Followed by RNA degradation by the viral RNase H, a plus-strand DNA containing U3-R-U5 sequences is synthesized by using (polypurine tract) PPT RNA as the primer, which is not degraded by the viral RNase H. And then this plus-strand DNA anneals to 3' end of minus-strand viral DNA, resulting in the synthesis of viral double-strand DNA (dsDNA) (Fig. 3).

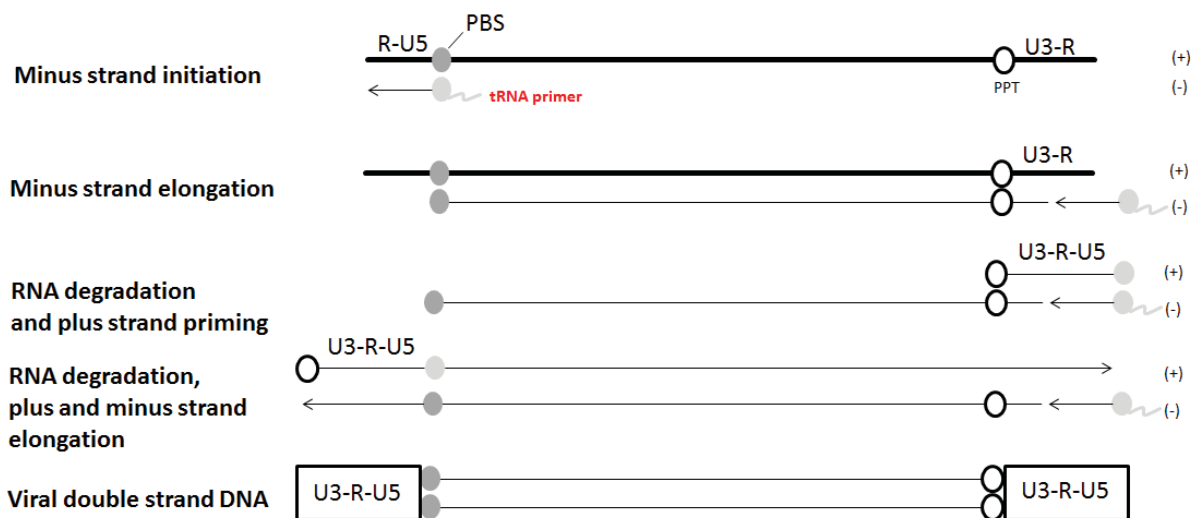


Figure 3: Retroviral reverse transcription. Reverse transcription starts by annealing a cellular tRNA to the viral primer binding site (PBS), leading to the synthesis of a minus-strand DNA. Then, this minus-strand DNA anneals to the 3' end of the viral genome, resulting in the extension of viral minus-strand DNA. Followed by RNA degradation, a plus-strand DNA containing U3-R-U5 sequences is synthesized by using (polypurine tract) PPT RNA as the primer. This plus-strand DNA anneals to 3' end of minus-strand viral DNA, priming the synthesis of viral double-strand DNA (dsDNA). All steps, the DNA synthesis on the RNA

template and the DNA synthesis on the DNA template and the degradation of the viral RNA is mediated by the viral reverse transcriptase/RNase H complex.

After the reverse transcription step, the viral reverse transcription complex (RTC) moves towards the cell nucleus along with the cellular microtubules. During the nuclear import, the retrovirus pre-integration complex (PIC) is formed. The PIC crosses the nuclear membrane and has access to the cell's chromosome before the integrase enzyme induces integration (Lusic and Siliciano, 2017). The retroviral integration is a unique process mediated by the viral integrase enzyme, and regulated by several cellular factors. Simply, we can separate integration as DNA cutting and joining steps. In the first step, also called as 3' end processing, two nucleotides are eliminated from each 3' end of linear viral DNA by viral integrase. In the joining step, each 3' sticky end of viral DNA attacks the phosphodiester bonds of the target DNA, resulting the covalent joining to the target DNA. Finally, the single-strand gaps are repaired by cellular enzymes to finish the integration, which leads to the duplication on the viral target DNA (Craigie and Bushman, 2012).

After integration, the retroviral genome (provirus) replicates together with the cellular chromosomal DNA. Reverse transcription and integration are the signature steps of retroviruses. Many drugs that inhibit reverse transcriptase and integrase have been used in the clinic to counteract the replication of HIV, but it is still impossible to eliminate the provirus DNA due to its integration with the host chromosome DNA. Many research groups are trying to find ways to solve this problem but HIV-1 integration in a quite stable population of resting and long-living blood cells (latency) is the barrier for curing HIV.

Transcription and splicing

Retroviral transcription is driven by the promoter and enhancer located in U3 part of the 5'LTR, and is mediated by cellular RNA polymerase II, which functions for the synthesis of host cellular mRNA and some small nuclear RNAs. During the early HIV-1 replication step, the provirus DNA expresses several multiply spliced mRNAs, including *tat*, *rev*, and *nef*. The export of these mRNAs from nuclear to cytoplasm is Rev-independent. The Tat protein is a 14-kDa nuclear protein that contains around 101 residues encoded by two exons, which acts as a transcriptional *trans-activator*. It can enter the nucleus, bind the LTR, and recruit cellular factors to activate and increase the level of transcription. The binding of HIV-1 Tat to viral LTR recruits several histone acetyltransferases, such as the CREB-binding protein, forming CBP/P300 complex, which induces acetylation of nucleosome, reducing the repression of the LTR promoter (Romani et al., 2010). In addition, the Tat proteins of primate lentiviruses also bind directly to a conserved stable stem-loop located in the 5' end of nascent viral RNAs, referred as TAR, strongly enhancing the LTR-directed viral transcription. Indeed, the binding of Tat to TAR recruits CDK9 and cyclinT1, forming the complex of TEFb. This complex is able to induce the phosphorylation of the CTD of RNA polymerase II, which results in successful synthesis of the full-length viral transcripts (Romani et al., 2010). The Tat protein of HIV-1 promotes a high level of viral transcription and replication and thus Tat is indispensable for HIV-1 (Carrier et al., 1994).

In the presence of Tat, cellular RNA polymerase II, and other factors, the HIV-1 provirus DNA can express many spliced viral pre-mRNAs. These spliced pre-mRNAs are regulated by different splicing acceptors (SA) and splicing donors (SD), which are located in the viral genome (Asang et al., 2008; Stoltzfus and Madsen, 2006). These spliced pre-mRNAs encode HIV-1 structural and accessory proteins, including Env, Vif, Vpu, and Vpr (Frankel and Young, 1998).

The HIV-1 provirus DNA also expresses full-length viral RNA that is used for Gag and Gag-Pol expression and viral genome packaging. The Gag-Pol product is expressed by occasional ribosomal frameshifting, altering the translation from *gag* frame into the adjacent *pol* gene. The full-length HIV-1 RNA and spliced pre-mRNAs are exported to the cytoplasm by the Rev protein (Fischer et al., 1994). Rev is a cytoplasm–nucleus shuttling protein. The localization is determined by two signals in Rev, the nuclear localization signal (NLS) and the nuclear export signal (NES) (Pollard and Malim, 1998). Rev exports the viral RNA by interacting with a highly conserved *cis*-acting sequence (the rev response element - RRE) in the *env* (Pollard and Malim, 1998). Thus, the Rev protein is also essential for HIV-1 replication.

Assembly and release

Retrovirus assembly and release are both mediated by the Gag protein. Gag is sufficient for assembly of immature virus-like-particles (VLP) (Fig. 2). However, production of infectious viral particles requires co-assembly of Gag with Env, the viral genome RNA, and the Gag-Pol precursor protein. Gag contains matrix (MA), capsid (CA), and nucleocapsid (NC) domains, as well as the late domain (L-domain) (Freed, 1998). The MA domain targets Gag to the site of viral assembly and facilitates Gag–membrane binding. The central CA domain mediates the Gag–Gag interaction and homo-oligomerization in an ordered manner during viral assembly and determines the particle morphology. The NC domain contains an RNA-binding domain and enables the packaging of the viral genome and Gag multimerization. The L-domain recruits cellular Endosomal Sorting Complexes Required for Transport (ESCRT) family factors to promote viral budding (Jouvenet et al., 2011; Martin-Serrano et al., 2003). The MA domain also interacts with phosphoinositide in the cellular membrane, which

determines the retroviral assembly sites (Weindel et al., 2010). The type of phosphoinositide and the degree of phosphoinositide binding may vary among different retroviruses and thus different retroviruses have distinct cellular assembly sites. For example, HIV-1 Gag assembly and budding occur predominantly on the plasma membrane (PM) and are mediated by the Gag N-terminal myristoylated MA domain (Jouvenet et al., 2006; Morikawa et al., 2000). EIAV Gag assembly and export are directed by matrix proteins through trans-Golgi networks and cellular vesicles (Zhang et al., 2015).

HIV/SIV and cross-species transmission of lentiviruses

HIV is a lentivirus that infects humans, which results in the acquired immune deficiency syndrome (AIDS). HIV destroys the host immune system and finally the patient is threatened by opportunistic infections or cancer. HIV infects human CD4⁺ T cells, macrophages, and dendritic cells, and the infection leads to the depletion of CD4⁺ T cells by pyroptosis, apoptosis, and other mechanisms. Macrophages and dendritic cells are not killed by HIV and can serve as cells that contribute to the latent viral reservoir. Antiretroviral therapy (ART) is able to control HIV-1 replication although patients need to take the drugs for the rest of their life. Stopping ART leads to a rebound of HIV-1, and the occurrence of drug-resistant HIV-1 may also cause the failure of therapy (Wensing et al., 2017).

The simian immunodeficiency viruses (SIVs) are a diverse group of retroviruses that naturally infect African monkeys (Klatt et al., 2012). Many African monkeys, such as the African green monkey, mangabeys, and mandrills, show infection by SIVs by serological and PCR-based tests (Klatt et al., 2012). Although SIVs are widespread among African monkeys, the infections rarely cause immunodeficiency or disease. Interestingly, Asian macaques can be

artificially infected by an SIV called SIVmac, and this infection may result in macaques' immunodeficiency syndrome, which is similar to human AIDS (Alexander et al., 1999). The SIVmac arose from the cross-species transmission of SIV from sooty mangabeys (SIVsm) (Apetrei et al., 2005). Infecting Asian pigtail macaques by genetically modified HIV-1 causes AIDS in macaques, which provides a good animal model for HIV-1 (Hatzioannou et al., 2014). The genome of SIV contains *LTR*, *gag*, *pol*, and *env*, and also accessory genes *vif*, *vpx*, and *vpr* (Fig. 4). The Vpx protein is unique to some SIVs, including SIVsm and SIVmac. HIV-2, which arose from SIVsm transmission from sooty mangabeys to humans, also contains the Vpx protein. The circulation of SIV in African monkeys can result in viral recombination or mutagenesis, which may cause the occurrence of new accessory proteins (Etienne et al., 2013).

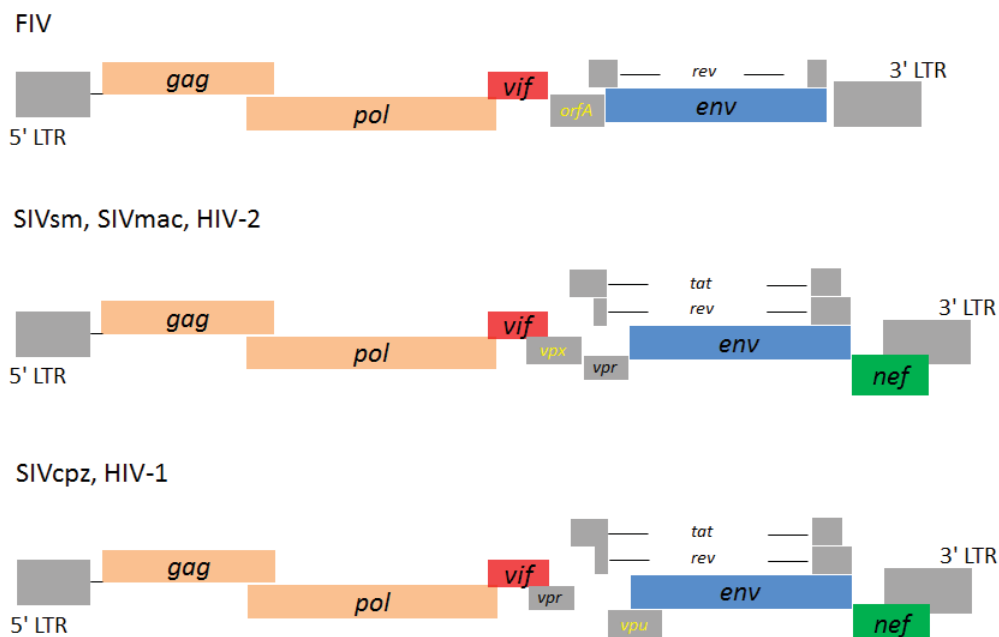


Figure 4: Genome structure of FIV, SIV and HIV. The structural genes (*gag*, *pol* and *env*) of indicated viruses are shown. All indicated viruses contain *vif* genes for counteraction their host APOBEC3. FIV has a unique *orfA* gene that localized between *vif* and *env*. *Vpx* gene presents in SIVsm, SIVmac and HIV-2. SIVcpz and HIV-1 contains *vpu* for overcoming the restriction of their host tetherin. LTR: the 5' and 3' Long terminal repeat containing the promoter/enhancer and the polyadenylation signal.

Chimpanzees (cpz), which are the evolutionarily closest extant primate to *Homo sapiens*, are also infected by SIVcpz (Sharp et al., 2005). The common chimpanzee includes four subspecies, only two of which, *Pan troglodytes troglodytes* (Ptt) and *Pan troglodytes schweinfurthii* (Pts), are infected by SIVcpz (SIVcpzPtt and SIVcpzPts, respectively) (Sharp et al., 2005). Genome analysis of SIVcpz indicates that SIVcpz originates from the cross-species transmission and recombination of three different SIV strains: SIVrcm from the red-capped mangabey (rcm), SIVgsn/mus/mon from the greater-spot-nosed (gsn), mustached (mus), and mona monkeys (mon), respectively, and a currently unidentified SIV (Bailes et al., 2003; Bell and Bedford, 2017; Etienne et al., 2013). It is still controversial to what extent SIVcpz causes AIDS in chimpanzees. However, one recent study showed that SIVcpz-associated immunodeficiency can be effectively treated with antiretroviral therapy (Barbian et al., 2017).

HIV-1 is believed to originate from the cross-species transmission of SIVcpz from chimpanzee to human. HIV-1 M and N groups originated from zoonotic transmission of SIVcpzPtt from west-central Africa (Keele et al., 2006; Van Heuverswyn et al., 2007). Additionally, recent studies indicate that SIVgor from gorillas (gor) is the origin of HIV-1 groups O and P (D'Arc et al., 2015; Takehisa et al., 2009). The HIV-1 M group is the pandemic virus, whereas viruses of groups N and P are only found in a few infected individuals (Plantier et al., 2009). The HIV-1 O group is mainly distributed in west-central Africa and has a low prevalence rate (less than 1% of global HIV-1 infections) (Peeters et al., 1997).

In addition to primate lentiviruses, it was also discovered that non-primate mammals are infected by related lentiviruses, such as FIV infection of domestic cat, BIV infection of cows, MVV infection of sheep. Similar to HIV and SIV, FIV

also contains a *vif* gene for counteraction of the restriction of feline APOBEC3 (Gu et al., 2016; Gu et al., 2017; Münk et al., 2008; Zielonka et al., 2010). However, FIV harbors a unique *orfA* gene that downregulates FIV primary receptor CD134 on the host cell surface and is important for viral infection (Hong et al., 2010) (Fig. 4). Similar to inter-species infections of primate lentiviruses, cross-species transmissions of FIV between several Felidae were observed (Troyer et al., 2008).

Restriction factors

Restriction factors are cell-intrinsic proteins that can potently suppress the replication of lentiviruses. In most cases, the restriction factors are induced by interferons (IFN). Many restriction factors have been identified that can suppress the replication of HIV-1, SIV, and FIV.

They are defined as follows: tripartite motif-containing protein 5 α (TRIM5 α), apolipoprotein B mRNA-editing enzyme, catalytic polypeptide-like 3 (APOBEC3), SAM and HD domain-containing protein 1 (SAMHD1), myxovirus resistance B (MxB), Tetherin, and serine incorporator protein 3/5 (SERINC3/5) (Doyle et al., 2015; Rosa et al., 2015; Usami et al., 2015). Simian TRIM5 α interacts with the HIV-1 capsid and inhibits viral uncoating. APOBEC3s decrease HIV-1 reverse transcription and induce hypermutation of the viral cDNA via the enzyme's cytidine deamination activity. SAMHD1 reduces the cellular dNTP level and inhibits viral reverse transcription. MxB prevents viral nuclear import and integration. Tetherin prevents HIV-1 release from the cell surface. SERINC3/5 can be packaged into viral particles and inhibit viral entry via an Env-dependent mechanism (Fig. 5) (Doyle et al., 2015).

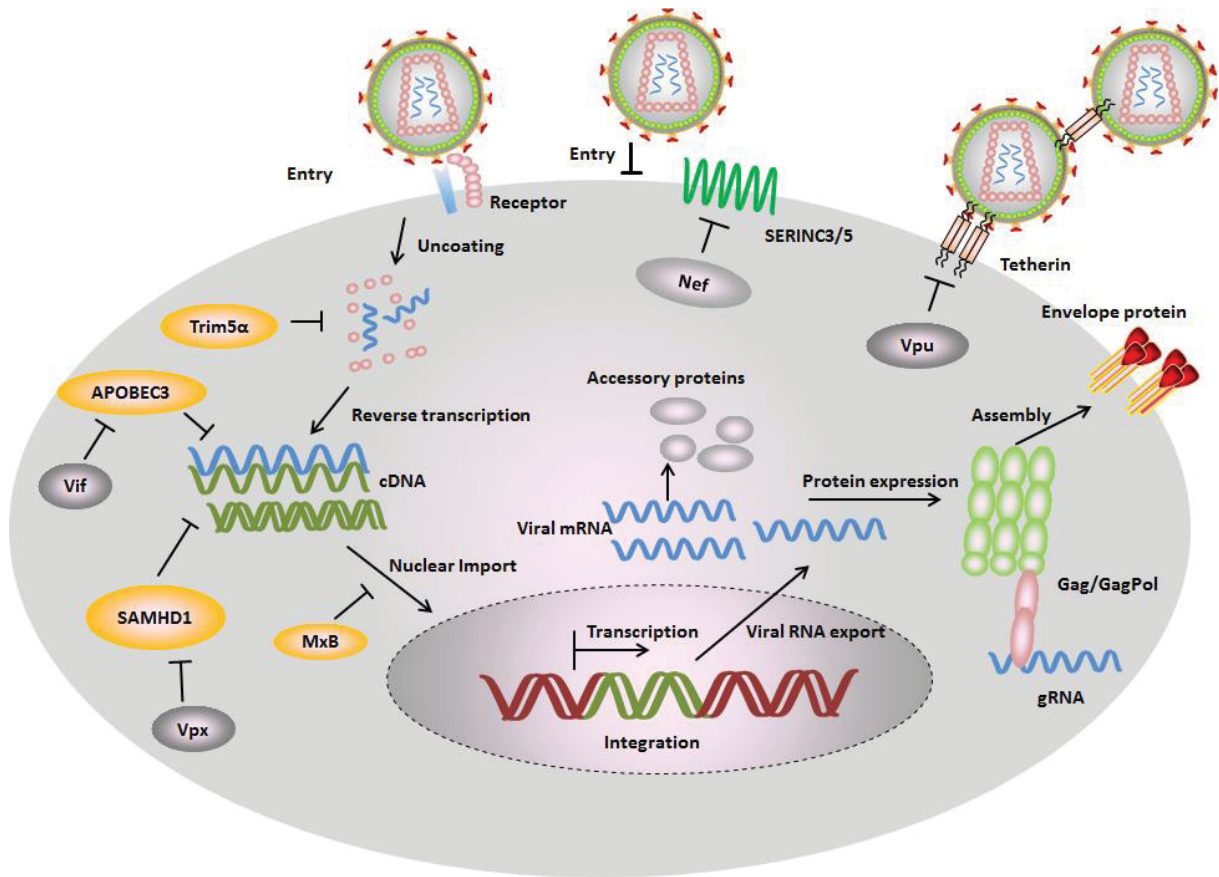


Figure 5: Restriction factors and HIV counteraction mechanisms. In the absence of viral antagonists, several cellular proteins called restriction factors inhibit different stages of the HIV-1 replication. Simian TRIM5 α interacts with HIV-1 capsid and inhibits viral uncoating. APOBEC3s decrease HIV-1 reverse transcription and induce hypermutations of viral cDNA by cytidine deamination. SAMHD1 reduces cellular dNTP level and inhibits viral reverse transcription. MxB prevents viral nuclear import and integration. Tetherin prevents HIV-1 release from cell surface. SERINC3/5 can be packaged into viral particles and inhibit viral entry by an Env-dependent mechanism. The restriction factors are counteracted by HIV-1 encoded proteins. HIV-1 capsid escapes the restriction of human TRIM5 α . HIV-1 Vif interacts with human APOBEC3s and induces their degradation by proteasome pathway. Vpx from SIVmac/smm and HIV-2 induce SAMHD1 degradation. HIV-1 Vpu counteracts the restriction of Tetherin. HIV-1 Nef antagonizes Serinc3/5.

To achieve sufficient lentiviral replication, the lentivirus antagonizes the cellular restriction factors by different mechanisms. Lentiviral Vif proteins directly interact with A3s and recruit them to an E3 ubiquitin ligase complex to induce A3 degradation by the proteasome (Guo et al., 2014; Yu et al., 2003). Similarly, HIV-1 Vpu interacts with Tetherin, preventing Tetherin trafficking to the cell surface and promoting its ubiquitination-mediated degradation (Neil, 2013).

HIV-1 Vpu also counteracts Tetherin by internalization of Tetherin from the cell surface to lysosomes (Neil, 2013). SIV Nef, HIV-2 and EIAV Env are Tetherin antagonists (Jia et al., 2009; Yin et al., 2014). Vpx from SIVmac/sm and HIV-2 induce SAMHD1 degradation by an E3 ubiquitin ligase complex that contains cullin 4A (CUL4A), DNA damage-binding protein (DDB1), and DDB1–CUL4-associated factor 1 (DCAF1) (Hrecka et al., 2011; Laguette et al., 2011). However, it remains unknown how HIV-1 escapes the restriction of SAMHD1 and subsequently achieves latency in myeloid cells. Nef of HIV-1 and SIV counteract SERINC3/5 by preventing packaging into viral particles (Fig. 5) (Rosa et al., 2015; Usami et al., 2015).

Studies on host restriction factors provide greater understanding not only of the lentivirus lifecycle but also the evolution of lentiviruses and lentivirus cross-species transmission. Studies on the interactions between viral proteins and host restriction factors also provide new targets for screening anti-viral inhibitors.

APOBEC3 and Vif

APOBEC3 inhibits lentivirus

The cellular restriction factors of the APOBEC3 (A3) family of DNA cytidine deaminases are an important arm of the innate immune defense system which can potentially serve as a barrier to lentiviral cross-species transmissions. Human A3s include seven genes that contain either one (A3A, A3C, and A3H) or two (A3B, A3D, A3F, and A3G) zinc (Z)-binding domains with the conserved motifs of HXE(X)23-28CXXC (X can be any residue) (Fig. 6) (LaRue et al., 2009). This Z domain includes three distinct phylogenetic clusters that named as Z1, Z2 and Z3, respectively (Fig. 6A).

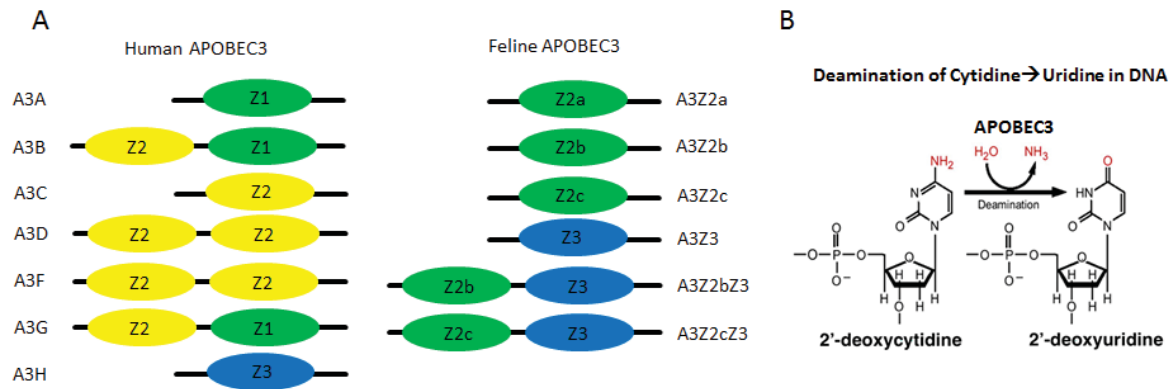


Figure 6: Human and Feline *APOBEC3* gene and APOBEC3 cytidine deamination activity. (A) Human A3 genes encode A3A, A3B, A3C, A3D, A3F, A3G and A3H. Domestic cat encodes A3Z2a, A3Z2b, A3Z2c and A3Z3. It also expresses A3Z2bZ3 and A3Z2cZ3 by read-through transcription and mRNA selective splicing. (B) A schematic of the single-stranded DNA cytidine deamination reaction catalyzed by APOBEC family members.

Among these seven genes, A3D, A3F, A3G and A3H inhibit HIV-1 Δ vif replication by deamination of cytidines in the viral single-strand DNA that is formed during reverse transcription, thereby introducing G-to-A hypermutations in the coding strand (Fig. 6B and 7). Additionally, some A3s inhibit virus replication by deaminase-independent mechanisms affecting reverse transcription and integration steps (Harris and Dudley, 2015) (Fig. 7). The domestic cat encodes three single-domain A3Z2s (A3Z2a - A3Z2c) and one A3Z3 protein as well as double domain A3Z2Z3 proteins by read-through transcription and mRNA alternative splicing (Münk et al., 2008; Zhang et al., 2016) (Fig. 6A). Previous studies demonstrated that feline A3Z3 and A3Z2Z3, but not A3Z2s, inhibit FIV Δ vif (Zielonka et al., 2010).

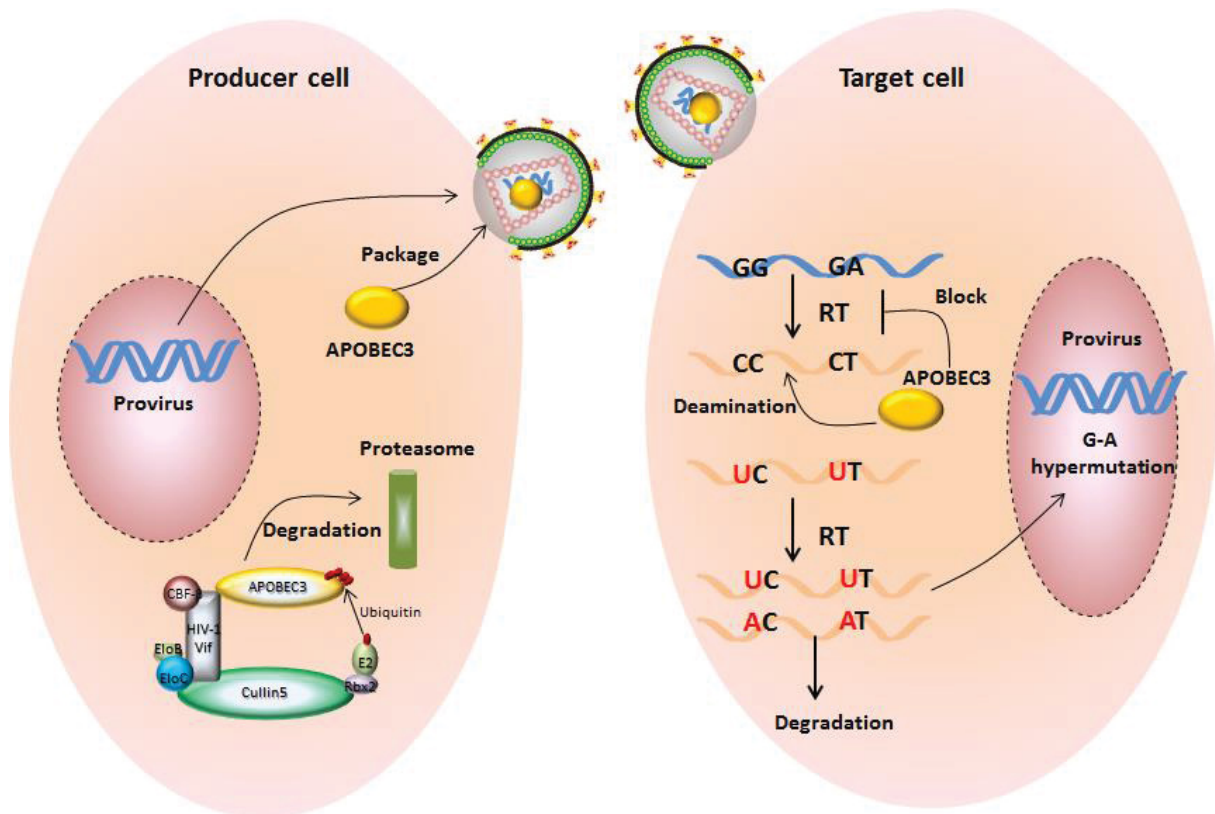


Figure 7: The mechanism of APOBEC3 inhibiting retrovirus. In the producer cell, APOBEC3 is packaged into viral particles and delivered to the next target cell when Vif is absent. During viral reverse transcription, APOBEC3 catalyzed deoxycytidine into deoxyuridine in single-stranded DNA. In the synthesis of viral next strand DNA, it will produce many G-A hypermutations. This viral genome with G-A mutations will be destroyed by some cellular enzymes. However, in the presence of Vif, Vif directly interacts with APOBEC3 and induces its degradation by proteasome pathway.

Recently, the structures of human APOBEC3 catalytic domains have been resolved. In figure 8, the X-ray structures of hA3C (Kitamura et al., 2012) and hA3H are shown, and they illustrate the A3 family's structural hallmarks. Each catalytic domain has an overall structure comprised of five β -strands and six α -helices. The β -strands form a hydrophobic β -sheet core, and this core is surrounded by six α -helices. The loops between β -strands and α -helices have variability of conformation and length. These loops may have essential roles in nucleic acids binding. Based the current human A3 structures, we can perform homology modelling for non-human A3s (Zhang et al., 2016).

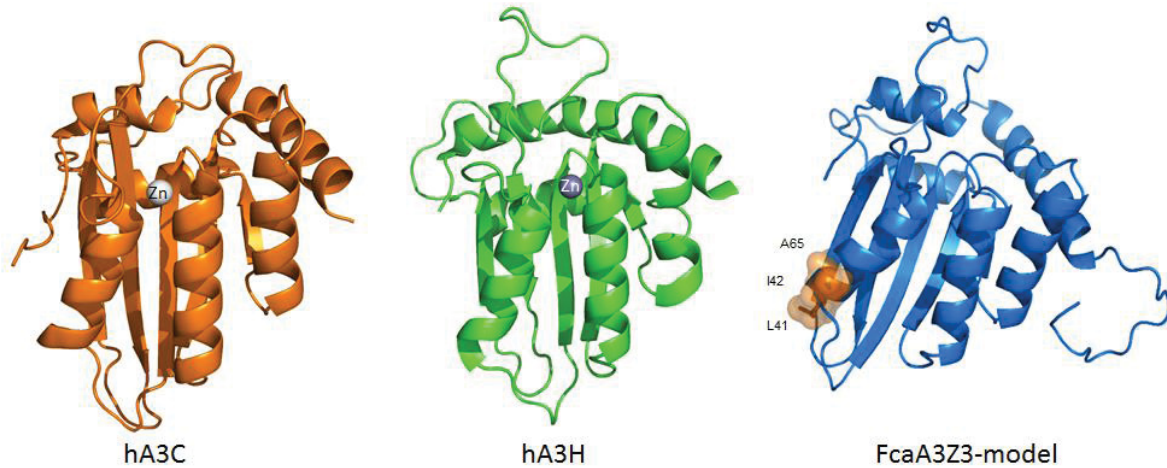


Figure 8: The structure of human A3C, A3H and a homology model of FcaA3Z3. The hA3C (3VOW) and hA3H (6B0B) are shown by ribbon presentation. The zinc-coordinating active sites of hA3C and hA3H are shown. The homology model of FcaA3Z3 is presented by blue. The essential sites of FcaA3Z3 that interact with FIV Vif are shown.

Vif counteraction of APOBEC3

To counteract the antiviral functions of A3, all lentiviruses except the equine infectious anemia virus encode the virion infectivity factor (Vif) that interacts with cognate A3 proteins and then recruit them to an E3 ubiquitin ligase complex containing Cullin5 (CUL5), Elongin B/C (ELOB/C), RING-box protein RBX2 and CBF β to induce degradation of the bound A3s by the proteasome (Fig. 9) (Guo et al., 2014; Yu et al., 2003).

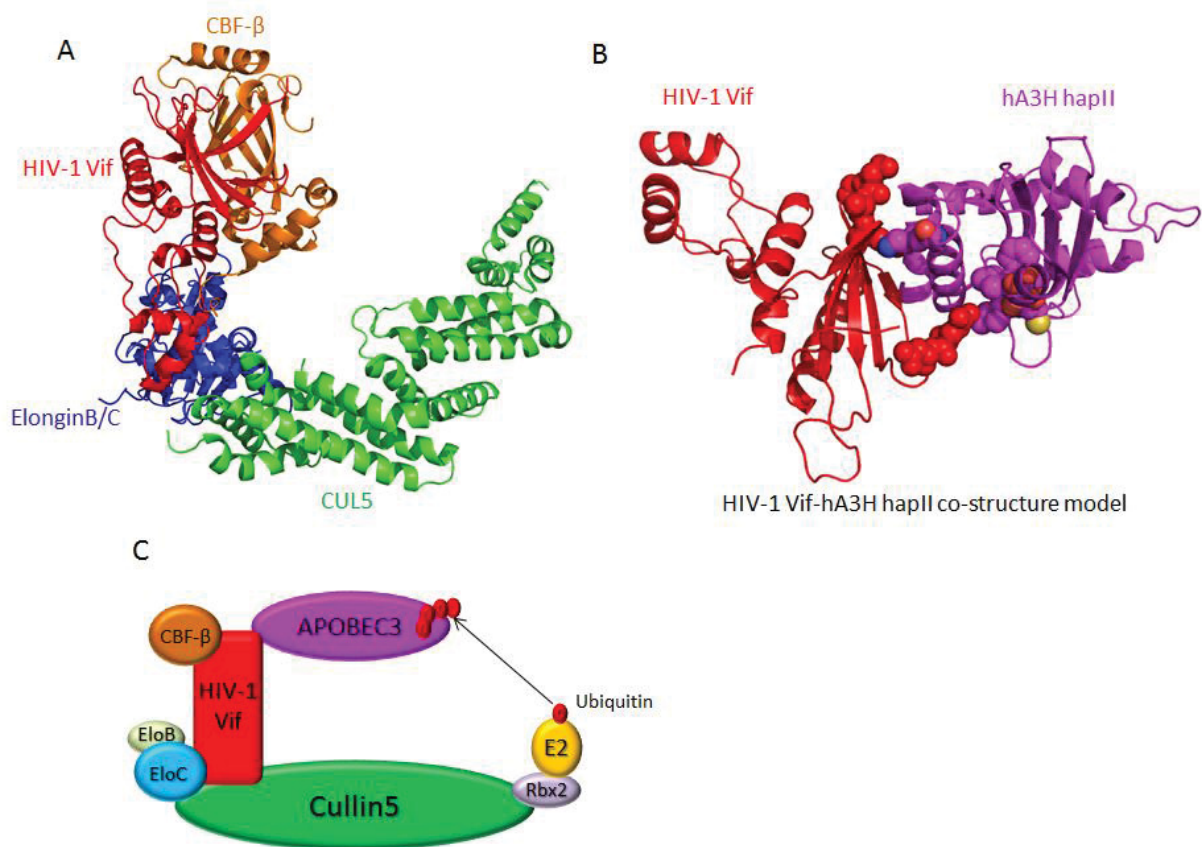


Figure 9: Structure basis of HIV-1 Vif E3 ubiquitination complex. (A) Overall structure of HIV-1 Vif-CBF-β-CUL5-ElonginB/C. Distinct colors indicate different proteins. (B) The HIV-1 Vif-hA3H hapII co-structure model. The interaction sites are indicated by spheres. (C) Cartoon presentation of HIV-1 Vif-APOBEC3 E3 ubiquitination complex.

However, the Vif-E3 complex also differs. For example, HIV-1 and SIV Vifs need the cofactor CBF-β to stabilize this complex (Fig. 9) (Kane et al., 2015), whereas FIV and other non-primate lentiviruses (e.g. maedi-visna virus (MVV), caprine arthritis encephalitis virus (CAEV) and bovine immunodeficiency virus (BIV)) Vifs do not require CBF-β. A recent study demonstrated that BIV Vif appears to operate independently of any cofactors, while MVV Vif hijacks cellular cyclophilin A (CYPA) as a cofactor. Whether FIV Vif recruits any additional protein is unclear (Kane et al., 2015).

References

- Alexander, L., Du, Z., Howe, A.Y., Czajak, S., and Desrosiers, R.C. (1999). Induction of AIDS in rhesus monkeys by a recombinant simian immunodeficiency virus expressing nef of human immunodeficiency virus type 1. *Journal of virology* 73, 5814-5825.
- Apetrei, C., Kaur, A., Lerche, N.W., Metzger, M., Pandrea, I., Hardcastle, J., Falkenstein, S., Bohm, R., Koehler, J., Traina-Dorge, V., *et al.* (2005). Molecular epidemiology of simian immunodeficiency virus SIVsm in U.S. primate centers unravels the origin of SIVmac and SIVstm. *Journal of virology* 79, 8991-9005.
- Arhel, N. (2010). Revisiting HIV-1 uncoating. *Retrovirology* 7, 96.
- Asang, C., Hauber, I., and Schaal, H. (2008). Insights into the selective activation of alternatively used splice acceptors by the human immunodeficiency virus type-1 bidirectional splicing enhancer. *Nucleic acids research* 36, 1450-1463.
- Bailes, E., Gao, F., Bibollet-Ruche, F., Courgnaud, V., Peeters, M., Marx, P.A., Hahn, B.H., and Sharp, P.M. (2003). Hybrid origin of SIV in chimpanzees. *Science* 300, 1713.
- Barbian, H.J., Jackson-Jewett, R., Brown, C.S., Bibollet-Ruche, F., Learn, G.H., Decker, T., Kreider, E.F., Li, Y., Denny, T.N., Sharp, P.M., *et al.* (2017). Effective treatment of SIVcpz-induced immunodeficiency in a captive western chimpanzee. *Retrovirology* 14, 35.
- Beck, J., and Nassal, M. (2007). Hepatitis B virus replication. *World journal of gastroenterology* 13, 48-64.
- Bell, S.M., and Bedford, T. (2017). Modern-day SIV viral diversity generated by extensive recombination and cross-species transmission. *PLoS pathogens* 13, e1006466.
- Belshaw, R., Pereira, V., Katzourakis, A., Talbot, G., Paces, J., Burt, A., and Tristem, M. (2004). Long-term reinfection of the human genome by endogenous retroviruses. *Proceedings of the National Academy of Sciences of the United States of America* 101, 4894-4899.
- Blumenthal, R., Durell, S., and Viard, M. (2012). HIV entry and envelope glycoprotein-mediated fusion. *The Journal of biological chemistry* 287, 40841-40849.
- Carrier, F., Gatignol, A., Hollander, M.C., Jeang, K.T., and Fornace, A.J., Jr. (1994). Induction of RNA-binding proteins in mammalian cells by DNA-damaging agents. *Proceedings of the National Academy of Sciences of the United States of America* 91, 1554-1558.
- Clapham, P.R., and McKnight, A. (2002). Cell surface receptors, virus entry and tropism of primate lentiviruses. *The Journal of general virology* 83, 1809-1829.
- Craigie, R., and Bushman, F.D. (2012). HIV DNA integration. *Cold Spring Harbor perspectives in medicine* 2, a006890.
- D'Arc, M., Ayoub, A., Esteban, A., Learn, G.H., Boue, V., Liegeois, F., Etienne, L., Tagg, N., Leendertz, F.H., Boesch, C., *et al.* (2015). Origin of the HIV-1 group O epidemic in western lowland gorillas. *Proceedings of the National Academy of Sciences of the United States of America* 112, E1343-1352.
- de Parseval, A., Chatterji, U., Sun, P., and Elder, J.H. (2004). Feline immunodeficiency virus targets activated CD4+ T cells by using CD134 as a binding receptor. *Proceedings of the National Academy of Sciences of the United States of America* 101, 13044-13049.
- Denner, J. (2016). How Active Are Porcine Endogenous Retroviruses (PERVs)? *Viruses* 8.
- Doyle, T., Goujon, C., and Malim, M.H. (2015). HIV-1 and interferons: who's interfering with whom? *Nature reviews Microbiology* 13, 403-413.
- Etienne, L., Hahn, B.H., Sharp, P.M., Matsen, F.A., and Emerman, M. (2013). Gene loss and adaptation to hominids underlie the ancient origin of HIV-1. *Cell host & microbe* 14, 85-92.
- Fischer, U., Meyer, S., Teufel, M., Heckel, C., Luhrmann, R., and Rautmann, G. (1994). Evidence that HIV-1 Rev directly promotes the nuclear export of unspliced RNA. *The EMBO journal* 13, 4105-4112.
- Frankel, A.D., and Young, J.A. (1998). HIV-1: fifteen proteins and an RNA. *Annual review of biochemistry* 67, 1-25.
- Freed, E.O. (1998). HIV-1 gag proteins: diverse functions in the virus life cycle. *Virology* 251, 1-15.

Gu, Q., Zhang, Z., Cano Ortiz, L., Franco, A.C., Häussinger, D., and Münk, C. (2016). Feline Immunodeficiency Virus Vif N-Terminal Residues Selectively Counteract Feline APOBEC3s. *Journal of virology* **90**, 10545-10557.

Gu, Q., Zhang, Z., Gertzen, C.G.W., Häussinger, D., Gohlke, H., and Münk, C. (2017). Identification of a conserved interface of HIV-1 and FIV Vifs with Cullin 5. *Journal of virology*.

Guo, Y., Dong, L., Qiu, X., Wang, Y., Zhang, B., Liu, H., Yu, Y., Zang, Y., Yang, M., and Huang, Z. (2014). Structural basis for hijacking CBF-beta and CUL5 E3 ligase complex by HIV-1 Vif. *Nature* **505**, 229-233.

Harris, R.S., and Dudley, J.P. (2015). APOBECs and virus restriction. *Virology* **479-480**, 131-145.

Hatzioannou, T., Del Prete, G.Q., Keele, B.F., Estes, J.D., McNatt, M.W., Bitzegeio, J., Raymond, A., Rodriguez, A., Schmidt, F., Mac Trubey, C., *et al.* (2014). HIV-1-induced AIDS in monkeys. *Science* **344**, 1401-1405.

Hong, Y., Fink, E., Hu, Q.Y., Kiosses, W.B., and Elder, J.H. (2010). OrfA downregulates feline immunodeficiency virus primary receptor CD134 on the host cell surface and is important in viral infection. *Journal of virology* **84**, 7225-7232.

Hrecka, K., Hao, C., Gierszewska, M., Swanson, S.K., Kesik-Brodacka, M., Srivastava, S., Florens, L., Washburn, M.P., and Skowronski, J. (2011). Vpx relieves inhibition of HIV-1 infection of macrophages mediated by the SAMHD1 protein. *Nature* **474**, 658-661.

Jia, B., Serra-Moreno, R., Neidermyer, W., Rahmberg, A., Mackey, J., Fofana, I.B., Johnson, W.E., Westmoreland, S., and Evans, D.T. (2009). Species-specific activity of SIV Nef and HIV-1 Vpu in overcoming restriction by tetherin/BST2. *PLoS pathogens* **5**, e1000429.

Jouvenet, N., Neil, S.J., Bess, C., Johnson, M.C., Virgen, C.A., Simon, S.M., and Bieniasz, P.D. (2006). Plasma membrane is the site of productive HIV-1 particle assembly. *PLoS biology* **4**, e435.

Jouvenet, N., Simon, S.M., and Bieniasz, P.D. (2011). Visualizing HIV-1 assembly. *Journal of molecular biology* **410**, 501-511.

Kane, J.R., Stanley, D.J., Hultquist, J.F., Johnson, J.R., Mietrach, N., Binning, J.M., Jonsson, S.R., Barelier, S., Newton, B.W., Johnson, T.L., *et al.* (2015). Lineage-Specific Viral Hijacking of Non-canonical E3 Ubiquitin Ligase Cofactors in the Evolution of Vif Anti-APOBEC3 Activity. *Cell reports* **11**, 1236-1250.

Keele, B.F., Van Heuverswyn, F., Li, Y., Bailes, E., Takehisa, J., Santiago, M.L., Bibollet-Ruche, F., Chen, Y., Wain, L.V., Liegeois, F., *et al.* (2006). Chimpanzee reservoirs of pandemic and nonpandemic HIV-1. *Science* **313**, 523-526.

Kitamura, S., Ode, H., Nakashima, M., Imahashi, M., Naganawa, Y., Kurosawa, T., Yokomaku, Y., Yamane, T., Watanabe, N., Suzuki, A., *et al.* (2012). The APOBEC3C crystal structure and the interface for HIV-1 Vif binding. *Nature structural & molecular biology* **19**, 1005-1010.

Klatt, N.R., Silvestri, G., and Hirsch, V. (2012). Nonpathogenic simian immunodeficiency virus infections. *Cold Spring Harbor perspectives in medicine* **2**, a007153.

Laguet, N., Sobhian, B., Casartelli, N., Ringard, M., Chable-Bessia, C., Segéral, E., Yatim, A., Emiliani, S., Schwartz, O., and Benkirane, M. (2011). SAMHD1 is the dendritic- and myeloid-cell-specific HIV-1 restriction factor counteracted by Vpx. *Nature* **474**, 654-657.

LaRue, R.S., Andresdottir, V., Blanchard, Y., Conticello, S.G., Derse, D., Emerman, M., Greene, W.C., Jonsson, S.R., Landau, N.R., Löchelt, M., *et al.* (2009). Guidelines for naming nonprimate APOBEC3 genes and proteins. *Journal of virology* **83**, 494-497.

Lusic, M., and Siliciano, R.F. (2017). Nuclear landscape of HIV-1 infection and integration. *Nature reviews Microbiology* **15**, 69-82.

Manel, N., Kim, F.J., Kinet, S., Taylor, N., Sitbon, M., and Battini, J.L. (2003). The ubiquitous glucose transporter GLUT-1 is a receptor for HTLV. *Cell* **115**, 449-459.

Martin-Serrano, J., Zang, T., and Bieniasz, P.D. (2003). Role of ESCRT-I in retroviral budding. *Journal of virology* **77**, 4794-4804.

Morikawa, Y., Hockley, D.J., Nermut, M.V., and Jones, I.M. (2000). Roles of matrix, p2, and N-terminal myristoylation in human immunodeficiency virus type 1 Gag assembly. *Journal of virology* **74**, 16-23.

Münk, C., Beck, T., Zielonka, J., Hotz-Wagenblatt, A., Chareza, S., Battenberg, M., Thielebein, J., Cichutek, K., Bravo, I.G., O'Brien, S.J., *et al.* (2008). Functions, structure, and read-through alternative splicing of feline APOBEC3 genes. *Genome biology* **9**, R48.

Neil, S.J. (2013). The antiviral activities of tetherin. *Current topics in microbiology and immunology* 371, 67-104.

Peeters, M., Gueye, A., Mboup, S., Bibollet-Ruche, F., Ekaza, E., Mulanga, C., Ouedrago, R., Gandji, R., Mpele, P., Dibanga, G., *et al.* (1997). Geographical distribution of HIV-1 group O viruses in Africa. *Aids* 11, 493-498.

Plantier, J.C., Leoz, M., Dickerson, J.E., De Oliveira, F., Cordonnier, F., Lemee, V., Damond, F., Robertson, D.L., and Simon, F. (2009). A new human immunodeficiency virus derived from gorillas. *Nature medicine* 15, 871-872.

Pollard, V.W., and Malim, M.H. (1998). The HIV-1 Rev protein. *Annual review of microbiology* 52, 491-532.

Romani, B., Engelbrecht, S., and Glashoff, R.H. (2010). Functions of Tat: the versatile protein of human immunodeficiency virus type 1. *The Journal of general virology* 91, 1-12.

Rosa, A., Chande, A., Ziglio, S., De Sanctis, V., Bertorelli, R., Goh, S.L., McCauley, S.M., Nowosielska, A., Antonarakis, S.E., Luban, J., *et al.* (2015). HIV-1 Nef promotes infection by excluding SERINC5 from virion incorporation. *Nature* 526, 212-217.

Sharp, P.M., Shaw, G.M., and Hahn, B.H. (2005). Simian immunodeficiency virus infection of chimpanzees. *Journal of virology* 79, 3891-3902.

Shimojima, M., Miyazawa, T., Ikeda, Y., McMonagle, E.L., Haining, H., Akashi, H., Takeuchi, Y., Hosie, M.J., and Willett, B.J. (2004). Use of CD134 as a primary receptor by the feline immunodeficiency virus. *Science* 303, 1192-1195.

Stoltzfus, C.M., and Madsen, J.M. (2006). Role of viral splicing elements and cellular RNA binding proteins in regulation of HIV-1 alternative RNA splicing. *Current HIV research* 4, 43-55.

Takehisa, J., Kraus, M.H., Ayoub, A., Bailes, E., Van Heuverswyn, F., Decker, J.M., Li, Y., Rudicell, R.S., Learn, G.H., Neel, C., *et al.* (2009). Origin and biology of simian immunodeficiency virus in wild-living western gorillas. *Journal of virology* 83, 1635-1648.

Troyer, J.L., Vandewoude, S., Pecon-Slaterry, J., McIntosh, C., Franklin, S., Antunes, A., Johnson, W., and O'Brien, S.J. (2008). FIV cross-species transmission: an evolutionary perspective. *Veterinary immunology and immunopathology* 123, 159-166.

Usami, Y., Wu, Y., and Gottlinger, H.G. (2015). SERINC3 and SERINC5 restrict HIV-1 infectivity and are counteracted by Nef. *Nature* 526, 218-223.

Van Heuverswyn, F., Li, Y., Bailes, E., Neel, C., Lafay, B., Keele, B.F., Shaw, K.S., Takehisa, J., Kraus, M.H., Loul, S., *et al.* (2007). Genetic diversity and phylogeographic clustering of SIVcpzPtt in wild chimpanzees in Cameroon. *Virology* 368, 155-171.

Weindel, S., Schmidt, R., Rammelt, S., Claes, L., v Campe, A., and Rein, S. (2010). Subtalar instability: a biomechanical cadaver study. *Archives of orthopaedic and trauma surgery* 130, 313-319.

Weiss, R.A. (1996). Retrovirus classification and cell interactions. *The Journal of antimicrobial chemotherapy* 37 Suppl B, 1-11.

Wensing, A.M., Calvez, V., Gunthard, H.F., Johnson, V.A., Paredes, R., Pillay, D., Shafer, R.W., and Richman, D.D. (2017). 2017 Update of the Drug Resistance Mutations in HIV-1. *Topics in antiviral medicine* 24, 132-133.

Whitcomb, J.M., and Hughes, S.H. (1992). Retroviral reverse transcription and integration: progress and problems. *Annual review of cell biology* 8, 275-306.

Yin, X., Hu, Z., Gu, Q., Wu, X., Zheng, Y.H., Wei, P., and Wang, X. (2014). Equine tetherin blocks retrovirus release and its activity is antagonized by equine infectious anemia virus envelope protein. *Journal of virology* 88, 1259-1270.

Yu, X., Yu, Y., Liu, B., Luo, K., Kong, W., Mao, P., and Yu, X.F. (2003). Induction of APOBEC3G ubiquitination and degradation by an HIV-1 Vif-Cul5-SCF complex. *Science* 302, 1056-1060.

Zerhouni, B., Nelson, J.A., and Saha, K. (2004). Isolation of CD4-independent primary human immunodeficiency virus type 1 isolates that are syncytium inducing and acutely cytopathic for CD8+ lymphocytes. *Journal of virology* 78, 1243-1255.

Zhang, Z., Gu, Q., Jaguva Vasudevan, A.A., Hain, A., Kloke, B.P., Hasheminasab, S., Mulnaes, D., Sato, K., Cichutek, K., Häussinger, D., *et al.* (2016). Determinants of FIV and HIV Vif sensitivity of feline APOBEC3 restriction factors. *Retrovirology* 13, 46.

Zhang, Z., Ma, J., Zhang, X., Su, C., Yao, Q.C., and Wang, X. (2015). Equine Infectious Anemia Virus Gag Assembly and Export Are Directed by Matrix Protein through trans-Golgi Networks and Cellular Vesicles. *Journal of virology* 90, 1824-1838.

Zielonka, J., Marino, D., Hofmann, H., Yuhki, N., Löchelt, M., and Münk, C. (2010). Vif of feline immunodeficiency virus from domestic cats protects against APOBEC3 restriction factors from many felids. *Journal of virology* 84, 7312-7324.

Chapter I

Vif Proteins from Diverse Human Immunodeficiency Virus/Simian Immunodeficiency Virus Lineages Have Distinct Binding Sites in A3C

This work was published in the Journal of Virology.

Zhang Z*, Gu Q*, Jaguva Vasudevan AA, Jeyaraj M, Schmidt S, Zielonka J, Perkovic M, Heckel JO, Cichutek K, Häussinger D, Smits SH, Münk C. 2016. Vif Proteins from Diverse Human Immunodeficiency Virus/Simian Immunodeficiency Virus Lineages Have Distinct Binding Sites in A3C. *Journal of virology* **90**:10193-10208.

* contributed equally to this work.

Zeli Zhang's contribution to this work:

Z. Z. performed the experiments in Fig 1; Fig 2; Fig 4; Fig 5; Fig 6; Fig 7B; Fig 8E and Fig 9B, D.

Z. Z. wrote the draft of the manuscript.



AMERICAN
SOCIETY FOR
MICROBIOLOGY

Title: Vif Proteins from Diverse Human Immunodeficiency Virus/Simian Immunodeficiency Virus Lineages Have Distinct Binding Sites in A3C

Author: Zeli Zhang, Qinyong Gu, Ananda Ayyappan Jaguva Vasudevan et al.

Publication: Journal of Virology

Publisher: American Society for Microbiology

Date: Nov 15, 2016

Copyright © 2016, American Society for Microbiology

LOGIN

If you're a [copyright.com](#) user, you can login to RightsLink using your copyright.com credentials. Already a [RightsLink](#) user or want to [learn more?](#)

Permissions Request

Authors in ASM journals retain the right to republish discrete portions of his/her article in any other publication (including print, CD-ROM, and other electronic formats) of which he or she is author or editor, provided that proper credit is given to the original ASM publication. ASM authors also retain the right to reuse the full article in his/her dissertation or thesis. For a full list of author rights, please see: http://journals.asm.org/site/misc/ASM_Author_Statement.xhtml

BACK

CLOSE WINDOW

Copyright © 2017 [Copyright Clearance Center, Inc.](#) All Rights Reserved. [Privacy statement](#). [Terms and Conditions](#).

Comments? We would like to hear from you. E-mail us at customercare@copyright.com

Vif Proteins from Diverse Human Immunodeficiency Virus/Simian Immunodeficiency Virus Lineages Have Distinct Binding Sites in A3C

Zeli Zhang,^a Qinyong Gu,^a Ananda Ayyappan Jaguva Vasudevan,^a Manimehalai Jeyaraj,^a Stanislaw Schmidt,^{b*} Jörg Zielonka,^{a*} Mario Perković,^{a,b*} Jens-Ove Heckel,^c Klaus Cichutek,^b Dieter Häussinger,^a Sander H. J. Smits,^d Carsten Münk^a

Clinic for Gastroenterology, Hepatology, and Infectiology, Medical Faculty, Heinrich-Heine-Universität Düsseldorf, Düsseldorf, Germany^a; Department of Medical Biotechnology, Paul-Ehrlich-Institut, Langen, Germany^b; Zoo Landau in der Pfalz, Landau in der Pfalz, Germany^c; Institute of Biochemistry, Heinrich-Heine-Universität Düsseldorf, Düsseldorf, Germany^d

ABSTRACT

Lentiviruses have evolved the Vif protein to counteract APOBEC3 (A3) restriction factors by targeting them for proteasomal degradation. Previous studies have identified important residues in the interface of human immunodeficiency virus type 1 (HIV-1) Vif and human APOBEC3C (hA3C) or human APOBEC3F (hA3F). However, the interaction between primate A3C proteins and HIV-1 Vif or natural HIV-1 Vif variants is still poorly understood. Here, we report that HIV-1 Vif is inactive against A3Cs of rhesus macaques (rhA3C), sooty mangabey monkeys (smmA3C), and African green monkeys (agmA3C), while HIV-2, African green monkey simian immunodeficiency virus (SIVagm), and SIVmac Vif proteins efficiently mediate the depletion of all tested A3Cs. We identified that residues N/H130 and Q133 in rhA3C and smmA3C are determinants for this HIV-1 Vif-triggered counteraction. We also found that the HIV-1 Vif interaction sites in helix 4 of hA3C and hA3F differ. Vif alleles from diverse HIV-1 subtypes were tested for degradation activities related to hA3C. The subtype F-1 Vif was identified to be inactive for degradation of hA3C and hA3F. The residues that determined F-1 Vif inactivity in the degradation of A3C/A3F were located in the C-terminal region (K167 and D182). Structural analysis of F-1 Vif revealed that impairing the internal salt bridge of E171-K167 restored reduction capacities to A3C/A3F. Furthermore, we found that D101 could also form an internal interaction with K167. Replacing D101 with glycine and R167 with lysine in NL4-3 Vif impaired its counteractivity to A3F and A3C. This finding indicates that internal interactions outside the A3 binding region in HIV-1 Vif influence the capacity to induce degradation of A3C/A3F.

IMPORTANCE

The APOBEC3 restriction factors can serve as potential barriers to lentiviral cross-species transmissions. Vif proteins from lentiviruses counteract APOBEC3 by proteasomal degradation. In this study, we found that monkey-derived A3C, rhA3C and smmA3C, were resistant to HIV-1 Vif. This was determined by A3C residues N/H130 and Q133. However, HIV-2, SIVagm, and SIVmac Vif proteins were found to be able to mediate the depletion of all tested primate A3C proteins. In addition, we identified a natural HIV-1 Vif (F-1 Vif) that was inactive in the degradation of hA3C/hA3F. Here, we provide for the first time a model that explains how an internal salt bridge of E171-K167-D101 influences Vif-mediated degradation of hA3C/hA3F. This finding provides a novel way to develop HIV-1 inhibitors by targeting the internal interactions of the Vif protein.

Simian immunodeficiency virus (SIV) naturally infects many Old World primate species in Africa. The pandemic of human immunodeficiency virus (HIV) originated from cross-species transmission events of SIVs to humans. HIV-1 was introduced into the human population by multiple transmissions of a chimpanzee (cpz) virus, which is known as SIVcpz. The less virulent human lentivirus, HIV-2, was derived from SIVsmm, which was obtained from sooty mangabey monkeys (smm) (1).

The cellular restriction factors of the APOBEC3 (A3) family of DNA cytidine deaminases are an important arm of the innate immune defense system which can potentially serve as a barrier to lentiviral cross-species transmissions (recently reviewed in references 2 and 3). Human A3s include seven genes that contain either one (A3A, A3C, and A3H) or two (A3B, A3D, A3F, and A3G) zinc (Z)-binding domains with the conserved motifs of HXE(X)_{23–28}CXXC (X can be any residue) (4, 5). Among these seven genes, A3D, A3F, A3G, and A3H inhibit HIV-1ΔVif replication by deamination of cytidines in the viral single-strand DNA that is formed during reverse transcription, thereby introducing G-to-A hypermutations in the coding strand (6–12). Additionally, some A3s inhibit virus replication by deaminase-indepen-

dent mechanisms affecting reverse transcription and integration steps (13–18). Human A3A and A3C are not antiviral against HIV-1, but human A3C could effectively restrict SIVmacΔVif and

Received 27 July 2016 Accepted 25 August 2016

Accepted manuscript posted online 31 August 2016

Citation Zhang Z, Gu Q, Jaguva Vasudevan AA, Jeyaraj M, Schmidt S, Zielonka J, Perković M, Heckel J-O, Cichutek K, Häussinger D, Smits SHJ, Münk C. 2016. Vif proteins from diverse human immunodeficiency virus/simian immunodeficiency virus lineages have distinct binding sites in A3C. *J Virol* 90:10193–10208. doi:10.1128/JVI.01497-16.

Editor: S. R. Ross, University of Illinois at Chicago

Address correspondence to Carsten Münk, carsten.muenk@med.uni-duesseldorf.de.

* Present address: Stanislaw Schmidt, Division of Pediatric Hematology and Oncology, Hospital for Children and Adolescents, Johann Wolfgang Goethe-Universität, Frankfurt, Germany; Jörg Zielonka, Roche Glycart AG, Schlieren, Switzerland; Mario Perković, TRON (Translational Oncology at the University Medical Center), Johannes Gutenberg-Universität Mainz, Mainz, Germany. Z.Z. and Q.G. contributed equally to this work.

Copyright © 2016, American Society for Microbiology. All Rights Reserved.

SIVagmΔVif (11, 19–23), and both A3A and A3C could decrease human papillomavirus infectivity (24, 25). However, some studies found that A3C inhibited HIV-1ΔVif by around 50% (26–28). Human A3B is a potent inhibitor against HIV-1, SIV, and human T cell leukemia virus (HTLV) (19, 29–32). In addition, human A3B was reported to be upregulated in several cancer cells and found to be degraded by virion infectivity factor (Vif) from several SIV lineages (33–39).

To counteract the antiviral functions of A3, all lentiviruses except the equine infectious anemia virus encode the Vif that interacts with A3 proteins and then recruit them to an E3 ubiquitin ligase complex containing Cullin5 (CUL5), Elongin B/C (ELOB/C), RING-box protein RBX2, and CBFβ to induce degradation of the bound A3s by the proteasome (40–42). The Bet of foamy viruses, the nucleocapsid of HTLV-1, and the glycosylated Gag (glyco-Gag) of murine leukemia virus (MLV) are also shown to have the ability to counteract A3s (21, 43–47). In many cases, this counteraction is species specific and depends on several specific A3/Vif interfaces. For example, HIV-1 Vif efficiently neutralizes human A3G, but it does not inactivate African green monkey A3G (agmA3G) and rhesus macaque A3G (rhA3G) despite a sequence identity of almost 75% (10, 48–50). The amino acid 128 of A3G determines this species-specific counteraction: human A3G with D128 is sensitive to HIV-1 Vif, while A3G.K128 is susceptible to SIVagm Vif (48–50). However, residue 129 in human A3G, but not adjacent position 128, determines the sensitivity to degradation by SIVsmm and HIV-2 Vif proteins (51). Several other cross-species counteractions were also observed: SIVmac Vif mediates the degradation not only of human A3s and rhesus macaque A3s but also of cat A3Z2Z3 (52–57); maedi-visna virus (MVV) Vif can induce the degradation of both sheep and human A3Z3s (58).

Although hA3G, hA3H hapII, and hA3F share a conserved zinc coordination motif, HIV-1 Vif targets different sites in these A3 proteins for degradation. For example, the ¹²⁸DPDY¹³¹ motif in hA3G is involved in direct interaction with the ¹⁴YRHHY¹⁷ domain of HIV-1 Vif (59, 60). The E121 residue in hA3H hapII determines its sensitivity to HIV-1 Vif derived from the NL4-3 strain (61, 62). hA3C and the C-terminal domain (CTD) of hA3F are conserved homologous Z2-typed A3s (4, 5), and 10 equivalent residues in these Z2-typed A3s are identified as being involved in HIV-1 Vif interaction (63). Additionally, A3F.E289 and HIV-1 Vif.R15 show a strong interaction by applying molecular docking (64). The equivalent residue E106 in A3C also determines A3-Vif binding (65). In contrast to this conserved A3-Vif interaction, it was also demonstrated that E324 in A3F is essential for HIV-1 Vif interaction but the equivalent residue E141 in A3C is not, which suggests that the Vif interaction interface differs between A3C and A3F (63, 66). In addition, previous studies have proved that these two glutamic acids vary in primate A3Fs and therefore determined the distinct sensitivities of primate A3F to HIV-1 Vif (67–69). However, the interaction between primate A3Cs and lentiviral Vifs is still less clear.

The N-terminal part of HIV-1 Vif is mainly involved in interaction with human A3s. For example, the ⁴⁰YRHHY⁴⁴ box is reported to be essential for A3G degradation, while the ¹⁴DRMR¹⁷ motif determines A3F degradation (70). Vif derived from HIV-1 clone LAI, but not that of NL4-3, could induce the degradation of hA3H hapII, which is determined by residues F39 and H48 (71). The C terminus of HIV-1 Vif consists of one zinc coordination motif that interacts with CUL5, one SLQ BC box that binds to

ELOB/C, and one Vif dimerization domain (reviewed in reference 72). Previously, it was also reported that the ¹⁷¹EDRW¹⁷⁵ motif in the C terminus of Vif determines the degradation of A3F (66, 73). However, A3 interaction sites in SIV Vif have not yet been identified. Recently, it was reported that the ¹⁶PXXME...PHXXV⁴⁷ domain and G48 of HIV-2 Vif and SIVsmm Vif are involved in the interaction with A3F and A3G, respectively (74).

In this study, we tested the sensitivities of primate A3Cs to several primate lentiviral Vif proteins. HIV-1 Vif had a distinct and restricted degradation profile for primate A3C proteins, while HIV-2, SIVagm, and SIVmac Vif degraded all tested A3C proteins. Additionally, three residues (106, 130, and 133) were identified in rhA3C and smmA3C that determined their resistance to HIV-1 Vif. We demonstrated that the equivalent residues in A3F (313 and 316) were unimportant for HIV-1 Vif sensitivity. Furthermore, two additional residues in the C terminus of the HIV-1 F-1 subtype Vif were identified as being involved in the interaction between HIV-1 Vif and hA3C/F. These observations suggest that Vif proteins from diverse HIV/SIV lineages have distinct interaction interfaces with A3C which mediate their degradation.

MATERIALS AND METHODS

Plasmids. HIV-1, HIV-2, SIVagm, and SIVmac Vif genes were inserted into pcWPRES containing a C-terminal V5 tag (75). SIVpts1 (Tan1; SIVCPZTAN1.910) and SIVpts2 (Tan2; SIVCPZTAN2.69) Vifs were amplified from a full-length molecular clone of SIVcpz (76). Amplicons were digested by EcoRI and NotI and inserted into pcWPRES containing a C-terminal V5 tag. The 21 different HIV-1 strain Vif expression plasmids were kindly provided by Viviana Simon (71). Recently described A3 expression plasmids for hA3C, hA3G, and hA3F (77) as well as rhA3C agmA3C (21) were used. According to the cpzA3C sequence in NCBI (NM_001251910.1), K85, D99, E103, and N115 in hA3C were replaced by N85, E99, K103, and K155 using overlapping PCR, which produced the cpzA3C expression plasmid. All A3s were inserted into pcDNA3.1(+) (Life Technologies, Darmstadt, Germany) expressing a C-terminal hemagglutinin (HA) tag. All A3 chimeras and mutants and Vif mutants were generated by overlapping PCR. PCR primers are shown in Table 1. A3 chimeras were inserted into pcDNA3.1(+), and Vif mutants were inserted into pCRV1 as described previously (78). The expression plasmid of smmA3C was generated by exon assembly from white-crowned mangabey (*Cercopithecus torquatus lunulatus*) genomic DNA. Three fragments were amplified separately using the primer pairs SmA3C-1.fw (5'-TAA GCGGAATTTCGAACATGAATCCACAGATCAGAAACCCG-3') and SmA3C-2.rv (5'-GATCGACCTGGTTTCGGAAG-3'), SmA3C-3.fw (5'-CTTCCGAAACCAGGTCGATC-3') and SmA3C-4.rv (5'-CAATATTTA AAATCTTCGTAGCCC-3'), and SmA3C-5.fw (5'-GGGCTACGAAGA TTTTAAATATTG-3') and SmA3C-6HA.rv (5'-AGGATAT CTCAAGCGTAATCTGGAACATCGTATGGATACTCGAGAATCT CCTG-3'). The fragments were fused through overlapping extension PCR, and the final fragment was amplified by using the forward SmA3C-1.fw and reverse SmA3C-6HA.rv primers. The amplicon was cloned into restriction sites EcoRI and EcoRV of the pcDNA3.1(+) plasmid and the sequence was verified. SIVmac-Luc (R-E-) and SIVmac-Luc (R-E-)ΔVif were provided by N. R. Landau (10). The HIV-1-Luc reporter system was described previously (79).

Cells, transfections, and infections. HEK293T (293T; ATCC CRL-3216) cells were maintained in Dulbecco's high-glucose modified Eagle's medium (DMEM; Biochrom, Berlin, Germany) supplemented with 10% fetal bovine serum (FBS), 2 mM L-glutamine, penicillin (100 U/ml), and streptomycin (100 μg/ml). A3 degradation experiments were performed in 24-well plates, and 1 × 10⁵ 293T cells were transfected with 150 ng hA3G, 150 ng hA3F, or 50 ng hA3C expression plasmids together with 350 ng HIV-1, SIVagm, or SIVmac Vif; pcDNA3.1(+) was used to increase the total transfected plasmid DNA to 500 ng. To produce SIVmac-luciferase

TABLE 1 Primers used in this study

Primer name	Product	Sequence (5'–3')
PmrRhAPO3C		TATAAGCTTTGAAGAGGAATGAATCCACAGATCAGAAACC
PmrRhAPOend		AGCTCGAGTCAAGCGTAATCTGGAACATCGTATGGATACTGAAGAATCTCCCGTAGGCG
CM28		AGCTCGAGTCAAGCGTAATCTGGAACATCGTATGGATACTGGAGACTCTCCCGTAGCCTT
PmrRhehu 9.1	rh/hA3C9	AAGGGCTCCAAGATGTGTAC
PmrRhehu 9.2		GTACACATCTTGGAGCCCTT
PmrRhehu 11.1	rh/hA3C11	CCACCTCCCCTGCACA
PmrRhehu 11.2		TGTGCAGGGGAGGTGG
PmrRhehu 1.1	rh/hA3C13	TCCACGGTGAAGCACAGC
PmrRhehu 1.2		GCTGTGCTTCACCGTGGA
PmrRhehu 3.1		GTGAGATTACGTTGCTGTGCCTGGCCAGGAACCTGG
PmrRhehu 3.2		CCAAGTTCTTGGCCAGGCACAGCAACGTGAATCTCAC
PmrRhehu 1.1	rh/hA3C15	TCCACGGTGAAGCACAGC
PmrRhehu 1.2		GCTGTGCTTCACCGTGGA
PmrRhehu 11.1		CCACCTCCCCTGCACA
PmrRhehu 11.2		TGTGCAGGGGAGGTGG
PmrRhehu 1.1	rh/hA3C17	TCCACGGTGAAGCACAGC
PmrRhehu 1.2		GCTGTGCTTCACCGTGGA
PmrRhehu 9.1		AAGGGCTCCAAGATGTGTAC
PmrRhehu 9.2		GTACACATCTTGGAGCCCTT
PmrRhehu 7.1	rh/hA3C31	AGGAAGCACCTTTCTGCATG
PmrRhehu 7.2		CATGCAGAAAGGTGCTTCTCT
PmrRhehu 3.1		GTGAGATTACGTTGCTGTGCCTGGCCAGGAACCTGG
PmrRhehu 3.2		CCAAGTTCTTGGCCAGGCACAGCAACGTGAATCTCAC
HuA3C-EcoRI-F		ATGAATTTCGCCACCATGAATCCACAGATCAGAAAC
HA-NotI-R		ATGCGGCCGCTCAAGCGTAATCTGGAACATC
HuSmmC1 + 2-F	smm/hA3C1 + 2	TCGGAACGAACTTGGCTGTGCTTC
HuSmmC1 + 2-R		GAAGCACAGCCAAGTTTCGTTCCGA
HuSmmC3 + 4-F	smm/hA3C3 + 4	CCATTGTCATGCAGAAAGGTGCTTCTCTC
HuSmmC3 + 4-R		GAGAGGAAGCACCTTTCTGCATGACAAATGG
HuSmmC5 + 6-F	smm/hA3C5 + 6	TGCAGGGGAGGTGGCCGAGTTCTTGGCCAGG
HuSmmC5 + 6-R		CCTGGCCAGGAACCTCGGCCACCTCCCCTGCA
HuSmmC7 + 8-F	smm/hA3C-7 + 8	AGATTTTAAATATTGTTGGGAAAACCTTTGTG
HuSmmC7 + 8-R		CACAAAGTTTTCACAACATATTTAAATCT
HuSmmC9 + 10-F	smm/hA3C-9 + 10	ATGAGCCATTCAAGCCTTGAAGGGA
HuSmmC9 + 10-R		TCCCTTCCAAGGCTTGAATGGCTCAT
RhA3CCE+QE-F	rhA3C-CE+QE	CAGTATCCGTGTTACCAGGAGGGGCTCCGCAGCCTGAGTCAGGAAGGAGTC
RhA3CCE+QE-R		GACTCCTTCTGACTCAGGCTGCGGAGCCCCCTCTGGTAACACGGATACTG
SmmA3CCE+QE-F	smmA3C-CE+QE	GGGATACATGTTACCAGGAGGGGCTCCGCAGCCTGAGTCAGGAAGGG
SmmA3CCE+QE-R		CCCTTCTGACTCAGGCTGCGGAGCCCCCTCTGGTAACATGTATCCC
HuA3CE106K-F	hA3C E106K	GGAGGTGGCCAAAGTTCTCTGGC
HuA3CE106K-R		GCCAGGAACCTTGGCCACCTCC
HuA3CQE-EK-F	hA3C QE-EK	AGCCTGAGTGAGAAAGGGGTGCTG
HuA3CQE-EK-R		CAGCGACCCCTTTCTCACTCAGGCT
HuA3CNQ+EK-F	hA3C NQ+EK	CAGTATCCAAATTACCAGCAGGGGCTCCGCAGCCTGAGTGAGAAAGGG
HuA3CNQ+EK-R		CCCTTTCTCACTCAGGCTGCGGAGCCCCCTGCTGGTAATTTGGATACTG
HuA3FDE-HQ-F	hA3F DE-HQ	CTGGGATACACATTACCAGCAGGGGCTC
HuA3FDE-HQ-R		GAGCCCCCTGCTGTAATGTGTATCCCAG
HuA3FQE-EK-F	hA3F QE-EK	GCAGCCTGAGTGAGAAAGGGGCTCCG
HuA3FQE-EK-R		CGGAGGCCCTTTCTCACTCAGGCTGC
HIV1Vif-EcoRI-F		ATGAATTTCGCCACCATGGAACAGATGGCAGG
HIV1Vif-NotI-R		ATGCGGCCGCTAGTGTCCATTCAATTGTATGGCTCCCTCTGTGGCCCTTGGTC
F1D-G-NotI-R	F-1 D-G	ATGCGGCCGCTAGTGTCCATTCAATTGTATGGCTCCCTCTGTGGCCCTTGGTC
F1KD-RG-F	F-1K D-RG	AAGCCACCTTTGCCCAGTGTTA
F1KD-RG-R		TAACTGGGCAAAGGTGGCTT
F1K-R-F	F-1 K-R	GCCAGTGTTAGGAACTGACAGAG
F1K-R-R		CTCTGTCAGTTTCTTAACACTGGGC
HIV1VIFRR-AA-F	B-NL4-3 RR-AA	GCAAGTAGACGCGATGGCGATTAACACATGG
HIV1VIFRR-AA-R		CCATGTGTTAATCGCCATCGCGTCTACTTGC
HIV1VIFED-AA-F	B-NL4-3 ED-AA	GAAACTGACAGCGGCCAGATGGAAC
HIV1VIFED-AA-R		GTTCCATCTGGCCGCTGTCAGTTTC
HIV1VIFD101G-F	B-NL4-3 D-G	CACAAGTAGACCCTGGCCTAGCAGACC
HIV1VIFD101G-R		GGTCTGCTAGGCCAGGCTCACTTGTG

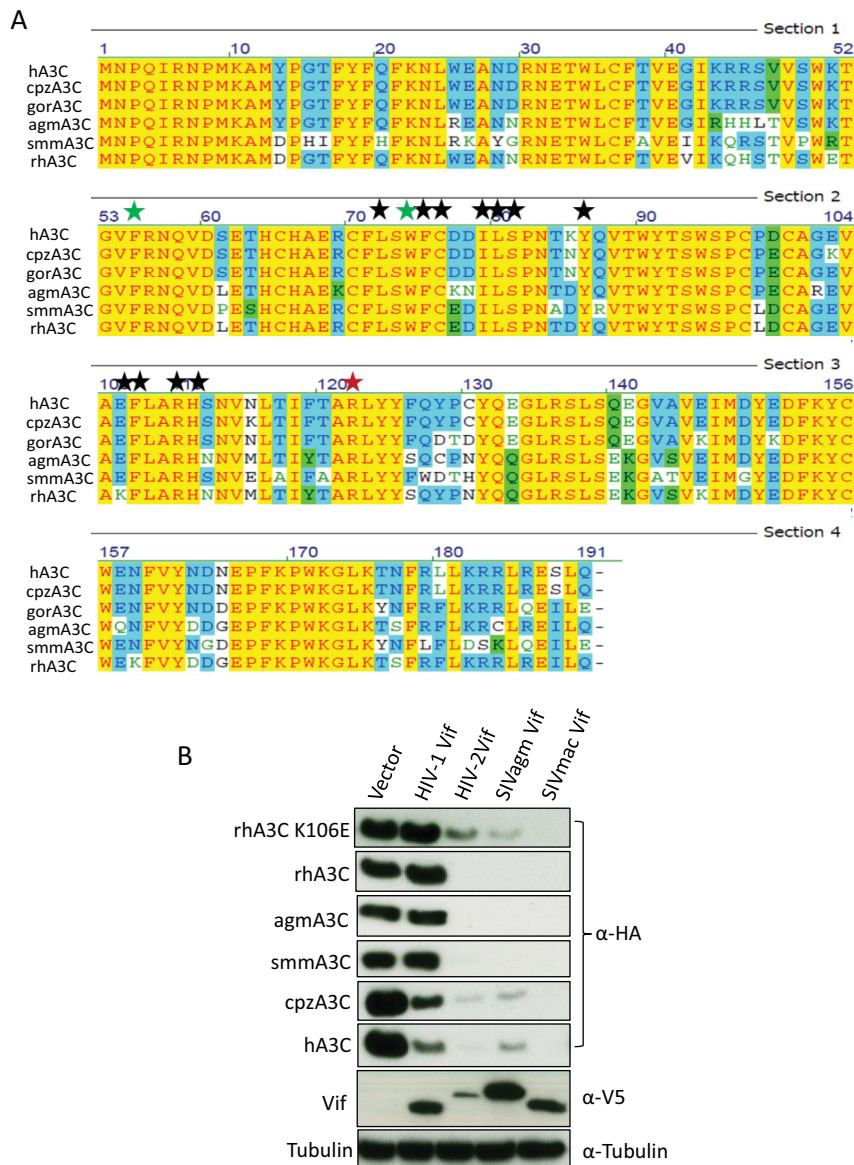


FIG 1 Sensitivity of primate A3C to lentiviral Vifs. (A) Sequence alignment of primate A3C proteins. Black stars represent important residues for HIV-1 Vif interaction. Green stars indicate the dimerization of A3C protein and anti-SIV activity. The red star is the A3C RNA binding site and indicates its viral incorporation. (B) 293T cells were cotransfected with A3C and HIV-1, HIV-2, SIVagm, or SIVmac Vif expression plasmids. Expression of A3Cs, Vifs, and tubulin was detected by immunoblotting using anti-HA, anti-V5, and anti-tubulin antibodies, respectively. h, cpz, gor, agm, smm, and rh represent human, chimpanzee, gorilla, African green monkey, sooty mangabey monkey, and rhesus monkey, respectively.

viruses, 293T cells were cotransfected with 650 ng SIVmac-Luc (R-E-) or SIVmac-Luc (R-E-)ΔVif, 150 ng A3C expression plasmid, 25 ng vesicular stomatitis virus glycoprotein (VSV-G) plasmid (pMD.G), or 200 ng HIV-1 Vif expression plasmid; in some experiments pcDNA3.1(+) was used instead of Vif or A3 expression plasmids. For HIV-1-luciferase viruses, transfection experiments in 6-well plates consisted of 300 ng of the HIV-1 packaging construct pMDLg/RRE, 130 ng of HIV-1 Rev expression plasmid pRSV-Rev, 300 ng of the HIV-1 reporter vector pSIN.PPT.CMV.Luc.IRES.GFP, 100 ng of the VSV-G expression plasmid pMD.G, and 800 ng HIV-1 Vif together with 800 ng hA3F expression plasmids. pcDNA3.1(+) was used instead of HIV-1 Vif or hA3F. At 48 h posttransfection, cells and supernatants were collected. The reverse transcriptase (RT) activity of SIVmac and HIV-1 was quantified by using the Cavid HS lenti RT kit (Cavidi Tech, Uppsala, Sweden). For reporter virus infection, 293T cells were seeded in 96-well plates 1 day before transduction. After

normalizing for RT activity, the same amounts of viruses were used for infection. Two days posttransduction, firefly luciferase activity was measured with the Steadylite HTS reporter gene assay system (Perkin-Elmer, Cologne, Germany) according to the manufacturer's instructions on a MicroLumat Plus luminometer (Berthold Detection Systems, Pforzheim, Germany). Each sample was analyzed in triplicate; the error bars for each triplicate are shown.

Immunoblot analysis. Transfected 293T cells were lysed in radioimmunoprecipitation assay (RIPA) buffer (25 mM Tris-HCl [pH 8.0], 137 mM NaCl, 1% NP-40, 1% glycerol, 0.5% sodium deoxycholate, 0.1% sodium dodecyl sulfate [SDS], 2 mM EDTA, and protease inhibitor cocktail set III [Calbiochem, Darmstadt, Germany]). To pellet virions, culture supernatants were centrifuged at 12,000 rpm for 10 min, subjected to centrifugation through a 20% sucrose cushion at 35,000 rpm in an SW40 Ti rotor for 1.5 h, and resuspended in RIPA buffer. The solution was

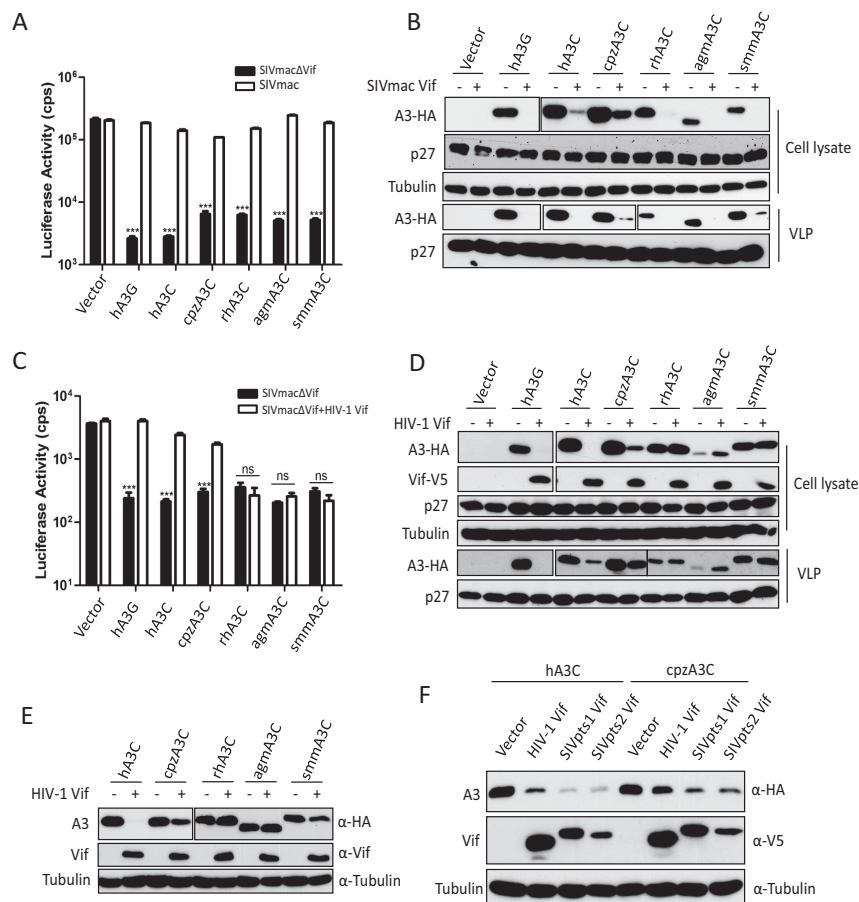


FIG 2 SIVmac Vif, but not HIV-1 Vif, counteracts primate A3Cs. (A and C) 293T cells were transfected with expression plasmids for SIVmacΔVif-Luc or SIVmac-Luc (A) or SIVmacΔVif-Luc or SIVmacΔVif-Luc plus HIV-1 Vif (C), together with expression plasmids for hA3G and primate A3Cs. pcDNA3.1(+) was used as a control (vector). After normalizing for reverse transcriptase activity, viral infectivity was determined by quantification of luciferase activity in 293T cells. (B and D) Lysates of SIVmac producer cells were used to detect the expression of A3s, SIVmac capsid (p27), or HIV-1 Vif by anti-HA, anti-p27, or anti-V5 antibody, respectively. Tubulin served as a loading control. Encapsidation of A3s into SIVmac was detected by anti-HA antibody. (E) Primate A3Cs and HIV-1 Vif (without tag) expression plasmids were cotransfected into 293T cells. The expression of A3C and HIV-1 Vif was detected by anti-HA and anti-Vif antibodies. (F) Expression plasmids for hA3C and cpzA3C were cotransfected with HIV-1 Vif or SIVcpz Vif into 293T cells. The expression of A3C and Vif was detected by anti-HA and anti-V5 antibodies. Pts, *Pan troglodytes schweinfurthii*. cps, counts per second. VLP, virus-like particle. Asterisks represent statistically significant differences: ***, $P < 0.001$; ns, no significance (Dunnett's t test).

boiled at 95°C for 5 min with Roti load-reducing loading buffer (Carl Roth, Karlsruhe, Germany) and resolved on an SDS-PAGE gel. The expression of A3s and lentivirus Vif was detected by mouse anti-HA antibody (1:7,500 dilution; MMS-101P; Covance, Münster, Germany) and mouse anti-V5 antibody (1:4,500 dilution; MCA1360; ABD Serotec, Düsseldorf, Germany) separately. HIV-1 Vifs from different subtype strains were detected by rabbit anti-Vif polyclonal antibody (1:1,000 dilution; catalog no. 2221; NIH AIDS Research and Reference Reagent Program) (80). Tubulin, SIVmac, and HIV-1 capsid proteins were detected using mouse anti- α -tubulin antibody (1:4,000 dilution; clone B5-1-2; Sigma-Aldrich, Taufkirchen, Germany) and mouse anti-capsid p24/p27 monoclonal antibody AG3.0 (1:50 dilution) separately (81), followed by horseradish peroxidase-conjugated rabbit anti-mouse or donkey anti-rabbit antibody (α -mouse or rabbit-IgG-horseradish peroxidase; GE Healthcare, Munich, Germany), and developed with ECL chemiluminescence reagents (GE Healthcare).

IP. To determine Vif and A3 binding, 293T cells were cotransfected with 1 μ g HIV-1 Vif.SLQ-AAA and 1 μ g wild-type or mutant A3 or with pcDNA3.1(+). Forty-eight hours later, the cells were lysed in immunoprecipitation (IP) lysis buffer (50 mM Tris-HCl pH 8, 1 mM phenylmethylsulfonyl fluoride [PMSF], 10% glycerol, 0.8% NP-40, 150 mM NaCl,

and complete protease inhibitor; Roche, Penzberg, Germany). The lysates were cleared by centrifugation. The supernatant were incubated with 20 μ l α -HA affinity matrix beads (Roche) at 4°C for 2 h. The samples were washed 5 times with lysis buffer. Bound proteins were eluted by boiling the beads for 5 min at 95°C in SDS loading buffer. Immunoblot analysis and detection were done as described above.

Model structure. To analyze the interaction surface between HIV-1 Vif and hA3C/A3F, the hA3C (PDB entry 3VOW), hA3F C-terminal (PDB entry 4J4J), and HIV-1 Vif (PDB entry 4N9F) structures were used. The structural models of F-1 Vif and mutants were built by the SWISS-MODEL online server (<http://www.swissmodel.expasy.org/>) (82) using B-NL4-3 Vif (PDB entry 4N9F) as a template. The graphical visualizations shown in Fig. 8 and 9 were constructed using PyMOL (PyMOL Molecular Graphics System, version 1.5.0.4; Schrödinger, Portland, OR).

Statistical analysis. Data are represented as the means with standard deviations (SD) in all bar diagrams. Statistically significant differences between two groups were analyzed using the unpaired Student's t test with GraphPad Prism, version 5 (GraphPad Software, San Diego, CA, USA). A minimum P value of 0.05 was considered statistically significant. A P value of <0.001 was extremely significant (***), 0.001 to 0.01 very significant (**), 0.01 to 0.05 significant (*), and >0.05 not significant (ns).

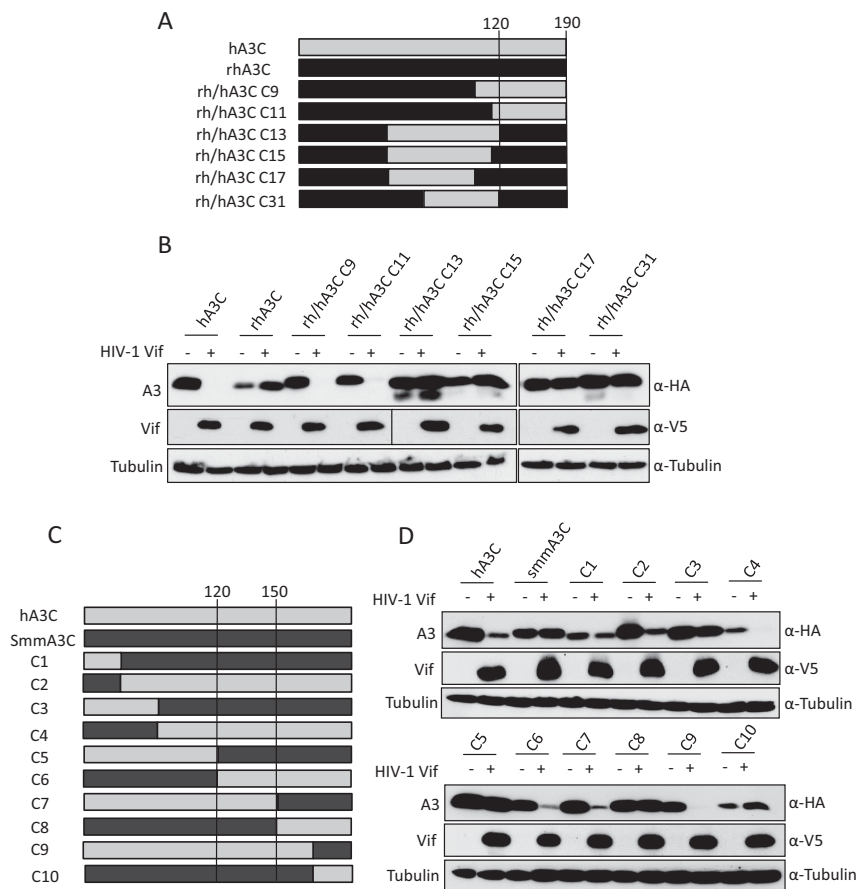


FIG 3 Sensitivity of rh/hA3C and h/smmA3C chimeras to HIV-1 Vif-mediated depletion. (A and C) Schematic structure of rh/hA3C and h/smmA3C chimeras. Amino acid positions 120, 150, and 190 in hA3C are indicated. (B and D) Immunoblots of protein lysates of cotransfected cells displaying the A3's sensitivity to HIV-1 Vif-triggered degradation. The expression of A3s and HIV-1 Vif were analyzed by using anti-HA and anti-V5 antibodies. Tubulin served as a loading control. +, with HIV-1 Vif; -, without HIV-1 Vif.

Accession number(s). Sequences for human A3C (NM_014508.2), chimpanzee A3C (NM_001251910.1), gorilla A3C (AH013821.1), African green monkey A3C (EU381232.1), sooty mangabey monkey A3C (KX405162), rhesus monkey A3C (JF714486.1), SIVpts1 (Tan1) (EF394356.1), and SIVpts2 (Tan2) (EF394357.1) were deposited in NCBI.

RESULTS

The sensitivity of primate A3C to lentiviral Vif. A previous study has identified several residues in the hydrophobic V-shaped groove formed by the $\alpha 2$ and $\alpha 3$ helices of A3C involved in HIV-1 Vif interaction (63). This interaction interface is conserved in primate A3C proteins, although rhA3C has one substitution (E to K) at position 106 (Fig. 1A). To test the sensitivities of these A3C proteins to HIV-1 Vif, cotransfections of expression plasmids for A3Cs and HIV-1 Vif were performed. A3C steady-state levels were assessed by immunoblotting protein lysates of coexpressing cells. Previous studies demonstrated that both SIVagm and HIV-1 Vif were able to induce the degradation of human A3C by the proteasome (83). Based on this finding, we assume that the dominant mechanism of Vif against A3C in our study is Vif-triggered degradation of A3 as well. Results show that HIV-1 Vif reduced the stability of hA3C and cpzA3C, while smmA3C, agmA3C, and rhA3C were resistant (Fig. 1B). smmA3C was cloned from a white-crowned mangabey (*Cercocebus torquatus lunulatus*), which is one of the three subspecies of sooty mangabey monkeys.

The resistance of smmA3C to HIV-1 Vif was unexpected, because the previously identified HIV-1 Vif interaction sites were identical between smmA3C and hA3C (Fig. 1A). HIV-1 Vif's block to deplete rhA3C may be caused by an E-to-K substitution at position 106. To prove this, we made a K106-to-E mutation in rhA3C and tested its sensitivity to HIV-1 Vif. However, the results showed that rhA3C.K106E still could not be degraded by HIV-1 Vif (Fig. 1B). These observations indicate that sites in addition to the already characterized residues in A3C are involved in the HIV-1 Vif interaction. We also observed that HIV-2, SIVmac, and SIVagm Vif depleted all A3C proteins, including rhA3C.K106E (Fig. 1B). These data suggest that Vif proteins from diverse HIV/SIV lineages have distinct binding sites in A3C which mediate its degradation.

We next tested the anti-SIVmac activities of these primate A3C proteins in the presence of SIVmac or HIV-1 Vif proteins. Luciferase reporter viruses of SIVmac, SIVmac Δ Vif, and SIVmac Δ Vif plus Vif of HIV-1 were produced with hA3G, hA3C, cpzA3C, rhA3C, agmA3C, or smmA3C. The Vif-proficient virus SIVmac-Luc expresses Vif in its natural expression context; however, Vif lacks an epitope tag for detection. Viral particles were normalized by RT activity, and the luciferase activity of infected cells was quantified 2 days postinfection. All A3C proteins strongly inhibited the infectivity of Vif-deficient SIVmac, which was fully coun-

teracted by SIVmac Vif, as was hA3G (Fig. 2A). The immunoblots of virus-producing cells indicated that SIVmac Vif reduced the stability of hA3G and all primate A3C proteins, which resulted in viral particles with much reduced A3 content (Fig. 2B). However, HIV-1 Vif counteracted the anti-SIVmac activity of hA3G, hA3C, and cpzA3C, and rhA3C, agmA3C, and smmA3C displayed resistance to HIV-1 Vif (Fig. 2C). The immunoblots showed that HIV-1 Vif decreased the protein level of hA3G, hA3C, and cpzA3C in cell lysates and viral particles but not that of rhA3C, agmA3C, and smmA3C (Fig. 2D). Since the HIV-1 Vif we used here contained a C-terminal V5 tag, we wondered whether the V5 tag in Vif would contribute to the Vif resistance of rhA3C, agmA3C, and smmA3C. We then tested the sensitivity of A3Cs to untagged HIV-1 Vif. We found that hA3C and cpzA3C were sensitive to antagonization by untagged HIV-1 Vif, whereas rhA3C, agmA3C, and smmA3C still were not degraded (Fig. 2E). Thus, the V5 tag in Vif did not contribute to the HIV-1 Vif resistance of rhA3C, agmA3C, and smmA3C. It is important to point out that cpzA3C was less efficiently depleted from cells by HIV-1 Vif (untagged and V5 tagged) than hA3C (Fig. 2D and E). The immunoblotting results showed that SIVcpz (SIVpts1 and SIVpts2) Vifs displayed stronger activity against hA3C and cpzA3C than HIV-1 Vif (Fig. 2F).

Identification of specific rh/smmA3C residues involved in resistance to HIV-1 Vif. The results from Fig. 1B suggest that additional sites in hA3C are involved in the interaction with HIV-1 Vif. To identify the additional determinants, several rh/hA3C chimeras were constructed. Structures of A3 chimeras are shown in Fig. 3A, and their sensitivities to HIV-1 Vif were determined by immunoblotting of cell lysates expressing Vif and individual A3 constructs. The results showed that hA3C chimera 9 and chimera 11 were sensitive to HIV-1 Vif-mediated depletion, while rhA3C chimeras 13, 15, 17, and 31 were resistant and not degraded (Fig. 3B). The composition of the chimeras indicated that the C terminus (from amino acids 120 to 190) of rhA3C determined the resistance to HIV-1 Vif. smmA3C was also resistant to HIV-1 Vif-induced degradation (Fig. 1A). To narrow the scope of residues in A3C that are involved in the HIV-1 Vif interaction, 10 chimeras of human A3C and smmA3C were produced. The structures of smm/hA3C chimeras are displayed in Fig. 3C. We found that hA3C chimeras 2, 4, 6, 7, and 9 could be depleted by HIV-1 Vif, while smmA3C and other chimeras evidently were not degraded (Fig. 3D). Based on these results, amino acids 120 to 150 of smmA3C were identified as an essential domain that confers resistance to HIV-1 Vif.

To identify the residues in rhA3C and smmA3C that are important for resistance to HIV-1 Vif-mediated counteraction, we compared the amino acids from 120 to 150 in primate A3C proteins, and four residues (130, 133, 140, and 141) were selected for further characterization. In hA3C and cpzA3C these residues are C130, E133, and 140QE141, while in agmA3C, rhA3C, and smmA3C these four positions are N/H130, Q133, and 140EK141, respectively (Fig. 1A). Thus, we mutated N130, Q133, and 140EK141 in rhA3C to the residues found in hA3C, termed rhA3C.CE+QE. Based on this construct, we performed the single-amino-acid substitution K106E, named rhA3C.K106E-CE+QE (Fig. 4A), because E106 in hA3C indicates it is binding to HIV-1 Vif (65). For smmA3C, four amino acid substitutions were produced, and the construct was termed smmA3C.CE+QE (Fig. 4A). The sensitivities of these constructs together with wild-type hA3C, rhA3C, and smmA3C to HIV-1 Vif-triggered de-

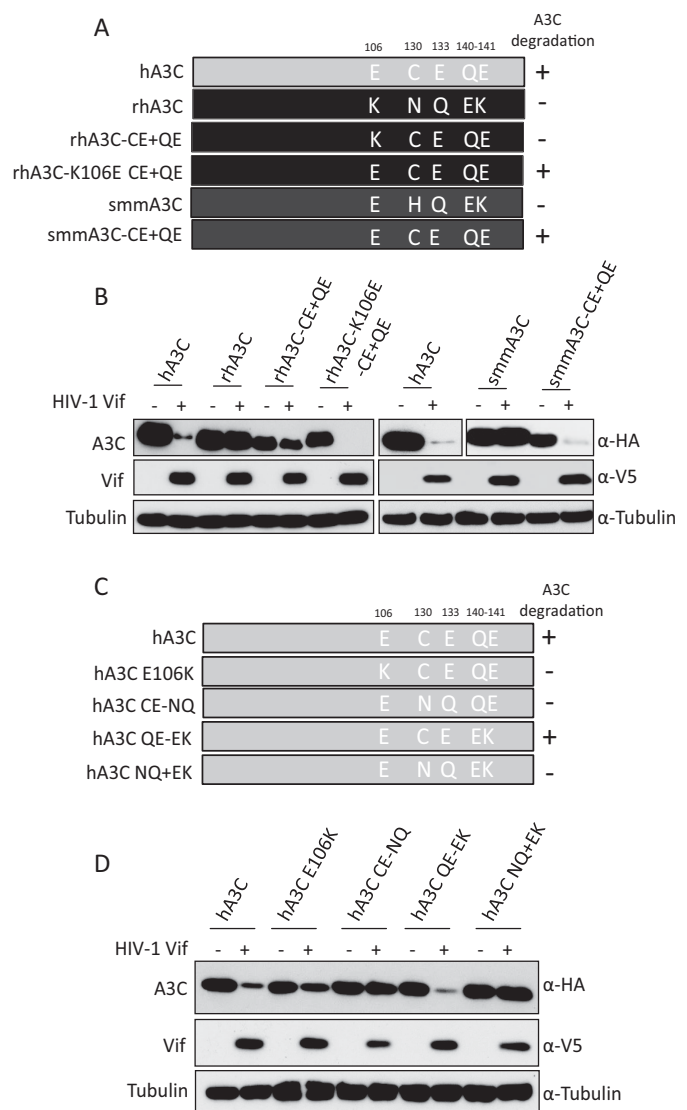


FIG 4 Identification of determinants in rhA3C and smmA3C that confer resistance to HIV-1 Vif. (A) The schematic structure of rhA3C and smmA3C mutants. The numbers represent amino acid positions in A3C. +, sensitive to HIV-1 Vif-induced degradation; -, resistant to HIV-1 Vif-induced degradation. (B and D) hA3C, rhA3C, smmA3C, or A3C mutants were cotransfected with HIV-1 Vif into 293T cells. A3, HIV-1 Vif, and tubulin were detected by using anti-HA, anti-V5, and anti-tubulin antibodies, respectively. (C) Schematic structure of hA3C mutants.

pletion were tested by immunoblotting. The results showed that rhA3C.CE+QE was still resistant to HIV-1 Vif, but rhA3C.K106E-CE+QE was sensitive to hA3C (Fig. 4B). This result confirmed the importance of E106 in hA3C involvement in the HIV-1 Vif interaction. The smmA3C.CE+QE protein was depleted by HIV-1 Vif, which suggests that C130, E133, and 140QE141 are also important for HIV-1 Vif-mediated degradation. In addition, the equivalent residues (C130, E133, and 140QE141) in hA3C were replaced by N130, Q133, and 140EK141, respectively, producing hA3C.CE-NQ, hA3C.QE-EK, and hA3C.NQ+QE (Fig. 4C). hA3C.E106K, which could not be antagonized by HIV-1 Vif, was used as a control. The results showed that hA3C.E106K was partially resistant to HIV-1 Vif but that hA3C.QE-EK was depleted (Fig. 4D), showing consis-

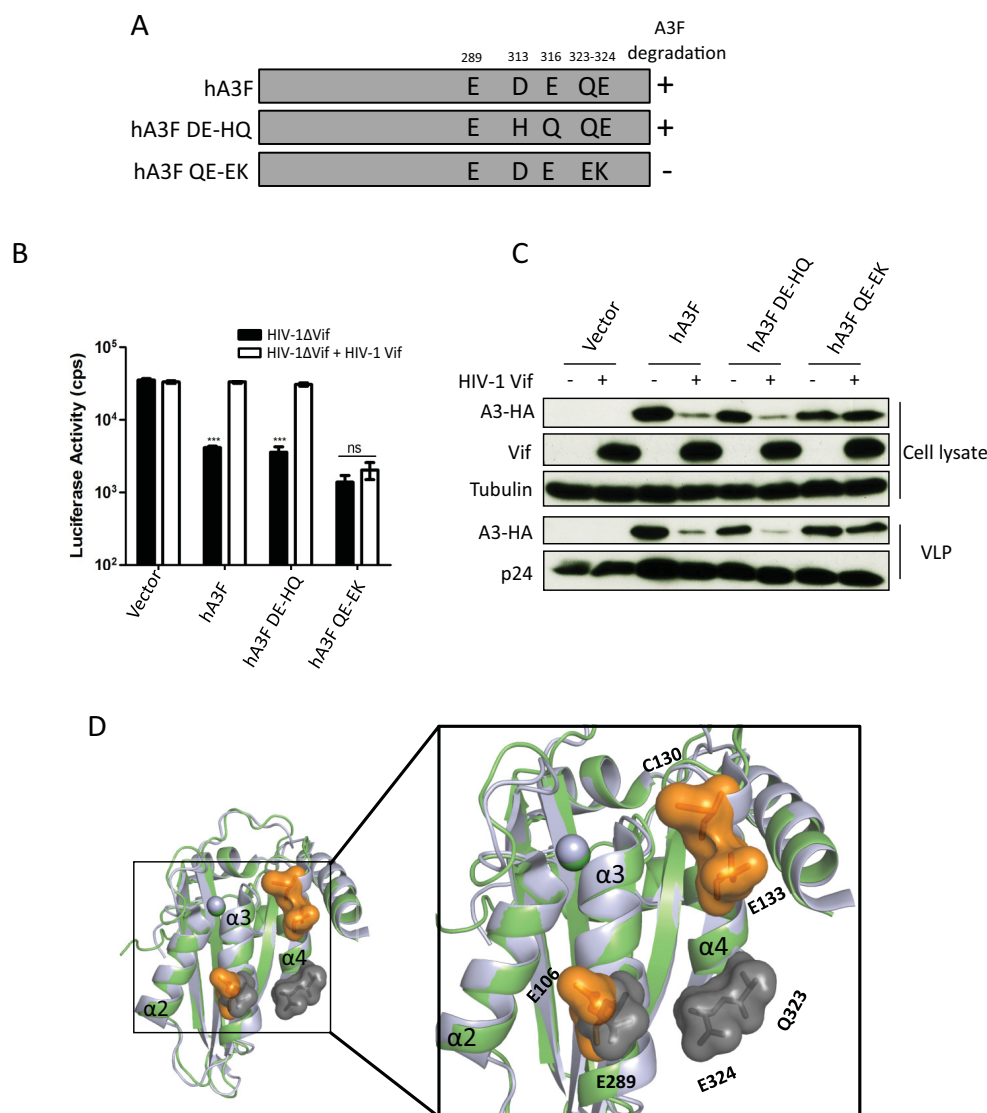


FIG 5 hA3F residues and HIV-1 Vif-induced depletion. (A) The schematic structure of hA3F mutants. +, sensitive to HIV-1 Vif induced degradation; –, resistant to HIV-1 Vif-induced degradation. (B) HIV-1ΔVifluciferase or HIV-1ΔVifluciferase plus HIV-1 Vif were produced in 293T cells in the presence of A3F or mutants. After normalizing for reverse transcriptase activity, viral infectivity was determined by quantification of luciferase activity in 293T cells. (C) A3s in HIV-1 producer cells and HIV-1 viral particles were detected by using anti-HA antibody. HIV-1 Vif and capsid (p24) were detected by anti-Vif and anti-p24 antibodies, respectively. Tubulin served as a loading control. (D) Superimposition of A3C crystal structure (PDB entry 3VOW) (green) and A3F-CTD crystal structure (PDB entry 4J4J) (light blue). Key residues E106, C130, and E133 are shown as orange surfaces in A3C with labels, and the essential residues (E289, Q323, and E324) in A3F are highlighted with gray surfaces and labels. cps, counts per second. Asterisks represent statistically significant differences: ***, $P < 0.001$; ns, no significance (Dunnett's t test).

tency with previous studies (63). Moreover, we found that hA3C.CE-NQ and hA3C.NQ+EK were resistant to HIV-1 Vif-mediated degradation (Fig. 4D). Taken together, these results demonstrate that residues 106, 130, and 133 of primate A3C proteins determine their sensitivities to HIV-1 Vif, but residues 140QE141 were unimportant for HIV-1 Vif interaction.

A3F and A3C have distinct Vif interaction interfaces. After identification of the residues C130 and E133 in hA3C as being important for interaction with HIV-1 Vif, we expanded our experiments to hA3F. The equivalent residues (D313 and E316) in hA3F were replaced by H313 and Q316, which were present in rhA3F. In addition, we altered amino acids Q323E and E324K in hA3F (Fig. 5A). We analyzed the anti-HIV-1 activity of these hA3F

mutants in the presence of HIV-1 Vif. HIV-1 Vif restored the infectivity in the presence of hA3F and hA3F.DE-HQ, while hA3F.QE-EK displayed antiviral activity in the presence and absence of HIV-1 Vif (Fig. 5B). The corresponding immunoblots of virus-producing cells showed that HIV-1 Vif reduced the steady-state level of hA3F and hA3F.DE-HQ but not of hA3F.QE-EK (Fig. 5C). Q323E and E324K alterations in hA3F impaired HIV-1 Vif-mediated depletion, consistent with previous studies (63, 67). However, we and other groups also observed that the equivalent residues (Q140 and E141) in hA3C were unimportant for HIV-1 Vif interaction (63) (Fig. 4D). We then compared the structures of hA3C and the C-terminal domain of hA3F and highlighted the HIV-1 Vif interaction surface investigated in our study. As shown

in Fig. 5D, residue E106 in hA3C and the corresponding residue E289 in hA3F, which are located in the $\alpha 3$ helices, were involved in HIV-1 Vif interaction. In the $\alpha 4$ helices, the HIV-1 Vif interaction surface differs in hA3C and hA3F, shifting from the top to the bottom of $\alpha 4$ helices (Fig. 5D). Taken together, these results indicate that the Vif-A3 interaction interfaces in hA3C and hA3F are different.

To clarify whether the identified residues of A3C and A3F were directly involved in Vif binding, coimmunoprecipitation (co-IP) assays of Vif.SLQ/AAA, which binds A3s without inducing their degradation, were performed with HA-tagged A3C and A3F. Because the expression levels of primate A3C and several mutants were distinct, ImageJ software was used to evaluate the band density of A3C and Vif from immunoprecipitation. The ratio of Vif to A3 was calculated as A3-Vif binding activity in which we set wild-type A3C-Vif or wild-type A3F-Vif binding activity as 100%. As shown in Fig. 6, rhA3C and its mutant, rhA3C-K106E-CE+QE, which was sensitive to HIV-1 Vif, immunoprecipitated with HIV-1 Vif (Fig. 6A); however, binding was much reduced compared to Vif binding to hA3C. The smmA3C and smmA3C.CE+QE protein levels were much lower in the cell lysates, so they precipitated less than hA3C in co-IP complexes, whereas the amount of detected HIV-1 Vif was similar to that of the hA3C-Vif complex (Fig. 6A), indicating that smmA3C has high binding activity to HIV-1 Vif (Fig. 6B). The hA3C.E106K and hA3C.QE-EK mutants showed very low HIV-1 Vif binding, which was consistent with a previous study (63). However, hA3C.CE-NQ, which was not degraded by HIV-1 Vif, pulled down similar amounts of Vif compared to the wild-type hA3C-Vif complex (Fig. 6A). The HIV-1 Vif binding capacities of hA3F and hA3F.DE-HQ were similar, corresponding to similar sensitivities to HIV-1 Vif (Fig. 5B and 6B). Significantly reduced amounts of Vif were pulled down by hA3F.QE-EK, suggesting hA3F residues 323QE324 were involved in Vif binding. RhA3C and smmA3C were totally resistant to HIV-1 Vif-induced degradation (Fig. 4B and D); however, both of these proteins showed robust binding to HIV-1 Vif, suggesting that the Vif binding detected by co-IPs is unrelated to Vif-mediated degradation.

Internal salt bridge of Vif protein influences degradation of hA3C/F. Previous studies have identified three motifs of HIV-1 Vif specifically involved in the interaction with hA3F: the F1 box (14DRMR17), F2 box (74TGEDW79), and F3 box (171EDRW174) (66, 84). To identify additional determinants in HIV-1 Vif relevant for interaction with hA3C/F, 21 HIV-1 Vif alleles (71) were used for detecting their hA3C counteractivity, including five Vifs isolated from HIV-1 N and O subtypes. All Vif alleles were detectable by anti-Vif polyclonal antibody (Fig. 7A). The Vif variants (C1, C2, and C3) displayed lower-level signals in the immunoblots than the other Vifs, which might be caused by weaker antibody recognition (Fig. 7A). The 21 Vif alleles depleted hA3C to various degrees. To evaluate the degree of this counteraction, ImageJ was used to calculate the density of hA3C bands in which hA3C cotransfected with empty vector plasmid was set as the control (100% expression). The results showed that 10 Vif variants (A2, B-NL4-3, B-LAI, C3, D2, F-3, F-4, O-119, O-127, and N-116) strongly depleted hA3C (Fig. 7A and B). All other Vif variants, except Vif from F-1, moderately reduced the protein level of hA3C. The F-1 Vif had an expression level similar to those of B-NL4-3 and B-LAI Vif, but almost 80% of hA3C could be detected in the presence of F-1 Vif (Fig. 7A and B). A previous

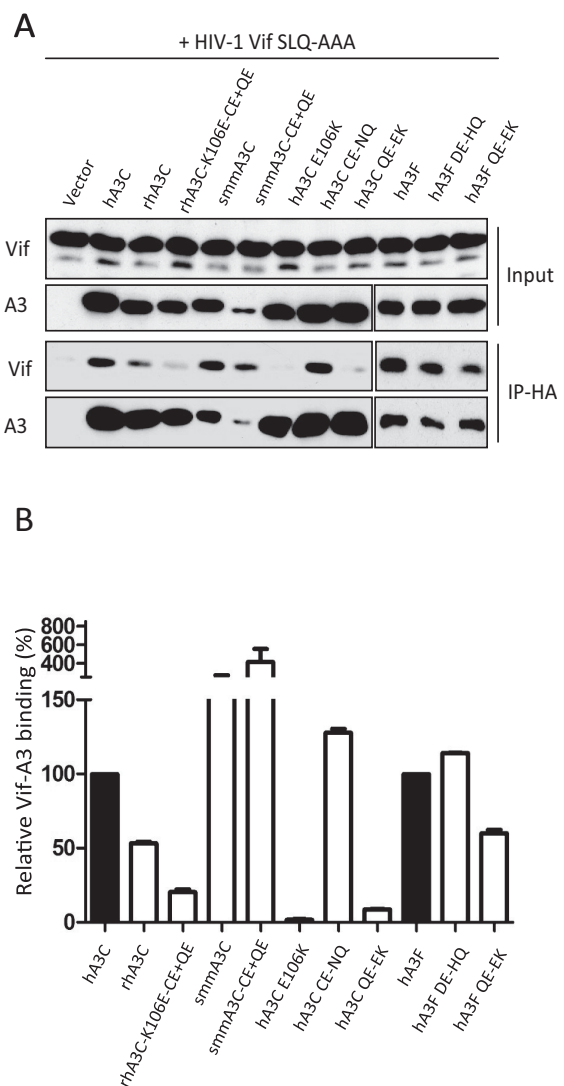


FIG 6 HIV-1 Vif binding to A3C and A3F mutants. (A) Coimmunoprecipitation of HIV-1 Vif SLQ/AAA with A3C and A3F mutants. Protein cell lysates (Input) and immunoprecipitated complexes (IP) were analyzed by immunoblotting with anti-Vif for HIV-1 Vif or anti-HA for A3. (B) ImageJ was used to evaluate the band density of A3C and Vif from immunoprecipitation. The ratio of Vif to A3 was calculated as A3-Vif binding activity. WT A3C-Vif and WT A3F-Vif binding activity was set as 100%.

study demonstrated that F-1 Vif, but not Vif from F-2 and B-NL4-3, could mediate the degradation of hA3H hapII (71). To understand whether the resistance of hA3C to F-1 Vif is specific, three Vif variants (B-NL4-3, F-1, and F-2) were tested for counteraction of hA3H hapII, hA3G, hA3F, and hA3C. The results showed that the protein levels of both hA3C and hA3F could be reduced by B-NL4-3 and F-2 Vif but displayed resistance to F-1 Vif. hA3G was strongly depleted by these three Vif variants, while hA3H hapII was resistant to B-NL4-3 and F-2 Vif but sensitive to F-1 Vif (Fig. 7C), consistent with previous data (71). Taken together, these results indicated that the differences between F-1, F-2, and B-NL4-3 Vifs determine specific degradation of hA3C/F.

After analyzing the sequences of B-NL4-3, F-1, and F-2 Vif, six residues outside the CUL5 and BC boxes were identified (positions 39, 48, 61, 62, 167, and 182) where all three Vifs differed from

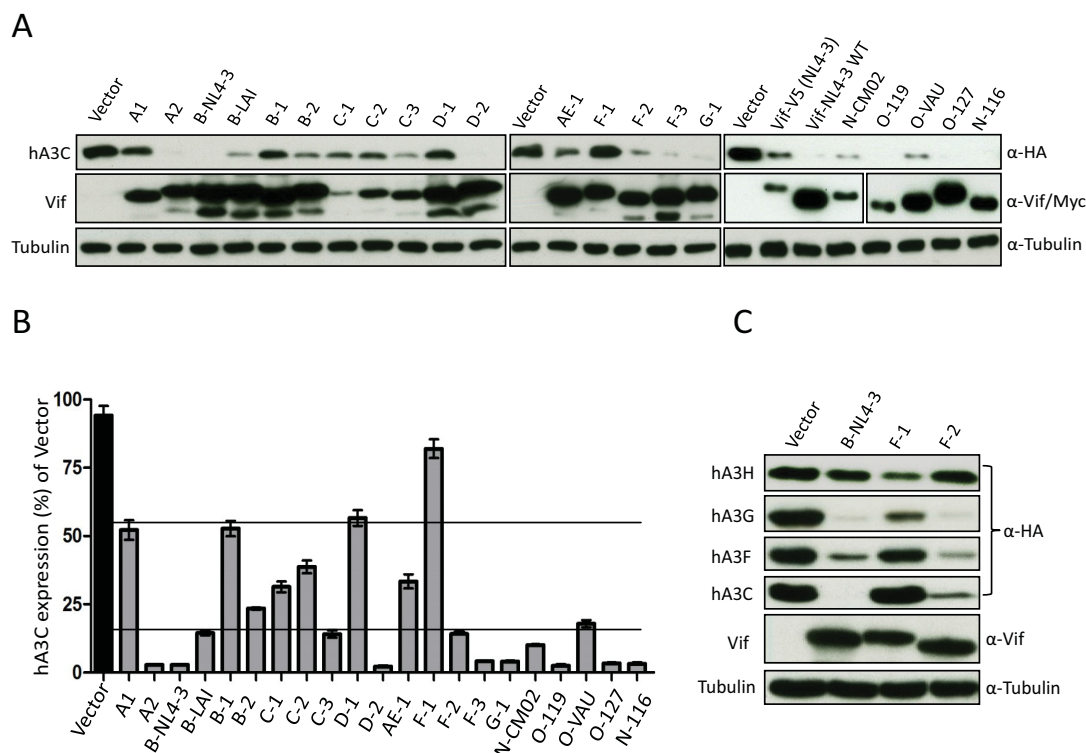


FIG 7 hA3C depletion activities of HIV-1 Vif alleles. (A) The 21 HIV-1 Vif alleles induced depletion of hA3C to various degrees. hA3C and Vif alleles were cotransfected into 293T cells. Protein extracts of transfected cells were used for detecting the expression of hA3C, Vif, and tubulin by anti-HA, anti-Vif, and anti-tubulin antibodies, respectively. Vifs from N and O subtypes were detected by anti-myc antibody. This A3C experiment was repeated at least three times with similar results. (B) ImageJ was used to evaluate the band density of A3C and tubulin. The ratio of A3C to tubulin was calculated as A3C expression efficiency. A3C plasmid cotransfected with empty vector plasmid was set as 100% expression. (C) hA3C, hA3F, hA3G, and hA3H hapII expression plasmids were transfected together with B-NL4-3 expression plasmids and F-1 and F-2 Vif variants. A3 and Vif were detected by using anti-HA and anti-Vif antibodies. Tubulin served as a loading control.

each other. Residues F39 and H48 in Vif determine the interaction with hA3H hapII (71). Based on the structure of Vif, residues 61 and 62 are on the other side of the F box that was identified for the interaction with hA3F. Thus, we focused on residues 167 and 182 in F-1 Vif. K167 and D182 in F-1 Vif were mutated to R and G, which are the corresponding residues in B-NL4-3 Vif both separately and in combination (Fig. 8A). Wild-type Vif and Vif mutants were tested in coexpression experiments for their effect on the steady-state levels of hA3C and hA3F. The immunoblot showed that replacing K167 with arginine recovered the F-1 Vif depletion activity against hA3C, while the introduction of glycine at position 182 did not help much to enhance A3C reduction (Fig. 8B). However, both K167R and D182G exchanges activated F-1 Vif counteraction of hA3F, which suggests that G182 is important for degradation of hA3F but not hA3C (Fig. 8B). We next replaced K167 in F-1 Vif by a negatively charged amino acid, D/E, as well as a nonpolar alanine, and analyzed their hA3C/hA3F inhibitory activities. We found that mutants K167A, K167D, and K167E depleted hA3C/hA3F as efficiently as B-NL4-3 Vif (Fig. 8C). The F3 box (171EDRW174) that interacts with hA3C/F is conserved in B-NL4-3 and F-1 Vif (Fig. 8A). Thus, we wondered whether the F3 box in F-1 Vif is still essential for inhibition of hA3C/hA3F. To address this question, 171ED172 to 171AA172 mutations were generated in both F-1 wild-type Vif and F-1 Vif.K167R constructs. The immunoblot revealed that replacing K167 with R recovered the F-1 Vif activity against hA3C/hA3F, but mutations in the F3

box together with K167R impaired degradation, suggesting that the F3 box in F-1 Vif is still key to the function of interaction with hA3C/hA3F (Fig. 8D). The Vifs from B-NL4-3 and F-1 share 90.3% identical residues. Thus, we modeled the structures of F-1 Vif and its mutants using the structure of B-NL4-3 Vif (PDB entry 4N9F) as a template and analyzed the interactions of residues 171 and 167 within these model variants. We found that E171 and K167 displayed a strong interaction in the F-1 Vif, while the models of K167A, K167D, and K167E displayed no interaction (Fig. 8E). Taken together, these results suggest that the side-chain interaction of E171 and K167 affect hA3C/hA3F-Vif interaction induced by E171, resulting in an F-1 Vif being inactive in the induction of the degradation of hA3C/hA3F.

Additionally, we exchanged R167 and G182 in B-NL4-3 Vif for K and D, which were found in F-1 Vif. As controls we included F2 and F3 box mutants (B-NL4-3.RR-AA and B-NL4-3.ED-AA). Wild-type Vif and Vif mutants were tested for affecting the protein stability of hA3C, hA3F, and hA3G in Vif/A3 coexpression experiments. The results showed that mutations in the F2 box and the F3 box indeed impaired Vif activity against hA3C and hA3F but not against hA3G (Fig. 9A). Surprisingly, substitution R167K or G182D or the combination of both mutations did not impair depletion of hA3C, hA3F, and hA3G by B-NL4-3 Vif (Fig. 9A). To analyze the internal structural changes of the R167K Vif mutant, we modeled the structures of B-NL4-3 Vif.R167K and analyzed the E171-K167 interaction. We found that residue K167 in

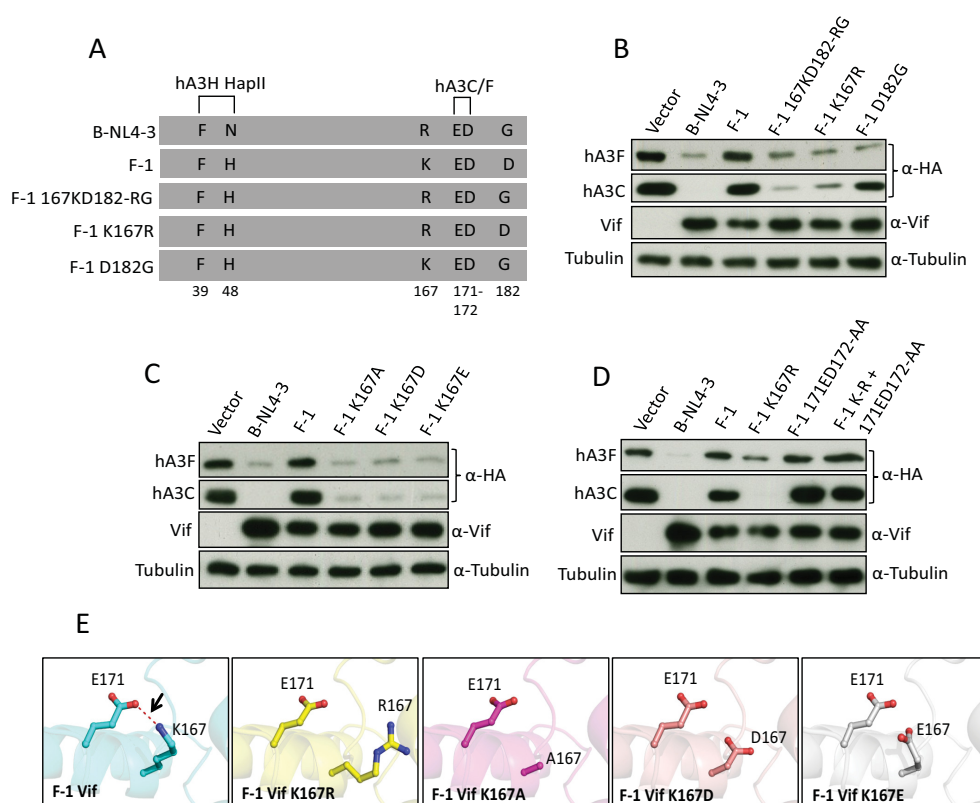


FIG 8 Identification of important residues in subtype F-1 Vif that determine its counteraction of hA3C/F. (A) Schematic structure of F-1 Vif mutants. The N-terminal hA3H HapII box and C-terminal hA3C/F box are shown. (B, C, and D) hA3C and hA3F were transfected into 293T cells together with B-NL4-3 Vif or with F-1 Vif or F-1 Vif mutant. A3 and Vif were detected by using anti-HA and anti-Vif antibodies. Tubulin served as a loading control. (E) The structures of wild-type F-1 Vif and F-1 Vif mutants were modeled by SWISS modeling. The internal interaction between residues 171 and 167 was analyzed by PyMOL and is shown as a red dashed line.

B-NL4-3 Vif.R167K preferred to interact with D101 but not with E171 (Fig. 9B). In F-1 Vif, a glycine was present at position 101 which had no chance to form an internal interaction with K167 (Fig. 9B). Thus, replacing D101 in B-NL4-3 Vif.R167K with glycine could rebuild the connection of E171-K167 (Fig. 9B). To test this hypothesis, we analyzed the counteractivity of B-NL4-3 Vif.D101G and B-NL4-3 Vif.D101G+R107K against different amounts of hA3C- or hA3F-transfected (150 ng, 250 ng, or 350 ng) expression plasmid. We found that B-NL4-3 Vif.D101G+R107K reduced the capacity to induce depletion of hA3F and hA3C compared with B-NL4-3 wild-type Vif (Fig. 9C). As shown in Fig. 9D, three discontinuous motifs (shown in red) in Vif (B-NL4-3) formed the hA3F and hA3C interaction surface, while the residues R167 and D101, which determined internal interaction with the F3 box, are shown in magenta (Fig. 9D). Taken together, these results suggest that internal interactions in the Vif protein can also influence the Vif-A3 interaction.

DISCUSSION

The antiviral activity of A3C against HIV-1ΔVif is not as potent as that of A3G and A3F. While several studies found no antiviral activity of hA3C, others reported that the infectivity of HIV-1ΔVif can be reduced by 50% by hA3C and restored by its Vif protein (11, 19–23, 26–28). We do not know whether ΔVif mutants of the various HIV-1 subtypes differ in their sensitivity to hA3C. However, of the 21 Vif isolates we tested here from HIV-1 group M, N,

and O subtypes, only four Vifs (A-1, B-1, D-1, and F-1) showed reduced counteractivity to hA3C. Thus, the capacity of HIV-1 Vifs to counteract hA3C is highly conserved. Our data indicate that HIV-1 Vif uses a different binding surface to interact with A3C and the related A3F and that impairing the anti-A3C/A3F activity does not prevent the counteraction of A3G.

A previous study identified several hydrophobic or negatively charged residues between the α2 and α3 helix of hA3C that bind to HIV-1 Vif (63), and it was also reported that C130A, C130L, and E133A substitutions in hA3C did not impair HIV-1 Vif-induced degradation. However, in our study, replacement of C130 and E133 in hA3C with residues N130 and Q133, which are found in rhA3C (hA3C CE-NQ mutant in Fig. 4C), resulted in resistance to HIV-1 Vif (Fig. 4D). Both cysteine and asparagine residues belong to polar amino acids, but the E133Q substitution alters the residue from negatively polar acidic to uncharged (whereas alanine is nonpolar). These observations suggest that the charge of residue 133 in hA3C is important for the interaction with HIV-1 Vif. In addition, we demonstrated the E324 of hA3F is essential for HIV-1 Vif interaction, while the equivalent residue E141 in hA3C is not. These results are consistent with Kitamura et al. (63). In the Vif protein, a recent study described that mutations in a basic Vif interface patch (R17, E171, and R173) had distinct influence on degradation of hA3C and hA3F (66). In our experiments, we found that the additional residue G182 of HIV-1 Vif had different effects on the counteraction of hA3C and

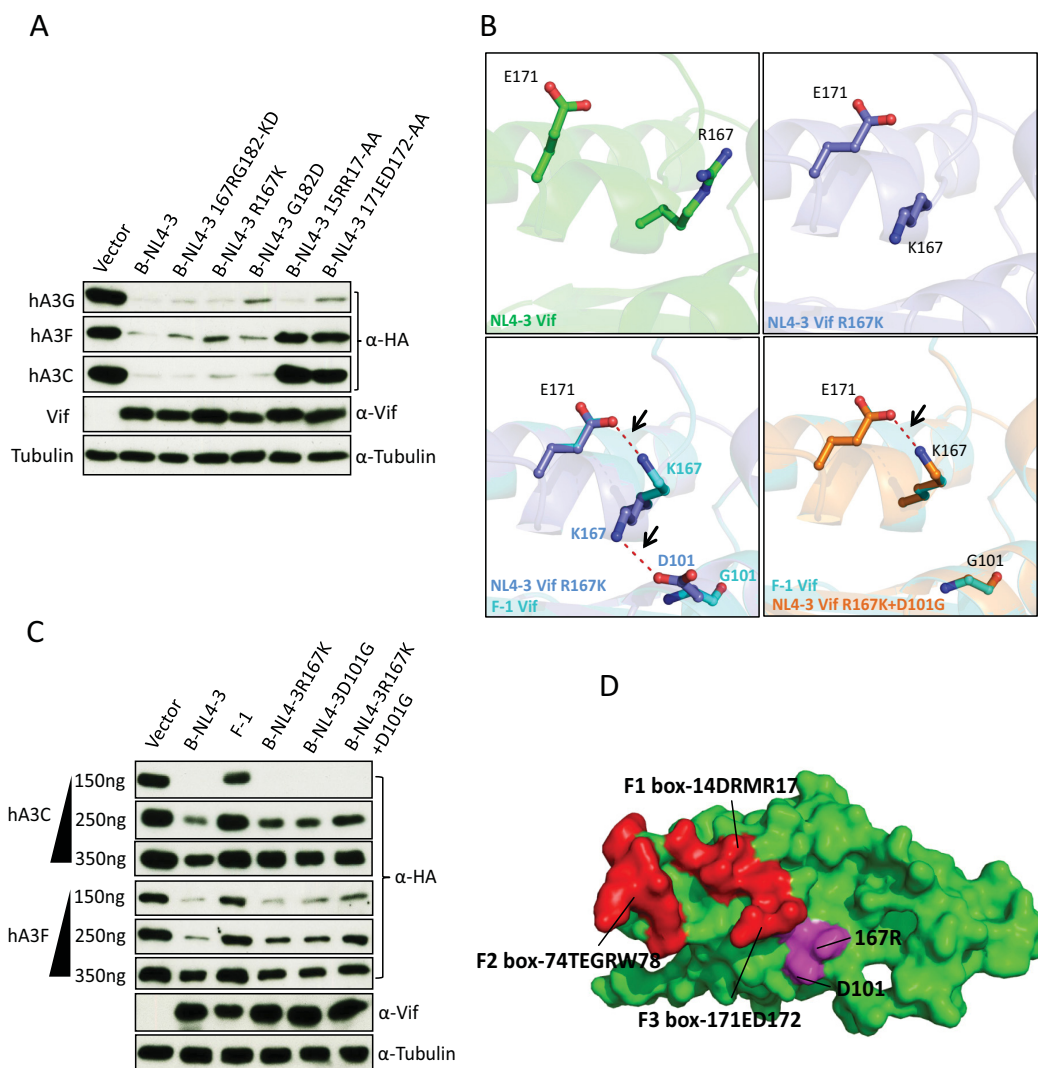


FIG 9 Structural differences between B-NL4-3 Vif and F-1 Vif. (A and C) hA3C and hA3F or hA3G expression plasmids were cotransfected together with B-NL4-3 Vif and its mutants. A3 and Vif were detected by using anti-HA and anti-Vif antibodies. Tubulin served as a loading control. (B) The structures of B-NL4-3, F-1 Vif, and their variants were modeled by SWISS modeling. The internal interaction between residues 171, 167, and 101 were analyzed by PyMOL, and the distances between interacting side chains are between 3.4 and 3.8 Å. The internal interaction is shown as a red dashed line. (D) Structure analysis of HIV-1 Vif (PDB entry 4N9F) for hA3C/hA3F interaction sites. Three discontinuous HIV-1 Vif motifs (F1 box, F2 box, and F3 box) that interact with hA3C/F are shown in red. 167R that contacted the F3 box is shown in magenta.

hA3F (Fig. 8B and 9C). These findings strongly support that HIV-1 Vif interaction interfaces in hA3C and hA3F are not identical.

A recent study reported that amino acids P16, M19, E20, P44, H45, and V47 of HIV-2 Vif are important for interaction with A3F, whereas the 140AGARV144 motif in the N-terminal half of A3F is critical for interaction with HIV-2 Vif (74). Here, we found that all tested A3C proteins were sensitive to HIV-2, SIVagm, and SIVmac Vif. hA3C and the C terminus of hA3F are homologous (5). A3C proteins are strong inhibitors of SIVΔVif, while SIVagm and SIVmac Vifs reduced the protein levels of hA3C, cpzA3C, smmA3C, agmA3C, and rhaA3C (Fig. 1B and 2). This counteraction might promote SIV cross-species transmissions between primates. Compared to HIV-1 Vif, SIVcpz Vif is more active against hA3C and cpzA3C (Fig. 2F). The role of the human A3C protein during SIVcpz transmission to the human population is currently

unclear. Letko et al. reported that gorilla A3G resists degradation of HIV-1 and most SIV Vifs, serving as a barrier to SIV transmission (51). Compared to the sequence of cpzA3C or hA3C, the region of amino acids 128 to 133 of gorA3C is quite different (128YPCYQE133 presents in cpzA3C and hA3C, 128DTDYQE133 in gorA3C). Whether the replacement of 128YPC130 with 128DTD130 affects gorA3C degradation by HIV-1 or SIV Vifs needs further investigation.

Here, we found that rhaA3C and smmA3C were resistant to HIV-1 Vif (Fig. 1B). However, coimmunoprecipitation assays showed that rhaA3C, smmA3C, and the hA3C.CE-NQ mutant, which was insensitive to HIV-1 Vif, still bound to HIV-1 Vif. These results indicate that binding detected by co-IPs is not a proper reporter for Vif-mediated counteraction affecting the protein levels. Indeed, several previous studies reported that binding of Vif and A3 is not the only determinant for complete Vif-mediated

ated degradation (53, 57, 83–85). Kitamura et al. identified several residues between $\alpha 2$ and $\alpha 3$ helices of A3C binding to HIV-1 Vif (63). These residues are conserved in smmA3C (Fig. 1A), which might be the reason that binding of smmA3C to HIV-1 Vif was observed in our study. Recently a wobble model of the evolution of the Vif-A3 interaction was presented (64), implicating that among the Vif-A3 interactions, some binding sites are essential while others provide additional stabilizing contacts. Based on this idea, where only Vif forms a sufficient network of interactions with A3s, a functional interaction is formed. Suboptimal, destabilized interactions could be restored by the evolution of compensatory changes in the Vif-A3 interface. Thus, it is possible that the Vif interaction sites in hA3C identified by Kitamura et al. are the main interactions (63), while C130 and E133 in hA3C represent one of the relevant additional interacting points for hA3C-Vif complex formation.

Previous studies have identified three discontinuous motifs of HIV-1 Vif specifically involved in interaction with hA3F: F1-(14DRMR17), F2-(74TGEDW79), and F3-(171EDRW174) (66, 84). In addition, conserved tryptophans in Vif outside the F1, F2, and F3 box have been reported to be important for hA3F degradation (86). Here, we identified HIV-1 Vif subtype F-1, which did not degrade hA3C and hA3F, as was determined by residue K167. Our experimental results suggest that the A3-Vif interaction surface differs in Vif proteins of B-NL4-3 and F-1. Structure modeling suggested that E171, K167, and D101 in HIV-1 Vif can form internal noncovalent interactions, while the mechanism of how this internal interaction influences the Vif-A3 interaction needs further investigation, especially due to its intrinsic disordered nature (87). Vif proteins of different F-1 isolates show variability at 101 and 167 sites (G101D or K167Q/R), but E171 is conserved (data not shown). The hA3F/hA3C degradation activities of these F-1 Vif variants require further investigation. Interestingly, Vif from the F-1 subtype did not degrade hA3C and hA3F, whereas it counteracted hA3G and hA3H hapII (Fig. 7C) (71). It is unknown how the F-1 subtype virus, an isolate from Brazil, escapes the restriction of hA3F. Recently, single-nucleotide polymorphism (SNP) haplotypes of hA3F were reported, and an I231V variant with an allele (V) frequency of 48% in European Americans was associated with significantly lower set-point viral load and lower rate of progression to AIDS (88). Thus, it is possible that the hA3F of the host of our F-1 subtype had a unique haplotype that can be counteracted by F-1 Vif.

In summary, we found that rhA3C and smmA3C were resistant, but hA3C was sensitive, to HIV-1 Vif-triggered depletion, which was regulated by residues 130 and 133. Moreover, we identified that the Vif of HIV-1 F-1 subtype could not degrade hA3C as well as hA3F but was counteractive against hA3G and hA3H hapII. Residues 167 and 182 of F-1 Vif were critical for its inactivity against hA3C and hA3F, which was due to the intramolecular interaction with the F3 box. These findings provide an important addition to the model of the HIV-1 Vif and hA3C/F interaction and also advance our understanding of host-virus interactions during cross-species transmission and viral evolution.

ACKNOWLEDGMENTS

We thank Wioletta Hörschken for excellent technical assistance. We thank Neeltje Kootstra, Nathaniel R. Landau, and Viviana Simon for reagents. The following reagents were obtained through the NIH AIDS

Research and Reference Reagent Program, Division of AIDS, NIAID, NIH: HIV-1 HXB2 Vif antiserum (number 2221) from Dana Gabuzda, monoclonal antibody to HIV-1 p24 (AG3.0) from Jonathan Allan, and SIVCPZTAN1.910 (number 11496) and SIVCPZTAN2.69 (number 11497) from Jun Takehisa, Matthias H. Kraus, and Beatrice H. Hahn.

FUNDING INFORMATION

This work, including the efforts of Carsten Münk, was funded by Heinz Ansmann Foundation. This work, including the efforts of Zeli Zhang and Qinyong Gu, was funded by China Scholarship Council (CSC).

REFERENCES

- Sharp PM, Hahn BH. 2011. Origins of HIV and the AIDS pandemic. *Cold Spring Harb Perspect Med* 1:a006841.
- Harris RS, Dudley JP. 2015. APOBECs and virus restriction. *Virology* 479-480:131–145.
- Simon V, Bloch N, Landau NR. 2015. Intrinsic host restrictions to HIV-1 and mechanisms of viral escape. *Nat Immunol* 16:546–553. <http://dx.doi.org/10.1038/ni.3156>.
- LaRue RS, Andresdottir V, Blanchard Y, Conticello SG, Derse D, Emerman M, Greene WC, Jonsson SR, Landau NR, Löchelt M, Malik HS, Malim MH, Münk C, O'Brien SJ, Pathak VK, Strebel K, Wain-Hobson S, Yu XF, Yuhki N, Harris RS. 2009. Guidelines for naming nonprimate APOBEC3 genes and proteins. *J Virol* 83:494–497. <http://dx.doi.org/10.1128/JVI.01976-08>.
- Münk C, Willemsen A, Bravo IG. 2012. An ancient history of gene duplications, fusions and losses in the evolution of APOBEC3 mutators in mammals. *BMC Evol Biol* 12:71. <http://dx.doi.org/10.1186/1471-2148-12-71>.
- Ooms M, Brayton B, Letko M, Maio SM, Pilcher CD, Hecht FM, Barbour JD, Simon V. 2013. HIV-1 Vif adaptation to human APOBEC3H haplotypes. *Cell Host Microbe* 14:411–421. <http://dx.doi.org/10.1016/j.chom.2013.09.006>.
- Refsland EW, Hultquist JF, Harris RS. 2012. Endogenous origins of HIV-1 G-to-A hypermutation and restriction in the nonpermissive T cell line CEM2n. *PLoS Pathog* 8:e1002800. <http://dx.doi.org/10.1371/journal.ppat.1002800>.
- Zhang H, Yang B, Pomerantz RJ, Zhang C, Arunachalam SC, Gao L. 2003. The cytidine deaminase CEM15 induces hypermutation in newly synthesized HIV-1 DNA. *Nature* 424:94–98. <http://dx.doi.org/10.1038/nature01707>.
- Mangeat B, Turelli P, Caron G, Friedli M, Perrin L, Trono D. 2003. Broad antiretroviral defence by human APOBEC3G through lethal editing of nascent reverse transcripts. *Nature* 424:99–103. <http://dx.doi.org/10.1038/nature01709>.
- Mariani R, Chen D, Schröfelbauer B, Navarro F, König R, Bollman B, Münk C, Nymark-McMahon H, Landau NR. 2003. Species-specific exclusion of APOBEC3G from HIV-1 virions by Vif. *Cell* 114:21–31. [http://dx.doi.org/10.1016/S0092-8674\(03\)00515-4](http://dx.doi.org/10.1016/S0092-8674(03)00515-4).
- Hultquist JF, Lengyel JA, Refsland EW, LaRue RS, Lackey L, Brown WL, Harris RS. 2011. Human and rhesus APOBEC3D, APOBEC3F, APOBEC3G, and APOBEC3H demonstrate a conserved capacity to restrict Vif-deficient HIV-1. *J Virol* 85:11220–11234. <http://dx.doi.org/10.1128/JVI.05238-11>.
- Wiegand HL, Doehe BP, Bogerd HP, Cullen BR. 2004. A second human antiretroviral factor, APOBEC3F, is suppressed by the HIV-1 and HIV-2 Vif proteins. *EMBO J* 23:2451–2458. <http://dx.doi.org/10.1038/sj.emboj.7600246>.
- Iwatani Y, Chan DS, Wang F, Maynard KS, Sugiura W, Gronenborn AM, Rouzina I, Williams MC, Musier-Forsyth K, Levin JG. 2007. Deaminase-independent inhibition of HIV-1 reverse transcription by APOBEC3G. *Nucleic Acids Res* 35:7096–7108. <http://dx.doi.org/10.1093/nar/gkm750>.
- Mbisa JL, Bu W, Pathak VK. 2010. APOBEC3F and APOBEC3G inhibit HIV-1 DNA integration by different mechanisms. *J Virol* 84:5250–5259. <http://dx.doi.org/10.1128/JVI.02358-09>.
- Wang X, Ao Z, Chen L, Kobinger G, Peng J, Yao X. 2012. The cellular antiviral protein APOBEC3G interacts with HIV-1 reverse transcriptase and inhibits its function during viral replication. *J Virol* 86:3777–3786. <http://dx.doi.org/10.1128/JVI.06594-11>.
- Holmes RK, Koning FA, Bishop KN, Malim MH. 2007. APOBEC3F can inhibit the accumulation of HIV-1 reverse transcription products in the

- absence of hypermutation. Comparisons with APOBEC3G. *J Biol Chem* 282:2587–2595.
17. Mbisa JL, Barr R, Thomas JA, Vandegraaff N, Dorweiler IJ, Svarovskaia ES, Brown WL, Mansky LM, Gorelick RJ, Harris RS, Engelman A, Pathak VK. 2007. Human immunodeficiency virus type 1 cDNAs produced in the presence of APOBEC3G exhibit defects in plus-strand DNA transfer and integration. *J Virol* 81:7099–7110. <http://dx.doi.org/10.1128/JVI.00272-07>.
 18. Gillick K, Pollpeter D, Phalora P, Kim EY, Wolinsky SM, Malim MH. 2013. Suppression of HIV-1 infection by APOBEC3 proteins in primary human CD4(+) T cells is associated with inhibition of processive reverse transcription as well as excessive cytidine deamination. *J Virol* 87:1508–1517. <http://dx.doi.org/10.1128/JVI.02587-12>.
 19. Yu Q, Chen D, König R, Mariani R, Unutmaz D, Landau NR. 2004. APOBEC3B and APOBEC3C are potent inhibitors of simian immunodeficiency virus replication. *J Biol Chem* 279:53379–53386. <http://dx.doi.org/10.1074/jbc.M408802200>.
 20. Stauch B, Hofmann H, Perkovic M, Weisel M, Kopietz F, Cichutek K, Münk C, Schneider G. 2009. Model structure of APOBEC3C reveals a binding pocket modulating ribonucleic acid interaction required for encapsidation. *Proc Natl Acad Sci U S A* 106:12079–12084. <http://dx.doi.org/10.1073/pnas.0900979106>.
 21. Perkovic M, Schmidt S, Marino D, Russell RA, Stauch B, Hofmann H, Kopietz F, Kloke BP, Zielonka J, Strover H, Hermle J, Lindemann D, Pathak VK, Schneider G, Löchelt M, Cichutek K, Münk C. 2009. Species-specific inhibition of APOBEC3C by the prototype foamy virus protein bet. *J Biol Chem* 284:5819–5826. <http://dx.doi.org/10.1074/jbc.M808853200>.
 22. Chaipan C, Smith JL, Hu WS, Pathak VK. 2013. APOBEC3G restricts HIV-1 to a greater extent than APOBEC3F and APOBEC3DE in human primary CD4+ T cells and macrophages. *J Virol* 87:444–453. <http://dx.doi.org/10.1128/JVI.00676-12>.
 23. Dang Y, Wang X, Esselman WJ, Zheng YH. 2006. Identification of APOBEC3DE as another antiretroviral factor from the human APOBEC family. *J Virol* 80:10522–10533. <http://dx.doi.org/10.1128/JVI.01123-06>.
 24. Warren CJ, Xu T, Guo K, Griffin LM, Westrich JA, Lee D, Lambert PF, Santiago ML, Pyeon D. 2015. APOBEC3A functions as a restriction factor of human papillomavirus. *J Virol* 89:688–702. <http://dx.doi.org/10.1128/JVI.02383-14>.
 25. Ahasan MM, Wakae K, Wang Z, Kitamura K, Liu G, Koura M, Imayasu M, Sakamoto N, Hanaoka K, Nakamura M, Kyo S, Kondo S, Fujiwara H, Yoshizaki T, Mori S, Kukimoto I, Muramatsu M. 2015. APOBEC3A and 3C decrease human papillomavirus 16 pseudovirion infectivity. *Biochem Biophys Res Commun* 457:295–299. <http://dx.doi.org/10.1016/j.bbrc.2014.12.103>.
 26. Marin M, Golem S, Rose KM, Kozak SL, Kabat D. 2008. Human immunodeficiency virus type 1 Vif functionally interacts with diverse APOBEC3 cytidine deaminases and moves with them between cytoplasmic sites of mRNA metabolism. *J Virol* 82:987–998. <http://dx.doi.org/10.1128/JVI.01078-07>.
 27. Bishop KN, Holmes RK, Sheehy AM, Davidson NO, Cho SJ, Malim MH. 2004. Cytidine deamination of retroviral DNA by diverse APOBEC proteins. *Curr Biol* 14:1392–1396. <http://dx.doi.org/10.1016/j.cub.2004.06.057>.
 28. Langlois MA, Beale RC, Conticello SG, Neuberger MS. 2005. Mutational comparison of the single-domained APOBEC3C and double-domained APOBEC3F/G anti-retroviral cytidine deaminases provides insight into their DNA target site specificities. *Nucleic Acids Res* 33:1913–1923. <http://dx.doi.org/10.1093/nar/gki343>.
 29. Ooms M, Krikoni A, Kress AK, Simon V, Münk C. 2012. APOBEC3A, APOBEC3B, and APOBEC3H haplotype 2 restrict human T-lymphotropic virus type 1. *J Virol* 86:6097–6108. <http://dx.doi.org/10.1128/JVI.06570-11>.
 30. Doehle BP, Schafer A, Cullen BR. 2005. Human APOBEC3B is a potent inhibitor of HIV-1 infectivity and is resistant to HIV-1 Vif. *Virology* 339:281–288. <http://dx.doi.org/10.1016/j.virol.2005.06.005>.
 31. Bogerd HP, Wiegand HL, Doehle BP, Cullen BR. 2007. The intrinsic antiretroviral factor APOBEC3B contains two enzymatically active cytidine deaminase domains. *Virology* 364:486–493. <http://dx.doi.org/10.1016/j.virol.2007.03.019>.
 32. Mahieux R, Suspene R, Delebecque F, Henry M, Schwartz O, Wain-Hobson S, Vartanian JP. 2005. Extensive editing of a small fraction of human T-cell leukemia virus type 1 genomes by four APOBEC3 cytidine deaminases. *J Gen Virol* 86:2489–2494.
 33. Burns MB, Temiz NA, Harris RS. 2013. Evidence for APOBEC3B mutagenesis in multiple human cancers. *Nat Genet* 45:977–983. <http://dx.doi.org/10.1038/ng.2701>.
 34. Land AM, Wang J, Law EK, Aberle R, Kirmaier A, Krupp A, Johnson WE, Harris RS. 2015. Degradation of the cancer genomic DNA deaminase APOBEC3B by SIV Vif. *Oncotarget* 6:39969–39979.
 35. Roberts SA, Lawrence MS, Klimczak LJ, Grimm SA, Fargo D, Stojanov P, Kiezun A, Kryukov GV, Carter SL, Saksena G, Harris S, Shah RR, Resnick MA, Getz G, Gordenin DA. 2013. An APOBEC cytidine deaminase mutagenesis pattern is widespread in human cancers. *Nat Genet* 45:970–976. <http://dx.doi.org/10.1038/ng.2702>.
 36. Alexandrov LB, Nik-Zainal S, Wedge DC, Aparicio SA, Behjati S, Biankin AV, Bignell GR, Bolli N, Borg A, Borresen-Dale AL, Boyault S, Burkhardt B, Butler AP, Caldas C, Davies HR, Desmedt C, Eils R, Eyfjord JE, Foekens JA, Greaves M, Hosoda F, Hutter B, Illic T, Imbeaud S, Imielinski M, Jager N, Jones DT, Jones D, Knappskog S, Kool M, Lakhani SR, Lopez-Otin C, Martin S, Munshi NC, Nakamura H, Northcott PA, Pajic M, Papaemmanuil E, Paradiso A, Pearson JV, Puente XS, Raine K, Ramakrishna M, Richardson AL, Richter J, Rosenstiel P, Schlesner M, Schumacher TN, Span PN, Teague JW, Totoki Y, Tutt AN, Valdes-Mas R, van Buuren MM, van't Veer L, Vincent-Salomon A, Waddell N, Yates LR, Australian Pancreatic Cancer Genome Initiative, ICGC Breast Cancer Consortium, ICGC MML-Seq Consortium, ICGC PedBrain I, Zucman-Rossi J, Futreal PA, McDermott U, Lichter P, Meyerson M, Grimmond SM, Siebert R, Campo E, Shibata T, Pfister SM, Campbell PJ, Stratton MR. 2013. Signatures of mutational processes in human cancer. *Nature* 500:415–421. <http://dx.doi.org/10.1038/nature12477>.
 37. Nik-Zainal S, Wedge DC, Alexandrov LB, Petljak M, Butler AP, Bolli N, Davies HR, Knappskog S, Martin S, Papaemmanuil E, Ramakrishna M, Shlien A, Simonic I, Xue Y, Tyler-Smith C, Campbell PJ, Stratton MR. 2014. Association of a germline copy number polymorphism of APOBEC3A and APOBEC3B with burden of putative APOBEC-dependent mutations in breast cancer. *Nat Genet* 46:487–491. <http://dx.doi.org/10.1038/ng.2955>.
 38. Taylor BJ, Nik-Zainal S, Wu YL, Stebbings LA, Raine K, Campbell PJ, Rada C, Stratton MR, Neuberger MS. 2013. DNA deaminases induce break-associated mutation showers with implication of APOBEC3B and 3A in breast cancer kataegis. *eLife* 2:e00534.
 39. Xu R, Zhang X, Zhang W, Fang Y, Zheng S, Yu XF. 2007. Association of human APOBEC3 cytidine deaminases with the generation of hepatitis virus B x antigen mutants and hepatocellular carcinoma. *Hepatology* 46:1810–1820. <http://dx.doi.org/10.1002/hep.21893>.
 40. Yu X, Yu Y, Liu B, Luo K, Kong W, Mao P, Yu XF. 2003. Induction of APOBEC3G ubiquitination and degradation by an HIV-1 Vif-Cul5-SCF complex. *Science* 302:1056–1060. <http://dx.doi.org/10.1126/science.1089591>.
 41. Jager S, Kim DY, Hultquist JF, Shindo K, LaRue RS, Kwon E, Li M, Anderson BD, Yen L, Stanley D, Mahon C, Kane J, Franks-Skiba K, Cimermanic P, Burlingame A, Sali A, Craik CS, Harris RS, Skiba JD, Krogan NJ. 2012. Vif hijacks CBF-beta to degrade APOBEC3G and promote HIV-1 infection. *Nature* 481:371–375.
 42. Zhang W, Du J, Evans SL, Yu Y, Yu XF. 2012. T-cell differentiation factor CBF-beta regulates HIV-1 Vif-mediated evasion of host restriction. *Nature* 481:376–379.
 43. Derse D, Hill SA, Princler G, Lloyd P, Heidecker G. 2007. Resistance of human T cell leukemia virus type 1 to APOBEC3G restriction is mediated by elements in nucleocapsid. *Proc Natl Acad Sci U S A* 104:2915–2920. <http://dx.doi.org/10.1073/pnas.0609444104>.
 44. Löchelt M, Romen F, Bastone P, Muckenfuss H, Kirchner N, Kim YB, Truyen U, Rosler U, Battenberg M, Saib A, Flory E, Cichutek K, Münk C. 2005. The antiretroviral activity of APOBEC3 is inhibited by the foamy virus accessory Bet protein. *Proc Natl Acad Sci U S A* 102:7982–7987. <http://dx.doi.org/10.1073/pnas.0501445102>.
 45. Stavrou S, Nitta T, Kotla S, Ha D, Nagashima K, Rein AR, Fan H, Ross SR. 2013. Murine leukemia virus glycosylated Gag blocks apolipoprotein B editing complex 3 and cytosolic sensor access to the reverse transcription complex. *Proc Natl Acad Sci U S A* 110:9078–9083. <http://dx.doi.org/10.1073/pnas.1217399110>.
 46. Rosales Gerpe MC, Renner TM, Belanger K, Lam C, Aydin H, Langlois MA. 2015. N-linked glycosylation protects gammaretroviruses against

- deamination by APOBEC3 proteins. *J Virol* 89:2342–2357. <http://dx.doi.org/10.1128/JVI.03330-14>.
47. Jaguva Vasudevan AA, Perkovic M, Bulliard Y, Cichutek K, Trono D, Häussinger D, Münk C. 2013. Prototype foamy virus Bet impairs the dimerization and cytosolic solubility of human APOBEC3G. *J Virol* 87:9030–9040. <http://dx.doi.org/10.1128/JVI.03385-12>.
 48. Bogerd HP, Doehle BP, Wiegand HL, Cullen BR. 2004. A single amino acid difference in the host APOBEC3G protein controls the primate species specificity of HIV type 1 virion infectivity factor. *Proc Natl Acad Sci U S A* 101:3770–3774. <http://dx.doi.org/10.1073/pnas.0307713101>.
 49. Schröfelbauer B, Chen D, Landau NR. 2004. A single amino acid of APOBEC3G controls its species-specific interaction with virion infectivity factor (Vif). *Proc Natl Acad Sci U S A* 101:3927–3932. <http://dx.doi.org/10.1073/pnas.0307132101>.
 50. Xu H, Svarovskaia ES, Barr R, Zhang Y, Khan MA, Strebel K, Pathak VK. 2004. A single amino acid substitution in human APOBEC3G anti-retroviral enzyme confers resistance to HIV-1 virion infectivity factor-induced depletion. *Proc Natl Acad Sci U S A* 101:5652–5657. <http://dx.doi.org/10.1073/pnas.0400830101>.
 51. Letko M, Silvestri G, Hahn BH, Bibollet-Ruche F, Gokcumen O, Simon V, Ooms M. 2013. Vif proteins from diverse primate lentiviral lineages use the same binding site in APOBEC3G. *J Virol* 87:11861–11871. <http://dx.doi.org/10.1128/JVI.01944-13>.
 52. Yoshikawa R, Takeuchi JS, Yamada E, Nakano Y, Ren F, Tanaka H, Münk C, Harris RS, Miyazawa T, Koyanagi Y, Sato K. 2015. Vif determines the requirement for CBF-beta in APOBEC3 degradation. *J Gen Virol* 96:887–892.
 53. Stern MA, Hu C, Saenz DT, Fadel HJ, Sims O, Peretz M, Poeschla EM. 2010. Productive replication of Vif-chimeric HIV-1 in feline cells. *J Virol* 84:7378–7395. <http://dx.doi.org/10.1128/JVI.00584-10>.
 54. Dang Y, Wang X, York IA, Zheng YH. 2010. Identification of a critical T(Q/D/E)x5ADx2(I/L) motif from primate lentivirus Vif proteins that regulate APOBEC3G and APOBEC3F neutralizing activity. *J Virol* 84:8561–8570. <http://dx.doi.org/10.1128/JVI.00960-10>.
 55. Gaur R, Strebel K. 2012. Insights into the dual activity of SIVmac239 Vif against human and African green monkey APOBEC3G. *PLoS One* 7:e48850. <http://dx.doi.org/10.1371/journal.pone.0048850>.
 56. Hatziioannou T, Princiotto M, Piatak M, Jr, Yuan F, Zhang F, Lifson JD, Bieniasz PD. 2006. Generation of simian-tropic HIV-1 by restriction factor evasion. *Science* 314:95. <http://dx.doi.org/10.1126/science.1130994>.
 57. Zhang Z, Gu Q, Jaguva Vasudevan AA, Hain A, Kloke BP, Hasheminasab S, Mulnaes D, Sato K, Cichutek K, Häussinger D, Bravo IG, Smits SH, Gohlke H, Münk C. 2016. Determinants of FIV and HIV Vif sensitivity of feline APOBEC3 restriction factors. *Retrovirology* 13:46. <http://dx.doi.org/10.1186/s12977-016-0274-9>.
 58. Larue RS, Lengyel J, Jonsson SR, Andresdottir V, Harris RS. 2010. Lentiviral Vif degrades the APOBEC3Z3/APOBEC3H protein of its mammalian host and is capable of cross-species activity. *J Virol* 84:8193–8201. <http://dx.doi.org/10.1128/JVI.00685-10>.
 59. Huthoff H, Malim MH. 2007. Identification of amino acid residues in APOBEC3G required for regulation by human immunodeficiency virus type 1 Vif and Virion encapsidation. *J Virol* 81:3807–3815. <http://dx.doi.org/10.1128/JVI.02795-06>.
 60. Letko M, Booiiman T, Kootstra N, Simon V, Ooms M. 2015. Identification of the HIV-1 Vif and human APOBEC3G protein interface. *Cell Rep* 13:1789–1799. <http://dx.doi.org/10.1016/j.celrep.2015.10.068>.
 61. Zhen A, Wang T, Zhao K, Xiong Y, Yu XF. 2010. A single amino acid difference in human APOBEC3H variants determines HIV-1 Vif sensitivity. *J Virol* 84:1902–1911. <http://dx.doi.org/10.1128/JVI.01509-09>.
 62. Ooms M, Letko M, Binka M, Simon V. 2013. The resistance of human APOBEC3H to HIV-1 NL4-3 molecular clone is determined by a single amino acid in Vif. *PLoS One* 8:e57744. <http://dx.doi.org/10.1371/journal.pone.0057744>.
 63. Kitamura S, Ode H, Nakashima M, Imahashi M, Naganawa Y, Kurosawa T, Yokomaku Y, Yamane T, Watanabe N, Suzuki A, Sugiura W, Iwatani Y. 2012. The APOBEC3C crystal structure and the interface for HIV-1 Vif binding. *Nat Struct Mol Biol* 19:1005–1010. <http://dx.doi.org/10.1038/nsmb.2378>.
 64. Richards C, Albin JS, Demir O, Shaban NM, Luengas EM, Land AM, Anderson BD, Holten JR, Anderson JS, Harki DA, Amaro RE, Harris RS. 2015. The binding interface between human APOBEC3F and HIV-1 Vif elucidated by genetic and computational approaches. *Cell Rep* 13:1781–1788. <http://dx.doi.org/10.1016/j.celrep.2015.10.067>.
 65. Smith JL, Pathak VK. 2010. Identification of specific determinants of human APOBEC3F, APOBEC3C, and APOBEC3DE and African green monkey APOBEC3F that interact with HIV-1 Vif. *J Virol* 84:12599–12608. <http://dx.doi.org/10.1128/JVI.01437-10>.
 66. Nakashima M, Ode H, Kawamura T, Kitamura S, Naganawa Y, Awazu H, Tsuzuki S, Matsuoka K, Nemoto M, Hachiya A, Sugiura W, Yokomaku Y, Watanabe N, Iwatani Y. 2016. Structural insights into HIV-1 Vif-APOBEC3F interaction. *J Virol* 90:1034–1047. <http://dx.doi.org/10.1128/JVI.02369-15>.
 67. Albin JS, LaRue RS, Weaver JA, Brown WL, Shindo K, Harjes E, Matsuo H, Harris RS. 2010. A single amino acid in human APOBEC3F alters susceptibility to HIV-1 Vif. *J Biol Chem* 285:40785–40792. <http://dx.doi.org/10.1074/jbc.M110.173161>.
 68. Land AM, Shaban NM, Evans L, Hultquist JF, Albin JS, Harris RS. 2014. APOBEC3F determinants of HIV-1 Vif sensitivity. *J Virol* 88:12923–12927. <http://dx.doi.org/10.1128/JVI.02362-14>.
 69. Zennou V, Bieniasz PD. 2006. Comparative analysis of the antiretroviral activity of APOBEC3G and APOBEC3F from primates. *Virology* 349:31–40. <http://dx.doi.org/10.1016/j.virol.2005.12.035>.
 70. Russell RA, Pathak VK. 2007. Identification of two distinct human immunodeficiency virus type 1 Vif determinants critical for interactions with human APOBEC3G and APOBEC3F. *J Virol* 81:8201–8210. <http://dx.doi.org/10.1128/JVI.00395-07>.
 71. Binka M, Ooms M, Steward M, Simon V. 2012. The activity spectrum of Vif from multiple HIV-1 subtypes against APOBEC3G, APOBEC3F, and APOBEC3H. *J Virol* 86:49–59. <http://dx.doi.org/10.1128/JVI.06082-11>.
 72. Salter JD, Morales GA, Smith HC. 2014. Structural insights for HIV-1 therapeutic strategies targeting Vif. *Trends Biochem Sci* 39:373–380. <http://dx.doi.org/10.1016/j.tibs.2014.07.001>.
 73. Dang Y, Davis RW, York IA, Zheng YH. 2010. Identification of 81LGxGxx-IxW89 and 171EDRW174 domains from human immunodeficiency virus type 1 Vif that regulate APOBEC3G and APOBEC3F neutralizing activity. *J Virol* 84:5741–5750. <http://dx.doi.org/10.1128/JVI.00079-10>.
 74. Smith JL, Izumi T, Borbet TC, Hagedorn AN, Pathak VK. 2014. HIV-1 and HIV-2 Vif interact with human APOBEC3 proteins using completely different determinants. *J Virol* 88:9893–9908. <http://dx.doi.org/10.1128/JVI.01318-14>.
 75. Zielonka J, Marino D, Hofmann H, Yuhki N, Löchelt M, Münk C. 2010. Vif of feline immunodeficiency virus from domestic cats protects against APOBEC3 restriction factors from many felids. *J Virol* 84:7312–7324. <http://dx.doi.org/10.1128/JVI.00209-10>.
 76. Takehisa J, Kraus MH, Decker JM, Li Y, Keele BF, Bibollet-Ruche F, Zambit KP, Weng Z, Santiago ML, Kamenya S, Wilson ML, Pusey AE, Bailes E, Sharp PM, Shaw GM, Hahn BH. 2007. Generation of infectious molecular clones of simian immunodeficiency virus from fecal consensus sequences of wild chimpanzees. *J Virol* 81:7463–7475. <http://dx.doi.org/10.1128/JVI.00551-07>.
 77. Muckenfuss H, Hamdorf M, Held U, Perkovic M, Lower J, Cichutek K, Flory E, Schumann GG, Münk C. 2006. APOBEC3 proteins inhibit human LINE-1 retrotransposition. *J Biol Chem* 281:22161–22172. <http://dx.doi.org/10.1074/jbc.M601716200>.
 78. Zennou V, Perez-Caballero D, Gottlinger H, Bieniasz PD. 2004. APOBEC3G incorporation into human immunodeficiency virus type 1 particles. *J Virol* 78:12058–12061. <http://dx.doi.org/10.1128/JVI.78.21.12058-12061.2004>.
 79. Bähr A, Singer A, Hain A, Vasudevan AA, Schilling M, Reh J, Riess M, Panitz S, Serrano V, Schweizer M, König R, Chanda S, Häussinger D, Kochs G, Lindemann D, Münk C. 2016. Interferon but not MxB inhibits foamy retroviruses. *Virology* 488:51–60. <http://dx.doi.org/10.1016/j.virol.2015.10.034>.
 80. Goncalves J, Jallepalli P, Gabuzda DH. 1994. Subcellular localization of the Vif protein of human immunodeficiency virus type 1. *J Virol* 68:704–712.
 81. Simm M, Shahabuddin M, Chao W, Allan JS, Volsky DJ. 1995. Aberrant Gag protein composition of a human immunodeficiency virus type 1 vif mutant produced in primary lymphocytes. *J Virol* 69:4582–4586.
 82. Bordoli L, Kiefer F, Arnold K, Benkert P, Battey J, Schwede T. 2009. Protein structure homology modeling using SWISS-MODEL workspace. *Nat Protoc* 4:1–13.
 83. Zhang W, Huang M, Wang T, Tan L, Tian C, Yu X, Kong W, Yu XF. 2008. Conserved and non-conserved features of HIV-1 and SIVagm Vif mediated suppression of APOBEC3 cytidine deaminases. *Cell Microbiol* 10:1662–1675. <http://dx.doi.org/10.1111/j.1462-5822.2008.01157.x>.

84. He Z, Zhang W, Chen G, Xu R, Yu XF. 2008. Characterization of conserved motifs in HIV-1 Vif required for APOBEC3G and APOBEC3F interaction. *J Mol Biol* 381:1000–1011. <http://dx.doi.org/10.1016/j.jmb.2008.06.061>.
85. Baig TT, Feng Y, Chelico L. 2014. Determinants of efficient degradation of APOBEC3 restriction factors by HIV-1 Vif. *J Virol* 88:14380–14395. <http://dx.doi.org/10.1128/JVI.02484-14>.
86. Tian C, Yu X, Zhang W, Wang T, Xu R, Yu XF. 2006. Differential requirement for conserved tryptophans in human immunodeficiency virus type 1 Vif for the selective suppression of APOBEC3G and APOBEC3F. *J Virol* 80:3112–3115. <http://dx.doi.org/10.1128/JVI.80.6.3112-3115.2006>.
87. Auclair JR, Green KM, Shandilya S, Evans JE, Somasundaran M, Schiffer CA. 2007. Mass spectrometry analysis of HIV-1 Vif reveals an increase in ordered structure upon oligomerization in regions necessary for viral infectivity. *Proteins* 69:270–284. <http://dx.doi.org/10.1002/prot.21471>.
88. An P, Penugonda S, Thorball CW, Bartha I, Goedert JJ, Donfield S, Buchbinder S, Binns-Roemer E, Kirk GD, Zhang W, Fellay J, Yu XF, Winkler CA. 2016. Role of APOBEC3F gene variation in HIV-1 disease progression and pneumocystis pneumonia. *PLoS Genet* 12:e1005921. <http://dx.doi.org/10.1371/journal.pgen.1005921>.

Chapter II

Determinants of FIV and HIV Vif sensitivity of feline APOBEC3 restriction factors

This work was published in the Retrovirology.

Zhang Z, Gu Q, Jaguva Vasudevan AA, Hain A, Kloke BP, Hasheminasab S, Mulnaes D, Sato K, Cichutek K, Häussinger D, Bravo IG, Smits SH, Gohlke H, Münk C. 2016. Determinants of FIV and HIV Vif sensitivity of feline APOBEC3 restriction factors. *Retrovirology* **13**:46.

(Open access)

Zeli Zhang's contribution to this work:

Z. Z. performed the experiments in Fig 1 a, b; Fig 2a, c; Fig 3d; Fig 4a, b, c; Fig 6; Fig 8; Fig 9; and Fig 10a, c, d. Z. Z. also performed most of experiments in additional files.


Z. Z. wrote most of Methods and Figure legends.

RESEARCH

Open Access



Determinants of FIV and HIV Vif sensitivity of feline APOBEC3 restriction factors

Zeli Zhang¹, Qinyong Gu¹, Ananda Ayyappan Jaguva Vasudevan¹, Anika Hain¹, Björn-Philipp Klope^{2,8}, Sascha Hasheminasab¹, Daniel Mulnaes⁴, Kei Sato^{5,6}, Klaus Cichutek², Dieter Häussinger¹, Ignacio G. Bravo⁷, Sander H. J. Smits³, Holger Gohlke⁴ and Carsten Münk^{1*} 

Abstract

Background: Feline immunodeficiency virus (FIV) is a global pathogen of Felidae species and a model system for Human immunodeficiency virus (HIV)-induced AIDS. In felids such as the domestic cat (*Felis catus*), APOBEC3 (A3) genes encode for single-domain A3Z2s, A3Z3 and double-domain A3Z2Z3 anti-viral cytidine deaminases. The feline A3Z2Z3 is expressed following read-through transcription and alternative splicing, introducing a previously untranslated exon in frame, encoding a domain insertion called linker. Only A3Z3 and A3Z2Z3 inhibit Vif-deficient FIV. Feline A3s also are restriction factors for HIV and Simian immunodeficiency viruses (SIV). Surprisingly, HIV-2/SIV Vifs can counteract feline A3Z2Z3.

Results: To identify residues in feline A3s that Vifs need for interaction and degradation, chimeric human–feline A3s were tested. Here we describe the molecular direct interaction of feline A3s with Vif proteins from cat FIV and present the first structural A3 model locating these interaction regions. In the Z3 domain we have identified residues involved in binding of FIV Vif, and their mutation blocked Vif-induced A3Z3 degradation. We further identified additional essential residues for FIV Vif interaction in the A3Z2 domain, allowing the generation of FIV Vif resistant A3Z2Z3. Mutated feline A3s also showed resistance to the Vif of a lion-specific FIV, indicating an evolutionary conserved Vif–A3 binding. Comparative modelling of feline A3Z2Z3 suggests that the residues interacting with FIV Vif have, unlike Vif-interacting residues in human A3s, a unique location at the domain interface of Z2 and Z3 and that the linker forms a homeobox-like domain protruding of the Z2Z3 core. HIV-2/SIV Vifs efficiently degrade feline A3Z2Z3 by possible targeting the linker stretch connecting both Z-domains.

Conclusions: Here we identified in feline A3s residues important for binding of FIV Vif and a unique protein domain insertion (linker). To understand Vif evolution, a structural model of the feline A3 was developed. Our results show that HIV Vif binds human A3s differently than FIV Vif feline A3s. The linker insertion is suggested to form a homeo-box domain, which is unique to A3s of cats and related species, and not found in human and mouse A3s. Together, these findings indicate a specific and different A3 evolution in cats and human.

Keywords: APOBEC3, FIV, Gene evolution, HIV, Homeobox, Homology modelling, Restriction factor, SIV, Vif

Background

APOBEC3 (A3) cytidine deaminases are anti-viral restriction factors containing either one or two zinc (Z)-binding domains found in different clade-specific gene

numbers and gene arrangements in placental mammals [1–4]. For example, primates have seven genes (A3A–A3D, A3F–A3H), while cats encode four genes (A3Z2a–A3Z2c, A3Z3) [3, 5]. These A3 proteins target broadly viruses and mobile genetic elements that depend on reverse transcription, but also show antiviral activity against unrelated viruses (for recent reviews see [6, 7]). Some retroviruses express viral A3-counteracting proteins, such as Vif of lentiviruses, Bet of foamy viruses,

*Correspondence: carsten.muenk@med.uni-duesseldorf.de

¹ Clinic for Gastroenterology, Hepatology, and Infectiology, Medical Faculty, Heinrich-Heine-University Düsseldorf, Building 23.12.U1.82, Moorenstr. 5, 40225 Düsseldorf, Germany

Full list of author information is available at the end of the article

the nucleocapsid of *Human T cell leukemia virus type 1* (HTLV-1), and the glycosylated (glyco)-Gag of *Murine leukemia virus* (MLV) [8–13]. The Vif protein prevents encapsidation of host-cell derived A3 proteins into nascent viral particles. In the absence of Vif, encapsidated A3s inhibit lentiviruses during infection by deamination of cytidines in the single-stranded DNA formed during reverse transcription, by introducing G-to-A mutations in the coding strand. Additionally, some A3s inhibit virus replication by reducing reverse transcription and integration via non-editing mechanisms [14–19].

The domestic cat *Felis catus* (Fca) is the host to many diverse retroviruses, such as the lentivirus *Feline immunodeficiency virus* (FIV), gammaretroviruses of the *Feline leukemia virus* (FeLV) group, and the spumaretrovirus *Feline foamy virus* (FFV) (for reviews see [20–23]). In a small proportion of naturally infected domestic cats, FIV causes an immunodeficiency disease similar to *Human immunodeficiency virus type 1* (HIV-1)-induced AIDS [24]. However, highly pathogenic FIV isolates can cause mortality up to 60 % under experimental conditions [25–27]. Thus, FIV infection of cats is a valuable animal model to study HIV-1 and AIDS [28–30]. In addition to the domestic cat, species-specific FIVs that might cause disease in some natural hosts have been isolated in many *Felidae* [31]. FFVs replicate in domestic cats and in other *Felidae* and are not causing disease [32–34]. In contrast, FeLVs are pathogenic and induce in domestic cats serious diseases such as lymphomas and anemia [24], but are rarely found in other *Felidae* [31].

The domestic cat, and likely all other *Felidae*, encode four A3 genes, three closely related A3Z2 genes (A3Z2a, A3Z2b, A3Z2c) and one A3Z3 gene [4, 35]. Besides the four canonical A3 proteins, the cat genome can express, by read-through transcription and alternative splicing, a fifth A3 protein, namely the double-domain A3Z2Z3, with two detected variants A3Z2bZ3 and A3Z2cZ3 (Fig. 1a). A3Z2Z3s are also found in big cats (Pantherinae), indicating evolutionary conserved gene regulation [4, 36]. FIV Vif induces proteasome-dependent degradation of feline A3Z2s, A3Z3, and A3Z2Z3 [4, 37]. The double-domain feline A3Z2Z3 contains two FIV Vif interaction regions, one in each Z-domain [36]. Interestingly, and currently unexplained, FIVΔvif can be inhibited by feline A3Z3 and A3Z2Z3, but not by A3Z2s [4, 36]. A reverse observation was made with FFVΔbet, where feline A3Z2s act as major inhibitors while A3Z3 and A3Z2Z3 only moderately reduce the infectivity of FFVΔbet [4, 10, 38, 39]. Recent data indicate that certain polymorphisms in feline A3Z3 genes correlate with the susceptibility to FIV and/or FeLV infections [40].

FIV Vif induces the poly-ubiquitination of feline A3s and bridges A3s to an E3 ubiquitin ligase complex containing

Cullin5 (Cul5), Elongin B/C (EloB/C), and RING-box protein RBX2 [37]; HIV-1 Vif forms a similar E3-ligase complex [41–43]. However, while HIV-1 Vif needs to additionally interact with the CBF-β protein to be stabilized and form this multiprotein complex [44, 45], FIV Vif does not bind CBF-β, and the FIV Vif-induced degradation of feline A3s does not require CBF-β to be expressed [46–49]. HIV-1 Vif cannot counteract feline A3s, and HIV-1 is therefore inhibited to various degrees by all feline A3s, with A3Z2Z3 displaying the strongest anti-HIV activity [36, 50–52]. The mechanistic reason preventing HIV-1 Vif from degrading feline A3s is unclear, especially because HIV-1 Vif and feline A3Z2Z3 are recovered together using co-immunoprecipitation assays [51]. In contrast to the Vif protein of HIV-1, Vif of Simian immunodeficiency virus from macaques (SIVmac) induces degradation of feline A3s [46, 51]. To assess the feasibility of generating an animal model for the human system based on FIV, we and others cloned FIV vif into HIV-1 and proved that in feline cell lines the A3 proteins are the dominant restriction factors against HIV-1 [36, 51].

In order to understand the FIV Vif interaction with feline A3 proteins, we identified in this study important A3 residues and used a homology model of feline A3Z2Z3 to describe the structure–function relationship of these potential FIV Vif binding amino acids.

Results

FIV and HIV-2/SIVmac/smm Vif induced degradation of felines A3s

In order to identify the molecular interaction of the FIV Vif protein and feline A3 proteins, we used FIV of domestic cats (*Felis catus*, Fca), hereafter referred as FIV. Co-transfection experiments of cat-derived A3s and FIV Vif expression plasmids were performed in 293T cells. All A3 constructs expressed the corresponding A3 protein as a C-terminal HA-tag, whereas Vif was expressed as a C-terminal V5-tag fusion protein. In addition, we also studied Vifs derived from HIV-1, HIV-2, SIVmac, and SIVsmm. Immunoblots of protein extracts from cells co-expressing both A3 and Vif were used as a read-out for degradation of the respective A3 protein. Results in Fig. 1b show that FIV Vif induces degradation of single-domain feline A3Z2a, A3Z2b, A3Z2c, A3Z3, and double-domain A3Z2bZ3 and A3Z2cZ3 in agreement with previous reports [4, 36, 37, 51]. The double-domain feline A3Z2bZ3 and A3Z2cZ3 were degraded by SIVmac Vif as seen before [46, 51], as well by the Vifs of SIVsmm and HIV-2. For subsequent experiments we used the expression plasmid FcaA3Z2bZ3, hereafter referred to as feline A3Z2Z3 for simplicity.

To understand, whether FIV Vif binds directly to feline A3s, we expressed A3Z2 and A3Z3 as GST fusion

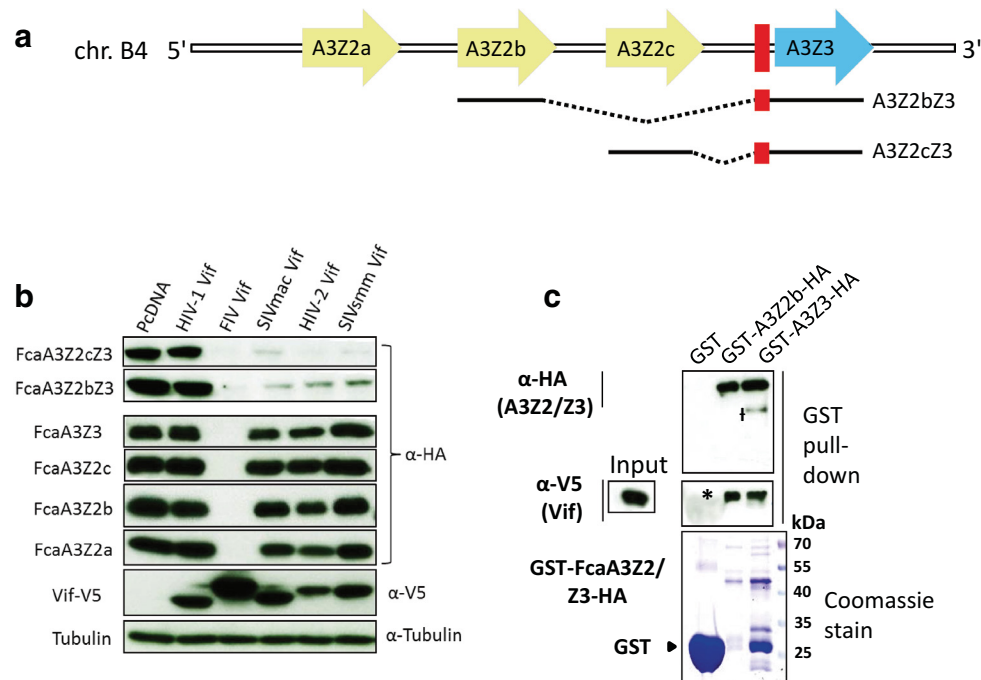


Fig. 1 The interaction of feline APOBEC3s with FIV Vif. **a** Representation of APOBEC3 (A3) genes in the genome of *Felis catus*, chromosome (chr.) B4. Coding regions of the A3 genes (A3Z2a, A3Z2b, A3Z2c, A3Z3) shown as arrows. Red rectangle exon 2 of A3Z3 that is untranslated in the A3Z3 mRNA, however translated ("linker domain") in readthrough transcripts A3Z2bZ3 and A3Z2cZ3. Spliced-out introns (dashed lines) are indicated, mRNAs for A3Z2s and A3Z3 not shown. For details, see references [4, 36]. **b** 293T cells were transfected with expression plasmids for FcaA3Z2a, FcaA3Z2b, FcaA3Z2c, FcaA3Z3, FcaA3Z2bZ3 and FcaA3Z2cZ3 together with HIV-1, SIVmac, HIV-2 and SIVsmm or FIV Vif or no Vif (replaced by pcDNA3.1). FcaA3s, Vifs and tubulin were visualized by immunoblot using anti-HA, anti-V5 and anti-tubulin antibodies. **c** Immunoprecipitation of *E. coli* expressed FcaA3Z2 and -Z3 (GST fusion proteins) after mixing with 293T-derived FIV Vif (Vif-V5). Asterisk indicates the impression of GST blob on the blot and Dagger denotes for a possible degradation product of FcaA3Z3

proteins in *E. coli*. Recombinant A3s were purified by affinity chromatography and mixed with lysates of 293T cells expressing FIV Vif. Following GST pulldown, immunoblots showed Vif binding to GST-A3Z2 and to GST-A3Z3 but not to GST (Fig. 1c). We further explored the interaction of FIV Vif with feline A3s by analyzing the cellular distribution in co-expressing cells. HOS cells were transfected either with plasmids encoding for feline A3Z2, A3Z3, or A3Z2Z3 alone or together with a plasmid encoding for FIV Vif-TLQAAA. The TLQ to AAA mutation in the Vif putative BC-box prevents its interaction with the E3 complex [37]. Feline A3 proteins showed a mostly cytoplasmic localization with no or very little nuclear A3, and feline A3Z3 localized in addition to the nucleoli (Additional file 1: Fig. S1, compare to Fig. S4). Nucleolar localization of A3Z3 proteins derived from humans and horses had been described before [53]. Very similar to the A3s, FIV Vif-TLQAAA showed a cytoplasmic distribution with little presence in the nucleus. Under these experimental conditions, strong co-localization of Vif and A3s was detected in cytoplasmic areas near the nucleus (Additional file 1: Fig. S1).

Identification of feline A3Z3 residues important for FIV Vif induced degradation

Feline A3Z3 and A3Z2Z3 are the restriction factors for FIV Δ vif, whereas A3Z2s are not active against FIV Δ vif [4, 36, 37, 51]. To characterize the Vif interaction with residues in feline A3Z3, A3Z3s derived from humans (A3H haplotype II, HsaA3H) and big cats (tiger, *Panthera tigris*, Pti; lion, *Panthera leo*, Ple; lynx, *Lynx lynx*, Lly; puma, *Puma concolor*, Pco) (protein alignments are highlighted in Additional file 1: Fig. S2) were used in co-transfection experiments with FIV Vif. A3s derived from tiger, lion, lynx, and puma were efficiently degraded by FIV Vif (Fig. 2a). Because A3H was resistant to FIV Vif-induced degradation, the construction of Hsa-Fca chimeric A3Z3s promised a rational approach to identify the A3Z3/FIV-Vif binding region. The chimeras Z3C1 and Z3C2 spanned respectively amino acids 1–22 and 1–50 of feline A3Z3, with the remaining part being derived from A3H, whereas Z3C6 and Z3C7 were mostly feline A3Z3 with residues 1–22 or 1–50 derived from A3H (Fig. 2b). Among the four A3Z3 chimeras, Z3C2 and Z3C6 were efficiently degraded by FIV Vif, while Z3C1

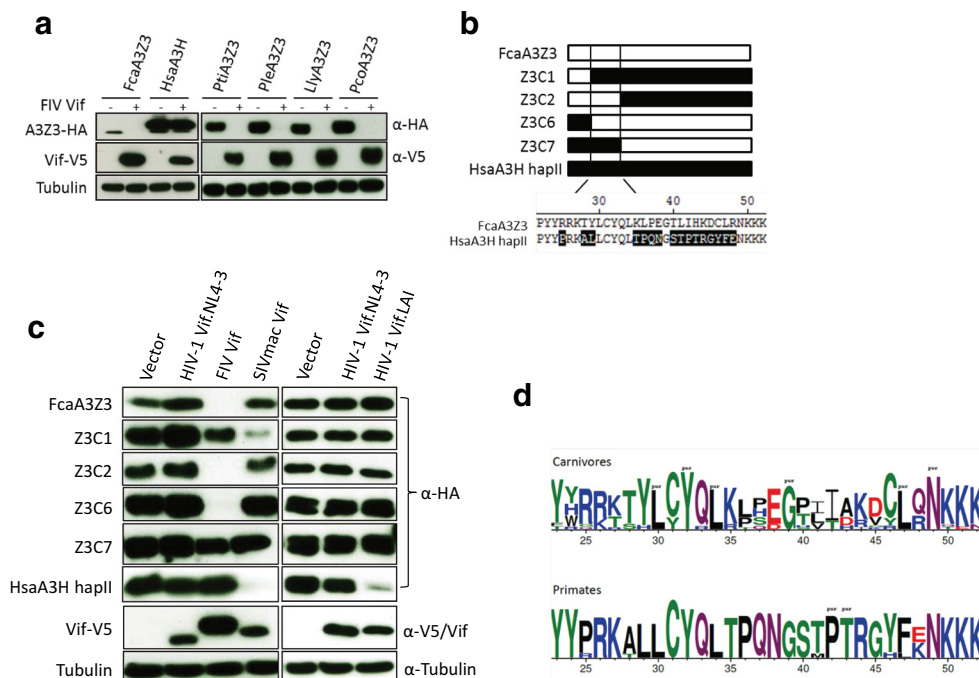


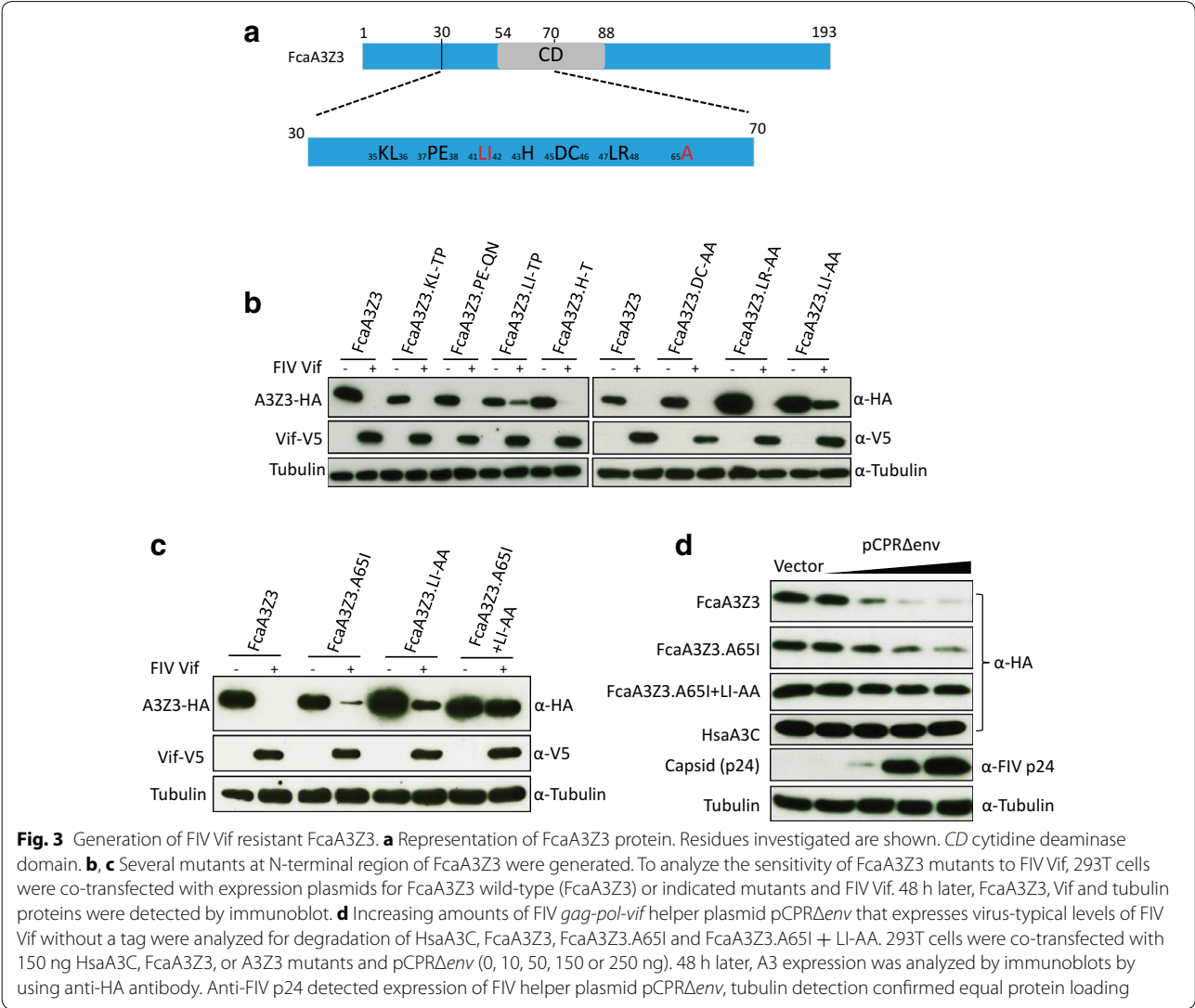
Fig. 2 Identification of residues in FcaA3Z3 for FIV Vif induced degradation. **a** Expression plasmids for FcaA3Z3, HsaA3H and big cat A3Z3s were co-transfected with FIV Vif into 293T cells. Cell lysates were analyzed by immunoblot. A3s contain a C-terminal HA-tag, Vifs contain a C-terminal V5-tag. FcaA3s represent domestic cat (*Felis catus*) APOBEC3s. Pti, Ple, Lly and Pco represent *Panthera tigris corbetti*; *Panthera leo bleyenberghi*; *Lynx lynx*; *Puma concolor*. **b** Scheme of FcaA3Z3/HsaA3H.hapll chimeras (Z3C1, -C2, -C6, -C7). Highlighted sequence diversity between HsaA3H and FcaA3Z3 in an N-terminal region. **c** 293T cells were co-transfected with expression plasmids for FcaA3Z3, Z3C1, Z3C2, Z3C6, Z3C7 or HsaA3H.hapll and FIV Vif, HIV-1 (NL4-3 or LAI) or SIVmac Vif. The expression of chimeras and Vif proteins were detected by using anti-HA and anti-V5 antibodies, respectively. Tubulin served as loading control. **d** Amino acid logo for the N-terminus in 15 A3Z3 sequences from ten Carnivores species (upper panel) and for eight A3Z3 sequences from eight Primates species (lower panel). Residues identified to evolve under purifying selection are labelled with “pur”. No residue was identified to evolve under diversifying selection in this A3Z3 stretch

and Z3C7 showed resistance to degradation (Fig. 2c). HIV-1 Vif (derived from clones NL4-3 or LAI) could not degrade any of the A3Z3 chimeras, but LAI Vif degraded A3H as reported before [54], and SIVmac Vif degraded Z3C1 and A3H but not Z3C2, Z3C6 and Z3C7 (Fig. 2c).

Our findings indicate that feline-derived residues shared by Z3C2 and Z3C6 (positions 23–50) are essential for FIV Vif interaction. This A3 stretch contained a number of positions evolving exclusively under purifying selection, for both carnivores and for primates (Fig. 2d). Globally, diversity among A3Z3 from carnivores was higher than among the primates’ orthologs (respectively 0.24 ± 0.02 vs 0.054 ± 0.007 , overall average pairwise nucleotide distance \pm bootstrap standard error estimate) (Additional file 1: Fig. S3A). During this analysis, we identified for the first time duplicated A3Z3s in the same genome (i.e. in-paralogs [55]) retrieved from different lineages within Caniformia (Ursidae, the giant panda and the polar bear; Phocidae, the Weddell seal; and Odobenidae, the walrus) but we could neither identify the two A3Z3 in-paralogs in Canidae (dog) nor in Mustelidae

(ferret) genomes. By contrast, in all Felidae genomes that we have screened we could only identify one of these in-paralogs (Additional file 1: Fig. S3A).

The A3Z3 region position 23–50 differs in 16 amino acids between human and feline A3Z3s, and contains certain highly conserved amino acid positions (Fig. 2b, d). We mutated thus most feline-specific residues in feline A3Z3, in positions 35–38 and 40–48. Residues in position 35 + 36 (KL), 37 + 38 (PE), 41 + 42 (LI) and 43 (H) in A3Z3 were substituted by the corresponding ones found in A3H. Additionally, we exchanged the A3Z3 residues at position 45 + 46 (DC), 47 + 48 (LR) and 41 + 42 (LI) against AA (Fig. 3a). These mutated A3s were characterized for resistance to degradation by co-expression with FIV Vif. We found that only A3Z3s mutated at position 41 + 42 (LI \gg TP and LI \gg AA) showed partial resistance to degradation by Vif (Fig. 3b). A65I in feline A3Z3 has been described in Brazilian cats and discussed to be a relevant resistance mutation against FIV [40, 56]. Under our experimental conditions, A3Z3 mutated in position 65 (A65I) displayed only little



resistance to Vif-mediated degradation (Fig. 3c). However, very important, the combination of mutations, A65I and L41A-I42A, resulted in an A3Z3 variant that showed complete resistance to FIV Vif degradation (Fig. 3c). We wondered whether experimental overexpression of the V5-tagged FIV Vif could mask the potency of the natural A65I variant to resist degradation. To address this question, we used as a source for Vif expression the replication-deficient FIV packaging construct pCPRΔenv [57]. Expression of increasing levels of pCPRΔenv in the presence of constant amounts of A3 revealed that the A65I mutation was degraded less efficiently than the wild-type A3Z3 (Fig. 3d). As a control we used A3C and A3Z3. A65I + LI-AA, which both showed no degradation by Vif derived by pCPRΔenv. Together, these findings indicate that the A65I mutation in feline A3Z3 mediates a

partial protection, and that a combination with L41A-I42A resulted in enhanced resistance to Vif.

The stretch involved in the interaction with Vif encompassed a number of highly conserved residues between A3Z3s from carnivores and primates, as well as residues under purifying selection (Fig. 2d). The L41–I42 residues in cat A3Z3 identified to interact with Vif are strictly conserved (L|I) in A3Z3 from felids, to the extent that even the codons used are also strictly conserved (CTT|ATT) for the five Felidae species analyzed. Interestingly, the two A3Z3 paralogs in Caniformia display different amino acid profiles in this Vif-binding region (Additional file 1: Fig. S3A), and albeit chemically related, amino acid residues in these positions are variable (I/L/V|I/T). Finally, this A3Z3 stretch is very different in the corresponding positions in A3Z3 from primates (T/M|P). Altogether,

evolutionary relationships for these two residues could thus at least partly explain species-specificity of the interaction between felidae A3Z3 and FIV Vif, reflecting adaptation and specific targeting.

Generation of a FIV Vif resistant feline A3Z2Z3

Our results demonstrate that feline A3Z2 can also be efficiently degraded by FIV Vif, thus implying a specific interaction between both proteins (Fig. 1b). In order to generate an A3Z2Z3 protein resistant to FIV Vif, we decided to mutate as well the A3Z2 moiety. To identify residues important for FIV Vif interaction with feline A3Z2, chimeric A3s of A3Z2 and human A3C, called Z2C1, -C4, -C5 and -C30 (Fig. 4a), were co-expressed with

FIV Vif. The chimeras Z2C1, Z2C4 and Z2C5 spanned the 1–22, 1–131 and 1–154 amino acids of feline A3Z2, respectively, the remaining parts being derived from A3C. Chimera Z2C30 was feline A3Z2, with amino acids 132–154 derived from A3C. Chimeras Z2C1 and Z2C4 showed moderately reduced protein levels when FIV Vif was co-expressed, chimera Z2C5 resistance to degradation, and chimera Z2C30 was efficiently degraded by FIV Vif (Fig. 4b). As controls, we investigated all chimeras for degradation by HIV-1 and SIVmac Vifs. HIV-1 Vif induced degradation of Z2C1 only, and SIVmac Vif completely degraded Z2C1, Z2C4 and Z2C30, and mostly Z2C5 (Fig. 4b). Because the Z2C5 chimera, in which the C-terminal 37 residues were of A3C origin, was resistant to FIV

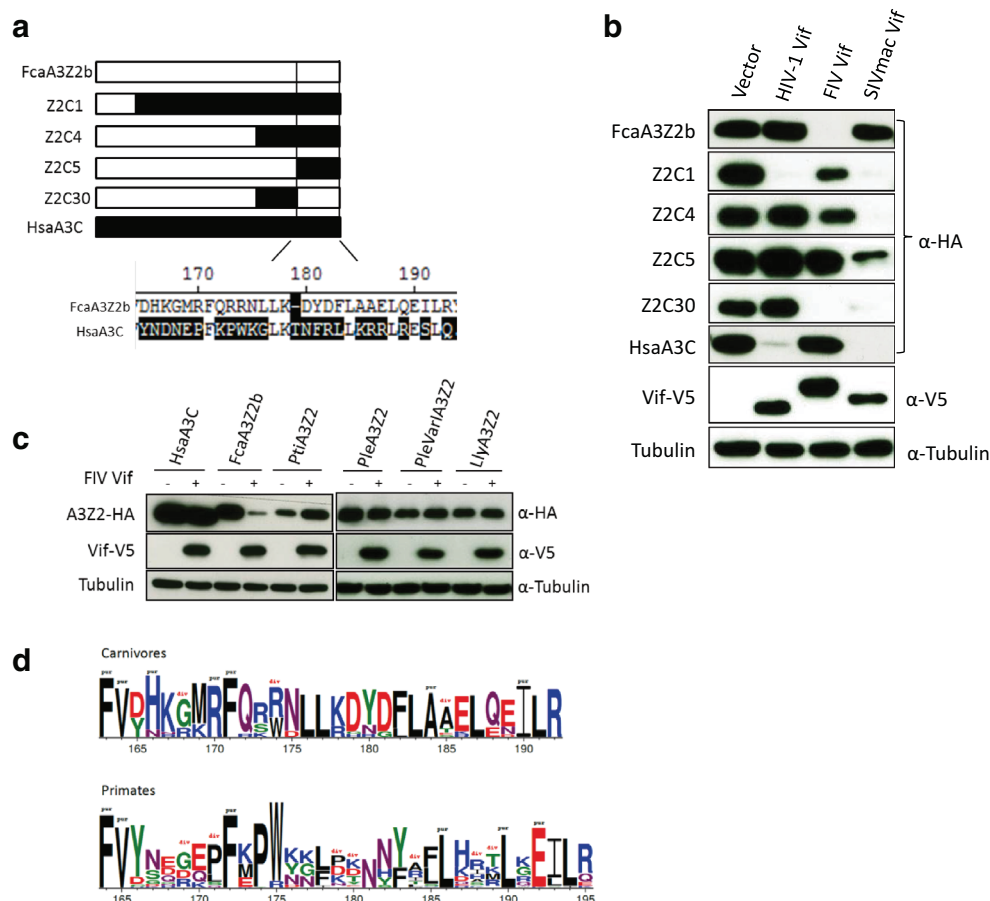


Fig. 4 FIV Vif requires C-terminal FcaA3Z2 (A3Z2b) residues for A3 degradation. **a** Scheme of A3Z2/A3C chimeras (Z2C1, -C4, -C5, -C30). Highlighted are C-terminal sequence differences between FcaA3Z2 and HsaA3C. **b** 293T cells were co-transfected with expression plasmids for Z2C1, Z2C4, Z2C5 or Z2C30 and FIV Vif, HIV-1 or SIVmac Vif. A3s contain a C-terminal HA-tag; Vifs contain a C-terminal V5-tag. The expression of chimeras and Vif proteins were detected by using anti-HA and anti-V5 antibodies, respectively. Cell lysates were also analyzed for equal amounts of total proteins using the anti-tubulin antibody. **c** Expression plasmids for A3C, FcaA3Z2, and big cat A3Z2s were co-transfected with FIV Vif into 293T cells. 48 h later, cells were analyzed by immunoblot. The expression of A3 and Vif proteins were detected by using anti-HA and anti-V5 antibodies, respectively. FcaA3s represent domestic cat (*Felis catus*); Pti, Ple, and Lly represent *Panthera tigris corbetti*; *Panthera leo bleyenberghi*; *Lynx lynx, varl, variant I*. **d** Amino acid logo for the C-terminus in 17 A3Z2 sequences from 12 Carnivores species (upper panel) and for 51 A3Z2 sequences from 17 Primates species (lower panel). Residues identified to evolve under purifying or diversifying selection are respectively labelled with “pur” (black) or with “div” (red)

Vif, we speculated that the C-terminal region of cat A3Z2 could be important for FIV Vif-induced degradation. SIVmac Vif, which cannot degrade feline A3Z2 (Fig. 4b), interacts presumably with C-terminal human-derived sequences spanning A3C sequences present in Z2C5 and Z2C30 (Fig. 4b). In addition we analyzed the degradation sensitivity of A3Z2 proteins from big cats and found that FIV Vif did not induce degradation of A3Z2 from tiger,

lion or lynx (Fig. 4c). These felid A3Z2s are very similar to FcaA3Z2 as they share 89–93 % identically conserved residues (Additional file 1: Figs. S2, S3B, Fig. 4d), whereas cat A3Z2 and human A3C are much more diverse and share only 47 % identical amino acids. Thus, we identified four positions in which all big cat A3Z2s differed from FcaA3Z2, in positions N18, T44, D165 and H166 (Additional file 1: Fig. S2, Fig. 5a). We mutated accordingly

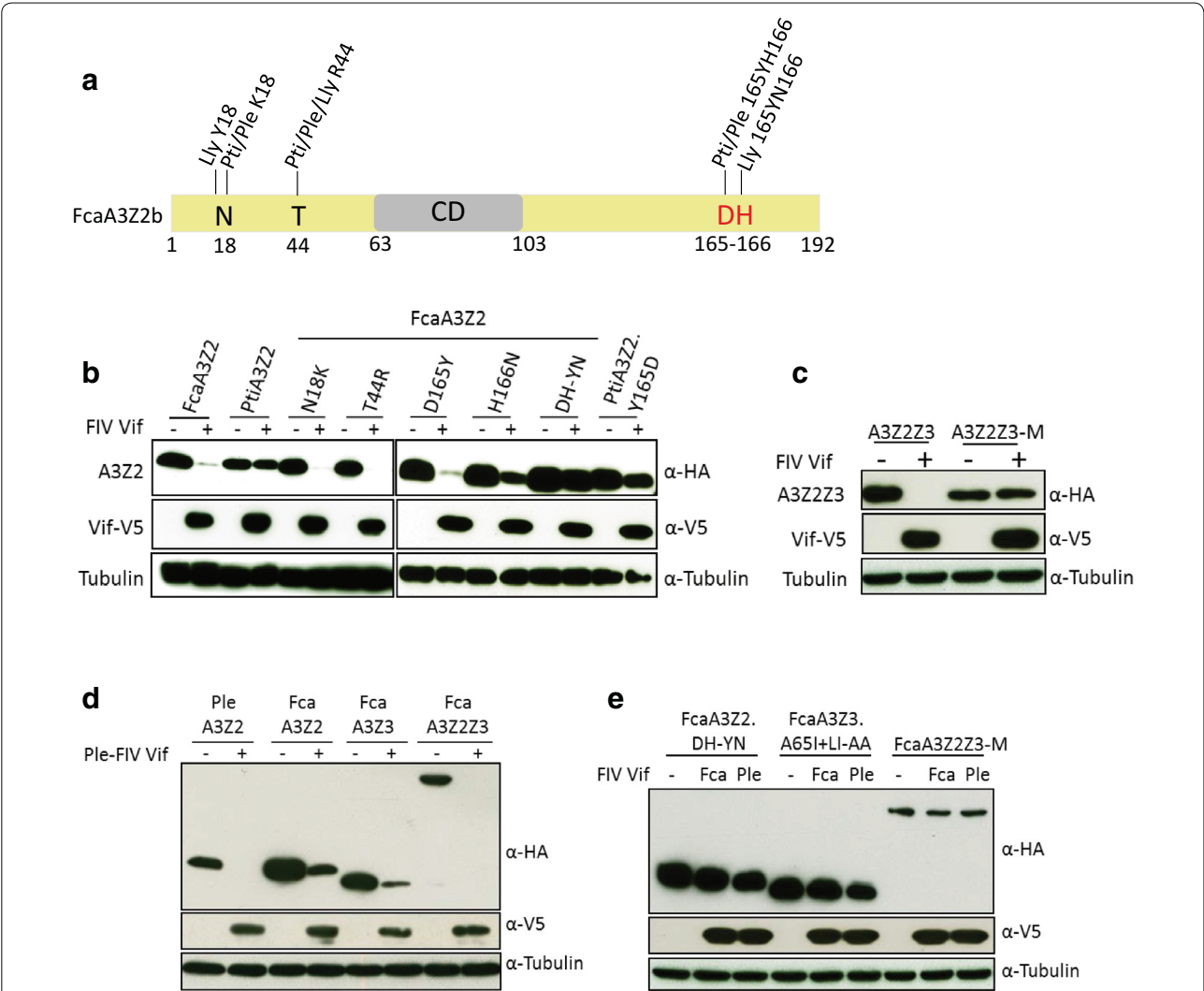


Fig. 5 FcaA3Z2 and FcaA3Z2Z3 mutations block degradation by feline Vifs. **a** Representation of FcaA3Z2b protein. Residues investigated are shown. CD cytidine deaminase domain. Residues different found in A3Z2 of the domestic cat and big cats indicated. Pti, Ple, and Lly represent *Panthera tigris corbetti*; *Panthera leo bleyenberghi*; *Lynx lynx*. **b** Expression plasmids for FIV Vif and FcaA3Z2, PtiA3Z2 or several mutants of feline A3Z2 were co-transfected into 293T cells. The expression of A3 and Vif proteins were detected by using anti-HA and anti-V5 antibodies, respectively. **c** FcaA3Z2Z3-M that contains DH-YN and A65I + LI-AA mutations in Z2- and Z3-domains was analyzed. Expression plasmids for FcaA3Z2Z3 wild-type or FcaA3Z2Z3-M were transfected together with FIV Vif plasmid into 293T cells. 48 h later, immunoblots were used to detect the expression of A3 and Vif by anti-HA and anti-V5 antibodies, respectively. **d** Vif from lion-derived FIV (FIVple) degrades wild-type FcaA3s (from domestic cat) and PleA3Z2 (from lion). 293T cells were co-transfected with expression plasmids for wild-type FcaA3Z2, PleA3Z2, FcaA3Z3 and FcaA3Z2Z3 and FIVple Vif. 48 h later, cells were harvested and lysates were used for detecting the expression of Vif and A3s by anti-HA and anti-V5, respectively. Cell lysates were also analyzed for equal amounts of total proteins using the anti-tubulin antibody. **e** Expression plasmids for FcaA3s with mutations (FcaA3Z2.DH-YN, FcaA3Z3.A65I + LI-AA or FcaA3Z2Z3-M) were co-transfected with lion FIV Vif (FIVple Vif) or domestic cat FIV Vif (FIVfca Vif) and 48 h later, cell lysates were used for detecting FcaA3s, Vif, and tubulin by anti-HA, anti-V5 and anti-tubulin, respectively. Fca, *Felis catus*; Ple, *Panthera leo bleyenberghi*

position 18 (N18K) and 44 (T44R) in FcaA3Z2, but found both mutants to be efficiently degraded by FIV Vif (Fig. 5b). Very similar, A3Z2.D165Y was depleted when co-expressed with FIV Vif. Interestingly, mutation of residue 166 (H166N) generated a partially Vif-resistant A3Z2 protein. We speculated that the adjacent D165 might enhance the Vif-resistance seen in the H166N variant. Indeed, the A3Z2.DH-YN mutant showed complete resistance to FIV Vif (Fig. 5b). We also analyzed tiger A3Z2.Y165D but could not reverse the resistance to degradation by FIV Vif (Fig. 5b). We conclude that D165-H166 in the C-terminal region of cat A3Z2 are important for Vif-mediated degradation together with other residues that remain to be characterized.

Finally, we constructed A3Z2Z3-M containing D165Y, H166N in Z2 and A65I + L41A, I42A in Z3. Co-expression experiments of A3Z2Z3-M with FIV Vif showed that this A3 variant was Vif-resistant (Fig. 5c). Importantly, the mutations that generated Vif-resistance did not impact the subcellular localization of the feline A3, as demonstrated by confocal microscopy of transiently transfected HOS cells (Additional file 1: Fig. S4). We also studied lion specific FIV (FIVple) Vif, which shares only 52 % identical residues with domestic cat FIV Vif (Additional file 1: Fig. S2C). FIVple Vif was able to induce degradation of PleA3Z2 and of FcaA3Z2, A3Z3 and A3Z2Z3 (Fig. 5d). Interestingly, FIVple Vif could not induce degradation of the mutated cat A3s A3Z2.DH-YN, A3Z3.A65I + LIAA and A3Z2Z3-M (Fig. 5e). These findings suggest that Vifs from lion and from domestic cat FIVs interact with identical residues in the domestic cat A3s.

To check whether the FIV Vif-resistant mutant A3s displayed modified binding to Vif, wild-type and mutated

A3s together with FIV Vif-TLQAAA were co-expressed and analyzed by anti-HA immuno-precipitation (Fig. 6). Wild-type cat A3Z3 precipitated FIV Vif (Fig. 6a), consistent with a direct interaction of both proteins (Fig. 1c). Only very little Vif bound to A3Z3.A65I and no Vif was detected in precipitations of A3Z3.LI-AA and A3Z3.A65I + LI-AA (Fig. 6a). However, when we examined wild-type A3Z2 and the DH-YN mutant, we detected similar amounts of Vif in both precipitations. Wild-type A3Z2Z3 bound high levels of Vif, and this binding was much reduced by the mutated variant A3Z2Z3-M (Fig. 6b). Globally, our observations suggest that A65I and LI-AA mutations in A3Z3 abolished FIV Vif binding, while hitherto not identified residues mediate Vif binding in A3Z2.

Structural analysis of feline A3Z2Z3

To identify the position of residues in feline A3s that, when mutated, prevent binding of FIV Vif and A3Z2Z3 degradation, a structural model of feline A3Z2Z3 was generated, initially aligning its sequence to the human full-length A3G model [58]. Surprisingly, the alignment indicated a large insertion in the Z2–Z3 linker region in the feline sequence that is not present in the human counterpart (Additional file 1: Fig. S5). This domain insertion spans 46 residues, extending the feline A3Z2Z3 linker to 83 residues compared to 27 residues in humans. The structure of the 83-residue linker was predicted using TopModel [59, 60]. Although the five identified template structures show only a low sequence identity with respect to the linker (up to 19.4 %; see “Methods” section), they all share a homeo-box domain fold [61]. The best three templates were aligned to the linker sequence

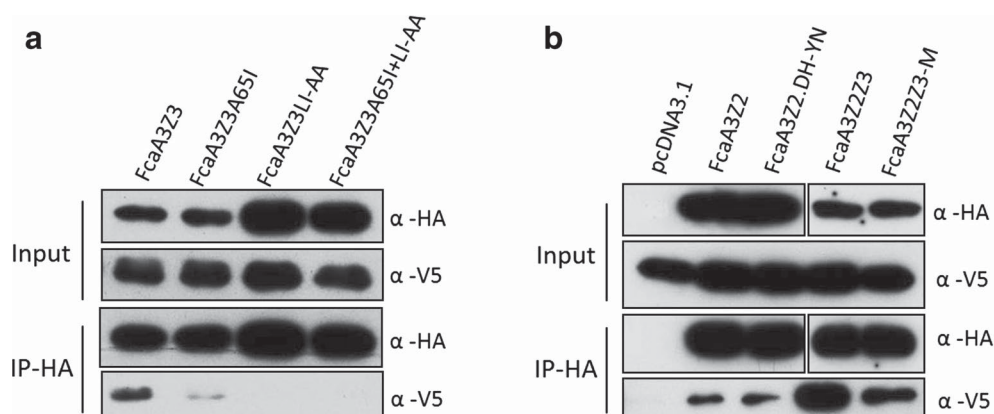


Fig. 6 Differential binding of FIV Vif to wild-type and mutant feline A3s. **a** Expression plasmids for FcaA3Z3s wild-type and mutants (all with HA-tag) and FIV Vif-TLQAAA (V5 tag) were co-transfected into 293T cells. The proteins were immunoprecipitated by α-HA beads and analyzed by immunoblots using anti-HA and anti-V5 antibodies. **b** Expression plasmids for FcaA3s (FcaA3Z2, FcaA3Z2.DH-YN, FcaA3Z2Z3 and FcaA3Z2Z3-M, all with HA-tag) and FIV Vif-TLQAAA (V5-tag) and were co-transfected into 293T cells, pcDNA3.1 (+) served as an A3-free control. 48 h later, cells were harvested, proteins were immunoprecipitated by α-HA beads. The FcaA3s and FIV Vif proteins were detected by anti-HA and anti-V5 antibodies, respectively

(Additional file 1: Fig. S5) and used for structure prediction. The rest of the feline A3Z2Z3 protein was predicted using the homology model of human A3G [58] as a template. Finally, the linker domain and the rest of the feline A3Z2Z3 protein were manually docked, sequentially connected, and unstructured parts of the linker domain were energy minimized (Fig. 7a). While this cannot be expected to result in an exact structural model, it provides a representation where the linker domain insertion could be located with respect to the rest of the feline A3Z2Z3 protein.

The five residues in feline A3s that, when mutated, prevent binding of FIV Vif and A3Z2Z3 degradation (D165, H166, L285, I286, A309; the last three corresponding to L41, I42 and A65 of A3Z3), are located opposite to the putative location of the linker domain and are at the boundary between the Z2 and Z3 domains (Fig. 7b). The predicted HIV-1 Vif binding regions in human A3G, A3C and A3H are additionally depicted in Fig. 7b–d, respectively. For A3C and A3H, the predicted HIV-1 Vif binding regions are spatially clearly separated from the respective five residues identified here in feline A3s (Fig. 7c, d). One may thus speculate that our findings indicate a FIV Vif binding region in feline A3 different from the ones described for HIV-1 Vif in human A3s.

FIV Vif-resistant feline A3s are antiviral

In the next set of experiments, we investigated whether feline A3s carrying the putative Vif-binding mutations displayed antiviral activity and resistance against Vif in FIV infections. We generated FIV luciferase reporter viruses by co-expression with either no A3 or with A3Z3, A3Z3.A65I, A3Z3.LI-AA or A3Z3.A65I + LI-AA and increasing levels of the FIV Vif plasmid (0–160 ng). Vector particles were normalized for reverse transcription (RT) activity, and luciferase activity was quantified 2 days post infection (Fig. 8a). All feline A3Z3s, either wild-type or mutants, were able to inhibit to the same extent Vif-deficient FIV, demonstrating that the described mutations do not hinder the potential for antiviral activity. Wild-type feline A3Z3 was fully counteracted by the lowest amount of Vif plasmid (40 ng) (Fig. 8a), matching well complete degradation observed in the lysates of FIV-producing cells (Fig. 8b). Opposite to the homogeneous behavior in the absence of Vif, mutated A3Z3s showed variable resistance to Vif-counteraction, as was obvious in the levels of remaining A3 signal in the cell lysates of the FIV-producing cells (Fig. 8b). Intermediate amounts of *vif*-encoding plasmid (40–80 ng) partially counteracted the inhibition of A3Z3.A65I or A3Z3.LI-AA mutants, and higher levels of Vif (160 ng plasmid) recovered infectivity of FIVs produced in the presence of

A3Z3.A65I and A3Z3.LI-AA. However, even the highest levels of Vif were not able to counteract the antiviral activity of A3Z3.A65I + LI-AA (Fig. 8a, b). The importance of Z2- and Z3-mutations in feline A3Z2Z3-M was characterized with 100 ng of FIV Vif plasmid. FIV luciferase viruses were produced and examined as described above using A3Z2Z3 and A3Z2Z3-M. FIV Vif restored the infectivity to levels similar to those in the absence of A3Z2Z3, while A3Z2Z3-M strongly inhibited FIV, either with or without Vif expression (Fig. 8c). The immunoblots of the corresponding FIV producing cells confirmed protein expression and Vif-dependent degradation of the wild-type A3Z2Z3 protein (Fig. 8d). To explore whether stable expression of A3Z2Z3-M can impact spreading infection, human HOS.CD4.CCR5 cells expressing either wild-type or mutated A3Z2Z3 were established (Fig. 8e, Additional file 1: Fig. S6) and infected by HIV-1 expressing FIV Vif (HIV-1 vif_{FIV}) [36]. FIV could not be investigated directly, because there are no feline cell lines known to be negative for A3 expression, and FIV cannot replicate in human cell lines. Whereas HIV-1 vif_{FIV} was detected at day six in the supernatant cells with wild-type A3Z2Z3, HOS cells expressing the A3Z2Z3-M showed a much delayed kinetic of viral replication (Fig. 8f). This observation suggests that the engineered A3Z2Z3-M protein also gained the capacity to restrict FIV Vif during multi-rounds of replication.

Encapsulation of A3 proteins in nascent virions is required for their antiviral activity. We investigated first whether mutated feline A3s could be differentially encapsidated into nascent virions. For this, we produced Vif-deficient FIV particles during expression of the different A3 proteins, measured the differential infectivity of the particles (Additional file 1: Fig. S7A) and subjected virus lysates to immunoblot analysis (Additional file 1: Fig. S7B). Results showed that wild-type and mutated feline A3s were detected in the concentrated FIVs (VLPs). However, while wild-type A3Z3 was less efficiently packaged compared with the A3Z3.A65I + LI-AA mutant, the wild-type A3Z2Z3 was detected in virions in higher abundance than the A3Z2Z3-M variant (Additional file 1: Fig. S7B). We addressed then the question whether encapsidated mutated feline A3s effectively exerted their cytidine deaminase activity onto the FIV genome in the virion. To tackle this question, cells were infected with FIV produced during cellular expression of feline A3Z3, A3Z3.A65I + LI-AA, A3Z2Z3 or A3Z2Z3-M, in the absence of A3 expression as a negative control, or during expression of human A3G as positive control. Total DNA was isolated from infected cells and subjected to differential DNA denaturing PCR (3D-PCR) [62] on the viral vector encoded luciferase gene 12 h post infection. Based on

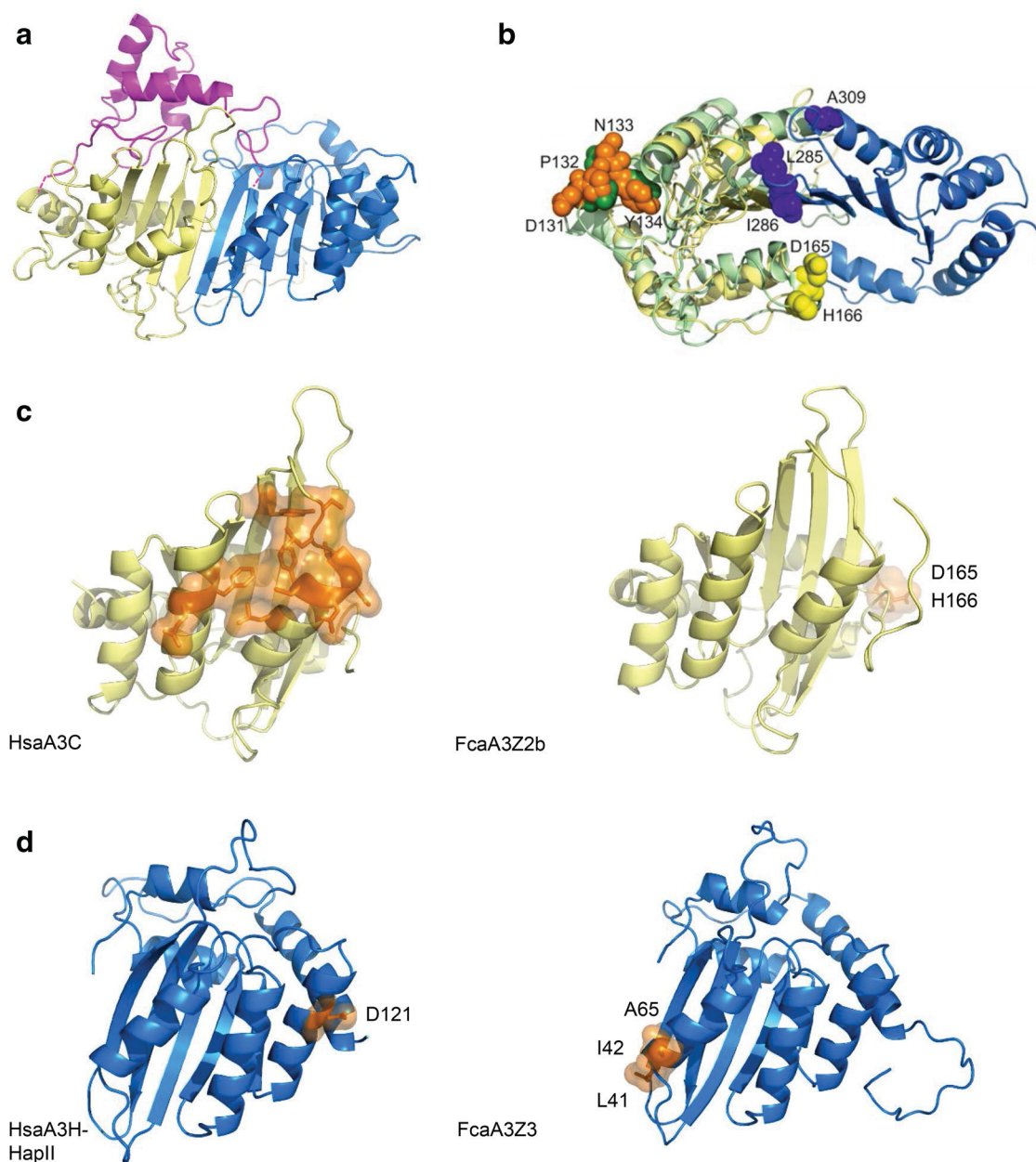
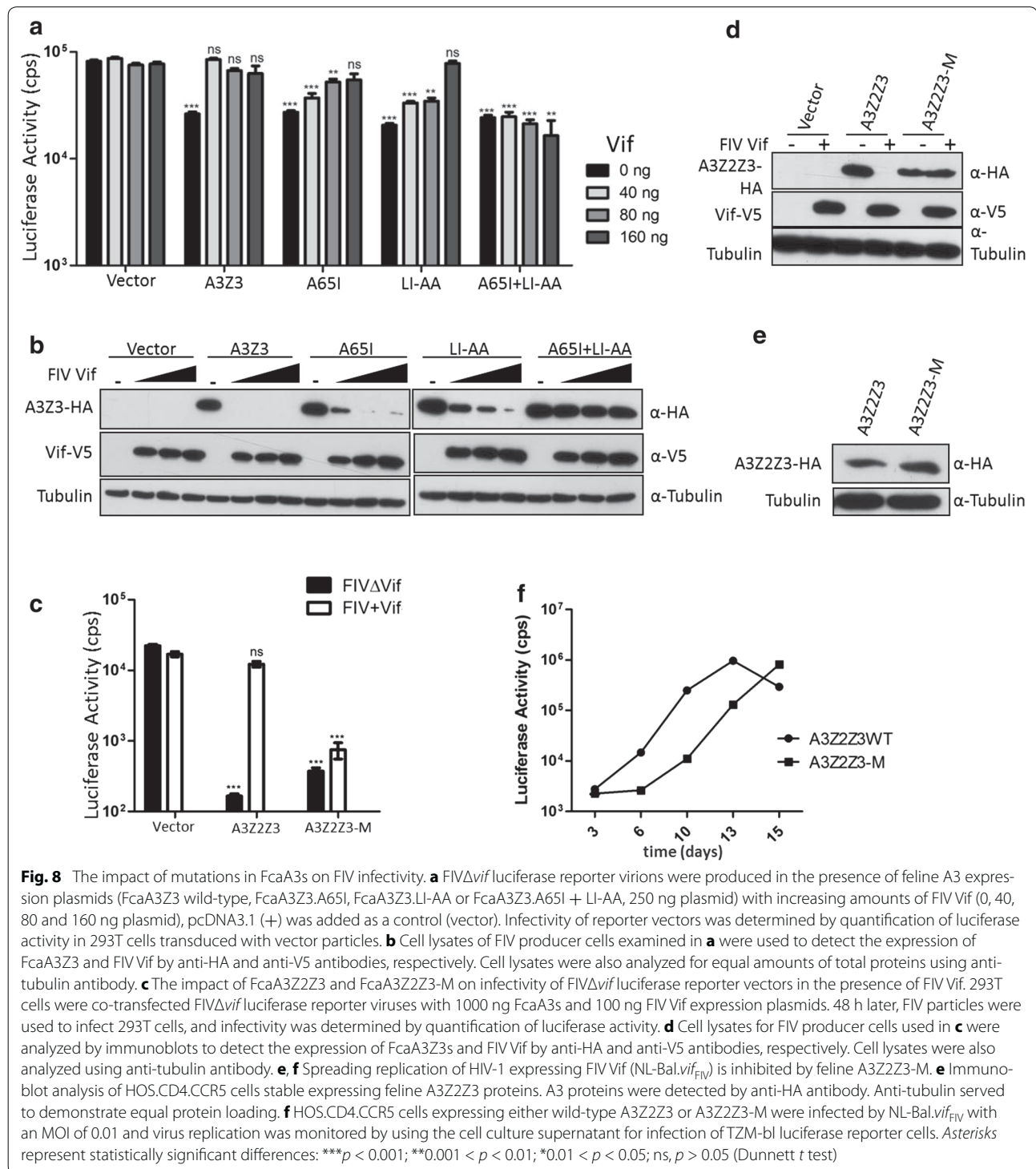


Fig. 7 Composite model of feline APOBEC3 and locations of residues mediating Vif binding. **a** Structural model of FcaA3Z2Z3 including the linker (pink) at a putative location above the Z2 (yellow) and Z3 (blue) domains; the linker connections to the Z2 and Z3 domains are highlighted by dashed lines. [69]. **b** Structural model of FcaA3Z2Z3 rotated by 90° with respect to **a** (Z2 domain: yellow; Z3 domain: blue; the linker region and parts of the N-terminus of Z2 and the C-terminus of Z3 for which no structure could be modeled were omitted for clarity). Residues in sphere representation in yellow (D165/H166), those in blue (L285/I286/A309), and those in orange (D131-Y134). Residues sequentially equivalent to the latter in the soluble N-terminal Vif-binding domain (sNTD) of A3G (PDB ID 2MZZ; pale green) are colored in green; these residues are part of the Vif-binding regions of the sNTD [68]. **c** Crystal structure of human A3C (PDB ID: 3VOW) and structural model of feline A3Z2b depicting the positions of respective HIV-1 Vif and FIV Vif binding sites. The domains are orientated as the Z2 domain in **a**. **d** Structural model of human A3H-HapII and feline A3Z3 depicting the positions of respective HIV-1 Vif and FIV Vif binding sites. The domains are orientated as the Z3 domain in **a**. Key residues involved in Vif binding are labelled (except human A3C), represented in sticks and highlighted with its surface in orange color

the overall nucleotide content, 3D-PCR amplifies PCR products at different denaturing temperatures (Td), with amplicons with higher A + T content displaying lower

denaturing temperatures than amplicons with higher G + C content. The net effect of the cytidine deaminase A3 activity is thus expected to lower the denaturing



temperature of the target DNA, leading to lower Tds values. Indeed, FIV virions produced in the absence of A3s yielded 3D-PCR products with the lowest Td of 86.3 °C, whereas all FIV virions produced during A3 expression

resulted in 3D-PCR products with decreased Tds (as low as 84.2 °C) (Additional file 1: Fig. S7C). This indicates that the wild-type and mutant feline A3s display enzymatic deamination activities.

The linker in feline A3Z2Z3 is targeted by HIV-2 and SIVmac/smm Vifs

We and others have observed that SIVmac Vif can induce degradation of feline A3Z2Z3 (Fig. 1b) [46, 51]. Figure 1b demonstrates that the Vifs of SIVsmm and HIV-2 also display this phenotype and are able to degrade feline A3Z2Z3. To elucidate this unexpected capacity of primate lentiviruses to counteract feline A3s in the context of viral infections, we generated luciferase reporter viruses for SIVmac and HIV-2 (Fig. 9). SIVmac or SIVmac Δ vif luciferase reporter viruses [63] were produced in the absence or presence of human A3G, feline A3Z2a, A3Z2b, A3Z2c, A3Z2bZ3, A3Z2cZ3 or A3Z2bZ3s that included polymorphic residues found in exon 4 of different *F. catus* breeding lines (Birman, Japanese Bobtail, British Shorthair, Turkish Van [36]). The Vif proficient virus SIVmac-Luc expresses Vif in its natural expression context; however Vif lacks a tag for detection. Viral particles were normalized for RT activity and luciferase activity of infected cells was quantified 2 days post infection (Fig. 9a). We found that double-domain feline A3s strongly inhibited Vif-deficient SIVmac, and that Vif expression fully counteracted this antiviral activity, showing therefore a similar pattern to human A3G. However, Vif expression did not affect inhibition of SIVmac by single domain A3s (Fig. 9a). The corresponding immunoblots of the virus producing cells showed Vif-dependent degradation of human A3G and of all feline A3Z2Z3s inspected. Feline A3Z2s and A3Z3 displayed a resistance to degradation by Vif proficient SIVmac (Fig. 9c). We performed a similar experiment using a HIV-2 luciferase reporter virus [64], which is a three-plasmid lentiviral vector system that requires Vif to be co-expressed from a separate plasmid (Fig. 9b). Using this system, we found that HIV-2 Vif counteracted the antiviral activity of human A3G, feline A3Z2bZ2 and of A3Z2cZ3. Again, the antiviral activity of feline single-domain A3s could not be inhibited by HIV-2 Vif (Fig. 9b). The immunoblots of the virus producing cells showed a Vif-dependent depletion of human A3G as well as of the feline double-domain A3s (Fig. 9d).

The Vif-mediated degradation profile exclusive to A3Z2Z3s may indicate that the HIV-2/SIVmac/smm Vifs require for interaction with the feline A3Z2Z3 a protein domain that is absent in the single-domain A3Z2 or A3Z3. We speculated that the homeo-box domain insertion (linker region) could play a central role in these Vif interactions. To test our hypothesis, three constructs were assayed: an A3Z2Z3 in which the linker was deleted (Δ Linker); and two versions of A3Z2Z3 in which either residues 223–240 (Δ 222) or residues 211–240 (Δ 210) in the linker were removed (Fig. 10a). All these constructs

successfully expressed protein upon transfection, and FIV Vif was able to degrade all of them. Only the linker truncations Δ 222 and Δ 210 were efficiently degraded by Vif of HIV-2/SIVmac/smm, whereas the Δ Linker construct showed very little degradation (Fig. 10b). We extended this experiment and analyzed the degradation with increasing levels (0, 20, 50, 150 or 250 ng) of SIVmac or HIV-2 Vif expression plasmid (Additional file 1: Fig. S8). Interestingly, the A3Z2Z3 lacking the linker domain (Δ Linker) showed dose-dependent moderate degradation, while mutants Δ 222 and Δ 210 showed a HIV-2/SIV Vif-dependent degradation similar as the wildtype A3Z2Z3 protein (Fig. 10b, Additional file 1: Fig. S8). To characterize the linker mutant A3s for functional antiviral activity, FIV Δ vif and SIVmac Δ vif luciferase reporter viruses were generated in the presence of wildtype and mutated A3s (Fig. 10c, d, Additional file 1: Fig. S9). Immunoblots of the viral particles showed that all A3s were encapsidated (Additional file 1: Fig. S9). Consistently in both viral systems, A3Z2Z3 moderately lost antiviral activity when part or the complete linker was deleted (Δ Linker, Δ 210, Δ 222) (Fig. 10c, d). Together, our results suggest that the linker domain enhances the antiviral activity of feline A3Z2Z3 but is not essentially required for it and that the linker is important for HIV-2/SIVmac/smm Vif degradation of feline A3Z2Z3. Whether the linker domain forms part of the HIV-2/SIV Vif interaction surface will be an important future question.

Because the linker insertion is absent in human A3s, we tried to learn more about the evolution of this unique domain. The DNA sequences in A3Z3 exon 2 encoding for the linker region in the double-domain A3Z2Z3 proteins are extremely conserved among members of Felinae and Pantherinae. The linker sequence is indeed more conserved than the corresponding Z2 and Z3 domains, the evolutionary distances being 0.044 ± 0.006 for the Z2 stretch, 0.011 ± 0.006 for the linker and 0.018 ± 0.004 for the Z3 stretch (overall average pairwise nucleotide distance \pm bootstrap standard error estimate). The evolutionary origin of the linker remains nevertheless obscure, as systematic BLASTn and BLAT searches using this linker sequence as seed did not retrieve hits beyond spurious matches. However, tBLASTn successfully retrieved hits associated with A3 genes: in the 5' untranslated region of the A3 gene (XR_434780) in the Weddell seal genome, in the 5' untranslated region of the A3 gene (FJ716808) in the camel genome, as well as in the 5' regulatory region of the A3 gene (FJ716803) in the pig genome. The only very remote hit in primates with linker-similar sequence could be located in an A3 gene of tarsier (XM_008049574.1), but similarity levels do not allow in this case claiming common ancestry.

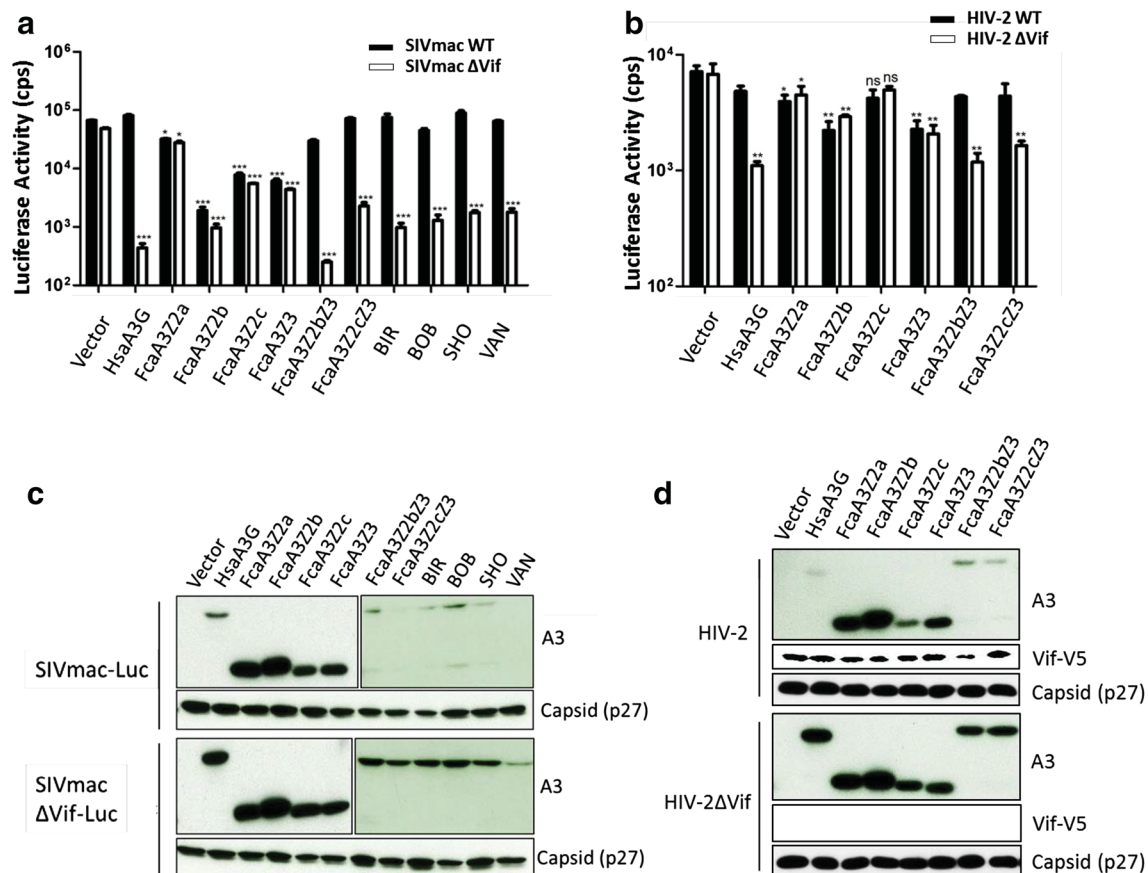


Fig. 9 SIVmac and HIV-2 escape inhibition by FcaA3Z2Z3. **a, b** 293T cells were transfected with expression plasmids for **a** SIVmacΔvif-Luc (SIVmacΔvif) or SIVmac-Luc (SIVmac WT) or **b** HIV-2Δvif-Luc (HIV-2Δvif) or HIV-2Δvif-Luc + HIV-2 Vif (HIV-2 WT), together with expression plasmids for HsaA3G or FcaA3s, pcDNA3.1 (+) was used as a control (vector). Reporter virus infectivity was determined by quantification of luciferase activity in 293T cells transduced with vector particles after normalizing for reverse transcriptase activity. *Luc* luciferase. **c** Lysates of SIVmac producer cells were used to detect the expression of FcaA3s and SIVmac capsid by anti-HA and anti-p27 antibodies, respectively. SIVmac Vif cannot be detected because of the unavailability of a suitable antibody. **d** Lysates of HIV-2 producer cells were used to detect the expression of FcaA3s and HIV-2 Vif by anti-HA and anti-V5 antibody, respectively. BIR, BOB, SHO and VAN represent FcaA3Z2Z3s including polymorphic sequences of exon 4 of four different *Felis catus* breeding lines: BIR Birman, BOB Japanese Bobtail, SHO British Shorthair, VAN Turkish Van. Asterisks represent statistically significant differences: *** $p < 0.001$; ** $0.001 < p < 0.01$; * $0.01 < p < 0.05$; ^{ns} $p > 0.05$ (Dunnett *t* test)

HIV-1 Vif weakly interacts with feline A3Z2Z3

The finding that HIV-2 Vif counteracts one of the feline A3s reinforces the view that the initially described species-specificity of Vifs [63] is not absolute [36, 52]. For the generation of an HIV-1 animal model based on the cat, it would of advantage to understand whether feline A3 proteins are structurally accessible for HIV-1 Vif. We show here that HIV-1 fails to degrade feline A3 proteins (Figs. 1b, 10b) and appears only to bind weakly to the feline A3Z2Z3 protein compared to FIV Vif (Additional file 1: Fig. S10A).

The structural model of feline A3Z2Z3 was used to rationalize the binding of HIV-1 Vif to A3Z2Z3. When comparing the amino acid sequences of A3G and feline A3s, we noticed that the HIV-1 Vif binding domain

124-YYFWDPDY-131 is conserved in feline A3Z2 (Additional file 1: Fig. S10B). This domain spans amino acid residues with a well-characterized role in Vif-binding, such as 128-DPD-130 [65] and the recently characterized Y125 [66] in the $\beta 4$ - $\alpha 4$ loop of human A3G [67]. In the feline A3Z2 domain we find DPN instead of the DPD motif; however, in human A3G DPN binds to HIV-1 Vif as wild-type DPD [65]. As our structural model of A3Z2Z3 in comparison to the soluble N-terminal domain (sNTD) of A3G [68] revealed that the two regions around these residues are similarly accessible (Fig. 7b), we attempted to restore binding of HIV 1 Vif to feline A3Z2Z3 by a N133D mutation, resulting in a YYFWDPD133Y motif sequentially identical to the one in A3G (Additional file 1: Fig. S10b). We did not observe degradation of A3Z2Z3.

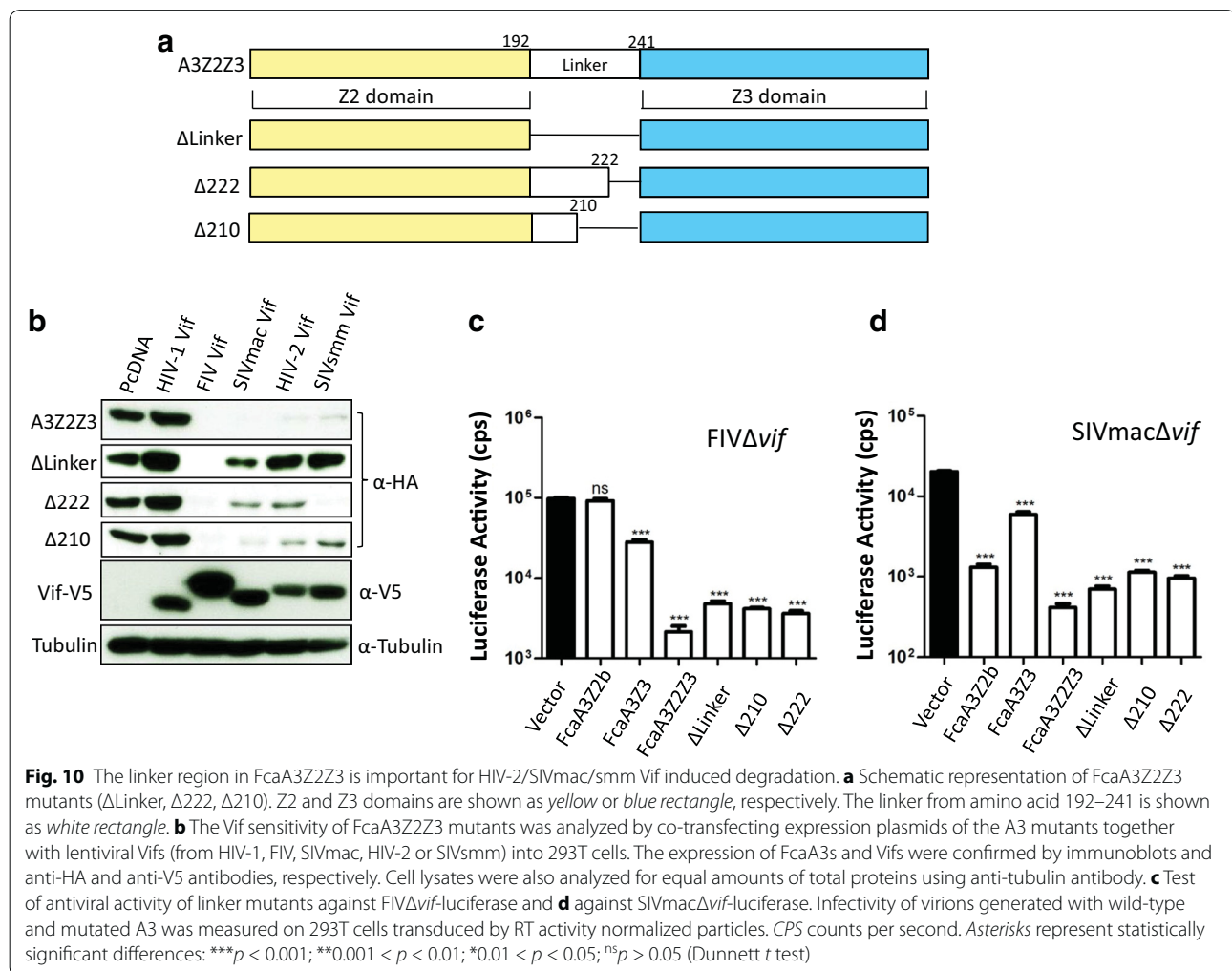


Fig. 10 The linker region in FcaA3Z2Z3 is important for HIV-2/SIVmac/smm Vif induced degradation. **a** Schematic representation of FcaA3Z2Z3 mutants (ΔLinker, Δ222, Δ210). Z2 and Z3 domains are shown as yellow or blue rectangle, respectively. The linker from amino acid 192–241 is shown as white rectangle. **b** The Vif sensitivity of FcaA3Z2Z3 mutants was analyzed by co-transfecting expression plasmids of the A3 mutants together with lentiviral Vifs (from HIV-1, FIV, SIVmac, HIV-2 or SIVsmm) into 293T cells. The expression of FcaA3s and Vifs were confirmed by immunoblots and anti-HA and anti-V5 antibodies, respectively. Cell lysates were also analyzed for equal amounts of total proteins using anti-tubulin antibody. **c** Test of antiviral activity of linker mutants against FIVΔvif-luciferase and **d** against SIVmacΔvif-luciferase. Infectivity of virions generated with wild-type and mutated A3 was measured on 293T cells transduced by RT activity normalized particles. CPS counts per second. Asterisks represent statistically significant differences: *** $p < 0.001$; ** $0.001 < p < 0.01$; * $0.01 < p < 0.05$; ns $p > 0.05$ (Dunnett t test)

N133D by HIV-1 Vif (Additional file 1: Fig. S10C), however; neither were mutations of P132 to introduce additional side chain interactions successful in that respect (Additional file 1: Figs. S10B, S10C). As to a possible explanation, for A3C, which is structurally highly similar to the sNTD of A3G [68], another motif of residues critical for Vif binding was found, centering on F75, Y86, F107, and H111 [69] (Fig. 7c). The sequentially equivalent residues of A3Z2Z3 are F78, Y89, F110, and Y114 such that the exchange of His versus Tyr may explain the failing of the binding of HIV-1 Vif. Another possible explanation for A3Z2Z3 is given by the occlusion of space required for HIV-1 Vif binding due to the presence of the predicted linker domain, where the long unstructured regions at the beginning and the end of the structured linker part may make it possible that the linker domain tips over the Z2 domain, that way shielding the putative HIV-1 Vif binding region (Fig. 7a, b).

Discussion

The A3 restriction factors are of extraordinary importance for the evolution and pathogenicity of lentiviruses and likely also of most other retroviruses. Here we identified A3 residues that are relevant for the FIV Vif interaction with both single-domain A3s, A3Z2 and A3Z3 (results are summarized in Table 1). In addition, we analyzed a unique A3 protein insertion domain called linker present in the feline A3Z2Z3 protein. The linker is suggested to form a homeo-box domain and mediates the sensitivity of A3Z2Z3 to degradation by Vifs of the HIV-2/SIVmac/smm group of primate lentiviruses.

Our knowledge about the interaction regions of A3s and of human and non-human lentivirus Vifs is limited. It was discussed that Vif is not simply a linker between the substrate A3 and the E3 ubiquitin ligase [70, 71]. In our study we investigated the interaction of three groups of Vif proteins (FIV, HIV-2/SIV, HIV-1) with feline A3s.

Table 1 Summary Vif-mediated A3 degradation

Feline A3 ^a	Degradation by Vif				Rescue of infection by Vif ^b		
	FIV	HIV-1	HIV-2	SIVmac/smm	FIV	HIV-2	SIVmac
A3Z2	++	—	—	—	ND	—	—
A3Z2.DH-YN	—	ND	ND	ND	ND	ND	ND
A3Z3	++	—	—	—	++	—	—
A3Z3.A65I	±	ND	ND	ND	±	ND	ND
A3Z3.LI-AA	±	ND	ND	ND	±	ND	ND
A3Z3.A65I + LI-AA	—	ND	ND	ND	—	ND	ND
A3Z2Z3	++	—	++	++	++	++	++
A3Z2Z3-M	—	ND	++	++	—	ND	ND
A3Z2Z3ΔLinker	++	—	±	±	ND	ND	ND

Degradation of A3 by Vif: ++, mostly degraded; ±, partial degradation with high amount of Vif; —, no degradation

Rescue of infection by Vif: ++, complete rescue; ±, partial rescue; —, no rescue

ND not done

^a Feline A3: A3s from domestic cat *Felis catus*

^b Experiments to rescue the infection were not done with HIV-1 and SIVsmm

Previous experimental evidence described residue A65 in feline A3Z3 in modulating the sensitivity to FIV Vif [56]. We identified here two additional residues (L41, I42) in feline A3Z3 whose combined mutation resulted in an A3 protein that was resistant even to degradation by very high amounts of co-expressed FIV Vif. The mutated feline A3Z3 protein clearly showed reduced binding to FIV Vif, supporting the model that Vif binding to A3 is needed for A3 degradation. In feline A3Z2 residues D165 and H166 were also found to regulate the FIV Vif induced degradation, but mutations in these positions did not block the binding to FIV Vif in co-immunoprecipitation assays. This observation demonstrates that Vif binding to A3s is not sufficient for A3 degradation. Supporting evidence that Vif interaction is necessary but not sufficient is coming from reports describing that HIV-1 NL4-3 Vif binds A3C mutants, A3B and A3H without inducing APOBEC3 degradation [71–73]. The qualitative co-immunoprecipitation assays used in our study did not much differentiate the binding strength of individual Vif-A3 pairs, and it is very well possible that a weak interaction of e.g. HIV-1 Vif with feline A3Z2Z3 is below a threshold to form a stable E3 ligase complex. However, the binding of mutated feline A3Z2.DH-YN to FIV Vif appeared to be robust, indicating a more complex mechanism. Studies on HIV-1 Vif binding to human A3B and A3H similarly concluded that the interaction strength is not the only determinant for complete Vif-mediated degradation, and the individual interfaces of the A3-Vif pair additionally regulate degradation [72].

Recently, Richards et al. [74] presented a wobble model of the evolution of the Vif-A3 interaction. This model implicates that Vif forms several interactions, of which

some are essential and some provide additional stabilizing contacts. Based on this idea, only if Vif forms a sufficient network of interactions with its A3 binding partner, a functional interaction is made. Suboptimal, destabilized interactions could be restored by the evolution of compensatory changes in Vif-A3 interface. It is thus possible that in feline A3Z3 residue A65 and L41, I42 are major independent interactions in the Vif-A3 interface, whereas in feline A3Z2 D165 and H166 represent one of the relevant interacting points for FIV Vif complex formation, while additional contact points still exist. Such a suboptimal Vif-A3 interaction might, for example, not be sufficient to facilitate E3 ligase conjugation of K48-linked polyubiquitin chains that are generally recognized by the proteasome.

The exact Vif-A3 interfaces are not known, because high-resolution structures have been only solved of single proteins such as of Z1- and Z2-domain human proteins (A3A, A3C), of the N-terminal Z2- and C-Terminal Z1-domain of human A3G, of the C-terminal Z2-domain of A3F and of HIV-1 Vif [67, 75, 76]. The structures of the full-length double domain A3s are unknown, however. Human A3Z1s and A3Z2s are globular proteins with six α -helices and five β -sheets arranged in a characteristic motif ($\alpha 1$ - $\beta 1$ - $\beta 2/2'$ - $\alpha 2$ - $\beta 3$ - $\alpha 3$ - $\beta 4$ - $\alpha 4$ - $\beta 5$ - $\alpha 5$ - $\alpha 6$) [67, 76]. In human A3C, A3D and A3E, the HIV-1 Vif binding site is conserved and located in a hydrophobic cavity and on the surrounding surface of the $\alpha 2$, $\alpha 3$ and $\alpha 4$ helices [69, 77, 78]. In human A3G, HIV-1 Vif binds a surface different to the binding region in A3C/D/E, with residues Y125, 128-DPN-130 in the $\beta 4$ - $\alpha 4$ loop being important for HIV-1 Vif binding [65, 66]. In the human Z3 protein A3H, binding of HIV-1 Vif is mediated by residue 121

(either E or D) [79, 80]. Based on our structural model of feline A3Z2Z3 (Fig. 7b), we locate the residues important for FIV Vif binding in feline A3Z2Z3 at the domain boundary of the Z2 and the Z3 domains, distant to the binding motifs in human A3s (Fig. 7c, d).

In feline A3Z2, the presumed HIV-1 Vif-binding domain of human A3G, the $\beta 4$ - $\alpha 4$ loop, is conserved. Nevertheless, HIV-1 Vif fails to degrade feline A3Z2 or A3Z2Z3 despite the presence of the well-characterized residues DPN (in A3G residues 128–130) and Y125 [65, 66]. Based on our structural model, we suggest that the $\beta 4$ - $\alpha 4$ loop of feline A3Z2 is surface exposed. This suggests that the Z2-domain of human A3G contains in addition to the Y125, 128-DPN-130 motif residues for HIV-1 Vif binding that are absent or hidden in feline A3Z2 or A3Z2Z3. Indeed, the presences of such important residues outside this motif in A3G were recently postulated [68, 81]. In addition to FIV Vif, we and others found previously that HIV-2/SIVmac/smm Vifs induce degradation of feline A3Z2Z3 [46, 51] by possibly targeting the unique linker domain. The previously called linker, a domain insertion in feline A3Z2Z3, is not found in any double-domain A3 protein of human or mouse origin. Our modelling results suggest that the insertion forms a homeo-box domain-like structure that protrudes the Z2-Z3 structure.

In general, it appears that double-domain A3 proteins display stronger antiviral activities than single-domain A3s. The evolution of double-domain encoding A3 genes could thus have been most likely adaptive, as it significantly increased the host fitness against retroviral infections. Our results suggest that primates and felids could have evolved double-domain A3s through different routes. The sequence of the linker insertion is located in 5'UTR of the felid A3Z3 gene in exon 2, which is exclusively translated in read-through transcripts spanning the A3Z2 and A3Z3 genes in felines (Fig. 1a). The sequence encoding for exon 2 seems to be restricted to members of Felinae and Pantherinae. In this sense, the A3Z2Z3 linker region resembles an orphan domain specific to Feliformia, and the linker could thus be a synapomorphy of this clade. Nevertheless, homology searches identified an enrichment of significantly remote tBLASTn hits associated with regulatory or non-coding regions of A3 genes in the genomes of different species, in the carnivore Weddell seal and in the artiodactyls pig and camel. This concentration of sequences with a possible common origin with the feline A3Z2Z3 linker found in the close vicinity of the A3 genes in other species within Laurasiatheria suggests that the linker could have been recruited as a coding sequence into the feline A3Z2Z3 mature mRNA from a pre-existent non-coding possibly

regulatory sequence, in an example of gain of function. This sequence could have been recruited after point mutation/s resulting in stop codon removal, introduction of frameshifts or unmasking previously cryptic functional sites [82] during the evolution of carnivores, after the split Caniformia/Feliformia but before the split Pantherinae/Felinae. In the case of primates and of rodents there are no descriptions of read-through transcripts of single domain A3s resulting in mRNAs encoding double-domain A3s. Instead, the human heterologous double domain A3s (i.e. A3B and A3G, both being A3Z2Z1) or homologous double domain A3s (i.e. A3D and A3F, both being A3Z2Z2) could have evolved after the fusion of head-to-tail duplicated genes, as the several rounds of gene duplication in the evolutionary history of the A3 locus in primates suggest [3].

During our evolutionary analysis of the A3Z3 genes, we found here for the first time duplicated A3Z3 genes. A3Z3 duplications were identified in the genomes of different carnivores (the giant panda, the polar bear, the Weddell seal and the walrus), but were not found in dog and ferret and also not in any felid. The most parsimonious hypothesis would be that a duplication event occurred within Caniformia, after the basal split of Canidae. However, given the inferred position of the most recent common ancestor of all A3Z3 in carnivores, and given the within-clades and between-clades evolutionary distances (Additional file 1: Fig. S3), we propose that an ancient A3Z3 duplication event may have occurred prior to the Caniformia/Feliformia split. One of the in-paralogs would have disappeared in the Felidae ancestor, and at least in the dog genome, while both copies would have been maintained in most lineages within Caniformia (the absence in the ferret genome should be confirmed when better quality data are available).

Conclusions

Host-virus arms races formed the Vif-A3 interactions. Our data support that the evolution of HIV-1, HIV-2 and FIV follow intrinsic currently unexplained evolutionary pathways adapting to the antiviral A3 repertoire. This study also revealed that the A3 gene evolution included newly identified duplications (in-paralogs) of A3Z3 genes in some caniformia and the inclusion of a homeobox-domain in the feline A3Z2Z3 protein. This homeobox domain insertion may reflect a transitional situation (read-through transcription) of the evolutionary development of double Z-domain containing A3 proteins. Further resolution of the interaction surface of feline A3s with Vif proteins will help us to understand the biochemistry of these interactions and may give us tools to explore the HIV-1 Vif interaction with human A3s.

Methods

Cells and transfections

HEK293T (293T, ATCC CRL-3216), HOS (ATCC CRL-1543) and TZM-bl cells (NIH AIDS Reagent program [83, 84]) were maintained in Dulbecco's high-glucose modified Eagle's medium (DMEM, Biochrom, Berlin, Germany) supplemented with 10 % fetal bovine serum (FBS), 2 mM L-glutamine, penicillin (100 U/ml), and streptomycin (100 µg/ml). Stable A3 expressing cells: FcaA3Z2Z3 wild type and mutant pcDNA-constructs were digested by BglII, and then were transfected into HOS.CD4.CCR5 cells using Lipofectamine LTX (Thermo Fisher Scientific, Schwerte, Germany) according to manufacturer's instruction, cells stably express feline A3s were selected by 750 µg/ml G418 (Biochrom, GmbH) in the following 3 weeks. The A3s degradation experiments were performed in 24-well plates, 1×10^5 293T cells were transfected with 250 ng A3s expression plasmids together with 250 ng HIV-1, HIV-2, SIVmac and SIVsmm Vif expression plasmids or 20 ng codon-optimized FIV Vif expression plasmid, pcDNA3.1 (+) (Life Technologies) was used to fill the total plasmid to 500 ng. To produce FIV-luciferase viruses, 293T cells were co-transfected with 0.6 µg FIV packaging construct, 0.6 µg FIV-luciferase vector, 1 µg A3 expression plasmid, 0.1 µg VSV-G expression plasmid; in some experiments pcDNA3.1 (+) (Life Technologies) was used instead of Vif or A3 expression plasmids. For HIV-2 and SIVmac-luciferase transfections, 1.2 µg HIV-2-Luc and SIVmac-Luc plasmids were used instead of FIV plasmids. At 48 h post transfection, cells and supernatants were collected.

Vif and A3 plasmids

FIV-34TF10 (codon-optimized), HIV-1, HIV-2, SIVmac and SIVsmm Vif genes were inserted into pcWPRE containing a C-terminal V5 tag [36]. HIV-1 Vif represents always HIV-1 Vif from clone NL4-3, except specifically stated LAI. HIV-1 Vif LAI is a gift from Viviana Simon and does not contain a protein tag [54]. pCPR Δenv FIV gag-pol plasmid that in addition expresses Vif was described previously [57]. FIV-Lion Vif gene (FIV_{ple} subtype B, accession number EU117991) was synthesized and codon-optimized. FIV-Lion Vif expression plasmid was generated by cloning codon-optimized FIV-Lion Vif fragment containing a V5 tag into pcWPRE using EcoRI and NotI. All A3s are expressed a carboxy-terminal hemagglutinin (HA) tag. Domestic cat and big cat (*Pantherinae*) A3s were described previously [36]. Human A3C (HsaA3C) and feline A3Z2b (FcaA3Z2b) chimeras were made by overlapping extension PCR. HsaA3C/FcaA3Z2 chimera Z2C1, Z2C4 and Z2C5 contain residues 1–22, 1–131 and 1–154 of FcaA3Z2, respectively; the remaining C-terminal fragments are derived from

human A3C. The 5' and 3' fragments were amplified separately by using primer pairs (Additional file 2: Table S1); two fragments were then mixed and amplified with the two external primers (Additional file 2: Table S1). To make HsaA3C/FcaA3Z2 chimera Z2C30, the first fragment was amplified by primers feApo3.fw and hufe3C 485.rv using chimera Z2C4 as a template, the second fragment was amplified by primers hufe3C 485.fw and HA-rv using FcaA3Z2 as a template, the two fragments were mixed and amplified with the two external primers. The FcaA3Z2b mutants were generated by fusion PCR using primer pairs described in Additional file 2: Table S1. The final products of HsaA3C/FcaA3Z2 chimeras and FcaA3Z2 mutants were cloned into pcDNA3.1 (+) using HindIII and XhoI restriction sites. The HsaA3H/FcaA3Z3 chimeras were constructed by the same method using primer pairs listed in Additional file 2: Table S2. To make FcaA3Z2bZ3-M, the PCR products of FcaA3Z2b DH-YN and FcaA3Z3 A65I + LI-AA were fused, and then inserted into pcDNA3.1 (+) by EcoRI and NotI restriction sites. The FcaA3Z2Z3 mutation constructs were generated by using the primers shown in Additional file 2: Table S3.

Viruses and infection

To produce FIV single-cycle luciferase viruses (FIV-Luc), 293T cells were co-transfected with the replication deficient packaging construct pFP93, a gift from Eric M. Poeschla [85], which only expresses *gag*, *pol*, and *rev*; the FIV luciferase vector pLinSin [4]; a VSV-G expression plasmid pMD.G; FcaA3s expression plasmids; FIV Vif expression plasmid; or empty vector pcDNA3.1 (+). To produce SIV-Luc viruses, 293T cells were co-transfected with SIVmac-Luc (R-E-); or SIVmac-Luc (R-E-) Δvif [63]; and FcaA3s expression plasmids. HIV-2-Luc was produced by co-transfecting 293T cells with HIV-2 packaging plasmid pHIV2 $\Delta 4$ [86]; transfer vector plasmid HIV-2-luc (SV40) [64]; pMD.G, together with FcaA3s expression plasmids or empty vector pcDNA3.1 (+) and HIV-2 Vif-V5 expression plasmid or pcDNA3.1 (+) empty vector. The reverse transcriptase (RT) activity of FIV, SIVmac and HIV-2 were quantified by using the Cavid HS lenti RT kit (Cavidi Tech, Uppsala, Sweden). For reporter virus infection, 293T cells were seeded in 96-well plate 1 day before transduction. After normalizing for RT activity, the same amounts of viruses were used for infection. Three days post transduction, firefly luciferase activity was measured with the Steadylite HTS reporter gene assay system (Perkin-Elmer, Cologne, Germany) according to the manufacturer's instructions on a MicroLumat Plus luminometer (Berthold Detection Systems, Pforzheim, Germany). Each sample was performed transduction in triplicates; the error bar of each triplicate

was shown. Replication-competent HIV-1 plasmids NL-BaL.vif_{FIV} were described previously [36]. NL-BaL.vif_{FIV} virus stocks were prepared by collecting the supernatant of transfected 293T cells. The kinetics of viral spreading replication was determined with HOS.CD4.CCR5.FcaA3s cells by infection with MOI 0.01 of NL-BaL.vif_{FIV}. Spreading virus replication was quantified over 15 days by infecting 10 µl supernatant to TZM-bl cells. All experiments were repeated independently at least three times.

Immunoblot analysis

Transfected 293T cells were lysed in radioimmunoprecipitation assay (RIPA) buffer (25 mM Tris-HCl [pH7.6], 150 mM NaCl, 1 % NP-40, 1 % sodium deoxycholate, 0.1 % sodium dodecyl sulfate [SDS], protease inhibitor cocktail set III [Calbiochem, Darmstadt, Germany]). The expression of FcaA3s and lentivirus Vif were detected by mouse anti-hemagglutinin (anti-HA) antibody (1:7500 dilution, MMS-101P; Covance, Münster, Germany) and mouse anti-V5 antibody (1:4500 dilution, MCA1360, ABDserotec, Düsseldorf, Germany) separately, the tubulin and SIV capsid protein were detected using mouse anti-α-tubulin antibody (1:4000, dilution, clone B5-1-2; Sigma-Aldrich, Taufkirchen, Germany), HIV Vif LAI was detected by HIV-1 Vif monoclonal antibody (#319) (NIH AIDS Reagent Program [87]) and mouse anti-capsid p24/p27 MAb AG3.0 (1:50 dilution [88]) separately, followed by horseradish peroxidase-conjugated rabbit anti-mouse antibody (α-mouse-IgG-HRP; GE Healthcare, Munich, Germany), and developed with ECL chemiluminescence reagents (GE Healthcare). Encapsulation of FcaA3 proteins into FIV particles: HEK293T cells were transfected with 600 ng pFP93, 600 ng of pLinSin, 100 ng pMD.G and 1000 ng of FcaA3 constructs. Viral supernatants were collected 48 h later, overlaid on 20 % sucrose and centrifuged for 4 h at 14,800 rpm in a table top centrifuge. Viral pellet was resuspended in RIPA buffer, boiled at 95 °C for 5 min with Roti load reducing loading buffer (Carl Roth, Karlsruhe, Germany) and resolved on a SDS-PAGE gel. The FcaA3s and tubulin proteins were detected as the above method. VSV-G and FIV p24 proteins were detected using mouse anti-VSV-G antibody (1:10,000 dilution; clone P5D4; Sigma-Aldrich) and mouse anti-FIV p24 antibody (1:2000 dilution; clone PAK3-2C1; NIH AIDS REPOSITORY) separately, followed by horseradish peroxidase-conjugated rabbit anti-mouse antibody (α-mouse-IgG-HRP; GE Healthcare, Munich, Germany), and developed with ECL chemiluminescence reagents (GE Healthcare).

Immunofluorescence and flow cytometry

HOS cells grown on polystyrene coverslips (Thermo Fisher Scientific, Langenselbold, Germany) were

transfected with expression plasmids for FcaA3 wild-type and mutants or together with FIV Vif-TLQAAA using Lipofectamine LTX (Life Technologies). At day one post transfection, cells were fixed in 4 % paraformaldehyde in PBS for 30 min, permeabilized in 0.1 % Triton X-100 in PBS for 15 min, incubated in blocking buffer (FBS in PBS) for 1 h, and then cells were stained by mouse anti-HA antibody in a 1:1000 dilution in blocking solution for 1 h. Donkey anti-mouse Alexa Fluor 488 (Life Technologies) was used as a secondary antibody in a 1:300 dilution in blocking solution for 1 h. FIV Vif-TLQAAA was stained by rabbit anti-V5 antibody in a 1:1000 dilution in blocking solution for 1 h. Donkey anti-rabbit Alexa Fluor 594 (Life Technologies) was used as a secondary antibody in a 1:300 dilution in blocking solution for 1 h. Finally, DAPI was used to stain nuclei for 2 min. The images were captured by using a 40× objective on a Zeiss LSM 510 Meta laser scanning confocal microscope (Carl Zeiss, Cologne, Germany). To analyze CD4 and CCR5 expression level of HOS.CD4.CCR5.FcaA3s, cells were stained by α-hCD4 PE mouse IgG1_k (Dako, Hamburg, Germany) and α-hCCR5 FITC (BD Bioscience, Heidelberg, Germany) separately according to the manufacturer's instruction. The measurement was carried out by BD FACSSanto (BD Bioscience). Data analysis was done with the Software FlowJo version 7.6 (FlowJo, Ashland, USA).

Immunoprecipitation

To determine Vif and A3 binding, 293T cells were co-transfected with 1 µg FIV Vif TLQAAA-V5 and 1 µg FcaA3 wild-type or mutants or pcDNA3.1 (+). 48 h later, the cells were lysed in IP-lysis buffer (50 mM Tris/HCl pH 8, 1 mM PMSE, 10 % Glycerol, 0.8 % NP-40, 150 mM NaCl, and protease inhibitor cocktail set III (Calbiochem, Darmstadt, Germany)). The lysates were cleared by centrifugation. The supernatant were incubated with 20 µl α-HA Affinity Matrix Beads (Roche) at 4 °C for 2 h. The samples were washed 5 times with lysate buffer on ice. Bound proteins were eluted by boiling the beads for 5 min at 95 °C in SDS loading buffer. Immunoblot analysis and detection were done as described.

3D-PCR

293T cells (5×10^5 cells/well in a 6-well plate) were transfected with 600 ng pFP93, 600 ng pLinSin, 100 ng pMD.G and 1000 ng FcaA3s expression plasmids or pcDNA3.1 (+) as a control. 48 h later, the viral supernatant was harvested, filtered (0.45 µm) and treated with DNase I (Life Technologies) at 37 °C for 1 h. 200 µl of supernatant was used for infecting 293T cells. 12 h post transduction, 293T cells were washed with PBS and DNA was isolated using DNeasy blood and tissue kit (Qiagen, Hilden, Germany). A 714-bp fragment of within the spliced luciferase

gene was amplified using the primers 5'-GATATGTG-GATTTCGAGTCGTC-3' and 5'-GTCATCGTCTTTC-CGTGCTC-3'. For selective amplification of the hypermutated products, the PCR denaturation temperature were lowered stepwise from 87.6 to 83.5 °C (83.5, 84.2, 85.2, 86.3, 87.6 °C) using a gradient thermocycler. The PCR parameters were as follows: (1) 95 °C for 5 min; (2) 40 cycles, with 1 cycle consisting of 83.5–87.6 °C for 30 s, 55 °C for 30 s, 72 °C for 1 min; (3) 10 min at 72 °C. PCRs were performed with recombination *Taq* DNA polymerase (Thermo Fisher Scientific).

Purification of GST tagged proteins and pull down assay

Feline A3Z2 and A3Z3 coding sequences were cloned in pGEX-6P2 vector (GE healthcare) with a C terminal HA tag to produce fusion proteins GST-FcaA3Z2-HA and GST-FcaA3Z3-HA (PCR primer in Additional file 2: Table S4). GST alone and fusion proteins were overexpressed in *E. coli* Rosetta (DE3) cells (EMD Millipore, Darmstadt, Germany) and purified by affinity chromatography using Glutathione Sepharose 4B beads (GE healthcare). After the culture of transformants until 0.6 OD₆₀₀, cells were induced with 1 mM isopropyl-beta-D-thiogalactopyranoside (IPTG) and 1 μM ZnSO₄ and cultured at 18 °C overnight. GST and Feline A3Z2/Z3 harboring cells were washed with PBS and lysed with 1× Bug buster protein extraction reagent (EMD Millipore) containing 50 mM Tris (pH 7.0), 10 % glycerol, and 1 M NaCl clarified by centrifugation and the soluble protein fraction was mixed with pre-equilibrated glutathione Sepharose beads. After 3 h incubation at 4 °C in end-over-end rotation, the beads were washed thrice with wash buffer containing 50 mM Tris (pH 8.0), 10 % glycerol and 500 mM NaCl and a single wash with the mild lysis buffer (50 mM Tris (pH 8), 1 mM PMSE, 10 % glycerol, 0.8 % NP-40, 150 mM NaCl and 1× complete protease inhibitor). These GST protein bound beads are used for the subsequent binding assay. GST pull down assay to detect direct binding with Vif of FIV: The protocol of protein–protein interactions was adapted from a previously described procedure [89]. HEK293T cells were transfected with 1.5 μg of FIV Vif-V5 coding plasmid and incubated for 48 h. Soluble protein fraction of HEK293T cells were obtained by lysing the cells with mild lysis buffer (50 mM Tris (pH 8), 1 mM PMSE, 10 % glycerol, 0.8 % NP-40, 150 mM NaCl, and 1× complete protease inhibitor (Calbiochem) and a 30 min centrifugation at 14,800 rpm. A fraction of the supernatant was kept for immunoblots; remaining lysates were equally added on the bead samples GST, GST-FcaA3Z2-HA and GST-FcaA3Z3-HA and incubated overnight at 4 °C in end-over-end rotation. Next day, the beads were washed thrice with the mild lysis buffer and the GST protein and protein complexes were eluted by adding wash

buffer containing 25 mM reduced glutathione. A fraction of the eluted proteins (equal amount) were boiled at 95 °C for 5 min with Roti load reducing loading buffer (Carl Roth) and resolved on a SDS-PAGE gel. FIV Vif and GST-FcaA3s were detected by anti-V5 and -HA antibody, respectively. Coomassie brilliant blue stained gel was also added to show the purity of GST and FcaA3 fusion proteins.

Evolutionary analyses

The initial set of A3 sequences was taken from Münk and coworkers [3]. These sequences were used as seeds for BLASTn, tBLASTn and BLAT searches to recover additional A3 sequences from genomes in Carnivora. The final dataset (closed on November 2015) contained four A3Z1 sequences from four Caniformia species, six A3Z2 sequences from six Caniformia species, eleven A3Z2 sequences from six Feliformia species, ten A3Z3 sequences from five Caniformia species and five A3Z3 sequences from five Feliformia species. Sequences were aligned at the amino acid level with MUSCLE [90]. The final alignment encompassed 629 and 269 alignment patterns at the nucleotide level and at the amino acid level, respectively. Phylogenetic inference was performed with RAXML_v8.2 [91, 92] using the GTR + 4Γ model at the nucleotide level and LG + Γ model at the amino acid level, the model choice done after initial maximum likelihood searches with RAXML. Additional phylogenetic inference was performed separately for the A3Z2 and A3Z3 genes using the same settings. In all cases, no significant differences between amino acid and nucleotide tree topologies were observed using the Shimodaira–Hasegawa test [93]. Phylogenetic supernetworks were constructed with SplitsTree_v4 [94] using 1000 either nucleotide or amino acid bootstrapped maximum likelihood trees. Selection on individual codons was inferred under a Bayesian framework with SELECTON V2.4 (<http://selecton.tau.ac.il/>) [95] contrasting the M8 and M8a models, and with DATAMONKEY (<http://www.datamonkey.org/>) using the Random Effects Likelihood (REL) model [96].

Statistical analysis

Data are represented as the mean with SD in all bar diagrams. Statistically significant differences between two groups were analyzed using the unpaired Student's t test with GraphPad Prism version 5 (GraphPad software, San Diego, CA, USA). Validity of the null hypothesis was verified with significance level at α value = 0.05.

Homology modelling of feline A3Z2Z3 protein

The homology modeling of the linker region of the feline A3Z2Z3 was performed in several steps: First, the

in-house meta-tool TopModel [59, 60] was used to compute a consensus alignment for the feline A3 sequences to the structural model of the human A3G [58] using 13 different alignment programs (Additional file 2: Table S5). From the consensus alignment, the feline A3 linker was identified and then submitted to TopModel for automated structure prediction using eight state-of-the-art threading programs (Additional file 2: Table S5). The identified templates (2YS9, chain A (19.4 %); 2MMB, chain A (17.1 %); 2DA4, chain A (14.7 %); 2LFB, chain A (9.2 %) and 1FTZ, chain A (12.9 %); sequence identities with respect to the linker are given in parentheses) were aligned to the linker sequence with TopModel using threading, sequence, and structural alignment programs, to produce a large alignment ensemble from every combination of the top three ranked templates and the target sequence. These alignments were modeled using Modeller9.1 [97], refined with RASP [98], and ranked using the in-house meta-tool for model quality assessment TopScore (D. Mulnaes, H. Gohlke, unpublished results), which combines quality assessments from eight different model quality assessment programs (Additional file 2: Table S5). The top ranked models for each template combination were refined with ModRefiner [99] and used as templates for a second round of modeling where bad scoring regions were removed. The resulting models were re-ranked and refined, and the top ranking model was selected as the linker representative. The model of the rest of the feline A3Z2Z3 was made with TopModel in a similar fashion using the feline–human consensus alignment. The linker domain was manually positioned near the linker region gap, unstructured parts were connected to the rest of the feline A3Z2Z3 and minimized using the MAB force field [100] as implemented in Moloc, thereby keeping all other protein atoms fixed.

Homology modelling of human A3H and feline A3Z2b and A3Z3 proteins

The models of the three proteins were built using the default settings in TopModel and all possible combinations of the top three ranked templates in each case. For the human A3H model, the templates were: PDB ID 4 J4 J, chain A, 35 % identity/96 % coverage; 2KBO, chain A, 37/95 %; 2RPZ, chain A, 30/94 %, resulting in a model with 84 % accuracy according to TopScore. For the feline A3Z2b model, the templates were: 3VM8, chain A, 42/94 %; 2KBO, chain A, 39/94 %; 1M65, chain A, 10/87 %, resulting in a model with 88 % accuracy according to TopScore. For the feline A3Z3 model, the templates were: 4J4J, chain A, 31/91 %; 2KBO, chain A, 36/90 %; 2RPZ, chain A, 24/92 %, resulting in a model with 84 % accuracy according to TopScore.

Additional files

Additional file 1: Figure S1. Cellular localization of feline A3s and FIV Vif. HOS cells were transfected with FcaA3Z2b, FcaA3Z3, or FcaA3Z2Z3 (all with HA-tag), together with FIV Vif-TLQAAA. To detect A3 (green) immunofluorescence, staining was performed with an anti-HA antibody. To detect FIV Vif (red) immunofluorescence, staining was performed with an anti-V5 antibody. Nuclei (blue) were visualized by DAPI staining. **Figure S2.** Comparison of protein sequences of A3s and Vif. (A, B) The sequence alignment of (A) FcaA3Z2 (FcaA3Z2b), (B) FcaA3Z3 and big cat A3 proteins. The D165-H166 and L40-I41 + A65 domains that are essential for FIV Vif induced degradation are marked by red boxes. (C) Sequence alignment of domestic cat FIV Vif (FIVfca subtype 34TF10) and lion FIV (FIVple subtype E) Vif. The C187 and C190 that are essential for induced FcaA3s degradation and marked the presumed BC box (TLQ/SLQ) marked by red boxes. (D) Sequence alignment of HIV-1 (strain NL4-3) and HIV-2 (strain RodA) Vif. The CUL5 box (HCCH) and BC box (SLQ) were marked by red boxes. Pti, Ple, Lly and Pco represent *Panthera tigris corbetti*; *Panthera leo bleyenberghi*; *Lynx lynx*; *Puma concolor*. **Figure S3.** Evolutionary supernetwork of A3 sequences retrieved from carnivores. The network was constructed with SplitsTree_v4 using 1,000 maximum likelihood bootstrapped trees created with RAxML_v8.2. Scale bar is given in substitutions per site. The approximate position of the root obtained using maximum likelihood inference with all A3Z1, A3Z2 and A3Z3 sequences from carnivores is indicated in grey. (A) The evolutionary distances among A3Z3 sequences within the two in-paralogs within Caniformia (upper branches and left branch) and within Feliformia (right branches) are indicated as overall average pairwise nucleotide distance \pm bootstrap standard error estimate. For each tip, the actual sequence orthologous to positions 38–44 in the *F. catus* A3Z3 gene are given in parentheses. The inset displays the evolutionary relationships among the Carnivora species for which we have identified A3Z3 paralogs. (B) The evolutionary distances among A3Z2 sequences within Caniformia (upper branches) and within Feliformia (lower branches) are indicated as overall average pairwise nucleotide distance \pm bootstrap standard error estimate. For each tip, the actual sequence orthologous to positions 165–170 in the *F. catus* A3Z2 genes are given in parentheses. **Figure S4.** The mutations in FcaA3 that cause resistance to FIV Vif do not alter the cellular distribution of FcaA3s. HOS cells were transfected with FcaA3Z2 (FcaA3Z2b), FcaA3Z2.DH-YN, FcaA3Z3, FcaA3Z3.A65I + LI-AA, FcaA3Z2Z3 or FcaA3Z2Z3-M (all with HA-tag). To detect A3 (green) immunofluorescence, staining was performed with an anti-HA antibody. Nuclei (blue) were visualized by DAPI staining. **Figure S5.** Sequence alignment of feline APOBEC3. Sequence alignment of feline A3Z2Z3 and human A3G as generated by the TopModel approach. The Z2 and Z3 domains are underlined in yellow and blue, respectively. The sequence of the linker domain is underlined in magenta. Helical regions and β -strands are depicted as red helices and green arrows, respectively. In addition, the alignments of three template structures used to model the structure of the linker domain are given (PDB IDs 2YS9, 2DA4, 2MMB). **Figure S6.** Expression of CD4 and CCR5 receptors on the surface of HOS (red) and HOS.CD4.CCR5 cells (blue) expressing feline A3Z2Z3 or A3Z2Z3-M. CD4 and CCR5 were detected by flow cytometry and anti-CD4 and anti-CCR5 antibodies. Numbers indicate the percentage of positive cells. HOS cells served as background control. **Figure S7.** The mutated FcaA3s are encapsidated and inhibit FIV by cytidine deamination. (A) The mutated FcaA3s can inhibit the infectivity of FIV Δ vif reporter viruses. 293T cells were co-transfected with plasmids for FIV Δ vif luciferase together with FcaA3s. 48 h later, supernatant normalized for reverse transcriptase activity was used to transduce 293T cells. Luciferase activity was determined two days post transduction. Asterisks represent statistically significant differences: ***, $p < 0.001$; **, $0.001 < p < 0.01$; *, $0.01 < p < 0.05$; ns, $p > 0.05$ [Dunnett's test]. (B) Immunoblot of FIV producer cells and VLPs used for (A). Encapsidation of wild-type and mutated feline A3s into FIV Δ vif virus like particles (VLPs), A3 proteins were detected by anti-HA antibody. Tubulin detection for equal loading of cell lysate was done using anti-tubulin, for demonstration of equal loading of FIV VLPs VSV-G and FIV p24 proteins were detected by anti-VSV-G and anti-FIV p24 antibodies separately. (C) Encapsidated wild-type and mutated FcaA3s deaminate cytidines FIV genomes. FIV Δ vif was produced in the absence and presence of wild-type and mutant FcaA3s (FcaA3Z3,

FcaA3Z3.A65I + LI-AA, FcaA3Z2Z3, FcaA3Z2Z3-M) or HsaA3G. The vector particles were used to infect 293T cells. 12 h later, the total cellular DNA was extracted and differential DNA denaturation PCR (3D-PCR) was performed. Td: denaturing temperature. **Figure S8.** *Vif titration on FcaA3 linker mutants.* Co-transfection of increasing amounts of expression plasmids for (A) HIV-2 Vif and (B) SIVmac Vif with constant amounts of the indicated A3 expression plasmids. The expression of FcaA3s and Vifs were analyzed by anti-HA and anti-V5 antibodies, respectively. Cell lysates were also analyzed for equal amounts of total proteins using anti-tubulin antibody.

Figure S9. *Expression and encapsidation of feline A3 linker mutants using (A) FIVΔvif and (B) SIVmacΔvif.* Immunoblots of corresponding experiments shown in Fig. 10C and 10D. Immunoblots of lysates of virus producer cells (cell) and virus particles (VLP). A3s were detected by anti-HA antibodies, cell lysates were also analyzed for equal amounts of total proteins using anti-tubulin antibody and VLP lysates using anti-VSV-G antibody.

Figure S10. *HIV-1 Vif cannot target the "YYFWDPN/DY" domain in FcaA3.* (A) CO-IP of feline A3Z2Z3 (HA tag) with either HIV-1 Vif (V5 tag) or FIV Vif (TLQAAA mutant, V5 tag). A3Z2Z3 immune precipitated and detected by anti-HA antibody, co-precipitated Vif was detected by anti-V5 antibody. (B) Comparison of the "YYFWDPN/DY" domain in HsaA3G and FcaA3Z2Z3 and derived mutations generated in FcaA3Z2Z3, the mutated residues shown in bold. (C) FcaA3Z2Z3 mutants were investigated for being sensitive for degradation by HIV-1 Vif. Expression plasmids of FcaA3Z2Z3 mutants of HsaA3G were co-transfected together with HIV-1 Vif into 293T cells. 48 h later, Cell lysates were used to detect the expression of FcaA3Z2Z3 and HIV-1 Vif by anti-HA and anti-V5 antibodies, respectively. Cell lysates were also analyzed for equal amounts of total proteins using anti-tubulin antibody.

Additional file 2: Table S1. Primer list used for HsaA3C/FcaA3Z2 chimeras and FcaA3Z2 mutants. **Table S2.** Primer list used for HsaA3H/FcaA3Z3 chimeras and FcaA3Z3 mutants. **Table S3.** Primer list used for FcaA3Z2Z3 mutants. **Table S4.** Primer used to clone GST fusion constructs. **Table S5.** The software used in TopModel for threading, alignment and model quality estimation^a.

Abbreviations

FIV: feline immunodeficiency virus; HIV: human immunodeficiency virus; SIV: simian immunodeficiency virus; APOBEC3: apolipoprotein B mRNA editing enzyme, catalytic polypeptide-like; Vif: viral infectivity factor; UTR: untranslated region.

Authors' contributions

ZZ, QG, AAJV, AH, BPK, and SH conducted experiments, DM, SHJS and HG generated the feline A3 homology model. IGB analyzed the evolutionary origin of feline A3s. KS, KC, DH, SHJS, HG and CM analyzed data and conceived experiments. IGB, SHJS, HG and CM wrote the manuscript. CM conceived the study. All authors read and approved the final manuscript.

Author details

¹ Clinic for Gastroenterology, Hepatology, and Infectiology, Medical Faculty, Heinrich-Heine-University Düsseldorf, Building 23.12.U1.82, Moorenstr. 5, 40225 Düsseldorf, Germany. ² Department of Medical Biotechnology, Paul-Ehrlich-Institute, Paul-Ehrlich-Str. 51-59, 63225 Langen, Germany. ³ Institute of Biochemistry, Heinrich Heine University Düsseldorf, Universitätsstr. 1, 40225 Düsseldorf, Germany. ⁴ Institute of Pharmaceutical and Medicinal Chemistry, Heinrich Heine University Düsseldorf, Universitätsstr. 1, 40225 Düsseldorf, Germany. ⁵ Laboratory of Viral Pathogenesis, Institute for Virus Research, Kyoto University, Kyoto 6068507, Japan. ⁶ CREST, Japan Science and Technology Agency, Saitama 3220012, Japan. ⁷ MIVEGEC (UMR CNRS 5290, IRD 224, UM), National Center of Scientific Research (CNRS), 34394 Montpellier, France. ⁸ Present Address: BioNTech RNA Pharmaceuticals GmbH, An der Goldgrube 12, 55131 Mainz, Germany.

Acknowledgements

We thank Wioletta Hörschken for excellent technical assistance, Rebecca Clemens for discussion and sharing of preliminary data, Yannick Bulliard and

Didier Trono for the model of the full-length A3G. We thank Nathaniel R. Landau, Garry Nolan, Eric Poeschla, and Viviana Simon for reagents. The following reagents were obtained through the NIH AIDS Reagent Program, Division of AIDS, NIAID, NIH: Monoclonal antibody to HIV-1 p24 (AG3.0) from Jonathan Allan, TZM-bl cells from John C. Kappes, Xiaoyun Wu and Tranzyme Inc., HIV-1 Vif monoclonal antibody (#319) from Michael H. Malim and anti-FIV p24 monoclonal (PAK3-2C1).

Competing interests

The authors declare that they have no competing interests.

Funding

ZZ and QG are supported by a scholarship from China Scholarship Council; CM is supported by the Heinz Ansmann foundation.

Received: 8 March 2016 Accepted: 9 June 2016

Published online: 01 July 2016

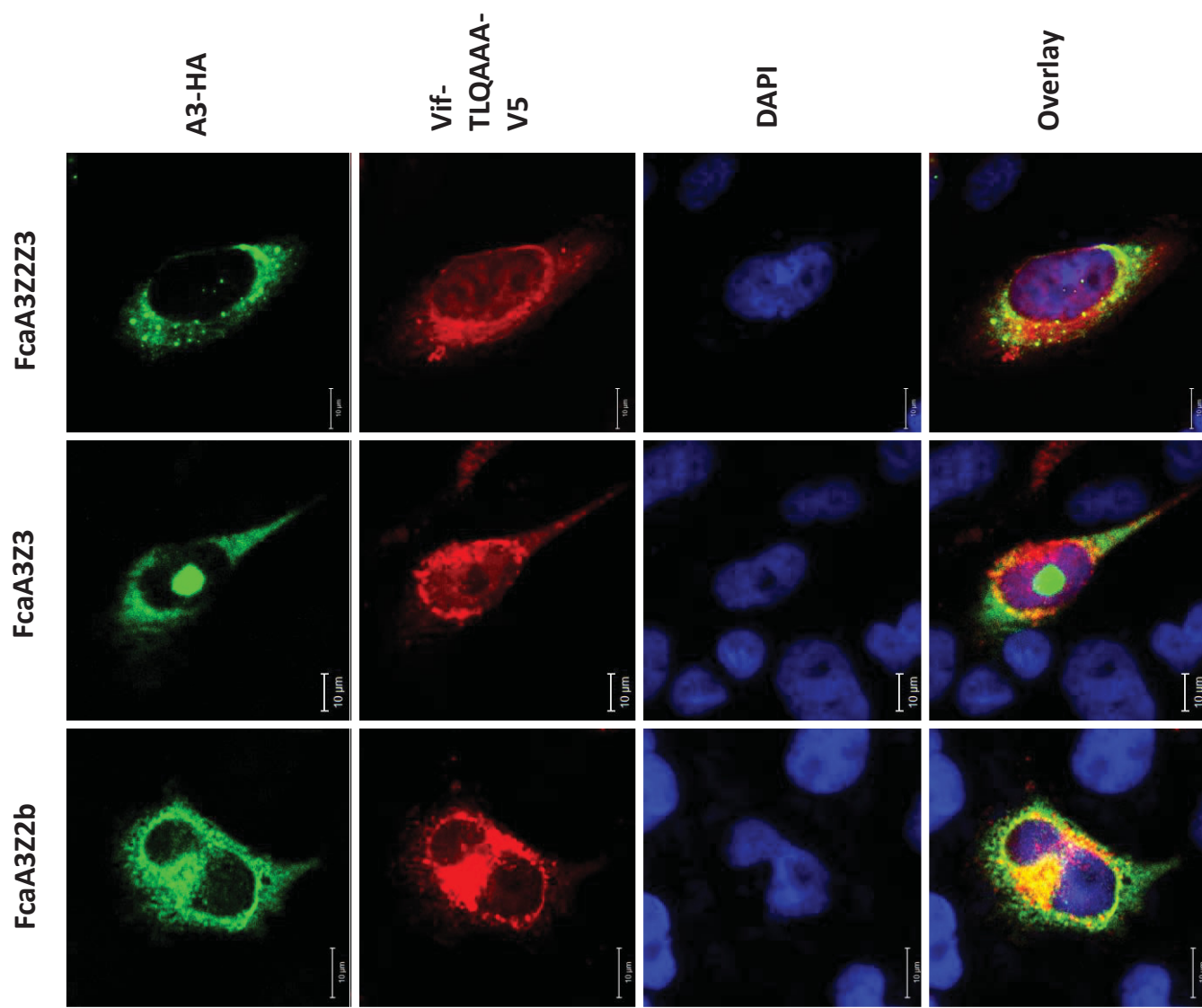
References

- LaRue RS, Jonsson SR, Silverstein KA, Lajoie M, Bertrand D, El-Mabrouk N, Hotzel I, Andresdottir V, Smith TP, Harris RS. The artiodactyl APOBEC3 innate immune repertoire shows evidence for a multi-functional domain organization that existed in the ancestor of placental mammals. *BMC Mol Biol*. 2008;9:104.
- LaRue RS, Andresdottir V, Blanchard Y, Conticello SG, Derse D, Emerman M, Greene WC, Jonsson SR, Landau NR, Löchelt M, et al. Guidelines for naming nonprimate APOBEC3 genes and proteins. *J Virol*. 2009;83(2):494–7.
- Münk C, Willemsen A, Bravo IG. An ancient history of gene duplications, fusions and losses in the evolution of APOBEC3 mutators in mammals. *BMC Evol Biol*. 2012;12:71.
- Münk C, Beck T, Zielonka J, Hotz-Wagenblatt A, Chareza S, Battenberg M, Thielebein J, Cichutek K, Bravo IG, O'Brien SJ, et al. Functions, structure, and read-through alternative splicing of feline APOBEC3 genes. *Genome Biol*. 2008;9(3):R48.
- Jarmuz A, Chester A, Bayliss J, Gisbourne J, Dunham I, Scott J, Navaratnam N. An anthropoid-specific locus of orphan C to U RNA-editing enzymes on chromosome 22. *Genomics*. 2002;79(3):285–96.
- Willems L, Gillet NA. APOBEC3 interference during replication of viral genomes. *Viruses*. 2015;7(6):2999–3018.
- Harris RS, Dudley JP. APOBECs and virus restriction. *Virology*. 2015;479–480:131–45.
- Sheehy AM, Gaddis NC, Choi JD, Malim MH. Isolation of a human gene that inhibits HIV-1 infection and is suppressed by the viral Vif protein. *Nature*. 2002;418(6898):646–50.
- Derse D, Hill SA, Prinler G, Lloyd P, Heidecker G. Resistance of human T cell leukemia virus type 1 to APOBEC3G restriction is mediated by elements in nucleocapsid. *Proc Natl Acad Sci USA*. 2007;104(8):2915–20.
- Löchelt M, Romen F, Bastone P, Muckenfuss H, Kirchner N, Kim YB, Truyen U, Rosler U, Battenberg M, Saib A, et al. The antiretroviral activity of APOBEC3 is inhibited by the foamy virus accessory Bet protein. *Proc Natl Acad Sci USA*. 2005;102(22):7982–7.
- Stavrou S, Nitta T, Kotla S, Ha D, Nagashima K, Rein AR, Fan H, Ross SR. Murine leukemia virus glycosylated Gag blocks apolipoprotein B editing complex 3 and cytosolic sensor access to the reverse transcription complex. *Proc Natl Acad Sci USA*. 2013;110(22):9078–83.
- Rosales Gerpe MC, Renner TM, Belanger K, Lam C, Aydin H, Langlois MA. N-linked glycosylation protects gammaretroviruses against deamination by APOBEC3 proteins. *J Virol*. 2015;89(4):2342–57.
- Kolokithas A, Rosenke K, Malik F, Hendrick D, Swanson L, Santiago ML, Portis JL, Hasenkrug KJ, Evans LH. The glycosylated Gag protein of a murine leukemia virus inhibits the antiretroviral function of APOBEC3. *J Virol*. 2010;84(20):10933–6.
- Holmes RK, Koning FA, Bishop KN, Malim MH. APOBEC3F can inhibit the accumulation of HIV-1 reverse transcription products in the absence of hypermutation. Comparisons with APOBEC3G. *J Biol Chem*. 2007;282(4):2587–95.
- Iwatani Y, Chan DS, Wang F, Maynard KS, Sugiura W, Gronenborn AM, Rouzina I, Williams MC, Musier-Forsyth K, Levin JG.

- Deaminase-independent inhibition of HIV-1 reverse transcription by APOBEC3G. *Nucleic Acids Res.* 2007;35(21):7096–108.
16. Gillick K, Pollpeter D, Phalora P, Kim EY, Wolinsky SM, Malim MH. Suppression of HIV-1 infection by APOBEC3 proteins in primary human CD4(+) T cells is associated with inhibition of processive reverse transcription as well as excessive cytidine deamination. *J Virol.* 2013;87(3):1508–17.
 17. Wang X, Ao Z, Chen L, Kobinger G, Peng J, Yao X. The cellular antiviral protein APOBEC3G interacts with HIV-1 reverse transcriptase and inhibits its function during viral replication. *J Virol.* 2012;86(7):3777–86.
 18. Mbisa JL, Barr R, Thomas JA, Vandegraaff N, Dorweiler JJ, Svarovskaia ES, Brown WL, Mansky LM, Gorelick RJ, Harris RS, et al. Human immunodeficiency virus type 1 cDNAs produced in the presence of APOBEC3G exhibit defects in plus-strand DNA transfer and integration. *J Virol.* 2007;81(13):7099–110.
 19. Mbisa JL, Bu W, Pathak VK. APOBEC3F and APOBEC3G inhibit HIV-1 DNA integration by different mechanisms. *J Virol.* 2010;84(10):5250–9.
 20. Kenyon JC, Lever AM. The molecular biology of feline immunodeficiency virus (FIV). *Viruses.* 2011;3(11):2192–213.
 21. Pecon-Slaterry J, Troyer JL, Johnson WE, O'Brien SJ. Evolution of feline immunodeficiency virus in Felidae: implications for human health and wildlife ecology. *Vet Immunol Immunopathol.* 2008;123(1–2):32–44.
 22. Willett BJ, Hosie MJ. Feline leukaemia virus: half a century since its discovery. *Vet J.* 2013;195(1):16–23.
 23. Rethwilm A, Bodem J. Evolution of foamy viruses: the most ancient of all retroviruses. *Viruses.* 2013;5(10):2349–74.
 24. Hartmann K. Clinical aspects of feline immunodeficiency and feline leukemia virus infection. *Vet Immunol Immunopathol.* 2011;143(3–4):190–201.
 25. de Rozieres S, Mathiason CK, Rolston MR, Chatterji U, Hoover EA, Elder JH. Characterization of a highly pathogenic molecular clone of feline immunodeficiency virus clade C. *J Virol.* 2004;78(17):8971–82.
 26. Diehl LJ, Mathiason-Dubard CK, O'Neil LL, Obert LA, Hoover EA. Induction of accelerated feline immunodeficiency virus disease by acute-phase virus passage. *J Virol.* 1995;69(10):6149–57.
 27. Obert LA, Hoover EA. Feline immunodeficiency virus clade C mucosal transmission and disease courses. *AIDS Res Hum Retrovir.* 2000;16(7):677–88.
 28. Lehman TL, O'Halloran KP, Hoover EA, Avery PR. Utilizing the FIV model to understand dendritic cell dysfunction and the potential role of dendritic cell immunization in HIV infection. *Vet Immunol Immunopathol.* 2010;134(1–2):75–81.
 29. Yamamoto JK, Sanou MP, Abbott JR, Coleman JK. Feline immunodeficiency virus model for designing HIV/AIDS vaccines. *Curr HIV Res.* 2010;8(1):14–25.
 30. Elder JH, Lin YC, Fink E, Grant CK. Feline immunodeficiency virus (FIV) as a model for study of lentivirus infections: parallels with HIV. *Curr HIV Res.* 2010;8(1):73–80.
 31. O'Brien SJ, Troyer JL, Brown MA, Johnson WE, Antunes A, Roelke ME, Pecon-Slaterry J. Emerging viruses in the Felidae: shifting paradigms. *Viruses.* 2012;4(2):236–57.
 32. German AC, Harbour DA, Helps CR, Gruffydd-Jones TJ. Is feline foamy virus really apathogenic? *Vet Immunol Immunopathol.* 2008;123(1–2):114–8.
 33. Winkler IG, Lochelt M, Flower RL. Epidemiology of feline foamy virus and feline immunodeficiency virus infections in domestic and feral cats: a seroepidemiological study. *J Clin Microbiol.* 1999;37(9):2848–51.
 34. Phung HT, Ikeda Y, Miyazawa T, Nakamura K, Mochizuki M, Izumiya Y, Sato E, Nishimura Y, Tohya Y, Takahashi E, et al. Genetic analyses of feline foamy virus isolates from domestic and wild feline species in geographically distinct areas. *Virus Res.* 2001;76(2):171–81.
 35. Zielonka J, Münk C. Cellular restriction factors of feline immunodeficiency virus. *Viruses.* 2011;3(10):1986–2005.
 36. Zielonka J, Marino D, Hofmann H, Yuhki N, Löchelt M, Münk C. Vif of feline immunodeficiency virus from domestic cats protects against APOBEC3 restriction factors from many felids. *J Virol.* 2010;84(14):7312–24.
 37. Wang J, Zhang W, Lv M, Zuo T, Kong W, Yu X. Identification of a Cullin5-ElonginB-ElonginC E3 complex in degradation of feline immunodeficiency virus Vif-mediated feline APOBEC3 proteins. *J Virol.* 2011;85(23):12482–91.
 38. Chareza S, Slavkovic LD, Liu Y, Rathe AM, Münk C, Zabogli E, Pistello M, Löchelt M. Molecular and functional interactions of cat APOBEC3 and feline foamy and immunodeficiency virus proteins: different ways to counteract host-encoded restriction. *Virology.* 2012;424(2):138–46.
 39. Münk C, Hechler T, Chareza S, Löchelt M. Restriction of feline retroviruses: lessons from cat APOBEC3 cytidine deaminases and TRIM5alpha proteins. *Vet Immunol Immunopathol.* 2010;134(1–2):14–24.
 40. de Castro FL, Junqueira DM, de Medeiros RM, da Silva TR, Costenaro JG, Knak MB, de Matos Almeida SE, Campos FS, Roehe PM, Franco AC. Analysis of single-nucleotide polymorphisms in the APOBEC3H gene of domestic cats (*Felis catus*) and their association with the susceptibility to feline immunodeficiency virus and feline leukemia virus infections. *Infect Genet Evol.* 2014;27:389–94.
 41. Mehle A, Goncalves J, Santa-Marta M, McPike M, Gabuzda D. Phosphorylation of a novel SOCS-box regulates assembly of the HIV-1 Vif-Cul5 complex that promotes APOBEC3G degradation. *Genes Dev.* 2004;18(23):2861–6.
 42. Yu Y, Xiao Z, Ehrlich ES, Yu X, Yu XF. Selective assembly of HIV-1 Vif-Cul5-ElonginB-ElonginC E3 ubiquitin ligase complex through a novel SOCS box and upstream cysteines. *Genes Dev.* 2004;18(23):2867–72.
 43. Yu X, Yu Y, Liu B, Luo K, Kong W, Mao P, Yu XF. Induction of APOBEC3G ubiquitination and degradation by an HIV-1 Vif-Cul5-SCF complex. *Science.* 2003;302(5647):1056–60.
 44. Jager S, Kim DY, Hultquist JF, Shindo K, LaRue RS, Kwon E, Li M, Anderson BD, Yen L, Stanley D, et al. Vif hijacks CBF-beta to degrade APOBEC3G and promote HIV-1 infection. *Nature.* 2012;481(7381):371–5.
 45. Zhang W, Du J, Evans SL, Yu Y, Yu XF. T-cell differentiation factor CBF-beta regulates HIV-1 Vif-mediated evasion of host restriction. *Nature.* 2012;481(7381):376–9.
 46. Yoshikawa R, Takeuchi JS, Yamada E, Nakano Y, Ren F, Tanaka H, Munk C, Harris RS, Miyazawa T, Koyanagi Y, et al. Vif determines the requirement for CBF-beta in APOBEC3 degradation. *J Gen Virol.* 2015;96(Pt 4):887–92.
 47. Kane JR, Stanley DJ, Hultquist JF, Johnson JR, Mietrach N, Binning JM, Jonsson SR, Barelier S, Newton BW, Johnson TL, et al. Lineage-specific viral hijacking of non-canonical E3 Ubiquitin ligase cofactors in the evolution of Vif anti-APOBEC3 activity. *Cell Rep.* 2015;11(8):1236–50.
 48. Ai Y, Zhu D, Wang C, Su C, Ma J, Ma J, Wang X. Core-binding factor subunit beta is not required for non-primate lentiviral Vif-mediated APOBEC3 degradation. *J Virol.* 2014;88(20):12112–22.
 49. Han X, Liang W, Hua D, Zhou X, Du J, Evans SL, Gao Q, Wang H, Viqueira R, Wei W, et al. Evolutionarily conserved requirement for core binding factor beta in the assembly of the human immunodeficiency virus/simian immunodeficiency virus Vif-cullin 5-RING E3 ubiquitin ligase. *J Virol.* 2014;88(6):3320–8.
 50. Münk C, Zielonka J, Constabel H, Kloke BP, Rengstl B, Battenberg M, Bonci F, Pistello M, Lochelt M, Cichutek K. Multiple restrictions of human immunodeficiency virus type 1 in feline cells. *J Virol.* 2007;81(13):7048–60.
 51. Stern MA, Hu C, Saenz DT, Fadel HJ, Sims O, Peretz M, Poeschla EM. Productive replication of Vif-chimeric HIV-1 in feline cells. *J Virol.* 2010;84(14):7378–95.
 52. LaRue RS, Lengyel J, Jonsson SR, Andresdottir V, Harris RS. Lentiviral Vif degrades the APOBEC3Z3/APOBEC3H protein of its mammalian host and is capable of cross-species activity. *J Virol.* 2010;84(16):8193–201.
 53. Zielonka J, Bravo IG, Marino D, Conrad E, Perkovic M, Battenberg M, Cichutek K, Münk C. Restriction of equine infectious anemia virus by equine APOBEC3 cytidine deaminases. *J Virol.* 2009;83(15):7547–59.
 54. Binka M, Ooms M, Steward M, Simon V. The activity spectrum of Vif from multiple HIV-1 subtypes against APOBEC3G, APOBEC3F, and APOBEC3H. *J Virol.* 2012;86(1):49–59.
 55. Sonnhammer EL, Koonin EV. Orthology, paralogy and proposed classification for paralog subtypes. *Trends Genet.* 2002;18(12):619–20.
 56. Yoshikawa R, Izumi T, Yamada E, Nakano Y, Misawa N, Ren F, Carpenter MA, Ikeda T, Münk C, Harris RS, et al. A naturally occurring domestic cat APOBEC3 variant confers resistance to FIV infection. *J Virol.* 2015;90(1):474–85.
 57. Curran MA, Kaiser SM, Achacoso PL, Nolan GP. Efficient transduction of nondividing cells by optimized feline immunodeficiency virus vectors. *Mol Ther.* 2000;1(1):31–8.
 58. Bulliard Y, Turelli P, Röhrig UF, Zoete V, Mangeat B, Michielin O, Trono D. Functional analysis and structural modeling of human APOBEC3G

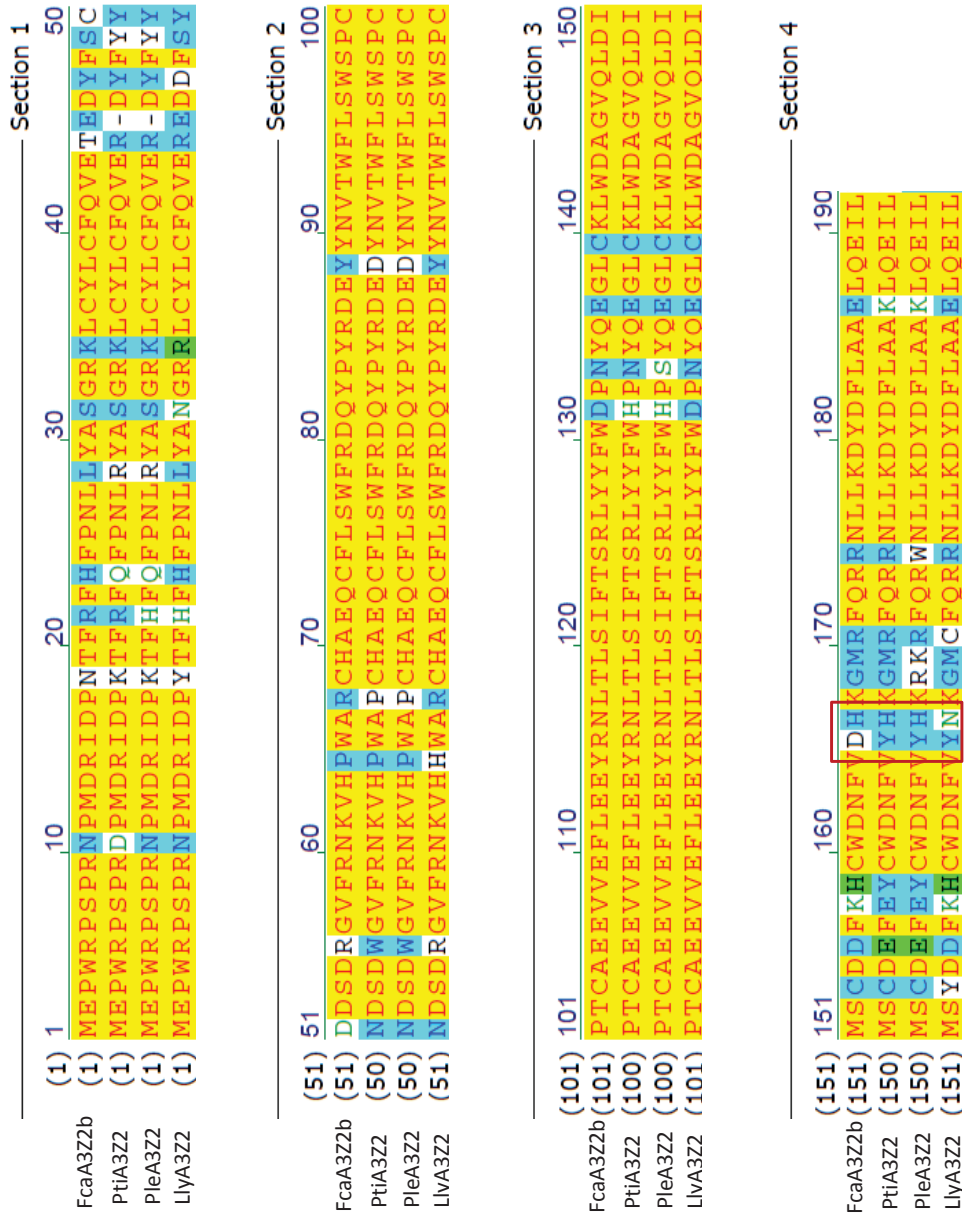
- reveal the role of evolutionarily conserved elements in the inhibition of human immunodeficiency virus type 1 infection and Alu transposition. *J Virol.* 2009;83(23):12611–21.
59. Gohlke H, Hergert U, Meyer T, Mulnaes D, Grieshaber MK, Smits SH, Schmitt L. Binding region of alanine dehydrogenase predicted by unbiased molecular dynamics simulations of ligand diffusion. *J Chem Inf Model.* 2013;53(10):2493–8.
 60. Widdrich N, Pittelkow M, Höppner A, Mulnaes D, Buckel W, Gohlke H, Smits SH, Bremer E. Molecular dynamics simulations and structure-guided mutagenesis provide insight into the architecture of the catalytic core of the ectoine hydroxylase. *J Mol Biol.* 2014;426(3):586–600.
 61. Gehring WJ. The homeobox in perspective. *Trends Biochem Sci.* 1992;17(8):277–80.
 62. Suspene R, Henry M, Guillot S, Wain-Hobson S, Vartanian JP. Recovery of APOBEC3-edited human immunodeficiency virus G → A hypermutants by differential DNA denaturation PCR. *J Gen Virol.* 2005;86(Pt 1):125–9.
 63. Mariani R, Chen D, Schröfelbauer B, Navarro F, König R, Bollman B, Münk C, Nymark-McMahon H, Landau NR. Species-specific exclusion of APOBEC3G from HIV-1 virions by Vif. *Cell.* 2003;114(1):21–31.
 64. Bähr A, Singer A, Hain A, Vasudevan AA, Schilling M, Reh J, Riess M, Panitz S, Serrano V, Schweizer M, et al. Interferon but not MxB inhibits foamy retroviruses. *Virology.* 2015;488:51–60.
 65. Huthoff H, Malim MH. Identification of amino acid residues in APOBEC3G required for regulation by human immunodeficiency virus type 1 Vif and Virion encapsidation. *J Virol.* 2007;81(8):3807–15.
 66. Letko M, Booiyan T, Kootstra N, Simon V, Ooms M. Identification of the HIV-1 Vif and human APOBEC3G protein interface. *Cell Rep* 2015;13(9):1789–99.
 67. Vasudevan AA, Smits SH, Höppner A, Häussinger D, Koenig BW, Münk C. Structural features of antiviral DNA cytidine deaminases. *Biol Chem.* 2013;394(11):1357–70.
 68. Kouno T, Luengas EM, Shigematsu M, Shandilya SM, Zhang J, Chen L, Hara M, Schiffer CA, Harris RS, Matsuo H. Structure of the Vif-binding domain of the antiviral enzyme APOBEC3G. *Nat Struct Mol Biol.* 2015;22(6):485–91.
 69. Kitamura S, Ode H, Nakashima M, Imahashi M, Naganawa Y, Kurosawa T, Yokomaku Y, Yamane T, Watanabe N, Suzuki A, et al. The APOBEC3C crystal structure and the interface for HIV-1 Vif binding. *Nat Struct Mol Biol.* 2012;19(10):1005–10.
 70. He Z, Zhang W, Chen G, Xu R, Yu XF. Characterization of conserved motifs in HIV-1 Vif required for APOBEC3G and APOBEC3F interaction. *J Mol Biol.* 2008;381(4):1000–11.
 71. Zhang W, Huang M, Wang T, Tan L, Tian C, Yu X, Kong W, Yu XF. Conserved and non-conserved features of HIV-1 and SIVagm Vif mediated suppression of APOBEC3 cytidine deaminases. *Cell Microbiol.* 2008;10(8):1662–75.
 72. Baig TT, Feng Y, Chelico L. Determinants of efficient degradation of APOBEC3 restriction factors by HIV-1 Vif. *J Virol.* 2014;88(24):14380–95.
 73. Marin M, Golem S, Rose KM, Kozak SL, Kabat D. Human immunodeficiency virus type 1 Vif functionally interacts with diverse APOBEC3 cytidine deaminases and moves with them between cytoplasmic sites of mRNA metabolism. *J Virol.* 2008;82(2):987–98.
 74. Richards C, Albin JS, Demir O, Shaban NM, Luengas EM, Land AM, Anderson BD, Holten JR, Anderson JS, Harki DA, et al. The binding interface between human APOBEC3F and HIV-1 Vif elucidated by genetic and computational approaches. *Cell Rep.* 2015;13(9):1781–8.
 75. Salter JD, Morales GA, Smith HC. Structural insights for HIV-1 therapeutic strategies targeting Vif. *Trends Biochem Sci.* 2014;39(9):373–80.
 76. Aydin H, Taylor MW, Lee JE. Structure-guided analysis of the human APOBEC3-HIV restrictome. *Structure.* 2014;22(5):668–84.
 77. Land AM, Shaban NM, Evans L, Hultquist JF, Albin JS, Harris RS. APOBEC3F determinants of HIV-1 Vif sensitivity. *J Virol.* 2014;88(21):12923–7.
 78. Siu KK, Sultana A, Azimi FC, Lee JE. Structural determinants of HIV-1 Vif susceptibility and DNA binding in APOBEC3F. *Nat Commun.* 2013;4:2593.
 79. Ooms M, Letko M, Binka M, Simon V. The resistance of human APOBEC3H to HIV-1 NL4-3 molecular clone is determined by a single amino acid in Vif. *PLoS One.* 2013;8(2):e57744.
 80. Zhen A, Wang T, Zhao K, Xiong Y, Yu XF. A single amino acid difference in human APOBEC3H variants determines HIV-1 Vif sensitivity. *J Virol.* 2010;84(4):1902–11.
 81. Lavens D, Peelman F, Van der Heyden J, Uyttendaele I, Catteuw D, Verhee A, Van Schoubroeck B, Kurth J, Hallenberger S, Clayton R, et al. Definition of the interacting interfaces of APOBEC3G and HIV-1 Vif using MAPPIT mutagenesis analysis. *Nucleic Acids Res.* 2010;38(6):1902–12.
 82. Tautz D, Domazet-Loso T. The evolutionary origin of orphan genes. *Nat Rev Genet.* 2011;12(10):692–702.
 83. Wei X, Decker JM, Liu H, Zhang X, Arani RB, Kilby JM, Saag MS, Wu X, Shaw GM, Kappes JC. Emergence of resistant human immunodeficiency virus type 1 in patients receiving fusion inhibitor (T-20) monotherapy. *Antimicrob Agents Chemother.* 2002;46(6):1896–905.
 84. Derdeyn CA, Decker JM, Sfakianos JN, Wu X, O'Brien WA, Ratner L, Kappes JC, Shaw GM, Hunter E. Sensitivity of human immunodeficiency virus type 1 to the fusion inhibitor T-20 is modulated by coreceptor specificity defined by the V3 loop of gp120. *J Virol.* 2000;74(18):8358–67.
 85. Loewen N, Barraza R, Whitwam T, Saenz DT, Kemler I, Poeschla EM. FIV Vectors. *Methods Mol Biol.* 2003;229:251–71.
 86. Morris KV, Gilbert J, Wong-Staal F, Gasmi M, Looney DJ. Transduction of cell lines and primary cells by FIV-packaged HIV vectors. *Mol Ther.* 2004;10(1):181–90.
 87. Simon JH, Southerling TE, Peterson JC, Meyer BE, Malim MH. Complementation of vif-defective human immunodeficiency virus type 1 by primate, but not nonprimate, lentivirus vif genes. *J Virol.* 1995;69(7):4166–72.
 88. Simm M, Shahabuddin M, Chao W, Allan JS, Volsky DJ. Aberrant Gag protein composition of a human immunodeficiency virus type 1 vif mutant produced in primary lymphocytes. *J Virol.* 1995;69(7):4582–6.
 89. Jaguva Vasudevan AA, Perkovic M, Bulliard Y, Cichutek K, Trono D, Häussinger D, Münk C. Prototype foamy virus Bet impairs the dimerization and cytosolic solubility of human APOBEC3G. *J Virol.* 2013;87(16):9030–40.
 90. Edgar RC. MUSCLE: multiple sequence alignment with high accuracy and high throughput. *Nucleic Acids Res.* 2004;32(5):1792–7.
 91. Stamatakis A, Ludwig T, Meier H. RAXML-III: a fast program for maximum likelihood-based inference of large phylogenetic trees. *Bioinformatics.* 2005;21(4):456–63.
 92. Stamatakis A. RAXML version 8: a tool for phylogenetic analysis and post-analysis of large phylogenies. *Bioinformatics.* 2014;30(9):1312–13.
 93. Shimodaira H, Hasegawa M. Multiple comparisons of log-likelihoods with applications to phylogenetic inference. *Mol Biol Evol.* 1999;16(8):1114.
 94. Huson DH, Bryant D. Application of phylogenetic networks in evolutionary studies. *Mol Biol Evol.* 2006;23(2):254–67.
 95. Stern A, Doron-Faigenboim A, Erez E, Martz E, Bacharach E, Pupko T. Selecton 2007: advanced models for detecting positive and purifying selection using a Bayesian inference approach. *Nucleic Acids Res.* 2007;35(Web Server issue):W506–11.
 96. Pond SK, Muse SV. Site-to-site variation of synonymous substitution rates. *Mol Biol Evol.* 2005;22(12):2375–85.
 97. Šali A, Blundell TL. Comparative protein modelling by satisfaction of spatial restraints. *J Mol Biol.* 1993;234(3):779–815.
 98. Miao Z, Cao Y, Jiang T. RASP: rapid modeling of protein side chain conformations. *Bioinformatics.* 2011;27(22):3117–22.
 99. Xu D, Zhang Y. Improving the physical realism and structural accuracy of protein models by a two-step atomic-level energy minimization. *Biophys J.* 2011;101(10):2525–34.
 100. Gerber PR, Muller K. MAB, a generally applicable molecular force field for structure modelling in medicinal chemistry. *J Comput Aided Mol Des.* 1995;9(3):251–68.

Suppl. Fig. S1



Suppl. Fig. S2

(A)



(B)

	Section 1									
	(1)	1	10	20	30	40	50	55		
FcaA3Z3	(1)	MNPLQEV	IFCRQFGNQHRVPKP	-	YYRRKTYLCYQLKLPEGT	LIH	KDCLRN	KKRRH		
PtiA3Z3	(1)	MNPLQED	IFYRQFGNQHRVPKP	Y	YYRRKTYLCYQLKLPEGT	LI	KDCLRN	KKRRH		
PleA3Z3	(1)	MNPLQED	IFYRQFGNQHRVPKP	-	YYRRKTYLCYQLKLPEGT	LI	KDCLRN	KKRRH		
LlyA3Z3	(1)	MNPLQED	IFYRQFGNQHRVPKP	Y	YYRRKTYLCYQLKLPEGT	LI	KDCLRN	EKKRH		
PcoA3Z3	(1)	MNPLQED	IFCRQFGNQHRVPKP	-	YYRRKTYLCYQLKLPEGT	LI	KDCLRN	KKRRH		

	Section 2									
	(56)	56	70	80	90	100	110			
FcaA3Z3	(55)	AEM	CFIDKIK	ILTRDTSQRFEI	ICYITWSPCPFCA	EELVAFVKDNP	PHLSLRI	FAS		
PtiA3Z3	(56)	AEI	CFIDKIKS	ILTRDTSQRFEI	ICYITWSPCPFCA	EELVAFVKDNP	PHLSLRI	FAS		
PleA3Z3	(55)	AEM	CFIDKIKS	ILTRDTSQRFEI	ICYITWSPCPFCA	EELVAFVKDNP	PHLSLRI	FAS		
LlyA3Z3	(56)	AEI	CFIDKIKS	ILTRDTSQRFEI	ICYITWSPCPFCA	EELVAFVKDNP	PHLSLRI	FAS		
PcoA3Z3	(55)	AEM	CFIDKIKS	ILTRDTSQRFEI	ICYITWSPCPFCA	KELVAFVKDNP	PHLSLRI	FAS		

	Section 3									
	(111)	111	120	130	140	150	165			
FcaA3Z3	(110)	RLYVHWRWKYQ	QGLRHLHA	SGIPVAV	MSLPEFEDCWRNFVDH	QDR	SFQWP	NLDQ		
PtiA3Z3	(111)	RLYVHWRWKYQ	QGLRHLHA	SGIPVAV	MSLPEFEDCWRNFVDH	QDR	L	FQWP	NLDQ	
PleA3Z3	(110)	RLYVHWRWKYQ	QGLRHLHA	SGIPVAV	I	SLPEFEDCWRNFVDH	QDR	SFQWP	HKLQ	
LlyA3Z3	(111)	RLYVHWRWKYQ	QGLRHLH	S	SGIPVAV	MSLPEFEDCWRNFVDH	QDR	L	FQWP	NLDQ
PcoA3Z3	(110)	RLYVHWRWKYQ	QGLRHLHA	SGIPVAV	MSLPEFEDCWRNFVDH	KDR	SFQWP	HNLQ		

	Section 4									
	(166)	166	180	190						
FcaA3Z3	(165)	YSK	SIKRRRLGKIL	T	PLNDLRNDFRN	LKLE				
PtiA3Z3	(166)	YSE	SIKRRRLGKIL	T	PLNDLRNDFRN	LKLE				
PleA3Z3	(165)	YSQ	SIKRRRLGKIL	T	PLNDLRNDFRN	LKLE				
LlyA3Z3	(166)	YSE	SIKRRRLGKIL	T	PLNDLRNDFRN	LKLE				
PcoA3Z3	(165)	YSK	SIKRRRLGKIL	M	PLNDLRNDFRN	LKLE				

(C)

Lion FIV Vif subtype E

Domestic cat FIV Vif-34TF10

1	10	20	30	40																																									
MSGE	DIS	QVSR	SLF	SVTL	GGPR	AM	YI	GS	I	D	E	R	E	R	C	S	K	R	K	D	L	K	K	R	L	C																			
MS	E	E	D	W	Q	V	S	R	R	L	F	A	V	L	Q	G	G	V	N	S	A	M	L	Y	I	S	R	L	P	P	D	E	-	R	E	K	Y	K	D	F	K	K	R	L	F

Lion FIV Vif subtype E

Domestic cat FIV Vif-34TF10

50	60	70	80	90																																												
KM	EN	R	F	I	Y	W	L	R	R	Q	E	G	I	L	W	S	F	H	T	R	D	Y	N	V	G	F	V	K	E	L	V	A	G	S	T	K	P	G	S	L	R	L	Y	C	Y	I	S	
D	T	E	T	G	F	I	K	R	L	R	K	A	E	G	I	K	W	S	F	H	T	R	D	Y	I	G	Y	V	R	E	M	V	A	G	S	T	T	S	L	S	L	R	M	Y	I	Y	I	S

Lion FIV Vif subtype E

Domestic cat FIV Vif-34TF10

100	110	120	130	140																																												
N	P	L	W	H	R	K	Y	R	P	T	L	Q	-	M	N	E	Q	F	P	Y	N	C	W	I	K	E	G	F	M	W	D	N	I	E	E	Q	I	M	K	G	P	I	P	C	K	G	W	
N	P	L	W	H	S	Q	Y	R	P	G	L	K	N	F	N	K	E	W	P	F	V	N	M	W	I	K	T	G	F	M	W	D	D	I	E	K	Q	N	I	C	I	G	E	V	S	P	G	W

Lion FIV Vif subtype E

Domestic cat FIV Vif-34TF10

150	160	170	180	190																																													
E	A	G	M	V	G	L	V	I	K	A	F	S	C	P	E	Q	K	R	E	V	S	I	L	Q	V	I	R	G	E	D	P	L	R	Y	C	G	D	C	W	N	L	I	V	V	R	N	T	S	
G	P	G	M	V	G	I	A	I	K	A	F	S	C	G	E	R	K	I	E	A	T	P	V	M	I	I	R	G	E	I	D	P	K	K	W	C	G	D	C	W	N	L	M	C	L	R	N	S	P

Lion FIV Vif subtype E

Domestic cat FIV Vif-34TF10

200	210	220	230	240	255																																																	
P	E	S	L	Q	R	L	A	M	K	A	C	G	R	K	T	R	E	W	V	G	C	C	N	H	R	F	L	S	P	F	R	T	P	T	D	C	Q	I	V	R	E	G	I	S	N	T	G	L	Y	L	I	G	K	G
F	K	T	L	Q	R	L	A	M	L	A	C	G	V	P	A	K	K	W	R	G	C	C	N	Q	R	F	V	S	P	Y	R	T	P	A	D	L	E	V	I	Q	S	K	P	S	W	N	L	L	W	S	G	E	L	

Section 1

HIV-1 Vif

HIV-2 Vif

Section 2

HIV-1 Vif
HIV-2 Vif

Section 3

HIV-1 Vif

Section 4

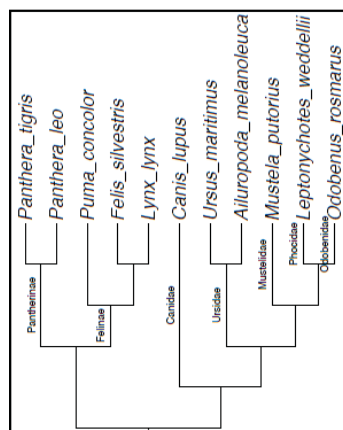
HIV-1 Vif

Section 5

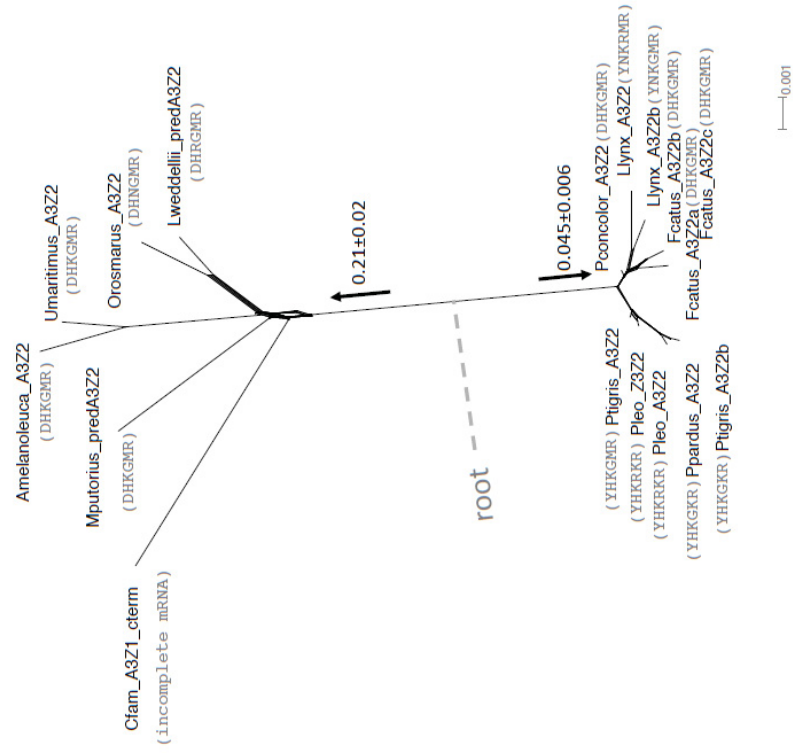
HIV-1 Vif

Suppl. Fig. S3

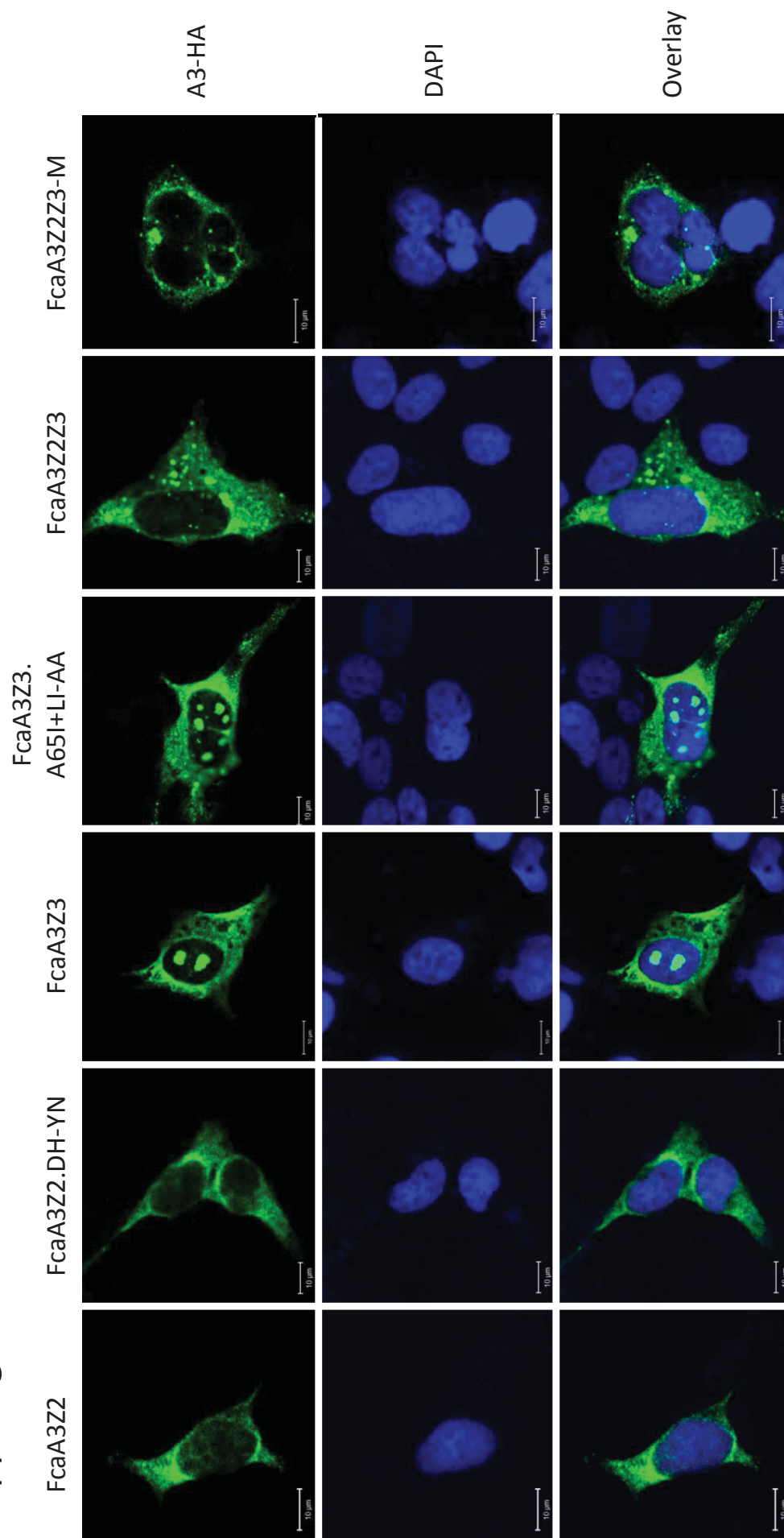
(A)



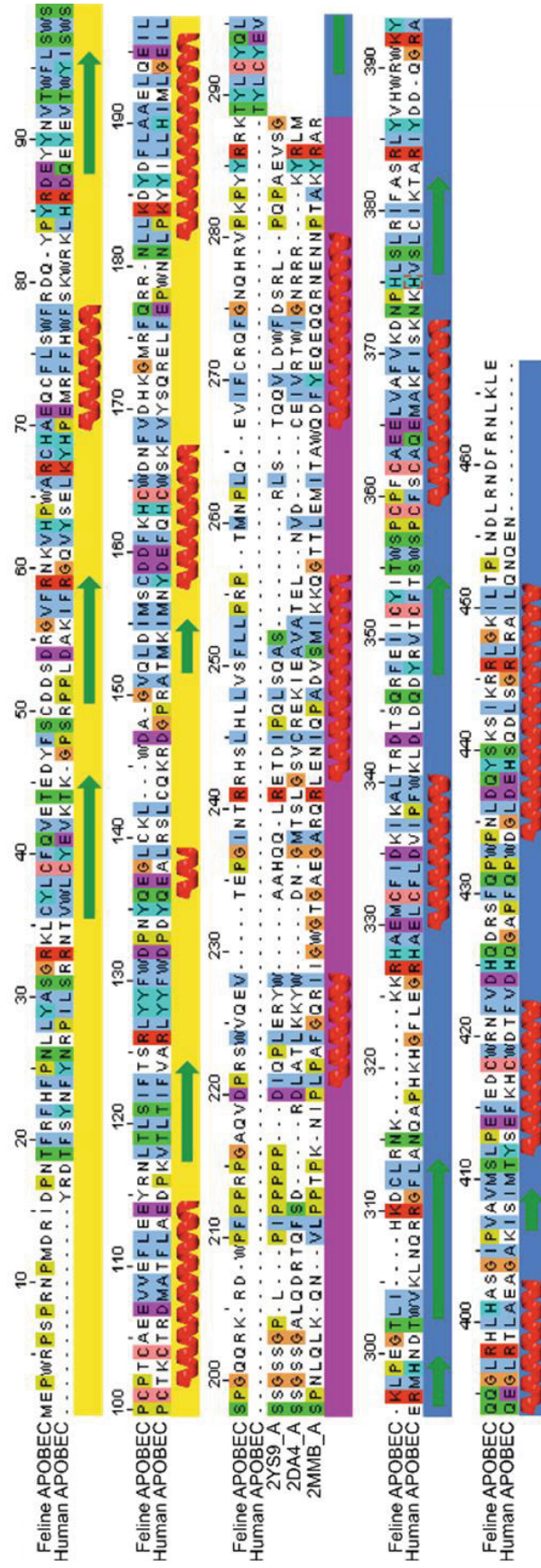
(B)



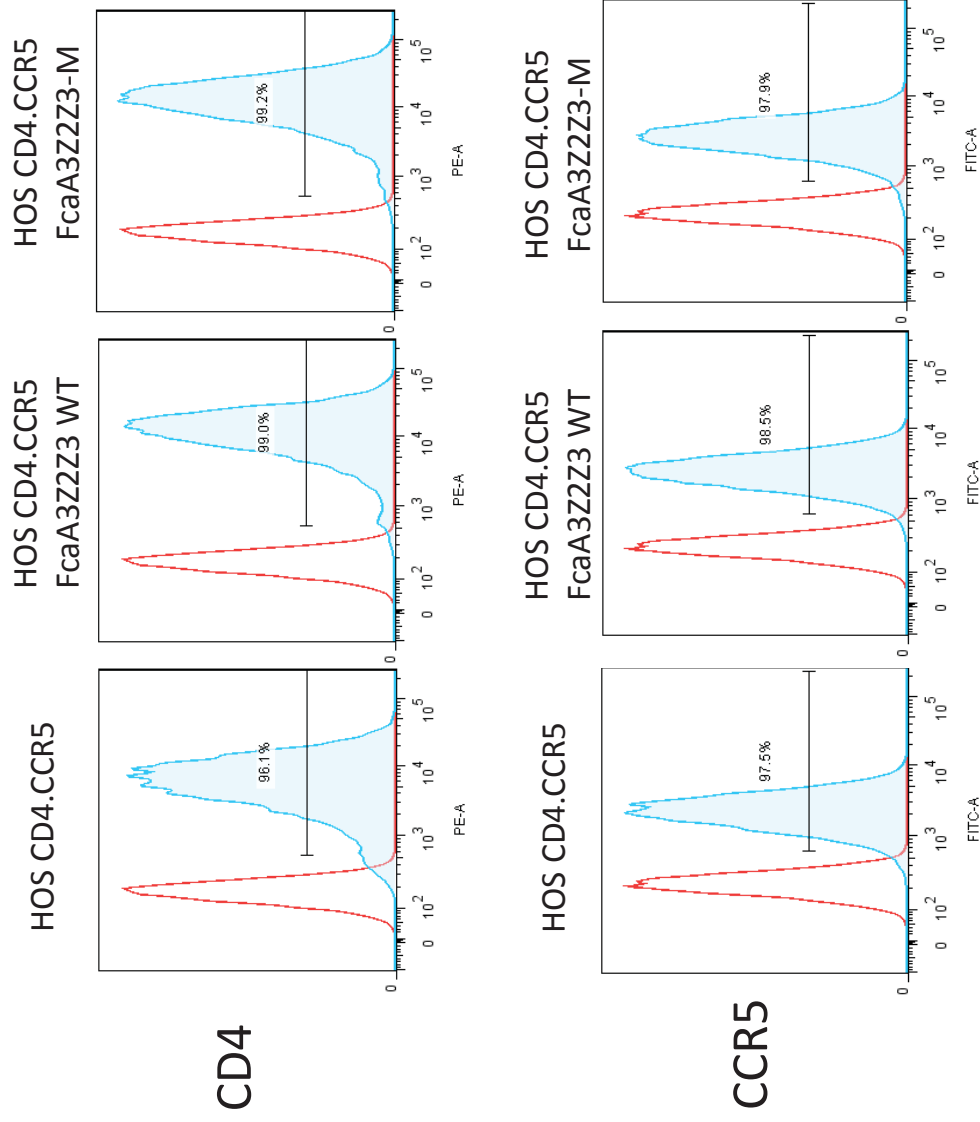
Suppl. Fig. S4



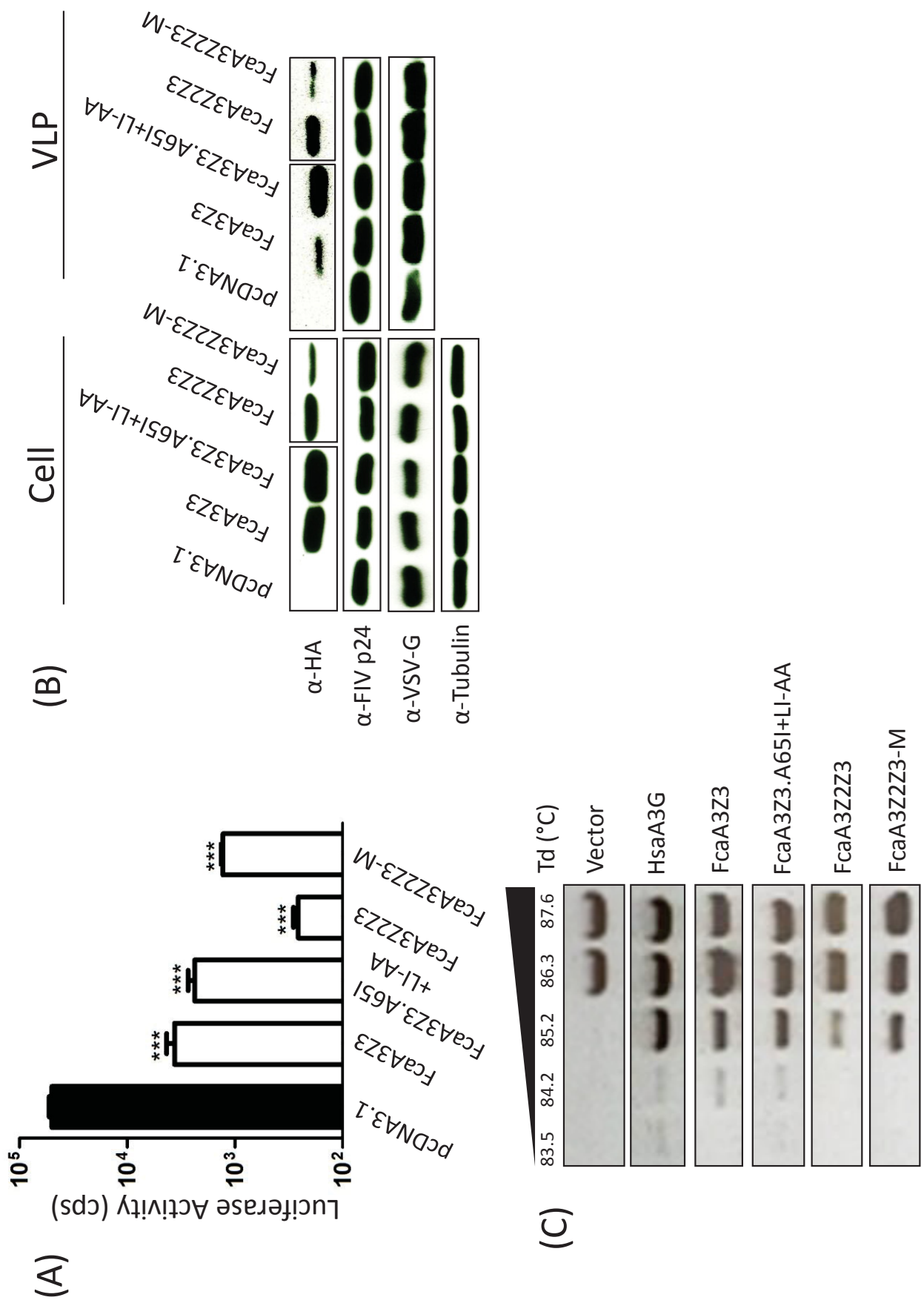
Suppl. Fig. S5



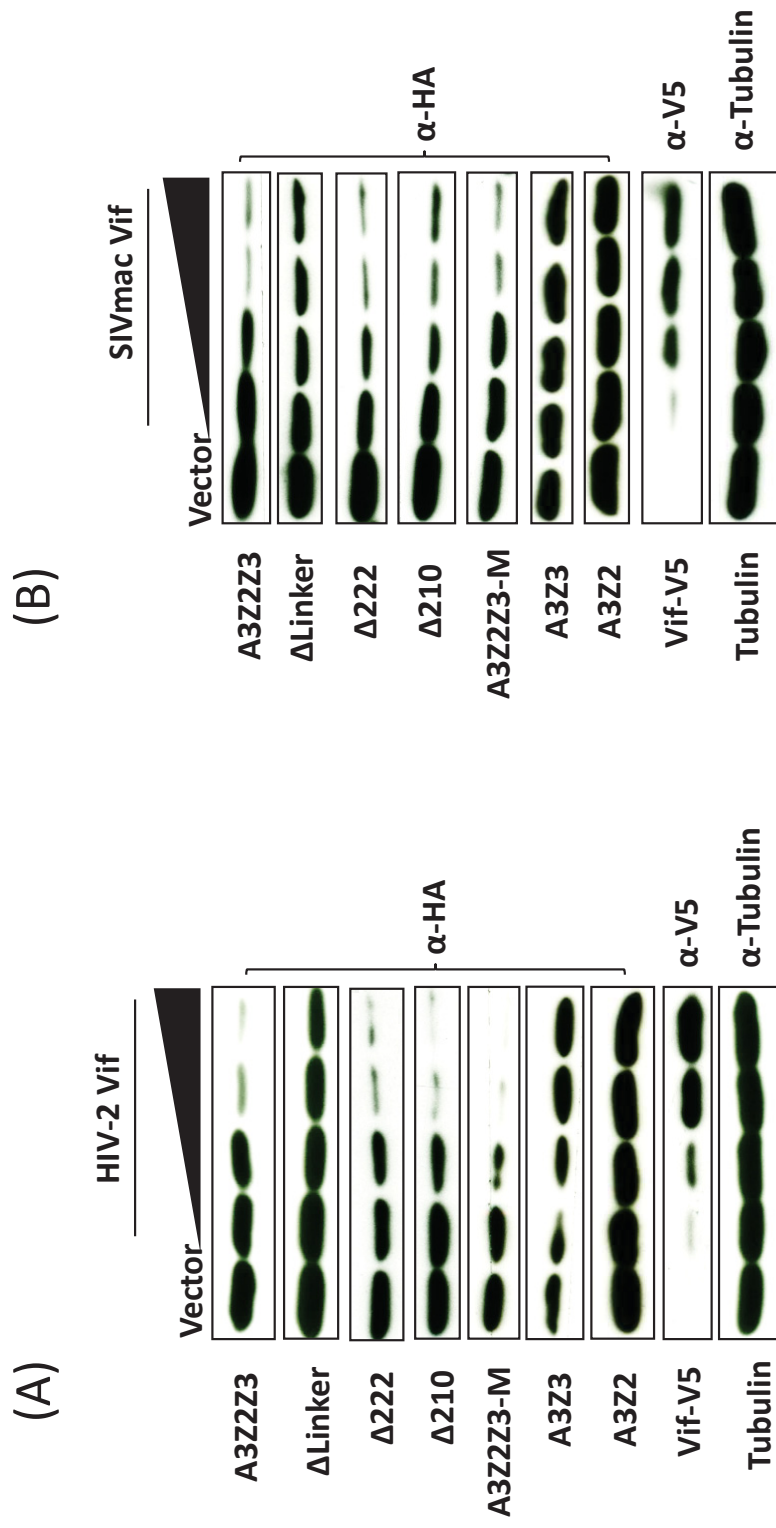
Suppl. Fig. S6



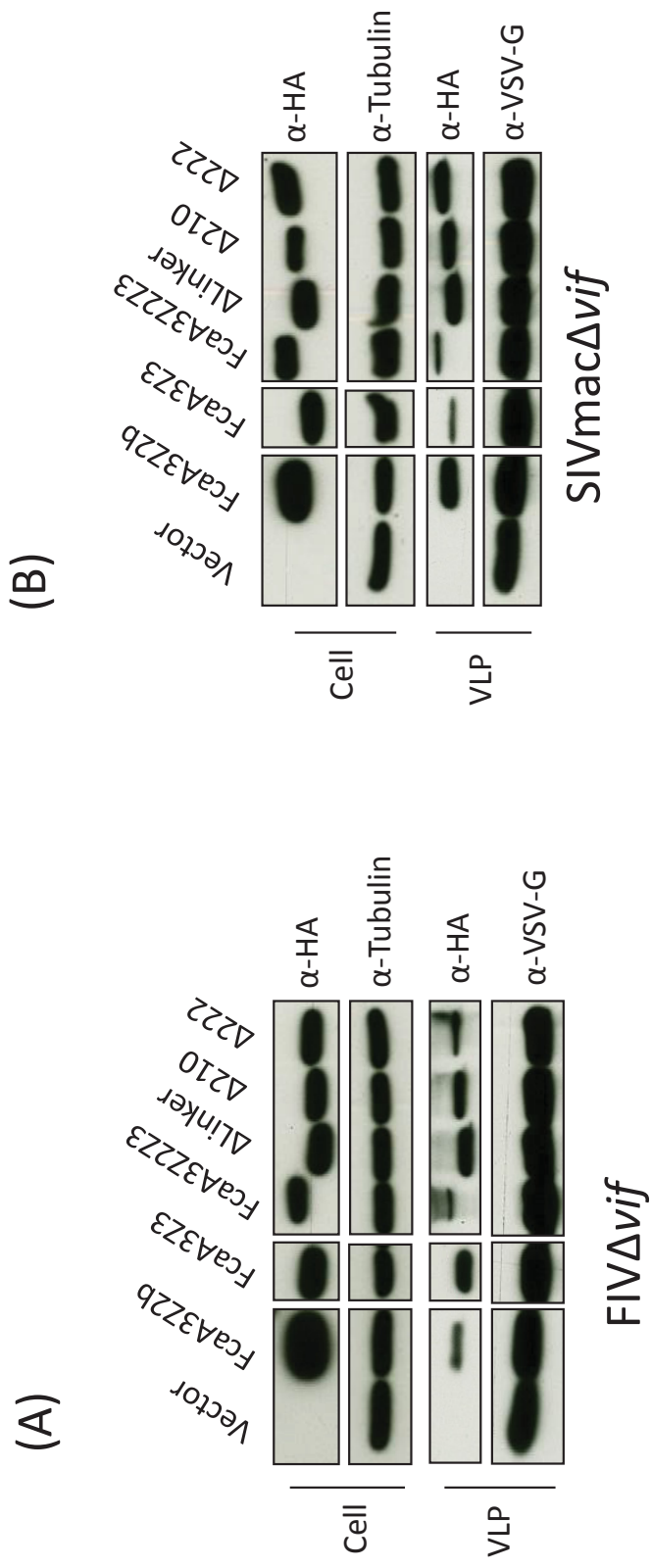
Suppl. Fig. S7



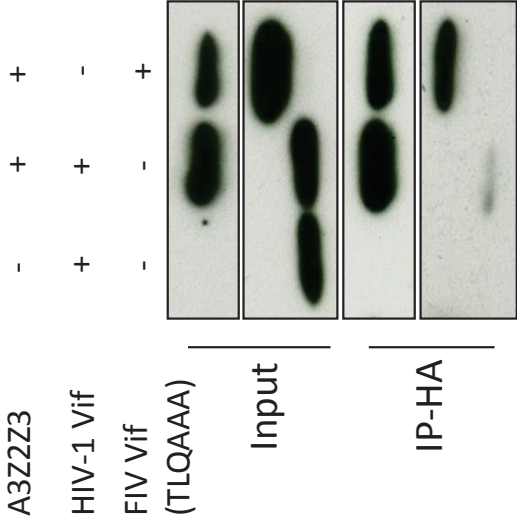
Suppl. Fig. S8



Suppl. Fig. S9



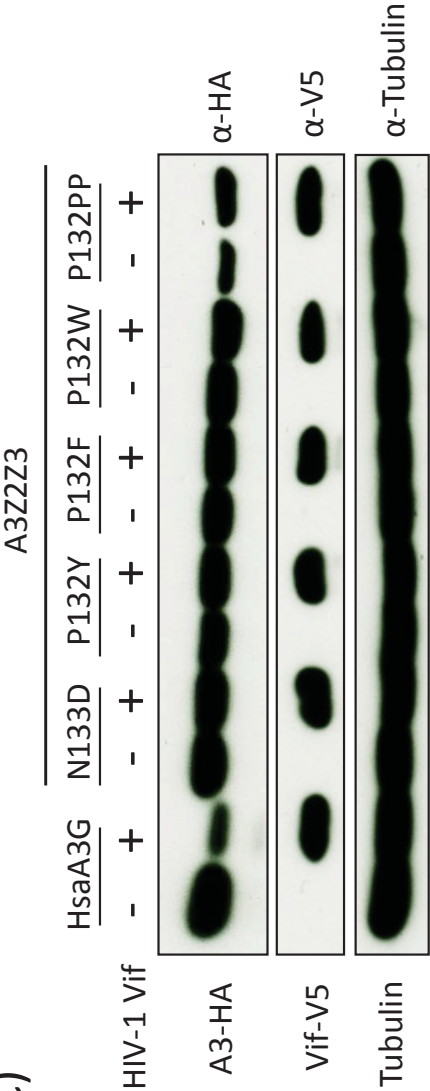
(A)



(B)

HsaA3G	YYFWDPDY
A3Z2Z3 WT	YYFWDPNY
N133D	YYFWDPDY
P132Y	YYFWDYNY
P132F	YYFWDFNY
P132W	YYFWDWNY
P132PP	YYFWDP P NY

(C)



Chapter III

STABLY EXPRESSED APOBEC3H FORMS A BARRIER FOR CROSS-SPECIES TRANSMISSION OF SIMIAN IMMUNODEFICIENCY VIRUS OF CHIMPANZEE TO HUMANS

The following data are published in the Plos Pathogens (selected as highlighted study with press release)

Zhang Z, Gu Q, de Manuel Montero M, Bravo IG, Marques-Bonet T, Häussinger D, Münk C. (2017) Stably expressed APOBEC3H forms a barrier for cross-species transmission of simian immunodeficiency virus of chimpanzee to humans. **PLoS Pathogens** 13(12): e1006746. (Open access)

Zeli Zhang's contribution to this work:

Z. Z. performed most experiments for this project and Z. Z. wrote the draft of the manuscript.

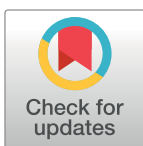
RESEARCH ARTICLE

Stably expressed APOBEC3H forms a barrier for cross-species transmission of simian immunodeficiency virus of chimpanzee to humans

Zeli Zhang¹, Qinyong Gu¹, Marc de Manuel Montero², Ignacio G. Bravo³, Tomas Marques-Bonet², Dieter Häussinger¹, Carsten Münk^{1*}

1 Clinic for Gastroenterology, Hepatology, and Infectiology, Medical Faculty, Heinrich-Heine-Universität Düsseldorf, Düsseldorf, Germany, **2** Institut Biologia Evolutiva (Universitat Pompeu Fabra/CSIC) ICREA, Barcelona, Spain, **3** Laboratory MIVEGEC, UMR CNRS 5290, UM, Montpellier, France

* carsten.muenk@med.uni-duesseldorf.de



OPEN ACCESS

Citation: Zhang Z, Gu Q, de Manuel Montero M, Bravo IG, Marques-Bonet T, Häussinger D, et al. (2017) Stably expressed APOBEC3H forms a barrier for cross-species transmission of simian immunodeficiency virus of chimpanzee to humans. *PLoS Pathog* 13(12): e1006746. <https://doi.org/10.1371/journal.ppat.1006746>

Editor: Susan R. Ross, University of Illinois at Chicago College of Medicine, UNITED STATES

Received: August 5, 2017

Accepted: November 12, 2017

Published: December 21, 2017

Copyright: © 2017 Zhang et al. This is an open access article distributed under the terms of the [Creative Commons Attribution License](https://creativecommons.org/licenses/by/4.0/), which permits unrestricted use, distribution, and reproduction in any medium, provided the original author and source are credited.

Data Availability Statement: All relevant data are within the paper and its Supporting Information files.

Funding: This work was supported by the Heinz Ansmann foundation and the China Scholarship Council (201406600029, 201508080057). The funders had no role in study design, data collection and analysis, decision to publish, or preparation of the manuscript.

Abstract

APOBEC3s (A3s) are potent restriction factors of human immunodeficiency virus type 1/ simian immunodeficiency viruses (HIV-1/SIV), and can repress cross-species transmissions of lentiviruses. HIV-1 originated from a zoonotic infection of SIV of chimpanzee (SIVcpz) to humans. However, the impact of human A3s on the replication of SIVcpz remains unclear. By using novel SIVcpz reporter viruses, we identified that human APOBEC3B (A3B) and APOBEC3H (A3H) haplotype II strongly reduced the infectivity of SIVcpz, because both of them are resistant to SIVcpz Vifs. We further demonstrated that human A3H inhibited SIVcpz by deaminase dependent as well independent mechanisms. In addition, other stably expressed human A3H haplotypes and splice variants showed strong antiviral activity against SIVcpz. Moreover, most SIV and HIV lineage Vif proteins could degrade chimpanzee A3H, but no Vifs from SIVcpz and SIV of gorilla (SIVgor) lineages antagonized human A3H haplotype II. Expression of human A3H hapII in human T cells efficiently blocked the spreading replication of SIVcpz. The spreading replication of SIVcpz was also restricted by stable A3H in human PBMCs. Thus, we speculate that stably expressed human A3H protects humans against the cross-species transmission of SIVcpz and that SIVcpz spillover to humans may have started in individuals that harbor haplotypes of unstable A3H proteins.

Author summary

Cellular cytidine deaminases of the APOBEC3 (A3) family are potent restriction factors that are able to inhibit retroviruses, this A3 restriction is counteracted by lentivirus Vif proteins. Human APOBEC3H (A3H) represents the most evolutionarily divergent A3 gene; it includes seven haplotypes and several splice variants. The polymorphism of human A3H has relevance for HIV-1 infection and AIDS progression. HIV-1 originated from cross-transmission of SIVcpz to humans. However, little is known about how

Competing interests: The authors have declared that no competing interests exist.

human A3s affect the replication or transmission of SIVcpz. In this study, we comprehensively analyzed the anti-SIVcpz activity of chimpanzee and human A3s. Human A3H haplotype II was identified as strong inhibitor against SIVcpz regardless of Vif. In addition, other stably expressed human A3H haplotypes and splice variants showed strong antiviral activity against SIVcpz. Moreover, based on the recent Great Ape Genome Project, we found that the polymorphism of chimpanzee A3H is lower compared with the diversity of human A3H. And chimpanzee A3H haplotypes identified in this study showed similar anti-SIVcpz activity and Vif sensitivity. Our results provide a model that stably expressed human A3H protects humans against the cross-species transmission of SIVcpz and that SIVcpz spillover to humans may have started in individuals that harbor haplotypes of unstable A3H proteins.

Introduction

Simian immunodeficiency virus (SIV) naturally infects many species of African Old-World monkeys, such as African green monkeys, mandrills and red-capped mangabey [1,2]. However, these viruses appear to be nonpathogenic in their natural hosts [2,3]. Chimpanzees (cpz), which are the evolutionarily closest extant primate to *Homo sapiens*, are infected by SIVcpz [4]. The common chimpanzee includes four subspecies, only two of which, *Pan troglodytes troglodytes* (Ptt) and *Pan troglodytes schweinfurthii* (Pts), are infected by SIVcpz (SIVcpzPtt and SIVcpzPts, respectively) [4]. Genome analysis of SIVcpz indicates that SIVcpz originates from the cross-species transmission and recombination of three different SIV strains: SIVrcm from the red-capped mangabey (rcm), SIVgsn/mus/mon from the greater-spot-nosed (gsn), mustached (mus), and mona monkeys (mon), respectively, and a currently unidentified SIV [5–7]. SIVcpzPts is thought to be the origin of SIVcpzPtt after intra-chimpanzee transmission [5].

SIVcpz is of particular interest because it is the ancestor of human immunodeficiency virus (HIV)-1. HIV-1 M and N groups originated from zoonotic transmission of SIVcpzPtt from west-central Africa [8,9]. Additionally, recent studies indicate that SIVgor from gorillas (gor) is the origin of HIV-1 groups O and P [10,11]. The HIV-1 M group is the pandemic virus, whereas viruses of groups N and P are only found in a few infected individuals [12,13]. The HIV-1 O group is mainly distributed in west-central Africa and has a low prevalence rate (less than 1% of global HIV-1 infections) [14,15]. The other HIV lentivirus, HIV-2, resulted from cross-species transmission of SIV from the sooty mangabey monkey (SIVsmm) [14].

Human intrinsic cellular antiviral factors may have direct relevance for the zoonotic infection of humans and the human-to-human spread of SIVs. Several restriction factors have been identified that repress lentiviral replication [16–18]. The family of human APOBEC3 (A3) restriction factors is formed by seven different proteins, A3A–D and A3F–H. Virion encapsidated APOBEC3D (A3D), A3F, A3G, and A3H inhibit HIV-1 that lacks the gene *vif* (HIV-1Δvif) by deaminating cytidines in the viral single-stranded DNA that is generated during reverse transcription, thereby introducing G-to-A hypermutations in the coding strand [19]. To achieve productive infections, lentiviral Vif proteins directly interact with A3s and recruit them to an E3 ubiquitin ligase complex to induce A3 degradation by the proteasome [20–22]. Several studies have investigated how A3G serves as a barrier for cross-species transmission of lentiviruses [23–25]. Human A3H represents the most evolutionarily divergent A3 gene; it includes seven haplotypes and several splice variants [26–28]. The protein stability of human A3H is one determinant of its antiviral activity [29–31]. The human A3H haplotype (hap) II, in contrast to A3G, is only sensitive to specific HIV-1 Vifs and adaptation of HIV-1 Vif to

A3H hapII has been described [32–35]. Thus, the polymorphism of human A3H has relevance for HIV-1 infection and AIDS progression [36,37].

To investigate how human A3s may affect the replication of SIVcpz, we generated novel luciferase reporter viruses based on two SIVcpz strains (SIVcpzPttMB897 and SIVcpzPttTAN1; S1 Fig). This system revealed that SIVcpz transmission to humans may have been significantly affected by the presence of stable A3H.

Results

Characterization of nanoluciferase reporter viruses for SIVcpz

To test SIVcpz, we first generated SIVcpz nanoluciferase (*NLuc*) reporter viruses using two SIV strains (SIVcpzPttMB897 and SIVcpzPttTAN1; S1 Fig). SIVcpzPttMB897 was isolated from wild chimpanzee (*Pan troglodytes troglodytes*) in southern Cameroon in 2007 [9,38], and this strain is regarded as the ancestor of the pandemic HIV-1 M group [14]. SIVcpzPttTAN1 was derived from chimpanzee subspecies *Pan troglodytes schweinfurthii*, and this strain does not cause sustained infections of humans [39]. The SIVcpz reporter constructs were generated by replacing most of the *nef* gene with *NLuc*. Additionally, the *vif* gene of SIVcpz was inactivated (S1 Fig). SIVcpz-NLuc reporter viruses pseudotyped with the glycoprotein of the vesicular stomatitis virus (VSV-G) were produced by plasmid transfection of 293T cells. When infected with the VSV-G pseudotyped viruses, SIVcpzPttMB897-NLuc and SIVcpzPttTAN1-NLuc, 293T cells showed high luciferase counts while very low nanoluciferase activity was detected when the viruses were not VSV-G pseudotyped (Fig 1). The luciferase activity of SIVcpzPttTAN1-NLuc was around 10-fold less than SIVcpzPttMB897-NLuc, even when equal amounts of virions normalized for reverse transcription activity were used for infection (Fig 1). Thus, these two novel SIVcpz reporter viruses transmitted the luciferase enzyme activity via glycoprotein-dependent infection.

Chimpanzee APOBEC3s have antiviral activity against diverse SIVs and are antagonized by SIVcpz Vif

Four SIV-luciferase reporter viruses based on SIV of macaques (SIVmac), African green monkeys (SIVagm) and chimpanzees (SIVcpzPtt, and SIVcpzPtt) were used to investigate the

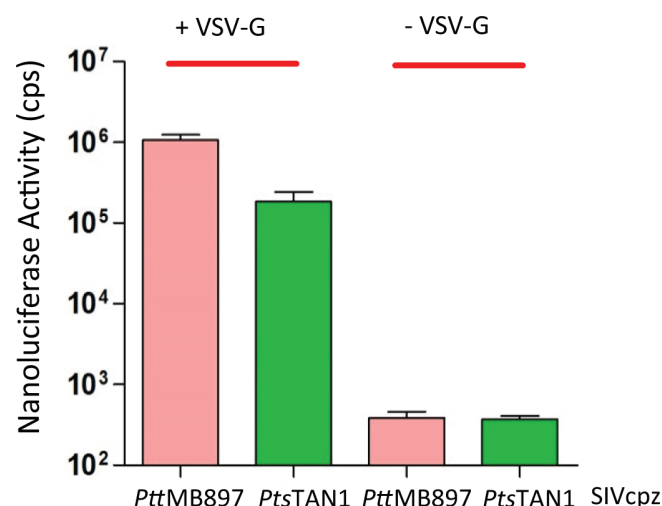


Fig 1. Single round infection assay of SIVcpz reporter viruses. SIVcpz-NLuc was produced in 293T cells in the presence (+) or absence (-) of VSV-G expression plasmid. Virions that had 20 pg reverse transcription activity were used for infection of 293T cells, viral infectivity was determined by quantification of nanoluciferase activity in lysates of infected cells, cps counts per second.

<https://doi.org/10.1371/journal.ppat.1006746.g001>

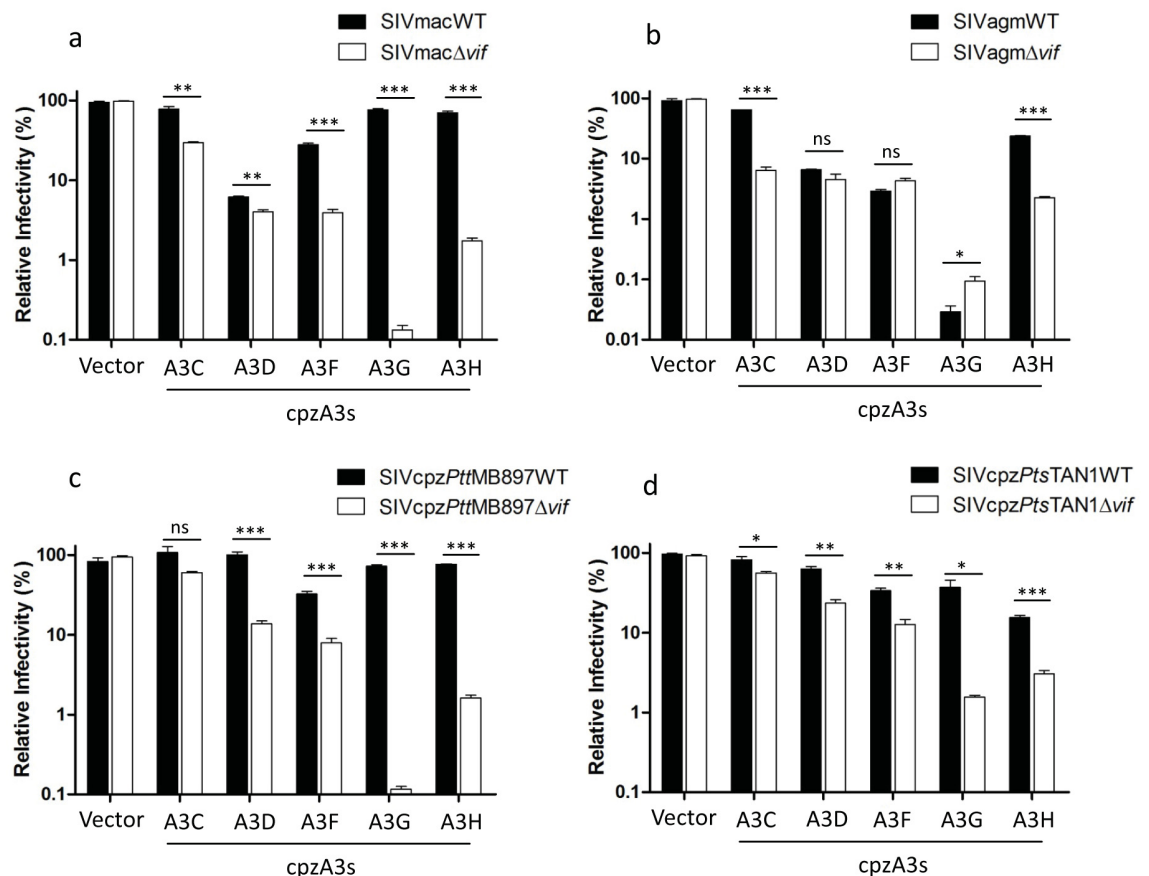


Fig 2. Chimpanzee APOBEC3s (cpzA3s) inhibit SIVs. (a, b) SIVmac or SIVagm wild type or delta *vif* reporter viruses were produced in 293T cells in the presence of cpzA3s. pcDNA3.1(+) was used as control (vector) for cpzA3s. Two days post-transfection, normalized amounts of viruses were used to infect 293T cells, firefly luciferase (relative light units-RLU) was measured two days post-infection. (c, d) SIVcpzPttMB897 or SIVcpzPttTAN1 wild type or delta *vif* reporter viruses were produced in 293T cells in the presence of cpzA3s. pcDNA3.1(+) was used as control (vector) for cpzA3s. Two days post-transfection, normalized amounts of viruses were used to infect 293T cells. Two days post-infection, 293T cells were carefully washed once with PBS, and nanoluciferase (relative light units-RLU) was measured, relative infectivity was shown. Values are means plus standard deviations (error bars) of a representative experiment performed in triplicate. Asterisks represent statistically significant differences: P value < 0.001 extremely significant (***), 0.001 to 0.01 very significant (**), 0.01 to 0.05 significant (*), >0.05 not significant (ns).

<https://doi.org/10.1371/journal.ppat.1006746.g002>

antiviral activity of chimpanzee A3s. We found that cpzA3C, D, F, G, and H reduced the infectivity of SIVmacΔvif (Fig 2A). SIVmac Vif fully antagonized restrictions of cpzA3C, G, and H, and to a large extent overcame cpzA3F, but it did not inhibit the restriction of cpzA3D (Fig 2A). Chimpanzee A3s showed a similar restriction pattern against SIVagmΔvif, but SIVagm Vif only abolished the restriction of cpzA3C and partly inhibited the restriction of cpzA3H. Even in the presence of SIVagm Vif, cpzA3D, F, and G significantly reduced the infectivity of SIVagm (Fig 2A). The expression of the cpzA3C, F, G, and H was detectable by immunoblotting using HA-tagged specific antibodies, while cpzA3D was not detectable using our immunoblotting system (S2A and S2C Fig).

In the absence of Vifs, cpzA3C reduced the infectivity of SIVmac and SIVagm by 5–10 fold and weakly inhibited SIVcpzPttMB897 and SIVcpzPttTAN1 by 1–2 fold (Fig 2C and 2D). cpzA3D, F, and H inhibited SIVcpzΔvif by 10–15-fold, while cpzA3G reduced the infectivity of both SIVcpzPttMB897Δvif and SIVcpzPttTAN1Δvif to an even greater extent (Fig 2C and 2D).

SIVcpzPttMB897 and SIVcpzPtsTAN1 Vifs are able to counteract all cpzA3s, but not all in cases to the same level, e.g. cpzA3F, the full viral infectivity (vector control) was restored, consistent with previous study [40] (Fig 2C and 2D). Taken together, these data indicate that chimpanzee A3s, such as cpzA3D and cpzA3G, can protect chimpanzees from infection with SIVs of rhesus macaques and African green monkeys.

Human APOBEC3H haplotype II strongly inhibits SIVcpz infectivity and is resistant to SIVcpz Vif

Our data and a previous study indicate that chimpanzee A3s, especially cpzA3D, play an important role as a barrier to cross-species transmission of SIVs from monkeys to chimpanzees (Fig 2A and 2B) [40]. Next, we asked whether human A3s (hA3s) form a barrier to SIVcpz infection of humans. Thus, we analyzed the anti-SIV activity of human A3s by using the four SIV reporter systems. Similar to chimpanzee A3s, hA3C, D, F, G, and H (including hapI and hapII) inhibited SIVmacΔvif and SIVagmΔvif infections, and SIVmac Vif abolished most of these restrictions but was only weakly active against hA3D (Fig 3A). SIVagm Vif only significantly overcame the restriction of hA3C, hA3H hapI, and hA3H hapII (Fig 3B). hA3D, hA3F and hA3G displayed resistance to SIVagm Vif counteraction, indicating that these three factors may protect humans against infection by SIVagm (Fig 3B). Consistent with a previous study, hA3B strongly reduced the infectivity of SIVmac and SIVagm regardless of Vif [41]. However, hA3A showed only a low-level inhibition of SIVmac and SIVagm and this restriction was resistant to both SIVmac and SIVagm Vifs (Fig 3A and 3B). The expression of hA3s in transfected 293T cells was detected by immunoblotting (S2B and S2C Fig). In the absence of Vif, hA3D, F, and G reduced the infectivity of SIVcpz, while Vif proteins from both SIVcpzPttMB897 and SIVcpzPtsTAN1 antagonized these hA3s (Fig 3C and 3D). In contrast to the experiments with SIVmacΔvif and SIVagmΔvif, no antiviral activity of hA3C was seen against SIVcpzΔvif (Fig 3C and 3D). Interestingly, two human A3s (hA3B and hA3H hapII) showed strong inhibition of SIVcpz regardless of Vif expression (Fig 3C and 3D). While hA3H is expressed in primary CD4⁺ lymphocytes and has the ability to inhibit HIV-1 [26,35], hA3B is not found in HIV target cells [35]. Together our data indicate that hA3H hapII may block SIVcpz cross-species transmission to humans.

To characterize the interaction between SIVcpz and A3H in more detail, the incorporation of cpzA3H and hA3H hapII into SIVcpz viral particles was analyzed by immunoblotting. In the absence of Vif, both cpzA3H and hA3H hapII were encapsidated into SIVcpzPttMB897 and SIVcpzPtsTAN1 (S2D Fig). Vif from both SIVcpz strains reduced the cpzA3H protein level in the cell lysate by depletion and decreased the cpzA3H incorporation into viral particles (S2D Fig). In agreement with the infectivity data of SIVcpz with cpzA3H (Fig 2C and 2D), SIVcpzPtt Vif was more active against cpzA3H than SIVcpzPts Vif [40]. However, the steady-state expression and particle encapsidation of hA3H hapII did not change in the presence of SIVcpz Vif, which corresponds with hA3H's hapII antiviral activity against wild-type SIVcpz (Fig 3C and 3D and S2D Fig). Furthermore, we investigated whether the cytidine deaminase activity is required for hA3H hapII inhibiting SIVcpz. We introduced the E56A mutation in the cytidine deaminase domain of hA3H hapII, which was previously reported to completely abolish the protein's deaminase activity [42]. The E56A mutant of A3H lost significantly antiviral activity compared with wild-type hA3H hapII, but remained a 10-fold inhibitory activity against SIVcpzΔvif (Fig 4A). Next we analyzed the presence of G-to-A mutations indicative of A3 deamination in the viral genome by amplifying a 700-bp fragment of the viral genome 12 h post-infection. Viruses prepared without co-expression of A3 showed no detectable G-to-A mutations. However, in the presence of hA3G, we found a hypermutation rate of around 2.8%

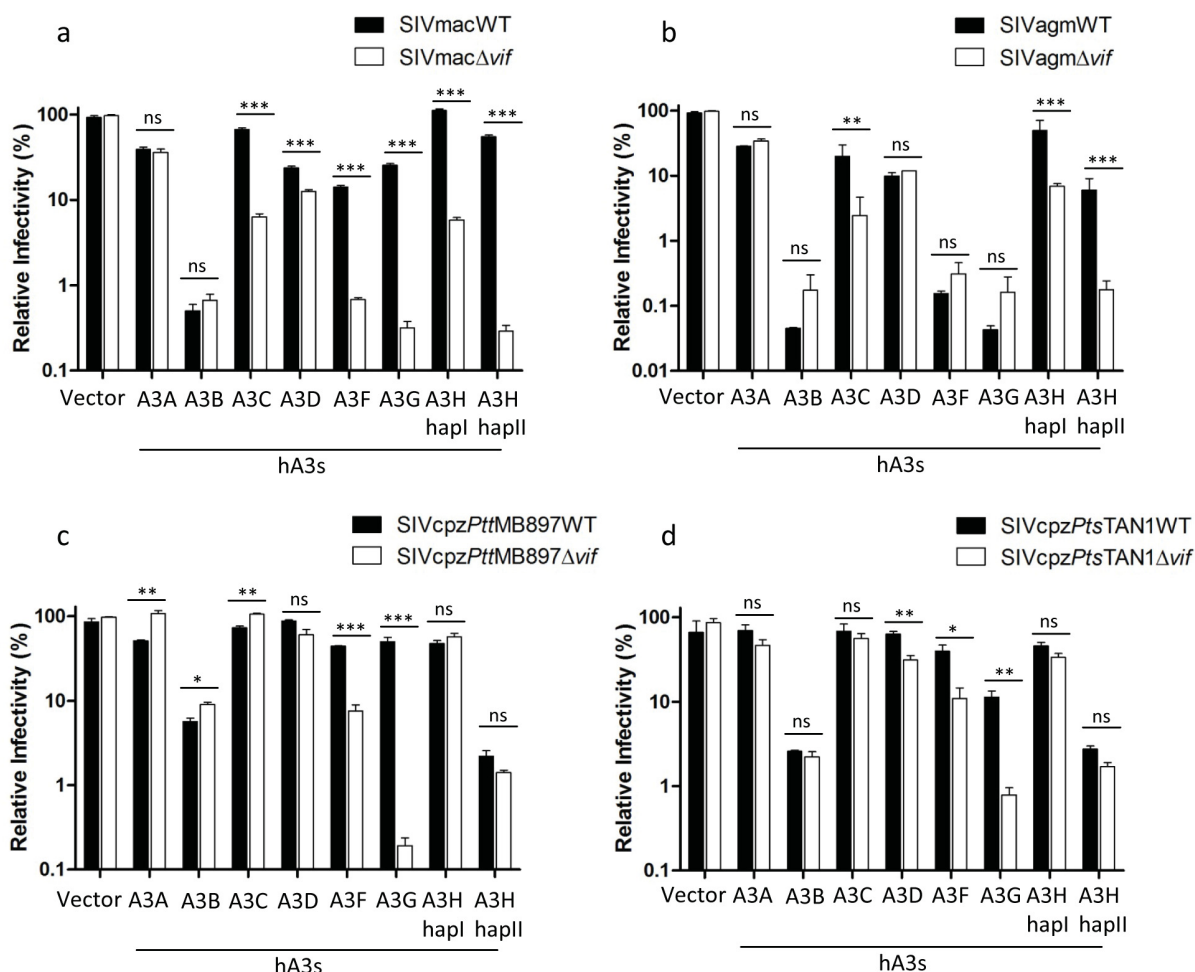


Fig 3. Human APOBEC3s (hA3s) inhibit SIVs. (a, b) SIVmac or SIVagm wild type or delta *vif* reporter viruses were produced in 293T cells in the presence of hA3s. PTR600 empty vector was used as control (vector) for hA3s. Two days post-transfection, normalized amounts of viruses were used to infect 293T cells, firefly luciferase (relative light units-RLU) was measured two days post-infection. (c, d) SIVcpzPttMB897 or SIVcpzPtsTAN1 wild type or delta *vif* reporter viruses were produced in 293T cells in the presence of hA3s. PTR600 empty vector was used as control (vector) for hA3s. Two days post-transfection, normalized amounts of viruses were used to infect 293T cells. Two days post-infection, 293T cells were carefully washed once with PBS, and nanoluciferase (relative light units-RLU) was measured. The relative infectivity was shown. Values are means plus standard deviations (error bars) of a representative experiment performed in triplicate. Asterisks represent statistically significant differences: P value < 0.001 extremely significant (***), 0.001 to 0.01 very significant (**), 0.01 to 0.05 significant (*), >0.05 not significant (ns).

<https://doi.org/10.1371/journal.ppat.1006746.g003>

in the SIVcpz genome (Fig 4B). Viruses made in the presence of hA3H hapII contained a mutation rate of around 0.9%, while hA3H hapII E56A did not edit the SIVcpz genome (Fig 4B). The sequence plots, confirmed that hA3G preferred GG motif (mutated G is underlined, which is CC in the deaminated minus strand), while hA3H hapII mutated a GA motif (TC in the minus strand) predominantly (Fig 4B), which is consistent to previous studies [42–44]. Taken together, these data indicate that hA3H hapII inhibits SIVcpz by both deaminase dependent and independent mechanisms.

To further characterize the level of anti-SIVcpz activity mediated by hA3H, different amounts (5–200 ng) of hA3H hapI or hA3H hapII expression plasmids were co-transfected with SIVcpzPttMB897 wild-type or Δvif reporter constructs and the viral infectivities were determined. The results indicate that the anti-SIVcpz activity of hA3H hapII increased with

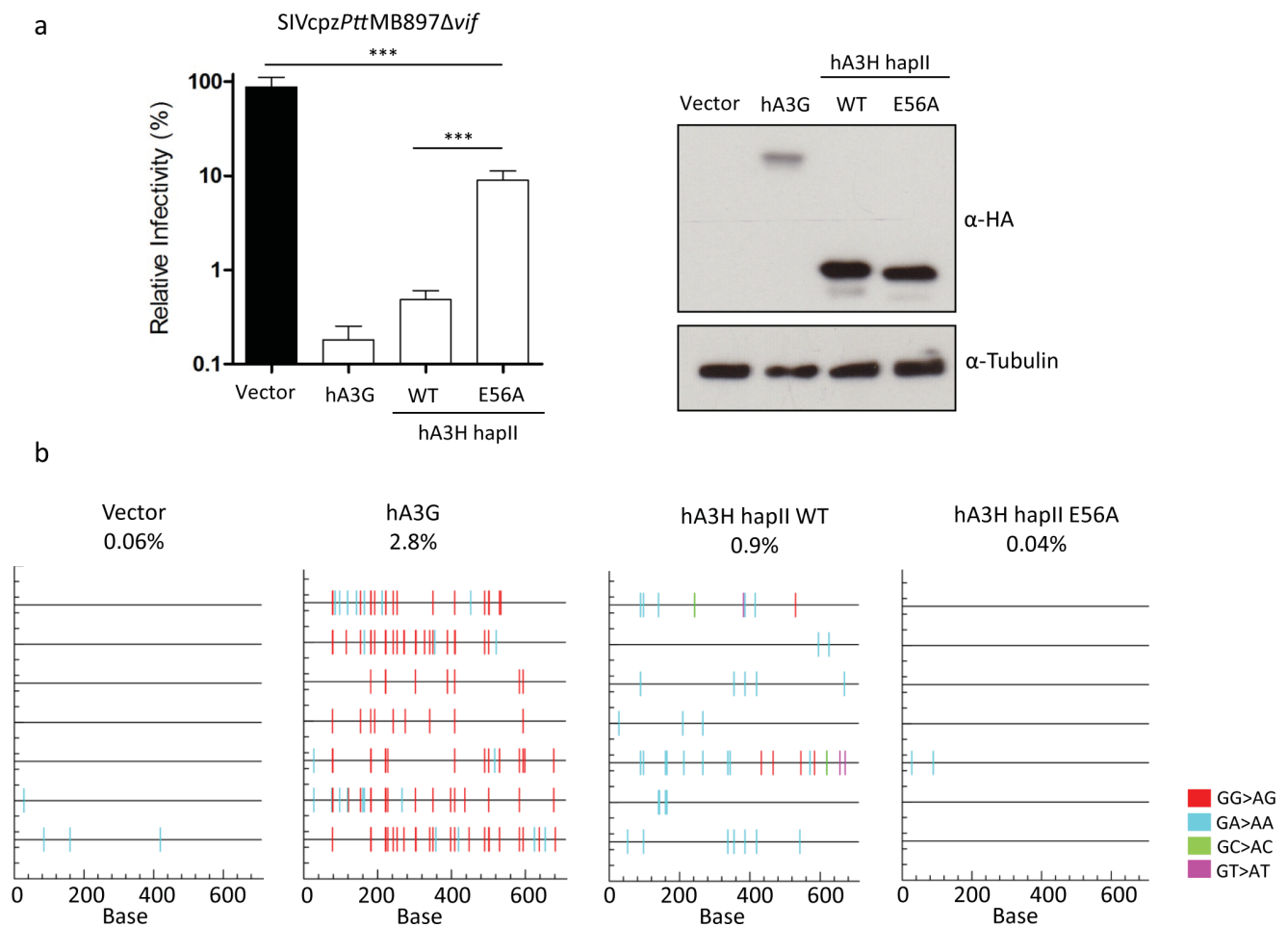


Fig 4. SIVcpz is inhibited by hA3H hapII by both deaminase dependent and independent mechanisms. (a) SIVcpzPttMB897Δvif reporter constructs were co-transfected with hA3G, hA3H hapII or hA3H hapII E56A expression plasmids, PTR600 empty vector was used as control (vector). Two days post-transfection, normalized amounts of viruses were used to infect 293T cells. The nanoluciferase (relative light units-RLU) was measured two days post-infection. The expression of A3s was detected by anti-HA antibody, tubulin served as loading control. (b) The viral supernatants from (a) were treated with DNase I (20 units for 1 ml viral supernatant) and used to infect 293T cells. 12 h post-infection, the cellular DNA was isolated. A 700-bp fragment of SIVcpz was amplified by PCR, cloned and sequenced.

<https://doi.org/10.1371/journal.ppat.1006746.g004>

the dose of transfected hA3H hapII plasmid regardless of Vif expression (Fig 5A and 5B). Even a low level of hA3H hapII (5 ng) displayed around 10-fold inhibition of SIVcpzPttMB897Δvif and Vif was not able to overcome this restriction. We also found that hA3H hapI showed around 20-fold inhibition of SIVcpzPttMB897, when 200 ng hA3H hapI expression plasmid was transfected (Fig 5A). 100 ng hA3H hapI and 10 ng hA3H hapII plasmids displayed similar protein expression levels, and they showed similar strength of inhibition of SIVcpzPttMB897 (Red box in Fig 5A and 5B), which is consistent with previous studies [45,46]. These results indicate that the protein expression level of A3H is one of the key determinants for its antiviral activity.

Human A3H has seven haplotypes and several splice variants, and the A3H protein stability determines the antiviral activity [29–31]. In the absence of Vif, cpzA3H, hA3H hapII, hA3H hapV, hA3H hapVII, and four hA3H hapII splice variants (SV182, SV183, and SV200) strongly inhibited SIVcpzPttMB897 (Fig 5C). However, Vif only counteracted the restriction of cpzA3H and was inactive against all the tested hA3H variants (Fig 5C). Corresponding

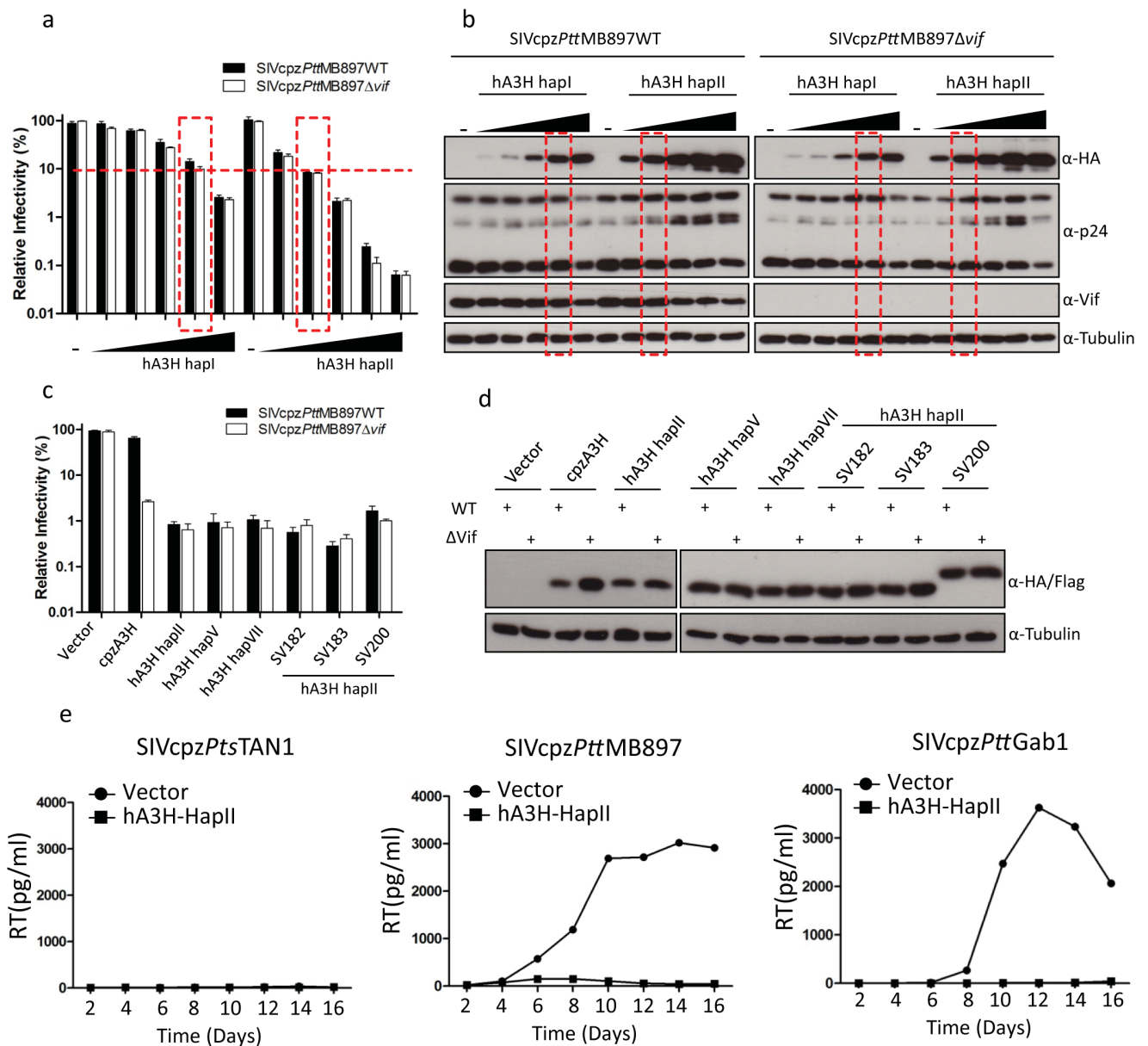


Fig 5. Inhibition of SIVcpz by hA3H haplotypes with stable protein expression. (a) SIVcpzPttMB897WT or SIVcpzPttMB897Δvif reporter constructs were co-transfected with increasing amounts of hA3H hapI or hapII expression plasmids (5, 10, 30, 100 or 200 ng), PTR600 empty vector was used to bring the total transfected plasmid DNA to 600 ng and also used as control (vector). Two days post-transfection, normalized amounts of viruses were used to infect 293T cells. The nanoluciferase (relative light units-RLU) was measured two days post-infection. (b) Cell lysates from (a) were used to detect the expression of A3s, SIVcpz capsid (p24), or SIVcpz Vif by anti-HA, anti-p24, or anti-Vif antibody, respectively. Tubulin served as a loading control. (c) SIVcpzPttMB897WT or SIVcpzPttMB897Δvif reporter constructs were co-transfected but with expression plasmids for different A3H haplotypes and splice variants. (d) Cell lysates from (c) were used to detect the expression of A3s by anti-HA antibody. Tubulin served as a loading control. (e) SupT11-vector-hCCR5 or SupT11-hA3H hapII-hCCR5 cells were infected with 1 ng RT activity of SIVcpzPttTAN1, SIVcpzPttMB897 or SIVcpzPttGab1, respectively, and culture supernatants were collected each second day and quantified by the RT assay.

<https://doi.org/10.1371/journal.ppat.1006746.g005>

immunoblotting results of lysates of the transfected cells confirmed that SIVcpzPttMB897 Vif only reduced the protein level of cpzA3H and protein levels of the hA3Hs were not changed by Vif co-expression (Fig 5D).

To learn more about the strength of hA3H's antiviral activity, the spreading replication of SIVcpz in human T cells (SupT11) that stably expressed hA3H hapII [47] was investigated. To facilitate replication of CCR5-tropic SIVcpz, we modified SupT11 cells to express human CCR5 (S3A and S3B Fig). The spreading replication was tested with full-length unmodified viruses (SIVcpzPttMB897, SIVcpzPttGab1, and SIVcpzPttTAN1). SIVcpzPttTAN1 did not replicate in the SupT11-hA3H hapII and SupT11-vector cells, regardless of the input of virus (1 ng reverse transcriptase (RT) activity or 50 ng RT) for the initial infection (Fig 5E and S3C Fig). Both SIVcpzPttMB897 and SIVcpzPttGab1 replicated efficiently in SupT11-vector cells, while no virus spreading was observed in SupT11-hA3H hapII cells (Fig 5E). These data indicate that hA3H hapII is a strong inhibitor of infection of SIVcpz in human T cells. We conclude, therefore, that stably expressed hA3H variants are Vif-resistant restriction factors of SIVcpz.

Identification of A3H residues that are important for antagonism by SIVcpz Vif

Both cpzA3H and hA3H hapII displayed strong anti-SIVcpz activity, while they had different sensitivities to SIVcpz Vif counteraction (Figs 2C, 2D, 3C and 3D). One recent study demonstrated that residue 97 of cpzA3H and hA3H hapII determines the sensitivity to HIV-1 clone NL4-3 Vif [48]. Thus, we tested whether residue 97 would also be important for SIVcpz Vif inhibition of A3H. The Q97K and K97Q mutations were introduced into cpzA3H and hA3H hapII, respectively. The results showed that cpzA3H Q97K and hA3H hapII K97Q retained their anti-SIVcpz activity in the absence of Vif (Fig 6A and 6C). While SIVcpzPttMB897 Vif almost fully overcame the inhibition of wild-type cpzA3H, it only partially antagonized cpzA3H Q97K and, similarly, SIVcpzPttTAN1 Vif did not counteract cpzA3H Q97K (Fig 6A and 6C). Additionally, hA3H hapII showed resistance to SIVcpzPttMB897 Vif, but this resistance was partially lost when the K97Q mutation was introduced (Fig 6A). In contrast to SIVcpzPttMB897 Vif, both wild-type hA3H hapII and its K97Q mutant showed resistance to SIVcpzPttTAN1 Vif (Fig 6C). Furthermore, we analyzed the protein expression level of these A3H mutants in the presence of SIVcpz Vifs. hA3H E121K was included as a control mutant that could not be degraded by HIV-1 Vif [48,49]. SIVcpzPttMB897 Vif slightly reduced the protein level of cpzA3H Q97K compared to the no-Vif control, which is consistent with the infectivity data (Fig 6A and 6B). SIVcpzPttTAN1 Vif did not affect the expression of cpzA3H Q97K (Fig 6D). hA3H hapII K97Q was depleted by co-expression of SIVcpzPttMB897 Vif, while the presence of SIVcpzPttTAN1 Vif did not affect hA3H protein levels (Fig 6B and 6D). We conclude that Vifs from SIVcpzPttMB897 and SIVcpzPttTAN1 have distinct interaction properties with hA3H hapII.

The polymorphism of the cpzA3H gene in chimpanzees

To find out how diverse A3H is in chimpanzees, we analyzed the deep-sequencing reads from the recent Great Ape Genome Project [50]. We mapped reads to the hA3H region (hg19, chr22:39496284–39498576) and the exons of A3H were isolated. The coding regions of A3H from 61 chimpanzees (10 *Pan troglodytes ellioti*, *Pte*; 16 *Pan troglodytes schweinfurthii*, *Pts*; 22 *Pan troglodytes troglodytes*, *Ptt*; 13 *Pan troglodytes verus*, *Ptv*) were analyzed. We found four single-nucleotide polymorphisms (SNPs) of cpzA3H (nucleotide positions 50, 359, 402, and 481; Table 1, Fig 7A and S4 Fig). Two of them (SNP_50 and SNP_359) were only present in *Ptv* with an overall frequency of 6.5% and 9.8%, respectively. SNP_402 was only found in *Pts* with a frequency of 9%. However, SNP_481 was detected in *Pte*, *Pts*, and *Ptt* with a frequency of 8.2%, 19.6%, and 34.4%, respectively. The detailed SNP and zygosity information is described in Table 1. These four SNPs including the reference cpzA3H were named from haplotype I (hapI) to haplotype V (hapV) (Fig 7A). In addition, we performed a phylogenetic

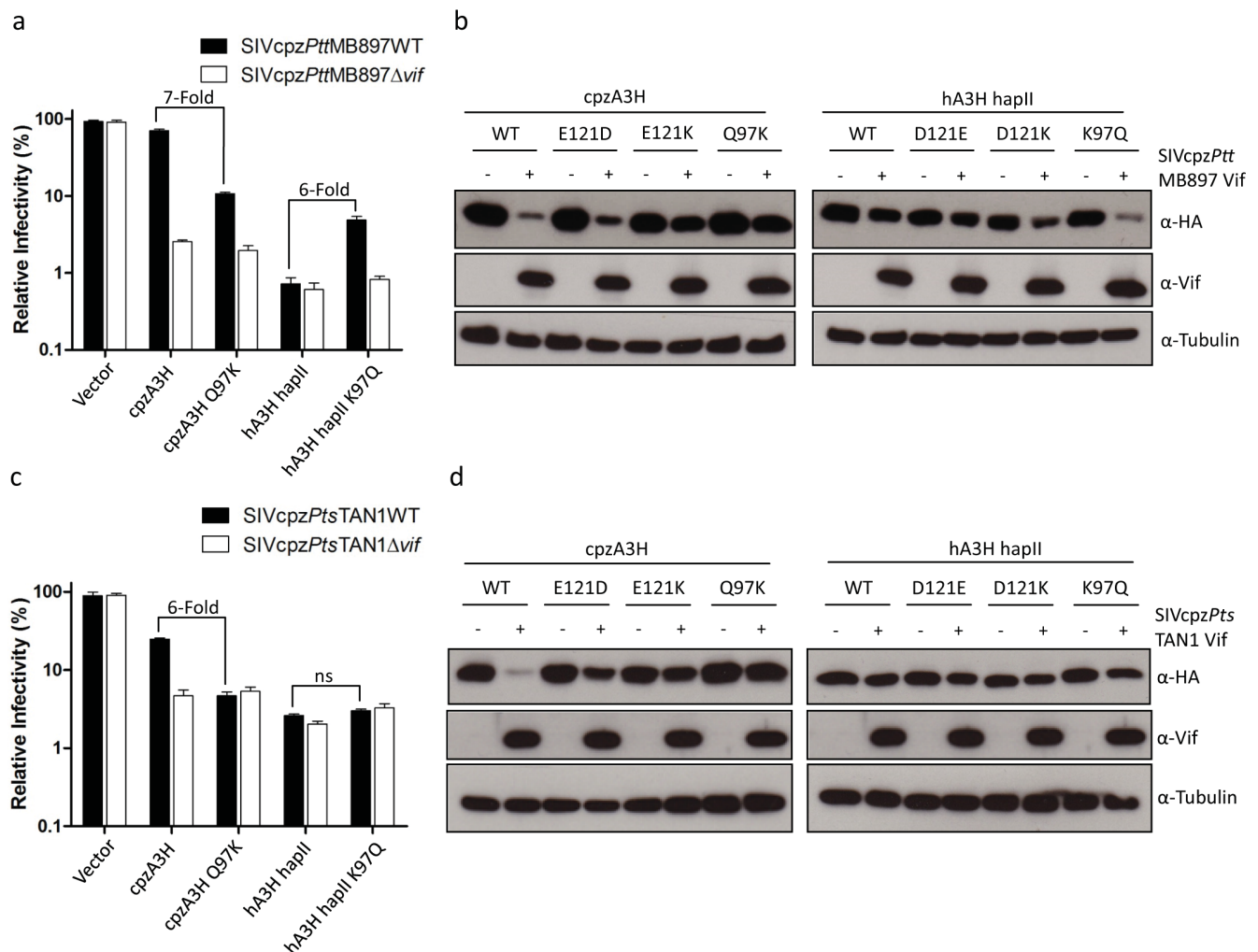


Fig 6. Residue 97 of A3H partially determines the sensitivity to SIVcpz Vifs. (a, b) SIVcpzPttMB897 or SIVcpzPttTAN1 wild type or delta vif reporter viruses were produced in 293T cells in the presence of A3H wild type or mutant expression plasmids, as indicated. The viral infectivity was determined by measuring the nanoluciferase of 293T cells infected with normalized amounts of SIVcpz reporter viruses. (c, d) cpzA3H, hA3H wild type or mutants expression plasmids were co-transfected with SIVcpz (SIVcpzPttMB897 or SIVcpzPttTAN1) Vif expression plasmids into 293T cells. The presence of A3H and Vif was detected by using anti-HA and anti-Vif antibodies, respectively. Tubulin served as a loading control.

<https://doi.org/10.1371/journal.ppat.1006746.g006>

Table 1. Genetic variants in the APOBEC3H gene in chimpanzee subspecies.

POS. NT ^a	REF	ALT	POS. AA ^b	REF	ALT	Summary of ALT ^c	HET ^d	HOM ALT ^e
50	G	A	17	R	H	4 Ptv	3	1
359	A	G	120	Q	R	6 Ptv	6	0
402	G	T	134	E	D	3 Pts	3	0
481	A	G	161	K	E	5 Pte, 12 Pts, 21 Ptt	18	20

a, position of nucleotide variant; REF, chimpanzee mRNA sequence from NCBI (NM_001142606.1); ALT, Variant.

b, position of corresponding amino acid in A3H protein.

c, summary of the individuals bearing the variant; Pts, *Pan troglodytes schweinfurthii*; Ptt, *P. t. troglodytes*; Pte, *P. t. ellioti*; Ptv, *P. t. verus*.

d, total number of individuals heterozygous.

e, total number of individuals homozygous for the variant.

<https://doi.org/10.1371/journal.ppat.1006746.t001>

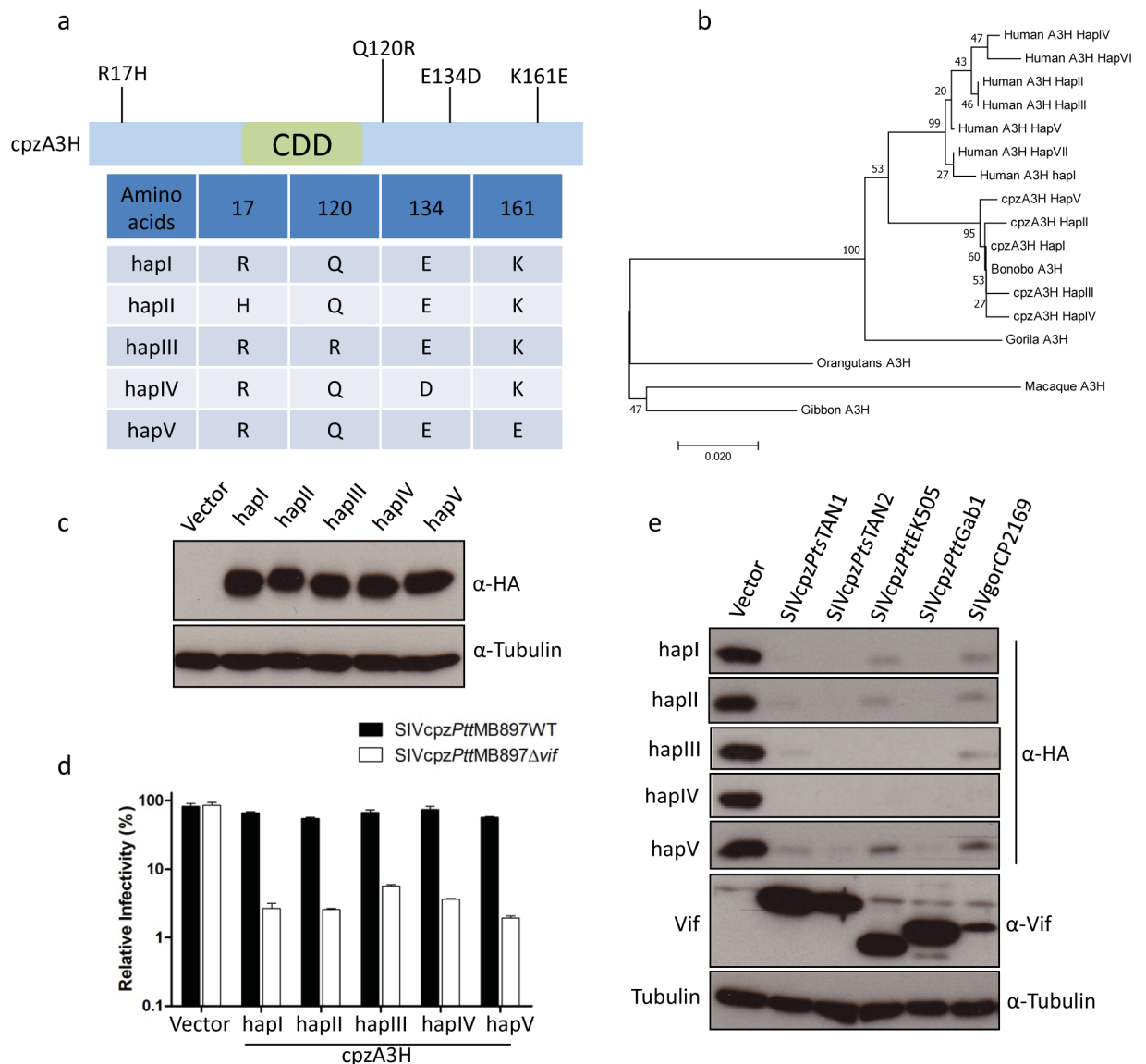


Fig 7. Similar anti-SIVcpz activity of cpzA3H haplotypes. (a) Four single nucleotide polymorphisms (SNPs) of cpzA3H were observed in 61 chimpanzees, see also Table 1. These four SNPs including reference cpzA3H were named haplotype I (hapI) to haplotype V (hapV). CDD, cytidine deaminase domain. (b) The phylogenetic relationship of primate A3H proteins. 500 bootstrap replications were performed during calculation. The number on each node indicates the bootstrap support. (c) cpzA3H expression plasmids for different haplotypes were transfected into 293T cells. After two days, the expression of cpzA3H was detected by using anti-HA antibody, respectively. Tubulin served as a loading control. (d) SIVcpzPttMB897WT or SIVcpzPttMB897Δvif reporter constructs were co-transfected with expression plasmids for cpzA3H haplotypes into 293T cells, pcDNA3.1(+) empty vector was used as control (vector). Two days post-transfection, normalized amounts of virus were used to infect 293T cells. The nanoluciferase (relative light units-RLU) was measured 2 days post-infection. (e) The expression plasmids of cpzA3H haplotypes were co-transfected with expression plasmids for Vifs (from different SIVcpz strains, as indicated) into 293T cells. The presence of A3H and Vif were detected by using anti-HA and anti-Vif antibodies, respectively. Tubulin served as a loading control.

<https://doi.org/10.1371/journal.ppat.1006746.g007>

analysis of A3H from apes (rhesus macaque A3H was also included). The results showed that gibbon, rhesus macaque, and orangutan A3H were classified into one clade. Gorilla A3H formed a separate clade, and human and chimpanzee A3H were classified into two clades, respectively (Fig 7B). Bonobo A3H was classified into the clade of chimpanzee A3H.

The protein stability differs in human A3H haplotypes and it is one of the determinants of its antiviral activity [29–31]. Thus, the expression of five cpzA3H haplotypes in 293T cells was tested by immunoblotting. All cpzA3H haplotypes produce stable proteins and had similar expression levels (Fig 7C). Moreover, these five cpzA3H haplotypes displayed similar anti-SIVcpz activities and were all sensitive to Vifs from SIVcpz lineages (Fig 7D and 7E). These data indicate that the polymorphism of cpzA3H does not affect its protein stability or antiviral activity.

Vifs from SIVcpz lineages fail to counteract human A3H haplotype II

There have been four independent transmissions from different SIVcpz/gor strains to the human population, which caused HIV-1 groups M, N, O, and P, respectively [11,14]. Thus, we tested the sensitivity of cpzA3H and hA3H hapII to Vifs from several SIVcpz/HIV-1 lineages. The immunoblots of co-expressing cells indicated that cpzA3H was depleted by all the tested SIVcpz Vifs, and it was also depleted by Vifs from HIV-1 B-LAI (M group), N-116, and O-127, but was not degraded by HIV-1 F-1 Vif (Fig 8A). hA3H hapII was resistant to depletion of all SIVcpz Vifs tested, including SIVgor Vif (Fig 8A). However, HIV-1 B-LAI, F-1, and N-116 Vifs induced the degradation of hA3H hapII (Fig 8A). Unexpectedly, HIV-1 O-127 Vif, which protein expression was not detectable was inactive against hA3H hapII (Fig 8A).

By testing chimeras of SIVcpzPttMB897 and HIV-1 LAI Vif, we identified that the Vif N-terminal region (residues 40–70) is essential for hA3H hapII depletion (Fig 8B and 8C). A previous study described the importance of HIV-1 Vif residues F39 and H48 for antagonism of hA3H hapII [33]. F39 is present in SIVcpzPttMB897 Vif, but at the 48 position, an asparagine (N) is found (Fig 8D). However, introducing an N48H mutation (construct M1) in SIVcpzPttMB897 Vif did not promote degradation of hA3H hapII (Fig 8E). However, the local area of residue 48 of SIVcpzPttMB897 Vif was important as an additional mutation revealed that changing residues 47EN48 to 47PH48 (construct M2) facilitated hA3H hapII depletion (Fig 8E). Furthermore, a replication-competent SIVcpzPttMB897_EN-PH with this substitution showed spreading replication in hA3H hapII-containing SupT11 cells (Fig 8F).

A previous study showed that HIV-1 Vif from a homozygous hA3H haplotype II patient had greater activity against hA3H hapII compared to other laboratory HIV-1 Vifs, which correlated with the presence of four amino acid substitutions (60GDAK63 to 60EKGE63) [32]. This substitution was introduced into SIVcpzPttMB897 Vif and led to enhanced hA3H hapII depletion (Fig 8E, Vif M2 compared to M3 and M4). Based on a recent HIV-1 Vif-hA3H hapII co-structure model [49], the co-structure of SIVcpzPttMB897 Vif-hA3H hapII was modeled. From the structure, we found that residues 47EN48 and 60GDAK63 of SIVcpzPttMB897 Vif were in close contact with hA3H hapII (Fig 8G). Both regions are diverse in Vifs from distinct SIVcpz and HIV-1 lineages (Fig 8H).

Next, we tested the replication of SIVcpz in human PBMCs from donors with different hA3H genotypes. We identified three donors who were homozygous for A3H hapI, hapIV and hapII, respectively. The protein expression of A3H in stimulated PBMCs was detected by immunoblotting, demonstrating highest protein levels in the PBMCs of hapII, moderate levels in PBMCs of hapI and weak levels in cells of hapIV (Fig 9A). However, the A3G expression in these PBMC was identical (Fig 9A). The viral replication experiments indicated that SIVcpzPttMB897 replicated fastest in PBMCs from the donor with haplotype IV, and moderately in PBMCs from the donor with haplotype I (Fig 9B and 9C). However, the replication of SIVcpzPttMB897 was inhibited in PBMCs from donor with haplotype II (Fig 9B and 9C). In summary, we speculate that stable hA3H forms a barrier for zoonotic transmission of SIVcpz to humans and Vif adaptation to stable hA3H would be needed for high-level infection of humans with this haplotype (Fig 10).

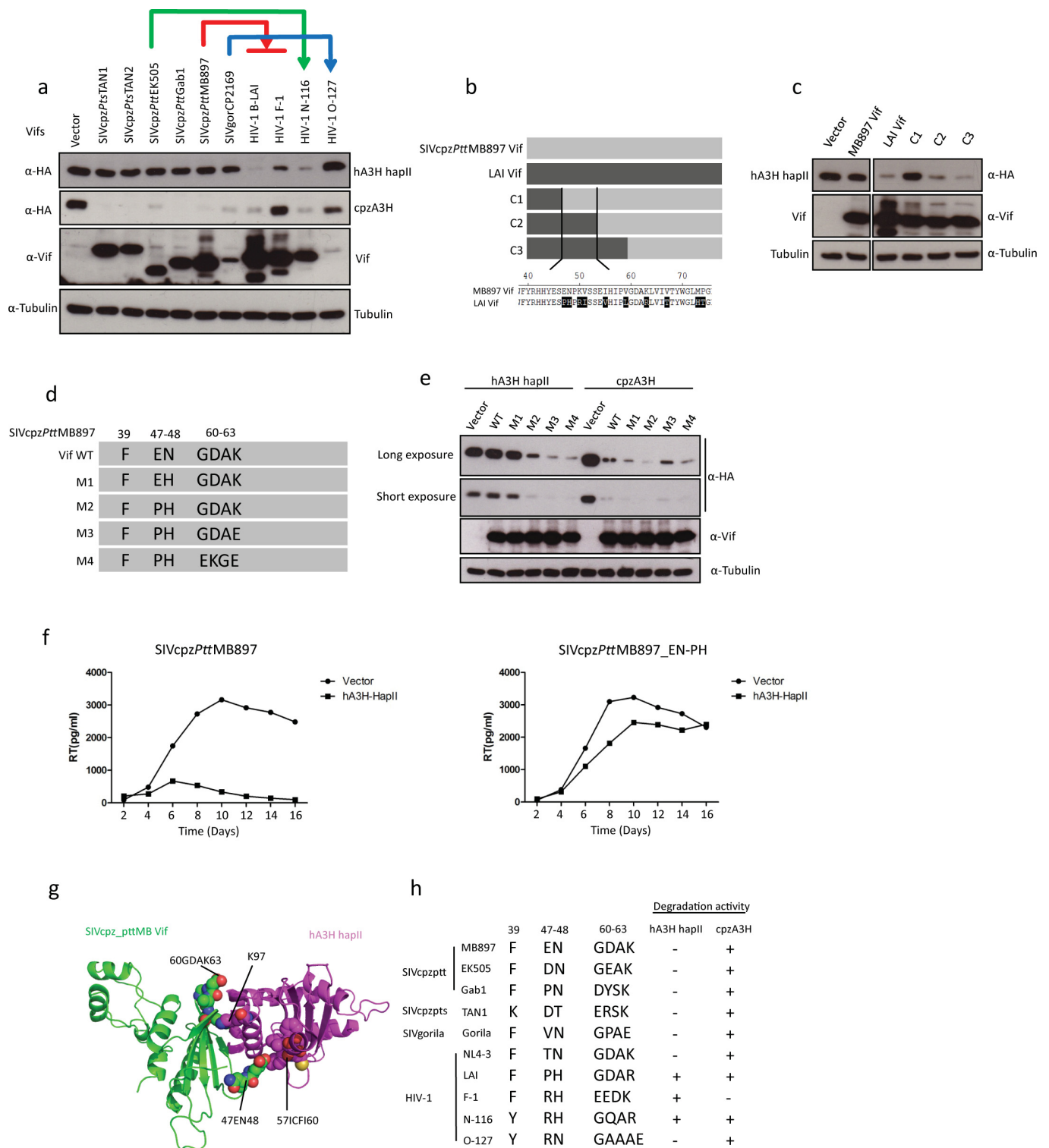


Fig 8. No counteraction of human A3H haplotype II by Vifs from different SIVcpz lineages. (a) cpzA3H or hA3H hapII wild type expression plasmids were co-transfected with expression plasmids for Vifs (different SIVcpz, SIVgor or HIV-1 strains, as indicated). The presence of A3H and Vif was detected by using anti-HA and anti-Vif antibodies, respectively. Tubulin served as a loading control. (b) The schematic structure of SIVcpzPttMB897 and HIV-1 LAI Vif chimeras. (c) hA3H hapII and Vif chimera expression plasmids were co-transfected into 293T cells. The presence of A3H and Vif was detected by using anti-HA and anti-Vif antibodies, respectively. Tubulin served as a loading control. (d) Schematic structure of SIVcpzPttMB897 Vif

mutants. (e) cpzA3H or hA3H hapII wild type expression plasmids were co-transfected with expression plasmids for different SIVcpzPttMB897 Vif mutants. The presence of A3H and Vif was detected by using anti-HA and anti-Vif antibodies, respectively. Tubulin served as a loading control. (f) SIVcpzPttMB897 with the mutation of 47EN48-47PH48 in Vif and wild type SIVcpz (5 ng RT activity) were used to infect SupT11-hA3H hapII-hCCR5 cells, respectively. The viral supernatants were collected each second day and quantified by RT assay. (g) Superimposition of SIVcpz Vif-hA3H hapII model structure. 47EN48 and 60GDAK63 motifs are shown by sphere, and their contact with hA3H hapII is displayed. (h) Summary: Correlation between Vif from different SIVcpz and HIV-1 lineages and antagonism activity against cpzA3H and hA3H hapII. Identity of amino acids at important positions (39, 47–48 and 60–63) of Vif was shown. -, + represents low and high A3H antagonism.

<https://doi.org/10.1371/journal.ppat.1006746.g008>

Discussion

SIVcpz originated from the cross-species transmission and recombination of three different SIVs [5,6]. After lentiviral transmission to a new host that differs in one or many A3 proteins, Vif adaptation is expected at the interface of both proteins [25,51]. In our study, all tested SIVcpz Vifs had the ability to counteract cpzA3Hs (Figs 2 and 7). Lucie Etienne *et al.* found that SIVrcm Vif acts like SIVcpz Vifs and can neutralize cpzA3H, while SIVmus Vif could not antagonize the restriction of cpzA3H [40]. Overcoming the restriction of cpzA3H may be one explanation for SIVcpz selectively acquiring the 5' region (including *vif*) from SIVrcm during

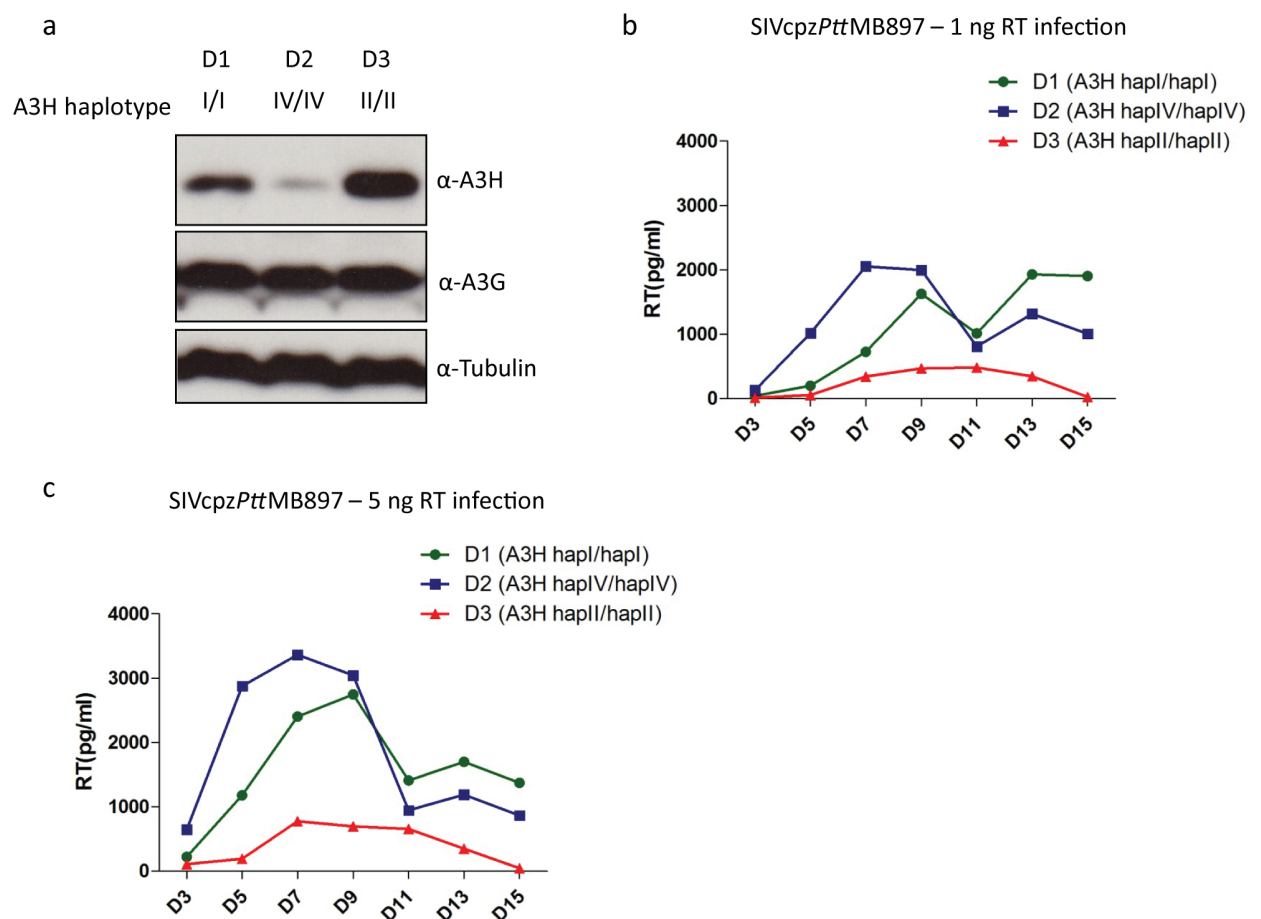


Fig 9. Stable hA3H inhibits SIVcpz replication in human PBMCs. (a) The genotypes of different donors were determined by sequencing the A3H mRNAs. Expression of A3H and A3G proteins in stimulated PBMCs were detected by immunoblots using anti-hA3H and anti-hA3G antibodies, respectively. Tubulin served as a loading control. (b, c) PBMCs from different donors were infected with 1 ng RT or 5 ng RT activity of SIVcpzPttMB897, respectively, and culture supernatants were collected each 2–3 day and analyzed for the RT activity.

<https://doi.org/10.1371/journal.ppat.1006746.g009>

recombination, and acquiring the 3' region (including *vpu*, *env*, and *nef*) from SIVgsn/SIVmus/SIVmon may have facilitated the counteraction of other restriction factors, such as Tetherin or Serinc3/5 [52–54]. Here, we also found that cpzA3D, F, and G were resistant to SIVagm Vif and similarly, cpzA3D was resistant to SIVmac Vif, confirming a previous report [40]. This observation indicates that cpzA3D and cpzA3G can protect chimpanzees from infection with SIVs of rhesus macaques and African green monkeys. On the other hand, SIVcpz Vifs could counteract all the tested cpzA3s. However, cpzA3F showed a moderate level of resistance to degradation induced by SIVcpz Vif (Fig 2C and 2D), possibly suggesting that cpzA3F may provide some repression of SIVcpz infection. Human and chimpanzee A3D, F, and G display a similar sensitivity to SIVcpz Vif, indicating that the inhibitory activity against cpzA3s by SIVcpz may be a prerequisite for the cross-species transmission of SIVcpz to the human population.

Here, we found that hA3C and hA3H hapI display a strong restriction against SIVmacΔvif and SIVagmΔvif; however, no antiviral activity was observed against SIVcpzΔvif (Fig 3) or HIV-1Δvif [26,41,55]. These data suggest that the viral sensitivity to hA3C and hA3H hapI was lost in the evolution of SIV lineages and not during the evolution of HIV-1. We cannot determine whether this happens during the creation of SIVcpz due to the lack of information regarding the antiviral activity of hA3C and hA3H hapI against SIVrcm/SIVgsn/SIVmus/SIVmon. We speculate that some SIVs similar to HIV-1 have the ability to escape hA3C and hA3H hapI restriction by a Vif-independent mechanism [55].

cpzA3H appears to be much less polymorphic than hA3H. However, A3F and A3G in chimpanzee are more diverse than the human orthologs [40]. Although our chimpanzee sample number was limited (61 chimpanzees), the results suggest that cpzA3H is relatively conserved among chimpanzees. Residues 15 and 105 of hA3H determine the protein stability and antiviral activity [28]. However, no variability was identified at these two positions in cpzA3H, which is in agreement with the comparable protein stability and anti-viral activity of the currently recognized five cpzA3H haplotypes (Fig 7). Vifs of different SIVcpz isolates degrade all haplotypes of cpzA3H indicating that cpzA3H is not a restriction factor for inter-subspecies transmission of SIVcpz. Compared to cpzA3H, human A3H is more diverse and includes seven haplotypes and several splice variants [28,30,31]. In our study, the stably expressed hA3H haplotypes were identified as Vif-resistant inhibitors against SIVcpz, indicating that these active hA3Hs are strong barriers to prevent SIVcpz infection of humans. After the zoonotic transmission of SIVcpz to humans expressing unstable A3H haplotypes, the very early human-to-human transmission was likely to be severely affected by humans expressing the A3H haplotypes with a stable protein (Figs 9 and 10). A possible mutation that would enhance SIVcpz Vif adaptation was investigated by replacing residues 47EN48 of SIVcpzPttMB897 Vif with 47PH48 (Fig 8). It is possible—but unlikely—that there are currently not identified viruses circulating in chimpanzees with vif genes encoding 47PH48 residues enhancing SIVcpz cross-species transmission to humans. In fact, the 47PH48 motif is also found in HIV-1 patients who harbor hA3H hapII [32,34]. The frequency of active hA3H varies significantly between populations, with the highest frequency in Africans (around 50% harbor stable A3H) [28,30]. This observation may be the result of a selective sweep caused by exposure to a retrovirus such as SIV or HTLV or other A3H-sensitive pathogens [56,57]. Several previous studies described a positive and balancing selection of human and chimpanzee MHC loci, caused by HIV-1/SIVcpz infections [56,58–60].

In addition to hA3H hapII, human tetherin is also a strong barrier against SIVcpz transmission to humans. SIVcpz Nef recognizes the cytoplasmic domain of chimpanzee tetherin and inhibits its restriction, but it cannot overcome the restriction of human tetherin due to a deletion in this domain [54]. However, the virus adapts to this restriction by regaining Vpu-

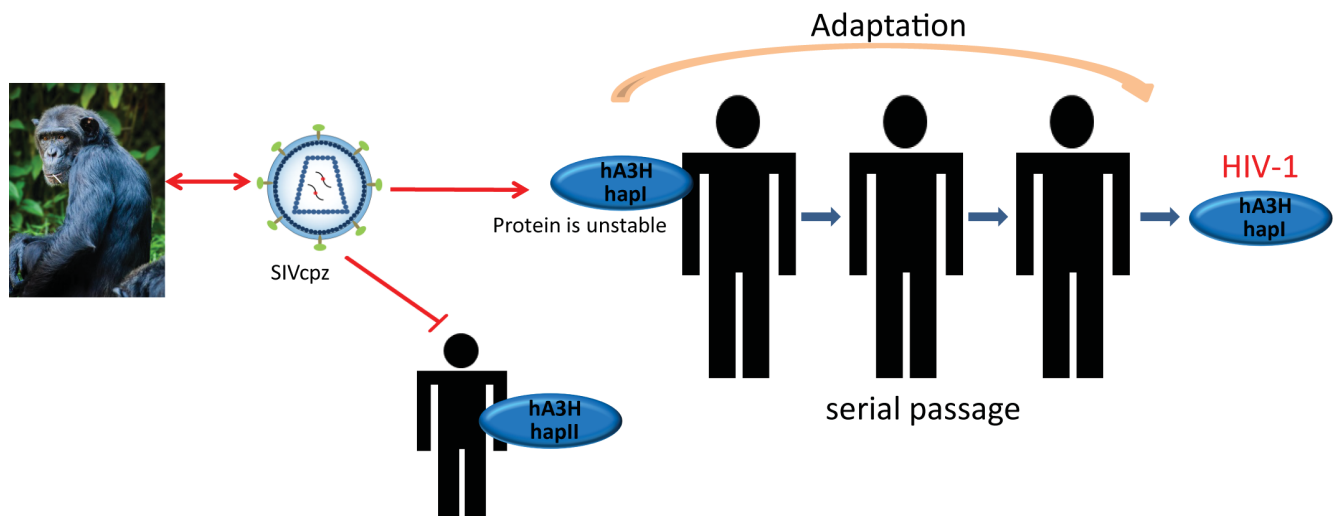


Fig 10. The model of SIVcpz cross species transmission to human. The model predicts that cross-species transmission of SIVcpz is blocked by hA3H hapII (or other stably expressed variants), but this transmission is easier obtained in humans with unstable A3H haplotypes.

<https://doi.org/10.1371/journal.ppat.1006746.g010>

mediated inhibition of tetherin after transmission of SIVcpz to humans [54]. In fact, other unknown restriction factors may exist to control the cross-transmission of SIVcpz to humans. For example, a recent study found that introducing a M30R/K mutation in the Gag matrix could enhance SIVcpz replication fitness in human tonsil explant cultures [38].

Overall, our study suggests that the stable active human A3Hs can protect humans against the spillover of SIVcpz, and SIVcpz cross-species transmission to humans may have started in those that harbored unstable A3H proteins.

Methods

Plasmids

Chimpanzee APOBEC3 (A3) expression plasmids (A3D, A3F, A3G and A3H) were provided by Michael Emerman [40], chimpanzee A3C plasmid was described recently [61]. Human A3s (A3A–A3H) were expressed by PTR600 vector with a carboxyl-terminal triple hemagglutinin (HA) tag [33]. Human A3H haplotype V, VII, splice variants and E56A of haplotype II expression plasmids with a carboxyl-terminal flag tag were provided by Viviana Simon [31]. Human A3H haplotype II with an N terminal HA tag was re-cloned into PTR600 vector by using standard PCR. All human and chimpanzee A3H mutants were generated by site direct mutagenesis and confirmed by sequencing. The MLV packaging construct pHIT60 was kindly provided by Jonathan Stoye, which encodes the *gag-pol* of MoMLV [62]. The Plasmid of pBABE.CCR5 that encodes human CCR5 was obtained from NIH AIDSREPOSITORY [63]. SIVmac-Luc (R-E-), SIVmac-Luc (R-E-)Δ*vif* and SIVagm-Luc (R-E-) and SIVagm-Luc (R-E-)Δ*vif* were provided by N. R. Landau [64]. The replication competent SIVcpzPtt clones MB897, EK505, Gab1 were kindly provided by Frank Kirchhoff [38,65]. SIVcpzPtt clones TAN1.910 and TAN2.69 and SIVgor clone CP2139 were obtained from NIH AIDSREPOSITORY [10,66]. To generate the Nanoluciferase reporter virus of SIVcpzPttMB897, the *nef* gene was replaced (the first 7 amino acids of Nef remained) by nanoluciferase gene by overlapping PCR using *NheI* and *XhoI* restriction sites. Additionally, two stop codons were inserted amino-terminal of Vif (amino acid position 40 and 44) by overlapping extension PCR using *PshAI* and *NheI* restriction sites.

The same method was performed to create nanoluciferase reporter virus of SIVcpzPttTAN1, and the restriction sites are shown in [S1 Fig](#). Simply, the *nef* gene was replaced (the first 7 amino acids of Nef remained) by nanoluciferase gene by overlapping PCR using *AclIII* and *XbaI* restriction sites. Additionally, two stop codons were inserted at the amino-terminal of Vif (amino acid position 40 and 44) by overlapping extension PCR using *PshAI* and *AclI* restriction sites. All constructs were verified by sequencing analysis. To generate the SIV Vif expression plasmids, Vif fragments from the following molecular clones: SIVcpzPtt EK505 (DQ373065), Gab1 (X52154), MB897 (EF535994) and SIVcpzPtt TAN1 (AF447763), TAN2 (DQ374657) and SIVgor CP2139 (FJ424866) were amplified and inserted into pCRV1 by *EcoRI* and *NotI*. Vif expression plasmids of HIV-1 LAI, F-1, N-116 and O-127 were provided by Viviana Simon [33,61]. All SIVcpzPttMB897 Vif mutants were generated by overlapping PCR and cloned into pCRV1 without any tag, verified by sequencing.

Cells and single-round infection assay

HEK293T (293T, ATCC CRL-3216) cells were maintained in Dulbecco's high-glucose modified Eagle's medium (DMEM, Biochrom, Berlin, Germany) supplemented with 10% fetal bovine serum (FBS), 2 mM L-glutamine, penicillin (100 U/ml), and streptomycin (100 µg/ml). SupT11 cells containing empty control and hA3H hapII were kindly provided by Reuben S. Harris and cultured in RPMI supplemented with 10% fetal bovine serum (FBS), 2 mM L-glutamine, penicillin (100 U/ml), and streptomycin (100 µg/ml) [47]. SupT11 cells with expression of hCCR5 were generated by MLV transduction. Simply, 1×10^6 SupT11 cells were transduced by MLV vector (produced by transfecting pBABE.CCR5, pHIT60 and VSV-G expression plasmid into 293T cells). 3 days after transduction, the SupT11 cells were selected for 3 weeks by using 1 µg/ml puromycin. For producing the single round infection of SIV reporter virus, 3×10^5 293T cells in 24-well plates were co-transfected with 300 ng SIVmac-Luc (R-E-), or SIVagm-Luc, or SIVcpzPttMB897-NLuc, or SIVcpzPttTAN1-NLuc; or the corresponding delta Vif versions, 30 ng human A3s or 200 ng chimpanzee A3s expression plasmids and 50 ng VSV-G (pMD.G), and pcDNA3.1(+) (Thermo Fisher Scientific) was used instead of A3 expression plasmids. Human A3s were expressed in plasmid PTR600, while chimpanzee A3s were expressed in plasmid pcDNA3.1(+). 30 ng of PTR600-human A3s constructs had comparable expression levels with 200 ng pcDNA3.1(+)-chimpanzee A3s plasmids. Transfections were performed by using Lipofectamine LTX (Thermo Fisher Scientific) according to manufacturer's instruction. The viral supernatants were collected 48 h post transfection. The reverse transcriptase (RT) activities of viruses were quantified by using the Cavid HS lenti RT kit (Cavidi Tech, Uppsala, Sweden). For SIVmac and SIVagm infections, 5×10^4 293T cells were seeded in 96-well plates one day before transduction, and 50 pg RT of viruses were used for infection. After 48 h, firefly luciferase activity was measured with Steady-Glo Luciferase system (Promega) according to the manufacturer's instructions on a MicroLumat Plus luminometer (Berthold Detection Systems, Pforzheim, Germany). For SIVcpz-NLuc, we observed high nanoluciferase enzyme activity in cell supernatant of transfected cells. 293T cells in 96-well plates were infected with 20 pg of SIVcpzPttMB897-NLuc or SIVcpzPttTAN1-NLuc. To eliminate the effect of contaminating nanoluciferase in the supernatant of virus producer cells, we changed the medium 8 h post infection. 48 h after transduction, the cells were carefully washed by PBS once, and the nanoluciferase activity was measured with Nano-Glo Luciferase system (Promega) on a MicroLumat Plus luminometer (Berthold Detection Systems). Each sample was analyzed in triplicates; the error bar of each triplicate was shown. Infections in which the VSV-G glycoprotein was omitted served as control for nanoluciferase enzyme background enzyme activity.

Detection of A3-mediated editing of SIVcpz transcripts

1 × 10⁶ 293T cells were infected with DNase I (Thermo Fisher, Germany) treated SIVcpzΔVif-Nluc produced in 293T cells together with hA3G, hA3H hapII, hA3H hapII E56A or pcDNA3.1(+). At 12 h post-infection, cells were washed with PBS, and DNA was isolated using a DNasy DNA isolation kit (Qiagen, Germany). A 700-bp fragment of the SIVcpz-Nluc (200-bp C terminal of *env* plus 500-bp nanoluciferase gene) was amplified using DreamTaq DNA polymerase (Thermo Fisher, Germany) with primers: 5'-attctccagtattgggacaagag-3' and 5'-ttacgccagaatgcgttcgcac-3'. The PCR parameters were: 95°C for 5 min; 30 cycles with 88°C for 30 s, 57°C for 30 s, 72°C for 1 min; 10 min at 72°C. PCR products were cloned using CloneJET PCR cloning kit (Thermo Scientific). Seven to ten clones were sequenced for each sample. A3 induced hypermutations were analyzed with the Hypermute online tool (<http://www.hiv.lanl.gov/content/sequence/HYPERMUT/hypermute.html>). The overall mutation rate was calculated by using the total number of G-A mutations divided by the total analyzed nucleotides.

Flow cytometry

To analyze CD4 and CCR5 expression level of SupT11 cell lines, 5 × 10⁵ cells were stained by α-hCD4 PE mouse IgG1_k (Dako, Hamburg, Germany) and α-hCCR5 FITC (BD Bioscience, Heidelberg, Germany) separately according to the manufacturer's instruction. The mouse IgG1/RPE isopeptidase was used as negative antibody control for CD4 staining. The measurement was carried out by BD FACSanto (BD Bioscience). Data analysis was done with the Software FlowJo version 7.6 (FlowJo, Ashland, USA).

Ethics statement

Buffy-coats obtained from anonymous blood donors were obtained from University Hospital Düsseldorf blood bank. Whole blood was obtained from healthy and de-identified African donors that signed an informed consent. The research has been approved by the Ethics Committee of the Medical Faculty of the Heinrich-Heine-University Düsseldorf (Reference No 4767R - 2014072657) and performed according to the principles expressed in the Declaration of Helsinki.

Determining of A3H haplotype expressed

Cellular RNA from PHA stimulated human PBMCs was isolated by using QIAGEN RNA extraction kit (Qiagen). 1 µg of total cellular RNA was used for reverse transcription with the RevertAid H Minus First Strand cDNA synthesis kit (Thermo Scientific). Human A3H cDNA was amplified with Q5 High-Fidelity DNA Polymerase (New England Biolabs) using primers: 5'-atggctctgttaacagccgaacattcc-3' and 5'-ggactgctttatcctgtcaagccgtcgc-3'. PCR products were cloned using CloneJET PCR cloning kit (Thermo Scientific). Six to ten clones were sequenced for each donor.

SIVcpz replication on SupT11 cell lines

To produce SIVcpz, 1 × 10⁶ 293T cells in 6-well plate were transfected with 2 µg SIVcpz molecular clone plasmids (SIVcpzP_{ts}Tan1, SIVcpzP_{tt}MB897 and SIVcpzP_{tt}Gab1). 2 days after transfection, the viral supernatants were collected and centrifuged at 12,000 rpm for 10 min to remove cell debris. Then the viral supernatants were concentrated through 20% sucrose cushion at 14,800 rpm 4 h, followed by resuspension in RPMI. The viral stock was quantified by using the Cavid HS lenti RT kit (Cavid Tech, Uppsala, Sweden). 5 × 10⁵ cells of each SupT11 cell lines (SupT11-vector-hCCR5 and SupT11-hA3H hapII-hCCR5) were infected with 1 ng

or 5 ng RT activity of SIVcpz in a 24-well plate (in 500 μ l) and cells were washed with PBS 1 day post-infection. Each second day, 200 μ l supernatant was collected, clarified, and stored at 80°C, and cultures were supplemented with fresh media. The replications were performed in two independent experiments, and each infection was performed in duplicates.

SIVcpz replication on PBMCs

3 x 10⁵ PHA stimulated PBMC from three donors were infected overnight with SIVcpzPttMB897 representing either 1 ng RT activity or 5 ng RT activity in the presence of 30 U/ml Interleukin-2 (IL-2) in 96-well round-bottom plates (total volume 200 μ l). After infection, cells were washed three times and maintained in complete RPMI with 30 U/ml of IL-2 for 15 days. 100 μ l culture supernatant was collected every 2–3 days, and cultures were supplemented with fresh media. The RT activities of viruses in culture supernatant were quantified by using the Cavid HS lenti RT kit (Cavid Tech, Uppsala, Sweden).

APOBEC3 degradation assay

A total of 3 x 10⁵ 293T cells in 24-well plates were co-transfected with 200 ng chimpanzee A3H expression plasmid or 50 ng hA3H haplotype II in PTR600 expression vector and 300 ng pCRV1 Vif expression plasmids, pcDNA3.1(+) (Thermo Fisher Scientific) was used to fill up the total transfected plasmid DNA to 500 ng. Transfections were performed by using Lipofectamine LTX (Thermo Fisher Scientific). 48 h post transfection, cells were lysed and clarified by 14,000 rpm/30 mins centrifugation. The expression of A3H and Vif were analyzed by immunoblots.

Immunoblot analysis

Transfected 293T cells were lysed in radioimmunoprecipitation assay (RIPA) buffer (25 mM Tris-HCl [pH 8.0], 137 mM NaCl, 1% NP-40, 1% glycerol, 0.5% sodium deoxycholate, 0.1% sodium dodecyl sulfate [SDS], 2 mM EDTA, and protease inhibitor cocktail set III [Calbiochem, Darmstadt, Germany]). To pellet virions, culture supernatant were centrifuged at 12,000 rpm for 10 min followed by centrifugation through 20% sucrose cushion at 14,500 rpm 4 h and resuspended in RIPA buffer, boiled at 95°C for 5 min with Roti load reducing loading buffer (Carl Roth, Karlsruhe, Germany) and resolved on a SDS-PAGE gel. The expression of A3s and SIV/HIV Vifs were detected by mouse anti-hemagglutinin (anti-HA) antibody (1:7,500 dilution, MMS-101P; Covance, Münster, Germany), rabbit anti-HA antibody (1:1,000 dilution, C29F4, cat. 3724, Cell Signaling, USA) and rabbit anti-Vif polyclonal antibody (1:1,000 dilution, NIH AIDSREAGENTS, cat. 2221) [67]; tubulin and SIVcpzPttMB897 capsid protein was detected using mouse anti- α -tubulin antibody (1:4,000 dilution, clone B5-1-2; Sigma-Aldrich, Taufkirchen, Germany) and mouse anti-capsid p24/p27 MAb AG3.0 (1:50 dilution) separately [68], followed by horseradish peroxidase-conjugated rabbit anti-mouse or donkey anti-rabbit antibodies (α -mouse or rabbit-IgG-HRP; GE Healthcare, Munich, Germany), and developed with ECL chemiluminescence reagents (GE Healthcare). The expression of A3H in SupT11 cell lines was detected by using anti-hA3H (1:1,000) antibody [35] followed by horseradish peroxidase-conjugated rabbit anti-mouse and developed with ECL chemiluminescence reagents. 8 x 10⁶ human PBMCs from three donors were lysed in 100 μ l RIPA buffer with protease inhibitor cocktail set III [Calbiochem, Darmstadt, Germany]). The expression of A3G, A3H and tubulin were detected by using anti-hA3H (1:1,000) [35], anti-hA3G (1:10,000, NIH AIDSREAGENTS, cat. 9906) [69] and anti-tubulin (1:4,000 dilution, clone B5-1-2; Sigma-Aldrich, Taufkirchen, Germany) antibodies, respectively.

Phylogenetic analysis

The primate A3H sequences were obtained from GenBank, the accession numbers are: EU861357, EU861358, EU861359, EU861360, EU861361, DQ408606 and DQ507277. CpzA3H SNPs were described in this study. The A3H sequences were aligned using the ClustalW in Mega 7 software. The phylogenetic analysis was performed in Mega 7 by using bootstrap neighbor joining method. Test parameters were estimated using 500 bootstrap replicates.

Model structure

To analyze the interaction surface between SIVcpz Vif and hA3H hapII, the structure of SIVcpz Vif was modeled using HIV-1 Vif (4N9F) [70] as template by using SWISS-MODEL online server (<http://www.swissmodel.expasy.org/>). The recent crystal structure of hA3H hapII (6B0B) was also used to model the structure of cpzA3H. The SIVcpz Vif and hA3H hapII co-structure was modeled based on the recent HIV-1 Vif-A3H interaction surface analysis [49]. The graphical visualization was constructed using PyMOL (PyMOL Molecular Graphics System, version 1.5.0.4; Schrödinger, Portland, OR).

Statistical analysis

Data are represented as the mean with SD in all bar diagrams. Statistically significant differences between two groups were analyzed using the unpaired Student's t-test with GraphPad Prism version 5 (GraphPad software, San Diego, CA, USA). A minimum p value of 0.05 was considered as statistically significant: P value < 0.001 extremely significant (**), 0.001 to 0.01 very significant (*), 0.01 to 0.05 significant (*), >0.05 not significant (ns).

Supporting information

S1 Fig. Schematic genome structure of SIVcpzPttMB897 and SIVcpzPtsTAN1. The restriction sites used for construction of nanoluciferase (NLuc) reporter viruses are shown. Stop codons were inserted in *vif* at positions for coding of amino acid 40 and 44. (TIF)

S2 Fig. Detection of A3 expression by immunoblots (a, b, c): 293T cells were transfected with 30 ng hA3s or 200 ng cpzA3s expression plasmids. Two days post-transfection, cell lysates were used to detect the expression of A3s by two different anti-HA antibodies. Tubulin served as a loading control. **(d)** SIVcpzPttMB897 or SIVcpzPtsTAN1 wild type or delta *vif* reporter viruses were produced in 293T cells in the presence of cpzA3H or hA3H hapII, pcDNA3.1(+) was used as control (vector). Two days post-transfection, cpzA3H and hA3H hapII in cell lysates and viral particles were detected by anti-HA antibody. Viral capsid (p24) was detected by anti-p24 antibody. Tubulin served as a loading control. VLP: Viral Like Particle. (TIF)

S3 Fig. (a) Characterization of SupT11-vector-hCCR5 or SupT11-hA3H hapII-hCCR5 cells for expression of hA3H hapII using immunoblots of cell lysates and anti-hA3H antibody. Tubulin served as a loading control and **(b)** for expression of CCR5 and CD4 by flow cytometry. Cells were stained by α -hCCR5 FITC, or α -hCD4 PE mouse IgG1_k separately. The mouse IgG1/RPE isopeptidase was used as negative antibody control for CD4 staining. **(c)** SupT11-vector-hCCR5 or SupT11-hA3H hapII-hCCR5 cells were infected with 50 ng RT activity of SIVcpzPtsTAN1, SIVcpzPttMB897 or SIVcpzPttMB897_EN-PH (47EN48 replaced by 47PH48 in Vif open reading frame), respectively, and culture supernatants were collected each second day

and quantified by the RT assay.
(TIF)

S4 Fig. Structural superimposition of cpzA3H (a) The recent crystal structure of hA3H hapII (6B0B) was used to model the structure of cpzA3H. The SNPs of cpzA3H identified in this study were shown. (b) The potential SIVcpz/HIV-1 Vif interaction sites in helix-3 and helix-4 of cpzA3H (green) are shown.
(TIF)

Acknowledgments

We thank Wioletta Hörschken for excellent technical assistance. We thank Viviana Simon, Michael Emerman, Frank Kirchhof, Nathaniel R. Landau, Marcel Ooms, Daniel Sauter and Jonathan Stoye for reagents. We thank Daniel Sauter for discussing the propagation of SIVcpz molecular clones.

Author Contributions

Conceptualization: Carsten Münk.

Data curation: Zeli Zhang, Qinyong Gu, Marc de Manuel Montero, Ignacio G. Bravo.

Formal analysis: Zeli Zhang, Marc de Manuel Montero, Ignacio G. Bravo, Tomas Marques-Bonet, Dieter Häussinger, Carsten Münk.

Funding acquisition: Dieter Häussinger, Carsten Münk.

Investigation: Zeli Zhang, Qinyong Gu.

Methodology: Zeli Zhang, Carsten Münk.

Project administration: Carsten Münk.

Resources: Marc de Manuel Montero, Ignacio G. Bravo, Tomas Marques-Bonet.

Software: Zeli Zhang, Marc de Manuel Montero, Ignacio G. Bravo, Tomas Marques-Bonet.

Supervision: Dieter Häussinger, Carsten Münk.

Validation: Qinyong Gu, Tomas Marques-Bonet, Dieter Häussinger.

Visualization: Carsten Münk.

Writing – original draft: Zeli Zhang.

Writing – review & editing: Carsten Münk.

References

1. Locatelli S, Peeters M (2012) Cross-species transmission of simian retroviruses: how and why they could lead to the emergence of new diseases in the human population. *AIDS* 26: 659–673. <https://doi.org/10.1097/QAD.0b013e328350fb68> PMID: 22441170
2. Klatt NR, Silvestri G, Hirsch V (2012) Nonpathogenic simian immunodeficiency virus infections. *Cold Spring Harb Perspect Med* 2: a007153. <https://doi.org/10.1101/cshperspect.a007153> PMID: 22315718
3. Pandrea I, Apetrei C (2010) Where the wild things are: pathogenesis of SIV infection in African nonhuman primate hosts. *Curr HIV/AIDS Rep* 7: 28–36. <https://doi.org/10.1007/s11904-009-0034-8> PMID: 20425055
4. Sharp PM, Shaw GM, Hahn BH (2005) Simian immunodeficiency virus infection of chimpanzees. *J Virol* 79: 3891–3902. <https://doi.org/10.1128/JVI.79.7.3891-3902.2005> PMID: 15767392

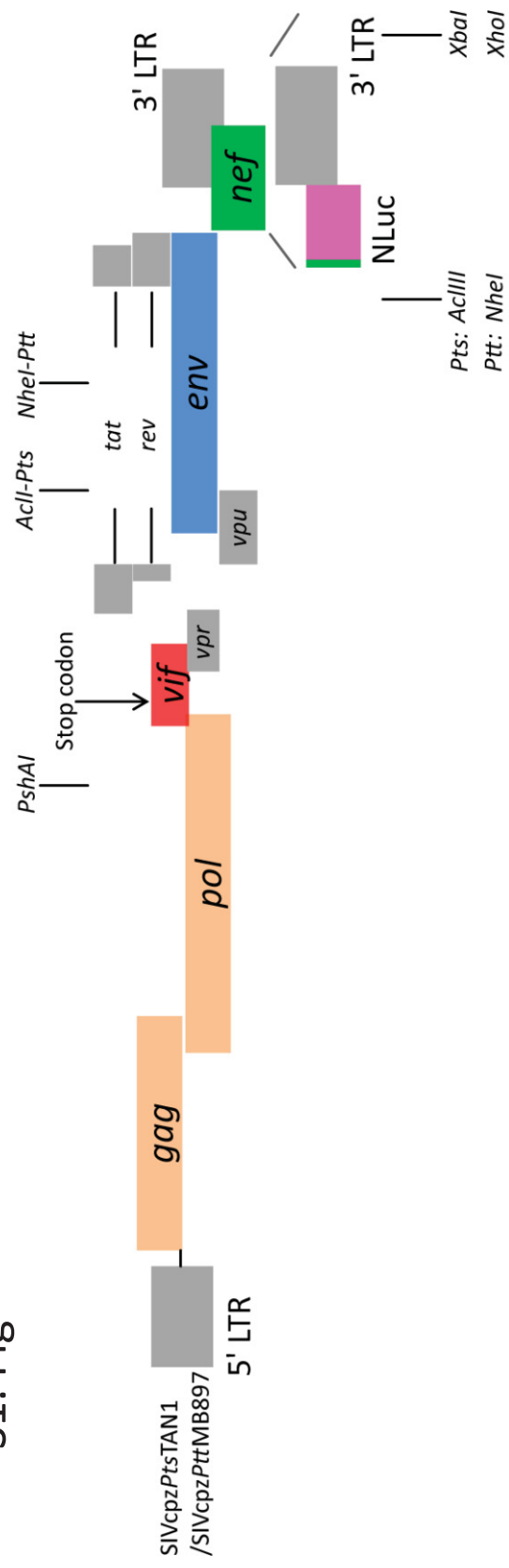
5. Bell SM, Bedford T (2017) Modern-day SIV viral diversity generated by extensive recombination and cross-species transmission. *PLoS Pathog* 13: e1006466. <https://doi.org/10.1371/journal.ppat.1006466> PMID: [28672035](#)
6. Bailes E, Gao F, Bibollet-Ruche F, Courgnaud V, Peeters M, et al. (2003) Hybrid origin of SIV in chimpanzees. *Science* 300: 1713. <https://doi.org/10.1126/science.1080657> PMID: [12805540](#)
7. Etienne L, Hahn BH, Sharp PM, Matsen FA, Emerman M (2013) Gene loss and adaptation to hominids underlie the ancient origin of HIV-1. *Cell Host Microbe* 14: 85–92. <https://doi.org/10.1016/j.chom.2013.06.002> PMID: [23870316](#)
8. Keele BF, Van Heuverswyn F, Li Y, Bailes E, Takehisa J, et al. (2006) Chimpanzee reservoirs of pandemic and nonpandemic HIV-1. *Science* 313: 523–526. <https://doi.org/10.1126/science.1126531> PMID: [16728595](#)
9. Van Heuverswyn F, Li Y, Bailes E, Neel C, Lafay B, et al. (2007) Genetic diversity and phylogeographic clustering of SIVcpzPtt in wild chimpanzees in Cameroon. *Virology* 368: 155–171. <https://doi.org/10.1016/j.virol.2007.06.018> PMID: [17651775](#)
10. Takehisa J, Kraus MH, Ayoub A, Bailes E, Van Heuverswyn F, et al. (2009) Origin and biology of simian immunodeficiency virus in wild-living western gorillas. *J Virol* 83: 1635–1648. <https://doi.org/10.1128/JVI.02311-08> PMID: [19073717](#)
11. D'Arc M, Ayoub A, Esteban A, Learn GH, Boue V, et al. (2015) Origin of the HIV-1 group O epidemic in western lowland gorillas. *Proc Natl Acad Sci U S A* 112: E1343–1352. <https://doi.org/10.1073/pnas.1502022112> PMID: [25733890](#)
12. Simon F, Maucel P, Roques P, Loussert-Ajaka I, Muller-Trutwin MC, et al. (1998) Identification of a new human immunodeficiency virus type 1 distinct from group M and group O. *Nat Med* 4: 1032–1037. <https://doi.org/10.1038/2017> PMID: [9734396](#)
13. Plantier JC, Leoz M, Dickerson JE, De Oliveira F, Cordonnier F, et al. (2009) A new human immunodeficiency virus derived from gorillas. *Nat Med* 15: 871–872. <https://doi.org/10.1038/nm.2016> PMID: [19648927](#)
14. Sharp PM, Hahn BH (2011) Origins of HIV and the AIDS pandemic. *Cold Spring Harb Perspect Med* 1: a006841. <https://doi.org/10.1101/cshperspect.a006841> PMID: [22229120](#)
15. Peeters M, Gueye A, Mboup S, Bibollet-Ruche F, Ekaza E, et al. (1997) Geographical distribution of HIV-1 group O viruses in Africa. *AIDS* 11: 493–498. PMID: [9084797](#)
16. Duggal NK, Emerman M (2012) Evolutionary conflicts between viruses and restriction factors shape immunity. *Nat Rev Immunol* 12: 687–695. <https://doi.org/10.1038/nri3295> PMID: [22976433](#)
17. Malim MH, Bieniasz PD (2012) HIV Restriction Factors and Mechanisms of Evasion. *Cold Spring Harb Perspect Med* 2: a006940. <https://doi.org/10.1101/cshperspect.a006940> PMID: [22553496](#)
18. Simon V, Bloch N, Landau NR (2015) Intrinsic host restrictions to HIV-1 and mechanisms of viral escape. *Nat Immunol* 16: 546–553. <https://doi.org/10.1038/ni.3156> PMID: [25988886](#)
19. Harris RS, Dudley JP (2015) APOBECs and virus restriction. *Virology* 479–480: 131–145. <https://doi.org/10.1016/j.virol.2015.03.012> PMID: [25818029](#)
20. Yu X, Yu Y, Liu B, Luo K, Kong W, et al. (2003) Induction of APOBEC3G ubiquitination and degradation by an HIV-1 Vif-Cul5-SCF complex. *Science* 302: 1056–1060. <https://doi.org/10.1126/science.1089591> PMID: [14564014](#)
21. Zhang W, Du J, Evans SL, Yu Y, Yu XF (2012) T-cell differentiation factor CBF-beta regulates HIV-1 Vif-mediated evasion of host restriction. *Nature* 481: 376–379.
22. Jager S, Kim DY, Hultquist JF, Shindo K, LaRue RS, et al. (2012) Vif hijacks CBF-beta to degrade APOBEC3G and promote HIV-1 infection. *Nature* 481: 371–375.
23. Hatzioannou T, Princiotto M, Piatak M Jr., Yuan F, Zhang F, et al. (2006) Generation of simian-tropic HIV-1 by restriction factor evasion. *Science* 314: 95. <https://doi.org/10.1126/science.1130994> PMID: [17023652](#)
24. Krupp A, McCarthy KR, Ooms M, Letko M, Morgan JS, et al. (2013) APOBEC3G polymorphism as a selective barrier to cross-species transmission and emergence of pathogenic SIV and AIDS in a primate host. *PLoS Pathog* 9: e1003641. <https://doi.org/10.1371/journal.ppat.1003641> PMID: [24098115](#)
25. Compton AA, Hirsch VM, Emerman M (2012) The host restriction factor APOBEC3G and retroviral Vif protein coevolve due to ongoing genetic conflict. *Cell Host Microbe* 11: 91–98. <https://doi.org/10.1016/j.chom.2011.11.010> PMID: [22264516](#)
26. OhAinle M, Kerns JA, Malik HS, Emerman M (2006) Adaptive evolution and antiviral activity of the conserved mammalian cytidine deaminase APOBEC3H. *J Virol* 80: 3853–3862. <https://doi.org/10.1128/JVI.80.8.3853-3862.2006> PMID: [16571802](#)
27. Dang Y, Siew LM, Wang X, Han Y, Lampen R, et al. (2008) Human cytidine deaminase APOBEC3H restricts HIV-1 replication. *J Biol Chem* 283: 11606–11614. <https://doi.org/10.1074/jbc.M707586200> PMID: [18299330](#)

28. OhAinle M, Kerns JA, Li MM, Malik HS, Emerman M (2008) Antiretroelement activity of APOBEC3H was lost twice in recent human evolution. *Cell Host Microbe* 4: 249–259. <https://doi.org/10.1016/j.chom.2008.07.005> PMID: [18779051](#)
29. Li MM, Emerman M (2011) Polymorphism in human APOBEC3H affects a phenotype dominant for sub-cellular localization and antiviral activity. *J Virol* 85: 8197–8207. <https://doi.org/10.1128/JVI.00624-11> PMID: [21653666](#)
30. Wang X, Abudu A, Son S, Dang Y, Venta PJ, et al. (2011) Analysis of human APOBEC3H haplotypes and anti-human immunodeficiency virus type 1 activity. *J Virol* 85: 3142–3152. <https://doi.org/10.1128/JVI.02049-10> PMID: [21270145](#)
31. Harari A, Ooms M, Mulder LC, Simon V (2009) Polymorphisms and splice variants influence the antiretroviral activity of human APOBEC3H. *J Virol* 83: 295–303. <https://doi.org/10.1128/JVI.01665-08> PMID: [18945781](#)
32. Li MM, Wu LI, Emerman M (2010) The range of human APOBEC3H sensitivity to lentiviral Vif proteins. *J Virol* 84: 88–95. <https://doi.org/10.1128/JVI.01344-09> PMID: [19828612](#)
33. Binka M, Ooms M, Steward M, Simon V (2012) The activity spectrum of Vif from multiple HIV-1 subtypes against APOBEC3G, APOBEC3F, and APOBEC3H. *J Virol* 86: 49–59. <https://doi.org/10.1128/JVI.06082-11> PMID: [22013041](#)
34. Ooms M, Brayton B, Letko M, Maio SM, Pilcher CD, et al. (2013) HIV-1 Vif adaptation to human APOBEC3H haplotypes. *Cell Host Microbe* 14: 411–421. <https://doi.org/10.1016/j.chom.2013.09.006> PMID: [24139399](#)
35. Refsland EW, Hultquist JF, Luengas EM, Ikeda T, Shaban NM, et al. (2014) Natural polymorphisms in human APOBEC3H and HIV-1 Vif combine in primary T lymphocytes to affect viral G-to-A mutation levels and infectivity. *PLoS Genet* 10: e1004761. <https://doi.org/10.1371/journal.pgen.1004761> PMID: [25411794](#)
36. Naruse TK, Sakurai D, Ohtani H, Sharma G, Sharma SK, et al. (2016) APOBEC3H polymorphisms and susceptibility to HIV-1 infection in an Indian population. *J Hum Genet* 61: 263–265. <https://doi.org/10.1038/jhg.2015.136> PMID: [26559750](#)
37. Sakurai D, Iwatani Y, Ohtani H, Naruse TK, Terunuma H, et al. (2015) APOBEC3H polymorphisms associated with the susceptibility to HIV-1 infection and AIDS progression in Japanese. *Immunogenetics* 67: 253–257. <https://doi.org/10.1007/s00251-015-0829-2> PMID: [25721876](#)
38. Bibollet-Ruche F, Heigle A, Keele BF, Easlick JL, Decker JM, et al. (2012) Efficient SIVcpz replication in human lymphoid tissue requires viral matrix protein adaptation. *J Clin Invest* 122: 1644–1652. <https://doi.org/10.1172/JCI61429> PMID: [22505456](#)
39. Santiago ML, Bibollet-Ruche F, Bailes E, Kamanya S, Muller MN, et al. (2003) Amplification of a complete simian immunodeficiency virus genome from fecal RNA of a wild chimpanzee. *J Virol* 77: 2233–2242. <https://doi.org/10.1128/JVI.77.3.2233-2242.2003> PMID: [12525658](#)
40. Etienne L, Bibollet-Ruche F, Sudmant PH, Wu LI, Hahn BH, et al. (2015) The Role of the Antiviral APOBEC3 Gene Family in Protecting Chimpanzees against Lentiviruses from Monkeys. *PLoS Pathog* 11: e1005149. <https://doi.org/10.1371/journal.ppat.1005149> PMID: [26394054](#)
41. Yu Q, Chen D, König R, Mariani R, Unutmaz D, et al. (2004) APOBEC3B and APOBEC3C are potent inhibitors of simian immunodeficiency virus replication. *J Biol Chem* 279: 53379–53386. <https://doi.org/10.1074/jbc.M408802200> PMID: [15466872](#)
42. Mitra M, Singer D, Mano Y, Hritz J, Nam G, et al. (2015) Sequence and structural determinants of human APOBEC3H deaminase and anti-HIV-1 activities. *Retrovirology* 12: 3. <https://doi.org/10.1186/s12977-014-0130-8> PMID: [25614027](#)
43. Yu Q, König R, Pillai S, Chiles K, Kearney M, et al. (2004) Single-strand specificity of APOBEC3G accounts for minus-strand deamination of the HIV genome. *Nat Struct Mol Biol* 11: 435–442. <https://doi.org/10.1038/nsmb758> PMID: [15098018](#)
44. Gu J, Chen Q, Xiao X, Ito F, Wolfe A, et al. (2016) Biochemical Characterization of APOBEC3H Variants: Implications for Their HIV-1 Restriction Activity and mC Modification. *J Mol Biol* 428: 4626–4638. <https://doi.org/10.1016/j.jmb.2016.08.012> PMID: [27534815](#)
45. Tan L, Sarkis PT, Wang T, Tian C, Yu XF (2009) Sole copy of Z2-type human cytidine deaminase APOBEC3H has inhibitory activity against retrotransposons and HIV-1. *FASEB J* 23: 279–287. <https://doi.org/10.1096/fj.07-088781> PMID: [18827027](#)
46. Zhen A, Wang T, Zhao K, Xiong Y, Yu XF (2010) A single amino acid difference in human APOBEC3H variants determines HIV-1 Vif sensitivity. *J Virol* 84: 1902–1911. <https://doi.org/10.1128/JVI.01509-09> PMID: [19939923](#)
47. Hultquist JF, Lengyel JA, Refsland EW, LaRue RS, Lackey L, et al. (2011) Human and rhesus APOBEC3D, APOBEC3F, APOBEC3G, and APOBEC3H demonstrate a conserved capacity to restrict Vif-deficient HIV-1. *J Virol* 85: 11220–11234. <https://doi.org/10.1128/JVI.05238-11> PMID: [21835787](#)

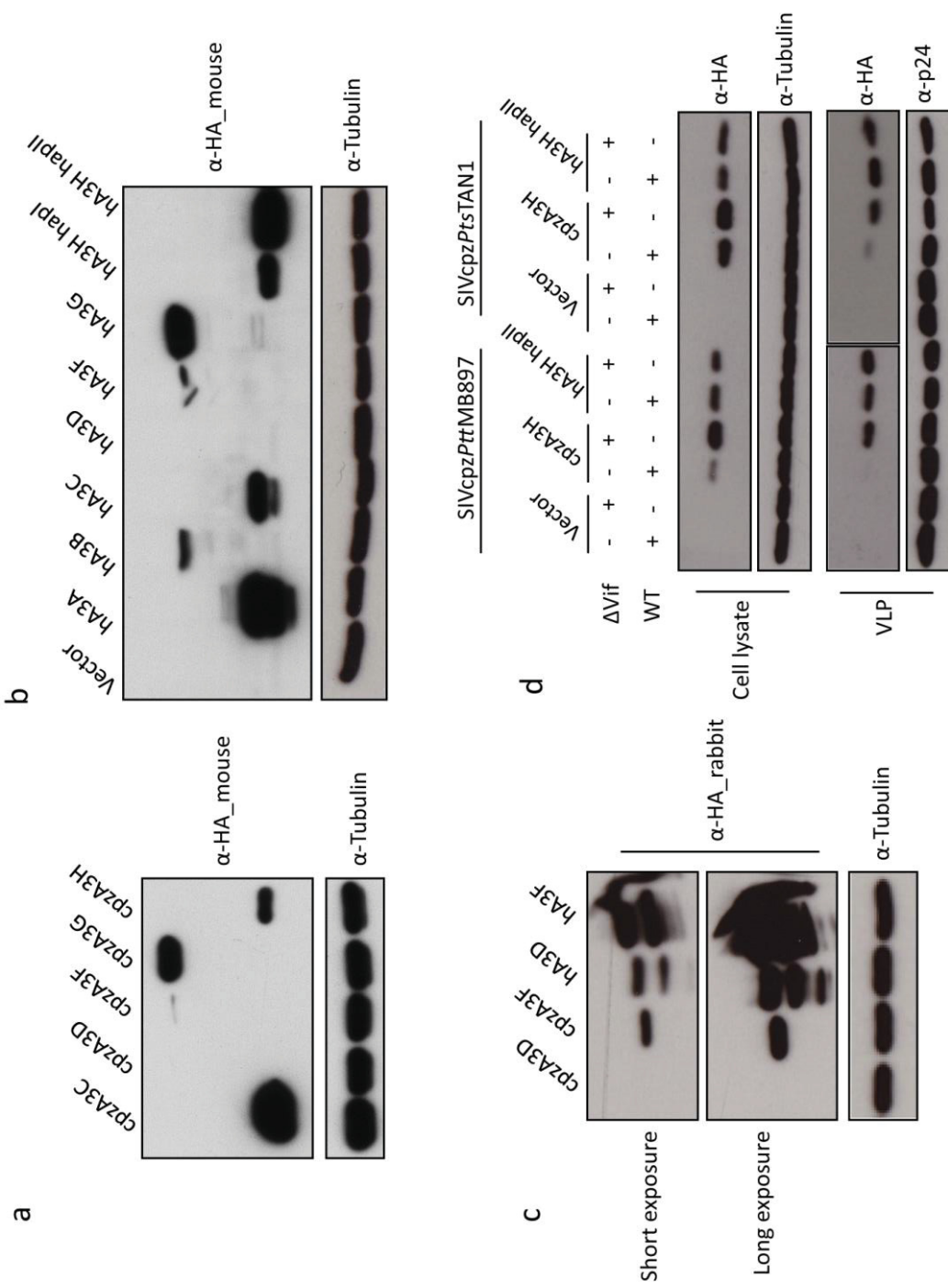
48. Nakashima M, Tsuzuki S, Awazu H, Hamano A, Okada A, et al. (2017) Mapping Region of Human Restriction Factor APOBEC3H Critical for Interaction with HIV-1 Vif. *J Mol Biol* 429: 1262–1276. <https://doi.org/10.1016/j.jmb.2017.03.019> PMID: 28336404
49. Ooms M, Letko M, Simon V (2017) The Structural Interface between HIV-1 Vif and Human APOBEC3H. *J Virol* 91.
50. Prado-Martinez J, Sudmant PH, Kidd JM, Li H, Kelley JL, et al. (2013) Great ape genetic diversity and population history. *Nature* 499: 471–475. <https://doi.org/10.1038/nature12228> PMID: 23823723
51. Harris RS, Anderson BD (2016) Evolutionary Paradigms from Ancient and Ongoing Conflicts between the Lentiviral Vif Protein and Mammalian APOBEC3 Enzymes. *PLoS Pathog* 12: e1005958. <https://doi.org/10.1371/journal.ppat.1005958> PMID: 27907174
52. Kluge SF, Mack K, Iyer SS, Pujol FM, Heigele A, et al. (2014) Nef proteins of epidemic HIV-1 group O strains antagonize human tetherin. *Cell Host Microbe* 16: 639–650. <https://doi.org/10.1016/j.chom.2014.10.002> PMID: 25525794
53. Heigele A, Kmiec D, Regensburger K, Langer S, Peiffer L, et al. (2016) The Potency of Nef-Mediated SERINC5 Antagonism Correlates with the Prevalence of Primate Lentiviruses in the Wild. *Cell Host Microbe* 20: 381–391. <https://doi.org/10.1016/j.chom.2016.08.004> PMID: 27631701
54. Sauter D, Schindler M, Specht A, Landford WN, Munch J, et al. (2009) Tetherin-driven adaptation of Vpu and Nef function and the evolution of pandemic and nonpandemic HIV-1 strains. *Cell Host Microbe* 6: 409–421. <https://doi.org/10.1016/j.chom.2009.10.004> PMID: 19917496
55. Jaguva Vasudevan AA, Hofmann H, Willbold D, Haussinger D, Koenig BW, et al. (2017) Enhancing the Catalytic Deamination Activity of APOBEC3C Is Insufficient to Inhibit Vif-Deficient HIV-1. *J Mol Biol* 429: 1171–1191. <https://doi.org/10.1016/j.jmb.2017.03.015> PMID: 28315663
56. de Groot NG, Bontrop RE (2013) The HIV-1 pandemic: does the selective sweep in chimpanzees mirror humankind's future? *Retrovirology* 10: 53. <https://doi.org/10.1186/1742-4690-10-53> PMID: 23705941
57. Ooms M, Krikoni A, Kress AK, Simon V, Münk C (2012) APOBEC3A, APOBEC3B, and APOBEC3H haplotype 2 restrict human T-lymphotropic virus type 1. *J Virol* 86: 6097–6108. <https://doi.org/10.1128/JVI.06570-11> PMID: 22457529
58. International HIVCS, Pereyra F, Jia X, McLaren PJ, Telenti A, et al. (2010) The major genetic determinants of HIV-1 control affect HLA class I peptide presentation. *Science* 330: 1551–1557. <https://doi.org/10.1126/science.1195271> PMID: 21051598
59. Thomas R, Apps R, Qi Y, Gao X, Male V, et al. (2009) HLA-C cell surface expression and control of HIV/AIDS correlate with a variant upstream of HLA-C. *Nat Genet* 41: 1290–1294. <https://doi.org/10.1038/ng.486> PMID: 19935663
60. Apps R, Qi Y, Carlson JM, Chen H, Gao X, et al. (2013) Influence of HLA-C expression level on HIV control. *Science* 340: 87–91. <https://doi.org/10.1126/science.1232685> PMID: 23559252
61. Zhang Z, Gu Q, Jaguva Vasudevan AA, Jeyaraj M, Schmidt S, et al. (2016) Vif Proteins from Diverse Human Immunodeficiency Virus/Simian Immunodeficiency Virus Lineages Have Distinct Binding Sites in A3C. *J Virol* 90: 10193–10208. <https://doi.org/10.1128/JVI.01497-16> PMID: 27581978
62. Bock M, Bishop KN, Towers G, Stoye JP (2000) Use of a transient assay for studying the genetic determinants of Fv1 restriction. *J Virol* 74: 7422–7430. PMID: 10906195
63. Deng H, Liu R, Ellmeier W, Choe S, Unutmaz D, et al. (1996) Identification of a major co-receptor for primary isolates of HIV-1. *Nature* 381: 661–666. <https://doi.org/10.1038/381661a0> PMID: 8649511
64. Mariani R, Chen D, Schröfelbauer B, Navarro F, König R, et al. (2003) Species-specific exclusion of APOBEC3G from HIV-1 virions by Vif. *Cell* 114: 21–31. PMID: 12859895
65. Huet T, Cheynier R, Meyerhans A, Roelants G, Wain-Hobson S (1990) Genetic organization of a chimpanzee lentivirus related to HIV-1. *Nature* 345: 356–359. <https://doi.org/10.1038/345356a0> PMID: 2188136
66. Takehisa J, Kraus MH, Decker JM, Li Y, Keele BF, et al. (2007) Generation of infectious molecular clones of simian immunodeficiency virus from fecal consensus sequences of wild chimpanzees. *J Virol* 81: 7463–7475. <https://doi.org/10.1128/JVI.00551-07> PMID: 17494082
67. Goncalves J, Jallepalli P, Gabuzda DH (1994) Subcellular localization of the Vif protein of human immunodeficiency virus type 1. *J Virol* 68: 704–712. PMID: 8289374
68. Simm M, Shahabuddin M, Chao W, Allan JS, Volsky DJ (1995) Aberrant Gag protein composition of a human immunodeficiency virus type 1 vif mutant produced in primary lymphocytes. *J Virol* 69: 4582–4586. PMID: 7769728
69. Kao S, Khan MA, Miyagi E, Plishka R, Buckler-White A, et al. (2003) The human immunodeficiency virus type 1 Vif protein reduces intracellular expression and inhibits packaging of APOBEC3G (CEM15), a cellular inhibitor of virus infectivity. *J Virol* 77: 11398–11407. <https://doi.org/10.1128/JVI.77.21.11398-11407.2003> PMID: 14557625

70. Guo Y, Dong L, Qiu X, Wang Y, Zhang B, et al. (2014) Structural basis for hijacking CBF-beta and CUL5 E3 ligase complex by HIV-1 Vif. *Nature* 505: 229–233. <https://doi.org/10.1038/nature12884> PMID: [24402281](https://pubmed.ncbi.nlm.nih.gov/24402281/)

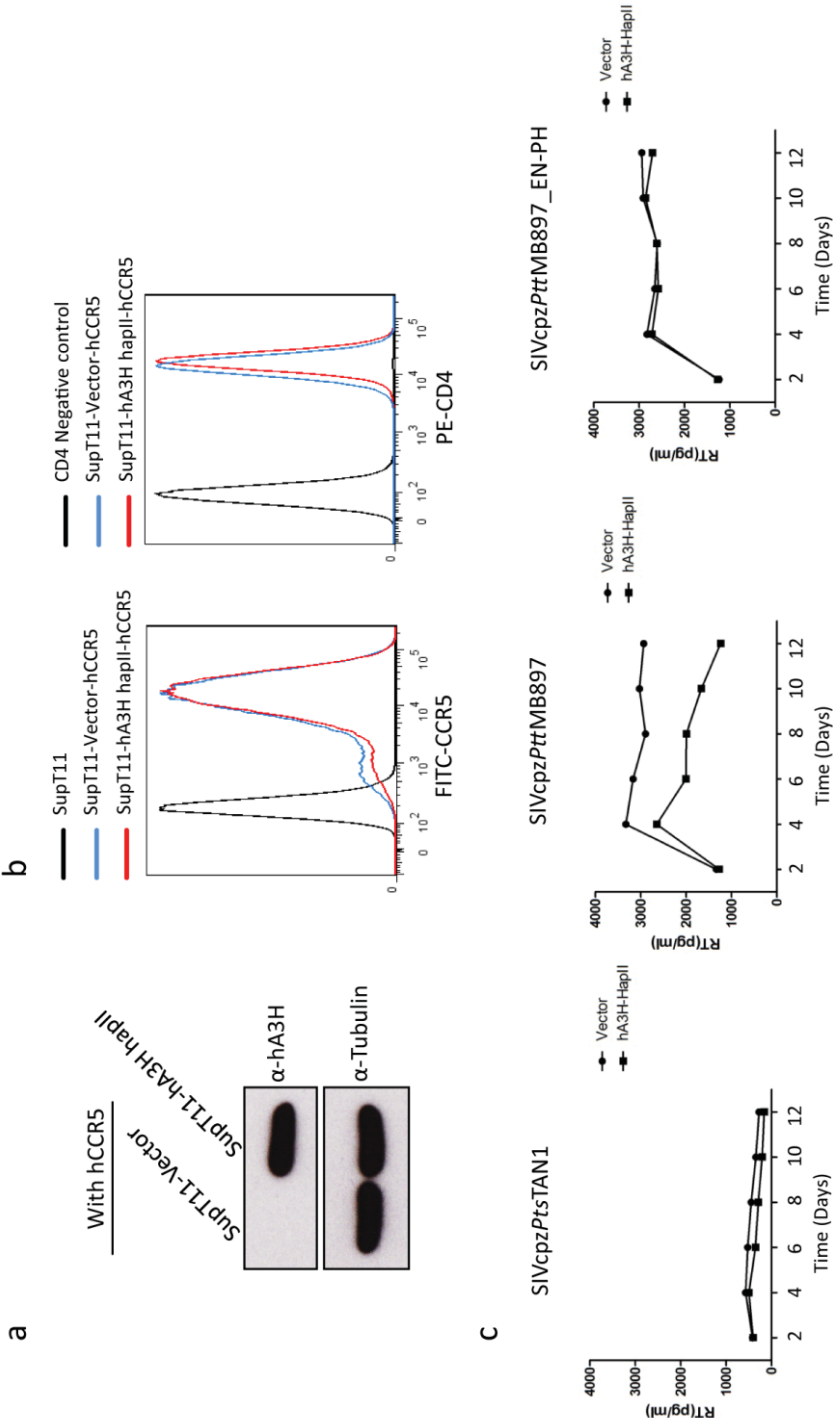
S1. Fig



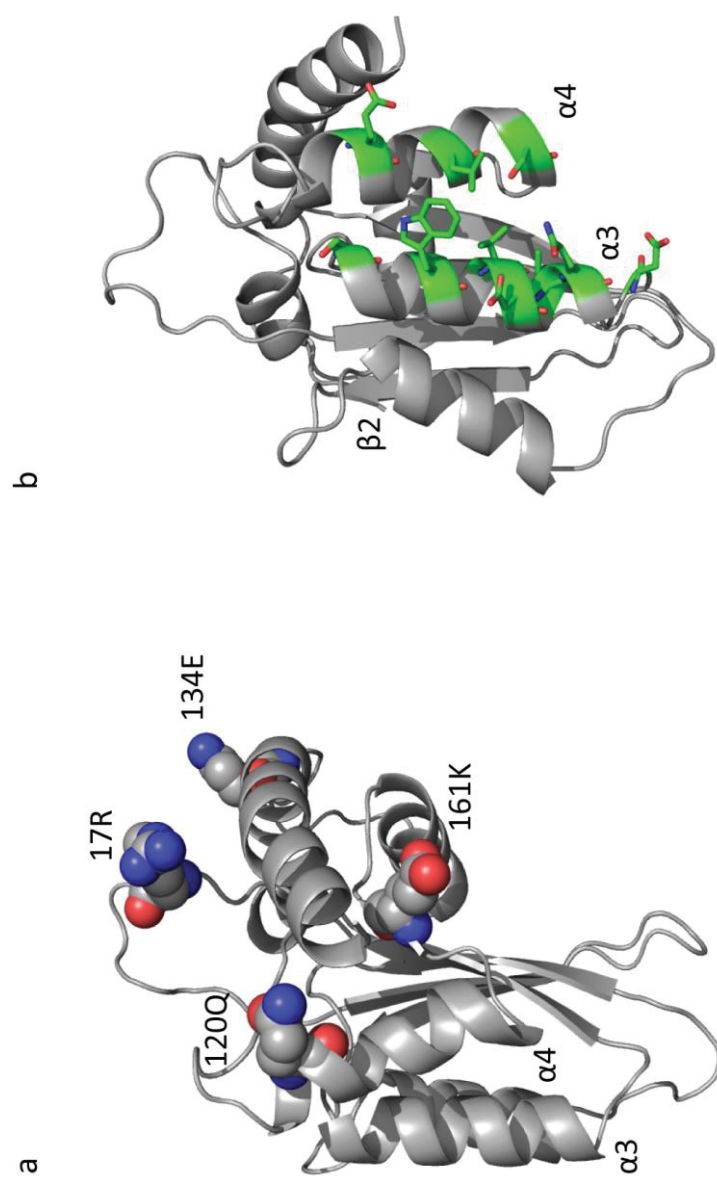
S2. Fig



S3. Fig



S4. Fig



Acknowledgements

I am really thankful to many people for long-time support and encouragement, which promotes my successful completion of current research. First of all, I would like to thank Chinese Scholarship Council who provides financial support to my study and life. I am grateful to my first supervisor Prof. Carsten Münk who gives chance to me for performing scientific research and provides continuous scientific assistance. I also appreciate my wife who provides abundance of happiness for my life, and abundance of support for my research. I am thankful to my second supervisor Prof. Holger Gohlke who gives lots of assistance and suggestions to my structural biology research. I thank all of my colleagues from AG Münk for providing a friendly and happy laboratory atmosphere. And I really enjoy cooperation with other groups.

Last, I appreciate all my friends for their relaxed and funny chatting in my life. I specially would like to thank my parents, uncle and aunty for their fully support and encouragement.

Declaration

I declare under oath that I have compiled my dissertation independently and without any undue assistance by third parties under consideration of the 'Principles for the Safeguarding of Good Scientific Practice at Heinrich Heine University Düsseldorf'

Düsseldorf

Date:

Zeli Zhang